

ADDRESSING SECURITY AND PRIVACY  
CHALLENGES IN INTERNET OF THINGS

ARSALAN MOSENIA

A DISSERTATION

PRESENTED TO THE FACULTY  
OF PRINCETON UNIVERSITY  
IN CANDIDACY FOR THE DEGREE  
OF DOCTOR OF PHILOSOPHY

RECOMMENDED FOR ACCEPTANCE

BY THE DEPARTMENT OF  
ELECTRICAL ENGINEERING  
ADVISER: NIRAJ K. JHA

JANUARY 2017

© Copyright by Arsalan Mosenia, 2017.

All rights reserved.

# Abstract

Internet of Things (IoT), also referred to as the Internet of Objects, is envisioned as a holistic and transformative approach for providing numerous services. The rapid development of various communication protocols and miniaturization of transceivers along with recent advances in sensing technologies offer the opportunity to transform isolated devices into communicating smart things. Smart things, that can sense, store, and even process electrical, thermal, optical, chemical, and other signals to extract user-/environment-related information, have enabled services only limited by human imagination.

Despite picturesque promises of IoT-enabled systems, the integration of smart things into the standard Internet introduces several security challenges because the majority of Internet technologies, communication protocols, and sensors were not designed to support IoT. Several recent research studies have demonstrated that launching security/privacy attacks against IoT-enabled systems, *in particular wearable medical sensor (WMS)-based systems*, may lead to catastrophic situations and life-threatening conditions. Therefore, security threats and privacy concerns in the IoT domain need to be proactively studied and aggressively addressed. In this thesis, we tackle several domain-specific security/privacy challenges associated with IoT-enabled systems.

We first target health monitoring systems that are one of the most widely-used types of IoT-enabled systems. We discuss and evaluate several energy-efficient schemes and algorithms, which significantly reduce total energy consumption of different implantable and wearable medical devices (IWMDs). The proposed schemes make continuous long-term health monitoring feasible while providing spare energy needed for data encryption.

Furthermore, we present two energy-efficient protocols for implantable medical devices (IMDs), which are essential for data encryption: (i) a secure wakeup protocol

that is resilient against battery draining attacks, along with (ii) a low-power key exchange protocol that shares the encryption key between the IMD and the external device while ensuring confidentiality of the key.

Moreover, we introduce a new class of attacks against the privacy of a patient who is carrying IWMDs. We describe how an attacker can infer private information about the patient by exploiting physiological information leakage, i.e., signals that continuously emanate from the human body due to the normal functioning of organs or IWMDs attached to (or implanted in) the body.

Further, we propose a new generic class of security attacks, called dedicated intelligent security attacks against sensor-triggered emergency responses (DISASTER), that is applicable to a variety of sensor-based systems. DISASTER exploits design flaws and security weaknesses of safety mechanisms deployed in cyber-physical systems (CPSs) to trigger emergency responses even in the absence of a real emergency. In addition to introducing DISASTER, we comprehensively describe its serious consequences and demonstrate the possibility of launching such attacks against the two most widely-used CPSs: residential and industrial automation/monitoring systems.

Finally, we present a continuous authentication system based on BioAura, i.e., information that is already gathered by WMSs for diagnostic and therapeutic purposes. We extensively examine the proposed authentication system and demonstrate that it offers promising advantages over one-time knowledge-based authentication systems, e.g., password-/pattern-based systems, and may potentially be used to protect personal computing devices and servers, software applications, and restricted physical spaces.



# Acknowledgments

This thesis would not have been possible without the help of so many people in so many ways. I would like to express my sincere appreciation to all those who supported me to complete the Ph.D. program at Princeton University.

I have had the honor and privilege to work under the supervision of Prof. Niraj K. Jha. who helped me take the first steps as a researcher. His guidance and support have helped me with academic research and writing from the first day of the Ph.D. program and have been very beneficial in shaping my Ph.D work. Apart from his immense wisdom and insight, his enthusiasm to explore new research directions and novel ideas has been a constant source of inspiration to me. His patience, kindness, understanding, and empathy towards his students are truly admirable. He has been extremely caring during my days of struggle. Although I have immensely benefited from his technical expertise, I still have so much to learn from his superior discipline and kind disposition.

I also received much advice and guidance from Profs. Anand Raghunathan, Susmita Sur-Kolay, and Mehran Mozaffari-Kermani. Discussion with them were always an exceptional source of new ideas. Without their continuous support, encouragement, and inspiration, preparing this thesis would not have been feasible.

I am deeply grateful for the guidance of Prof. Prateek Mittal, who inspired me in many ways and offered me the opportunity to become a teaching assistant in ELE 432 that he taught in Spring 2016. I have also been fortunate to collaborate with him on a research study during my last year of Ph.D. work.

I would like to thank my thesis readers, Profs. Niraj K. Jha, Susmita Sur-Kolay, and Prateek Mittal, for the extensive efforts in polishing and revising this thesis. I am also thankful to Profs. Niraj K. Jha, Anand Raghunathan, and David Wentzlaff for agreeing to be on my final public oral committee.

Prof. Niraj K. Jha, Prateek Mittal, and Sharad Malik kindly offered me teaching opportunities in their courses. Those were extremely valuable and enjoyable experiences from which I realized how much devotion makes perfection. I greatly appreciate their help, guidance, and trust in me.

The faculty in the Electrical Engineering and Computer Science Departments have been a phenomenal source of knowledge and guidance. I would like to thank all of them. I am also thankful to have group-mates like Mehran Mozaffari-Kermani, Mohammad Shoaib, Sourindra Choudhuri, Abdullah Guler, Fisher Wu, Xiaoliang Dai, Debajit Bhattacharya, Bochao Wang, Hongxu Yin, Ozge Akmandor, and Ajay Bhoj for their companionship. I would like to express my sincere gratitude towards Colleen Conrad, Lori Bailey, Heather L. Evans, and Stacey Weber as well; they have been extremely helpful throughout my time in the Department of Electrical Engineering.

I also appreciate the help I received from my friends who have made this journey unforgettable. I have had so many great moments with Behsan Behzadi, Pouya Sharifi, Amir Mazaheri, Fariborz Mirzaei, Siamak Garabaglu, Hooman Mohajeri, Mohammad Shahradi, Hossein Valavi, Hasan Nosratabadi, Moein Malekaghlagh, Mehdi Yazdi, Hesam Aklaghpour, Vahid Askari, Hooman Kayyatzadeh, and Ali Jamal. I have been fortunate to have them in my life.

Finally, my heartfelt thanks to my beloved parents, grandparents, and my wonderful brother Arman. I would not be able to accomplish anything without their unwavering love, support, and understanding.

This work was supported by NSF under Grant no. CNS-1219570 and CNS-1617628 and Project X Fund from Princeton University.

To my beloved parents and family who have supported me throughout my  
education.

# Contents

Abstract . . . . .	iii
Acknowledgments . . . . .	v
List of Tables . . . . .	xiv
List of Figures . . . . .	xvi
<b>1 Introduction</b>	<b>1</b>
1.1 The IoT paradigm . . . . .	2
1.1.1 IoT reference models . . . . .	2
1.1.2 Scope of applications . . . . .	5
1.1.3 Definition of security in the scope of IoT . . . . .	8
1.1.4 Potential attackers and their motivations . . . . .	10
1.2 WMS-based systems . . . . .	10
1.2.1 History and market growth . . . . .	12
1.2.2 Scopes of applications . . . . .	13
1.2.3 Main components of WMS-based systems . . . . .	20
1.2.4 Design goals . . . . .	24
1.3 Contributions of the thesis . . . . .	27
1.4 Thesis outline . . . . .	29
<b>2 Related Work</b>	<b>31</b>
2.1 Vulnerabilities of IoT and their countermeasures . . . . .	31

2.1.1	Known vulnerabilities . . . . .	31
2.1.2	Existing countermeasures . . . . .	43
2.2	Emerging research directions in the domain of WMS-based systems .	53
2.2.1	Design of low-power sensors . . . . .	54
2.2.2	Minimally-invasive capture methods . . . . .	57
2.2.3	Security and privacy . . . . .	58
2.2.4	Calibration and noise cancellation . . . . .	60
2.2.5	Big data . . . . .	61
2.2.6	Cloud computing . . . . .	63
<b>3</b>	<b>Energy-Efficient Long-term Continuous Personal Health Monitoring</b>	<b>65</b>
3.1	Introduction . . . . .	66
3.2	Different components of a general-purpose health monitoring system .	69
3.2.1	Health monitoring with networked wireless biomedical sensors	70
3.2.2	Communication protocol . . . . .	71
3.3	Baseline continuous health monitoring system . . . . .	72
3.3.1	Baseline WBAN . . . . .	72
3.3.2	Energy and storage requirements . . . . .	76
3.4	Analytical models for the evaluation of WBAN's energy and storage requirements . . . . .	77
3.4.1	Analytical models . . . . .	78
3.4.2	Evaluation of the baseline WBAN . . . . .	82
3.5	Improving the energy efficiency of continuous health monitoring . . .	84
3.5.1	Sample aggregation . . . . .	85
3.5.2	Anomaly-driven transmission . . . . .	87
3.5.3	CS-based computation and transmission . . . . .	89
3.5.4	Summary of proposed schemes . . . . .	94

3.6	Storage requirements . . . . .	95
3.7	Choosing the appropriate scheme and hardware platform . . . . .	97
3.7.1	The appropriate scheme for each sensor . . . . .	97
3.7.2	The hardware platform . . . . .	100
3.8	Chapter summary . . . . .	101
<b>4</b>	<b>OpSecure: A Secure Optical Communication Channel for Im-</b>	
	<b>plantable Medical Devices</b>	<b>102</b>
4.1	Introduction . . . . .	103
4.2	Problem definition . . . . .	106
4.2.1	Wakeup and key exchange protocols . . . . .	106
4.2.2	Related work . . . . .	107
4.3	The proposed channel and protocols . . . . .	110
4.3.1	OpSecure: The proposed channel . . . . .	110
4.3.2	The proposed protocols . . . . .	112
4.4	The prototype implementation and body model . . . . .	115
4.4.1	Prototype implementation . . . . .	115
4.4.2	The bacon-beef body model . . . . .	117
4.5	Evaluation of the proposed protocols . . . . .	117
4.5.1	Transmission range . . . . .	118
4.5.2	Transmission quality . . . . .	118
4.5.3	Wakeup/exchange time . . . . .	119
4.5.4	Size and energy overheads . . . . .	120
4.5.5	Security analysis . . . . .	122
4.5.6	Summary of evaluations . . . . .	124
4.6	Chapter summary . . . . .	124

<b>5</b>	<b>Physiological Information Leakage</b>	<b>126</b>
5.1	Introduction . . . . .	127
5.2	Threat model . . . . .	129
5.2.1	Adversary . . . . .	129
5.2.2	Potential risks . . . . .	129
5.3	Information leakage . . . . .	130
5.3.1	Leakage sources . . . . .	131
5.3.2	Leakage types . . . . .	131
5.4	Leaked signals and capture methods . . . . .	135
5.4.1	Capturing acoustic signals emanating from body organs . . . . .	136
5.4.2	Capturing acoustic signal generated by IWMDs . . . . .	137
5.4.3	Capturing unintentional EM signals . . . . .	138
5.4.4	Capturing the metadata of wireless communication . . . . .	138
5.5	Proposed privacy attacks . . . . .	139
5.5.1	Acoustic signal based body-related attacks . . . . .	140
5.5.2	Acoustic signal based IWMD-related attacks . . . . .	142
5.5.3	EM radiation based IWMD-related attacks . . . . .	153
5.6	Possible countermeasures . . . . .	157
5.7	Chapter summary . . . . .	159
<b>6</b>	<b>DISASTER: Dedicated Intelligent Security Attacks on Sensor-triggered Emergency Responses</b>	<b>161</b>
6.1	Introduction . . . . .	162
6.2	Threat model . . . . .	164
6.2.1	Problem definition . . . . .	165
6.2.2	Potential attackers . . . . .	166
6.3	Typical components and weaknesses of safety mechanisms . . . . .	167
6.3.1	Typical CPS architecture . . . . .	167

6.3.2	Common design flaws and security weaknesses . . . . .	169
6.4	Potential consequences of launching DISASTER . . . . .	172
6.4.1	Life-threatening conditions . . . . .	172
6.4.2	Economic collateral damage . . . . .	173
6.4.3	Overriding access control mechanisms . . . . .	173
6.4.4	Unintended ignorance . . . . .	174
6.5	Launching DISASTER . . . . .	174
6.5.1	Creating and transmitting illegitimate packets . . . . .	175
6.5.2	DISASTER case studies . . . . .	177
6.6	Suggested countermeasures . . . . .	189
6.6.1	Proactive countermeasures . . . . .	189
6.6.2	Unpredictable situations . . . . .	192
6.7	Chapter summary . . . . .	193
<b>7</b>	<b>CABA: Continuous Authentication Based on BioAura</b>	<b>194</b>
7.1	Introduction . . . . .	195
7.2	Desirable authentication requirements . . . . .	198
7.2.1	Design-octagon . . . . .	198
7.2.2	Addressing desirable requirements . . . . .	200
7.3	BioAura . . . . .	202
7.4	Scope of applications . . . . .	204
7.5	Implementation and experimental setup . . . . .	206
7.5.1	Prototype implementation . . . . .	207
7.5.2	Experimental setup and metrics . . . . .	211
7.6	Authentication results . . . . .	214
7.6.1	Authentication accuracy . . . . .	214
7.6.2	CABA scalability . . . . .	219
7.7	Using BioAura for identification . . . . .	221



7.8	Real-time adaptive authorization . . . . .	222
7.9	Potential threats and countermeasures . . . . .	225
7.10	Comparison between CABA and previously-proposed systems . . . . .	227
7.11	Discussion . . . . .	229
7.11.1	Health information leakage . . . . .	229
7.11.2	One-time authentication based on BioAura . . . . .	230
7.11.3	The impact of temporal conditions . . . . .	230
7.12	Chapter summary . . . . .	231
<b>8</b>	<b>Conclusion</b>	<b>232</b>
8.1	Thesis summary . . . . .	232
8.2	Future directions . . . . .	235
	<b>Bibliography</b>	<b>237</b>

# List of Tables

1.1	Security requirements . . . . .	9
1.2	Common WMSs . . . . .	22
3.1	Resolution, sampling rate, and maximum transmission rate . . . . .	76
3.2	Variables, unit, and description . . . . .	78
3.3	Upper-bound values of $E_s$ . . . . .	80
3.4	Minimum and maximum values of total energy consumption . . . . .	83
3.5	Minimum and maximum battery lifetimes of different sensors . . . . .	83
3.6	Minimum and maximum storage required for long-term storage . . . . .	84
3.7	Maximum number of samples in one packet . . . . .	86
3.8	Minimum and maximum values of total energy consumption while using the sample aggregation scheme . . . . .	87
3.9	Minimum and maximum battery lifetimes of different sensors while using sample aggregation scheme . . . . .	87
3.10	Average total energy consumption of the EEG sensor for the anomaly-driven method . . . . .	89
3.11	Average battery lifetimes for the EEG sensor for the anomaly-driven method . . . . .	89
3.12	Average total energy consumption of the EEG sensor for CS-based computation . . . . .	94
3.13	Average battery lifetimes of the EEG sensor for CS-based computation . . . . .	94

3.14	Average storage required for long-term storage of processed data . . . . .	97
3.15	Comparison of different schemes . . . . .	99
4.1	Summary of evaluations . . . . .	124
5.1	Sources of leakage, types of leakage, and descriptions . . . . .	135
5.2	Accuracy of the three methods for eavesdropping on the alarm system of an insulin pump . . . . .	149
6.1	Different sensors used in a typical residential CPS, their descriptions, and services . . . . .	178
6.2	Maximum recording distance and maximum retransmission distance for each sensor in Experimental scenario 1 . . . . .	182
6.3	Communication frequency, modulation type, and pin length of each residential sensor . . . . .	183
6.4	Maximum transmission distance for each residential sensor in Experi- mental scenario 2 . . . . .	184
6.5	Communication frequency, modulation type, and pin length for each level sensor . . . . .	188
6.6	Maximum transmission distance for each industrial level sensor exam- ined in Experimental scenario 2 . . . . .	189
7.1	Biostreams, their abbreviations/notations, and units . . . . .	204
7.2	Classifiers and their $EER_{t=7h}$ . . . . .	216
7.3	Classifiers and their $FAW$ and $FRW$ . . . . .	216
7.4	Classifiers and their $FRR$ ( $FAR \approx 0$ ) . . . . .	217
7.5	Classifiers and their $FAR$ ( $FRR \approx 0$ ) . . . . .	217

# List of Figures

1.1	Three IoT reference models . . . . .	3
1.2	Different applications of IoT [1] . . . . .	6
1.3	The scope of applications of WMS-based systems . . . . .	14
1.4	The three main components of WMS-based systems: WMSs, the base station, and Cloud servers [2]. . . . .	21
1.5	Goal-heptagon: Desiderata for WMS-based systems [2]. . . . .	25
2.1	Summary of attacks and countermeasures [1] . . . . .	32
3.1	A personal health care system. . . . .	70
3.2	Scatter plot of the reported $E_{ADC}$ vs. ENOB bits for different ADC architectures: asynchronous ( $\circ$ ), cyclic ( $\square$ ), delta-sigma ( $\triangleleft$ ), flash (+), folding ( $\triangle$ ), pipeline ( $\times$ ), successive approximation ( $\diamond$ ), subranging ( $\triangleright$ ), n-Slope ( $*$ ), n-Step ( $\star$ ), and other ( $\nabla$ ) . . . . .	79
3.3	Energy consumption and battery lifetime of the ECG sensor for the anomaly-driven method with respect to frequency of occurrence of arrhythmia in a day. . . . .	90
3.4	Traditional CS vs. on-sensor CS-based computation. . . . .	91

3.5	Sensitivity and FA/h of seizure detection classification with respect to compression ratio. Sensitivity and FA/h CS-based method using $\alpha = 8\times$ are almost equal to the sensitivity and FA/h of the traditional method using Nyquist sampling ( $\alpha = 1\times$ ). . . . .	93
3.6	Energy consumption and battery lifetime of the ECG sensor for the CS-based method with respect to frequency of occurrence of arrhythmia in a day. . . . .	94
3.7	Energy reduction in each sensor when the sensor accumulates multiple samples in one packet. Raw data are assumed to be gathered at the maximum frequency. . . . .	95
3.8	Energy reduction in EEG and ECG sensors. The number of arrhythmia events in a day is assumed to be 32, and raw data are assumed to be gathered at the maximum frequency. . . . .	95
3.9	The amount of storage required for storing important chunks of ECG signals based on the results of computation. . . . .	97
4.1	Overall system architecture: IMD and external device have a bidirectional RF channel that supports symmetric encryption, e.g., Bluetooth Low Energy. . . . .	106
4.2	The IMD (pacemaker) has an embedded light sensor, and the smartphone flashlight acts as a light source. . . . .	112
4.3	<i>keySegmentation</i> outputs <i>segments</i> [] given <i>Keypacket</i> . . . . .	114
4.4	The smartphone generates a 4-bit key and transmits the key over OpSecure. The application allows the user to control both the key length ( $N$ ) and transmission rate ( $R$ ). . . . .	116
4.5	Experimental setup: The smartphone is placed on top of the bacon layer above a transparent plastic sealing. . . . .	117

5.1	Sources of leakage and different types of signals that are continuously leaking from the human body and IWMDs. . . . .	132
5.2	The displacement-based laser microphone. . . . .	137
5.3	Schematic for displacement-based laser microphone: The laser beam forms a small incident angle with the surface. The fraction of light beam received by the light sensor depends on the vibration of the surface. . . . .	137
5.4	Different types of privacy attacks, capture methods, and the private information that each type of attack can extract from different leaked signals . . . . .	140
5.5	A schematic view of an insulin pump. The components marked in red (motor and buzzer) generate the acoustic signals that can be interpreted to reveal the medical data. . . . .	143
5.6	Dose of injected insulin vs. the number of rotation steps of the electrical motor. . . . .	144
5.7	Acoustic signal generated by the electrical motor of an insulin pump while injecting 0.8 unit of insulin. . . . .	144
5.8	Dose of injected insulin vs. injection duration. . . . .	147
5.9	Acoustic signal generated by the electrical motor of an insulin pump when 0.8 unit of insulin is injected. For a large fraction of time, the acoustic signal is dominated by background noise, and counting the number of rotation steps is not feasible. . . . .	148
5.10	Acoustic signal generated by the safety system of an insulin pump when the user tries to inject 0.8 unit of insulin. . . . .	150
5.11	Block diagram of an ambulatory BP monitoring device. The components shown in red are the major sources of acoustic leakage. . . . .	151

5.12	Acoustic signal generated by the ambulatory BP monitoring device. Three phases of measurement are shown. . . . .	151
6.1	Common architecture of CPS. Upon the detection of an emergency, the safety unit directly controls the physical objects or warns the users by activating the passive components. . . . .	168
6.2	The implementation of an OOK demodulator in GNURadio . . . . .	177
6.3	The door sensor generates a packet as soon as it detects the door is open. The spike in the fast Fourier transform of the analog signal shows a single transmission using OOK modulation. . . . .	181
6.4	The bitstream transmitted by the door sensor to the base station of the residential CPS. The door sensor repeatedly transmits a single static packet, which includes its 4-bit pin number, to its base station. . . . .	183
6.5	A simple industrial automation/monitoring CPS . . . . .	187
6.6	The bitstream transmitted by one of the level sensors to the base sta- tion of the industrial CPS. . . . .	188
7.1	Design-octagon: Desiderata for a continuous authentication system. . .	198
7.2	A continuous health monitoring system consisting of several small lightweight WMSs that transmit biomedical data to the smartphone. . . . .	203
7.3	The tablet wants to authenticate the user. The vertical arrows depict the timeline. . . . .	206
7.4	The laptop wants to authenticate the user before allowing the user to utilize its resources or software applications. . . . .	207
7.5	User authentication phase: The user's smartphone provides $Y$ and the user ID, and CABA outputs the decision. . . . .	209
7.6	Two possible output sequences over a ten-minute authentication time- frame. A (R) refers to an accept (reject) decision. . . . .	214

7.7	Average $EER_t$ for different classifiers with respect to $TRW$ . . . . .	218
7.8	Moving training window. . . . .	218
7.9	$EER_{t=7h}$ for different classifiers when Biostreams are dropped one at a time. The green bar depicts the baseline scenario in which no feature is dropped. The abbreviations/notations provided in Table 7.1 are used to label other bars. . . . .	219



# Chapter 1

## Introduction

Internet of Things (IoT) does not have a unique definition. However, a broad interpretation of IoT is that it provides any service over the traditional Internet by enabling human-to-thing, thing-to-thing, or thing-to-things communications [3]. IoT represents the interconnection of heterogeneous entities, where the term entity refers to a human, sensor, or potentially anything that may request/provide a service [4].

The emergence of the IoT paradigm is one of the most spectacular phenomena of the last decade. The development of various communication protocols, along with the miniaturization of transceivers, provides the opportunity to transform an isolated device into a communicating thing. Moreover, computing power, energy capacity, and storage capabilities of small computing or sensing devices have significantly improved while their sizes have decreased drastically. Boosted by the rapid development of IoT-enabled systems in recent years, Internet-connected wearable medical sensors (WMSs) are garnering an ever-increasing attention in both academic and industrial research. Although WMSs were initially developed to enable low-cost solutions for continuous health monitoring, the applications of WMS-based systems now range far beyond health care. As discussed later in this chapter, several research efforts have

proposed the use of such systems in diverse application domains, e.g., education, human-computer interaction, and security.

As a side effect of rapid advances in the design and development of IoT-enabled systems, the number of potential threats and possible attacks against security of such systems, *in particular WMS-based systems that rely on resource-constrained sensors*, and privacy of their users has grown drastically. Thus, security threats and common privacy concerns need to be studied and addressed in depth. This would greatly simplify the development of secure smart devices that enable a plethora of services for human beings, ranging from building automation to health monitoring, in which very different things, e.g., temperature sensor, light sensor, and medical sensors, might interact with each other or with a human carrying a smart computing device, e.g., a smartphone, tablet, or laptop. This dissertation aims to explore and address different security/privacy issues associated with IoT-enabled systems with a special focus on WMS-based systems.

In the rest of this chapter, we first describe the IoT paradigm, and then discuss WMS-based systems.

## **1.1 The IoT paradigm**

In this section, we first discuss different IoT reference models described in the literature. Then, we describe the scope of IoT applications. Thereafter, we explain what security means in the scope of IoT. Finally, we discuss who the attackers that target the IoT might be, and what motivations they might have.

### **1.1.1 IoT reference models**

Three IoT reference models have been widely discussed in academic and industrial publications. Fig. 1.1 shows these models and their different levels. The three-level

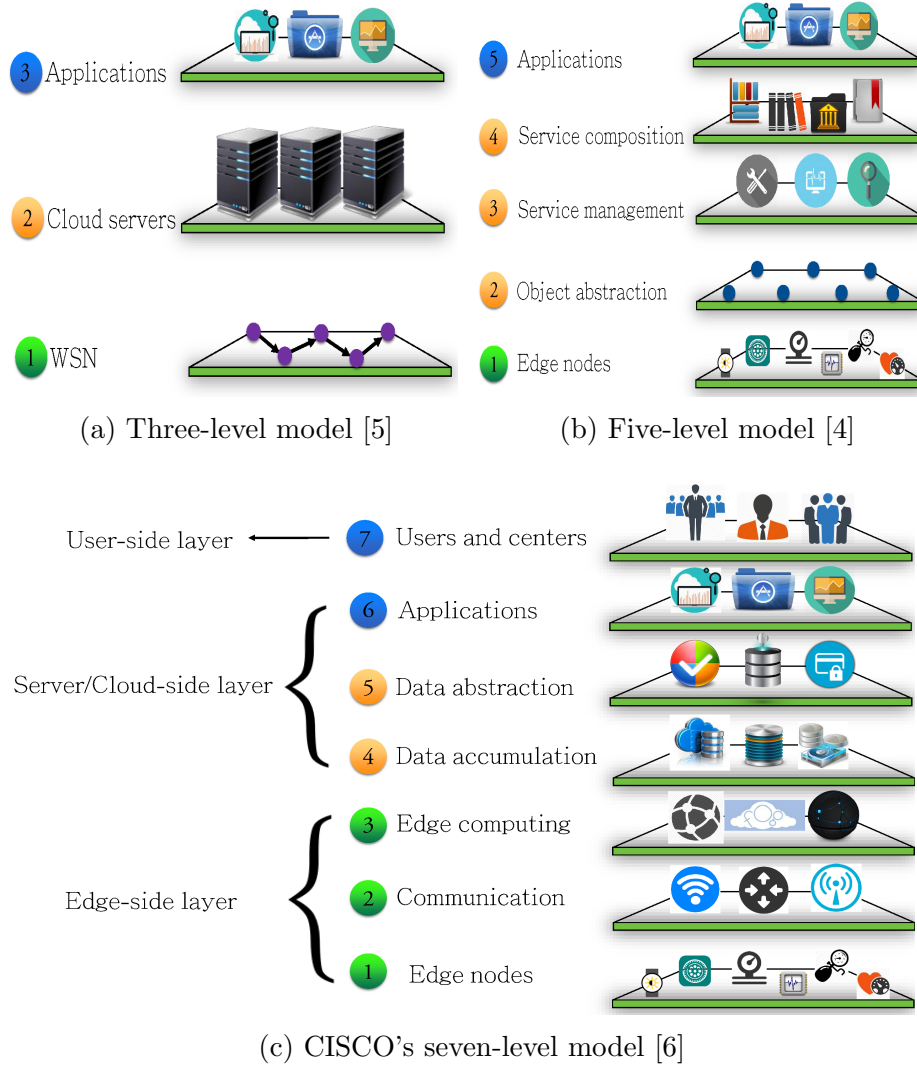


Figure 1.1: Three IoT reference models

model [5] is among the first reference models proposed for IoT. It depicts IoT as an extended version of wireless sensor networks (WSNs). In fact, it models IoT as a combination of WSNs and cloud servers, which offer different services to the user. The five-level model [4] is an alternative that has been proposed to facilitate interactions among different sections of an enterprise by decomposing complex systems into simplified applications consisting of an ecosystem of simpler and well-defined components [4]. In 2014, CISCO suggested a comprehensive extension to the traditional three-level and five-level models. CISCO's seven-level model has the potential to be

standardized and thus create a widely-accepted reference model for IoT [6]. In this model, data flow is usually bidirectional. However, the dominant direction of data flow depends on the application. For example, in a control system, data and commands travel from the top of the model (applications level) to the bottom (edge node level), whereas, in a monitoring scenario, the flow is from bottom to top.

In order to summarize IoT security attacks and their countermeasures in a level-by-level fashion, we use the CISCO reference model in Chapter 2. Next, we briefly describe each level of this model.

***Level 1-Edge devices:*** The first level of this reference model typically consists of computing nodes, e.g., smart controllers, sensors, RFID readers, etc., and different versions of RFID tags. Data confidentiality and integrity must be taken into account from this level upwards.

***Level 2-Communication:*** The communication level consists of all the components that enable transmission of information or commands: (i) communication between devices in the first level, (ii) communication between the components in the second level, and (iii) transmission of information between the first and third levels (edge computing level).

***Level 3-Edge computing:*** Edge computing, also called fog computing, is the third level of the model in which simple data processing is initiated. This is essential for reducing the computation load in the higher level as well as providing a fast response. Most real-time applications need to perform computations as close to the edge of the network as possible. The amount of processing in this level depends on the computing power of the service providers, servers, and computing nodes. Typically, simple signal processing and learning algorithms are utilized here.

***Level 4-Data accumulation:*** Most of the applications may not need instant data processing. This level enables conversion of data in motion to data at rest, i.e., it allows us to store the data for future analysis or to share with high-level computing

servers. The main tasks of this level are converting the format from network packets to database tables, reducing data through filtering and selective storing, and determining whether the data are of interest to higher levels.

**Level 5-Data abstraction:** This level provides the opportunity to render and store data such that further processing becomes simpler or more efficient. The common tasks of entities at this level include normalization, de-normalization, indexing and consolidating data into one place, and providing access to multiple data stores.

**Level 6-Applications:** The application level provides information interpretation, where software cooperates with data accumulation and data abstraction levels. The applications of IoT are numerous and may vary significantly across markets and industrial needs.

**Level 7-Users and centers:** The highest level of the IoT is where the users are. Users make use of the applications and their analytical data.

### 1.1.2 Scope of applications

In this section, we first discuss the scope of IoT applications.

Smart homes and buildings, electronic health aids, and smarter vehicles are just some of the IoT instances [7–9]. Each smart device may provide several services to enable a more intuitive environment. However, we are not even close to exhausting the possible uses of IoT. IoT provides an opportunity to combine sensing, communication, networking, authentication, identification, and computing, and enables numerous services upon request such that access to the information of any smart thing is possible at any time. Fig. 1.2 demonstrates various applications of the IoT, which we describe next:

**1. Smart vehicles:** Smart vehicles have started to revolutionize traditional transportation. Small IoT-based systems can enable remote locking/unlocking of cars, download of roadmaps, and access to traffic information. Moreover, Internet-



Figure 1.2: Different applications of IoT [1]

connected cars provide significant protection against theft.

**2. Smart buildings:** Smart homes and buildings enable effective energy management. For example, smart thermostats, which have embedded sensors and data analysis algorithms, can control air conditioners based on user preferences and habits. Moreover, smart controllers can adjust lighting based on user's usage. Several household items, e.g., refrigerators, televisions, and security systems, could have their own processing units, and provide over-the-Internet services. These smart devices greatly enhance users' convenience. Remotely-controllable devices receive commands from users to perform actions that have an effect on the surrounding environment. Thus, attacks on these devices may lead to physical consequences [10].

**3. Health monitoring:** Recent advances in biomedical sensing and signal processing, low-power devices, and wireless communication have revolutionized health care. IoT-based long-term personal health monitoring and drug delivery systems, in which various physiological signals are captured, analyzed, and stored for future use,

provide a fundamentally new approach to health care [11]. Smart medical devices are already in use in fitness, diet, and health monitoring systems [12]. The future of IoT-based health care systems lies in designing personal health monitors that enable early detection of illnesses.

**4. *Energy management:*** Use of smart IoT-based systems, which integrate embedded sensors and actuation components, enables a proactive approach to optimizing energy consumption. In particular, power outlets, lamps, fridges, and smart televisions, which can be controlled remotely, are expected to share information with energy supply companies to optimize the energy consumption in smart homes. Moreover, such things allow the users to remotely control or manage them, and enable scheduling that can lead to a significant reduction in energy consumption.

**5. *Construction management:*** Monitoring and management of modern infrastructure, e.g., bridges, traffic lights, railway tracks, and buildings, are one of the key IoT applications [13]. IoT can be used for monitoring any sudden changes in structural conditions that can lead to safety and security risks. It can also enable construction and maintenance companies to share information about their plans. For example, a construction company can let GPS companies know its maintenance plans for the roads and, based on that, the smart GPS devices can choose an alternative route, which avoids the road under construction.

**6. *Environmental monitoring:*** The use of smart things with embedded sensors enables environmental monitoring as well as detection of emergency situations, e.g., a flood, which require a fast response. In addition, the quality of air and water can be examined by IoT-based devices. Moreover, humidity and temperature can be easily monitored [14].

**7. *Production and assembly line management:*** IoT-based smart systems allow rapid manufacturing of new products and an interactive response to demands by enabling communication between sensors and controlling/monitoring systems [15].

Moreover, intelligent management approaches that use real-time measurements can also enable energy optimization and safety management.

**8. Food supply chain:** The food supply chain model is fundamentally distributed and sophisticated. IoT can provide valuable information for managers of this chain. Although IoT is already in use within the supply management systems, its current benefits are limited. One of the most obvious and significant advantages of IoT in supply management is that it ensures security and safety of the products by utilizing IoT-based tracking [16]. These devices can raise a warning in case of a security breach at any unauthorized level of the supply management system.

### **1.1.3 Definition of security in the scope of IoT**

Next, we define two of the most commonly-used terms in the scope of IoT: a secure thing and a security attack. When defining what a secure thing is, it is important to understand the characteristics that define security. Traditionally, security requirements are broken down into three main categories: (i) confidentiality, (ii) integrity, and (iii) availability, referred to as the CIA-triad. Confidentiality entails applying a set of rules to limit unauthorized access to certain information. It is crucial for IoT devices because they might handle critical personal information, e.g., medical records and prescription. For instance, an unauthorized access to personal health devices may reveal personal health information or even lead to life-threatening situations [17]. Integrity is also necessary for providing a reliable service. The device must ensure that the received commands and collected information are legitimate. An integrity compromise may lead to serious adverse consequences. For example, integrity attacks against medical devices, e.g., an insulin pump [18] or a pacemaker [19], may have life-threatening outcomes. IoT availability is essential for providing a fully-functioning Internet-connected environment. It ensures that devices are available for collecting data and prevents service interruptions.



Table 1.1: Security requirements

Requirement	Definition	Abbreviations
Confidentiality	Ensuring that only authorized users access the information	C
Integrity	Ensuring completeness, accuracy, and absence of unauthorized data manipulation	I
Availability	Ensuring that all system services are available, when requested by an authorized user	A
Accountability	An ability of a system to hold users responsible for their actions	AC
Auditability	An ability of a system to conduct persistent monitoring of all actions	AU
Trustworthiness	An ability of a system to verify identity and establish trust in a third party	TW
Non-repudiation	An ability of a system to confirm occurrence/non-occurrence of an action	NR
Privacy	Ensuring that the system obeys privacy policies and enabling users to control their data	P

The insufficiency of the CIA-triad in the context of security has been addressed before [20–22]. Cherdantseva et al. [20] show that the CIA-triad does not address new threats that emerge in a collaborative security environment. They provide a comprehensive list of security requirements by analyzing and examining a variety of information, assurance, and security literature. This list is called the IAS-octave and is proposed as an extension to CIA-triad. Table 1.1 summarizes the security requirements in the IAS-octave, and provides their definitions and abbreviations. We define:

- *Secure thing*: A thing that meets all of the above-mentioned security requirements.
- *Security attack*: An attack that threatens at least one of the above-mentioned security requirements.

### 1.1.4 Potential attackers and their motivations

Next, we briefly discuss who the attackers that target the IoT might be, and what motivations they may have.

IoT-based systems may manage a huge amount of information and be used for services ranging from industrial management to health monitoring. This has made the IoT paradigm an interesting target for a multitude of attackers and adversaries, such as occasional hackers, cybercriminals, hacktivists, government, etc.

Potential attackers might be interested in stealing sensitive information, e.g., credit card numbers, location data, financial accounts' passwords, and health-related information, by hacking IoT devices. Moreover, they might try to compromise IoT components, e.g., edge nodes, to launch attacks against a third-party entity. Consider an intelligence agency that infects millions of IoT-based systems, e.g., remote monitoring systems, and smart devices, e.g., smart televisions. It can exploit the infected systems and devices to spy on a person of interest or to conduct an attack on a large scale. Also, hacktivists or those in opposition might be interested in attacking smart devices to launch protests against an organization.

## 1.2 WMS-based systems

Aging population and rapidly-rising costs of health care have triggered a lot of interest in WMSs. Traditionally, in-hospital monitoring devices, such as electrocardiogram (ECG) and electroencephalogram (EEG) monitors, have been used to sense and store raw medical data, with processing being performed later on another machine, e.g., an external computer [11, 23]. Several trends in communication, signal processing, machine learning, and biomedical sensing have converged to advance continuous health monitoring from a distant vision to the verge of reality. Foremost among these trends is the development of Internet-connected WMSs, which can non-invasively sense, col-

lect, and even process different types of body-related data, e.g., electrical, thermal, and optical signals generated by the human body.

WMSs enable proactive prevention and remote detection of health issues, thus with the potential to significantly reduce health care costs [24, 25]. Since the introduction of the first wearable heart monitor in 1981 [26], numerous types of WMS-based systems have been proposed, ranging from simple accelerometer-based activity monitors [25, 27] to complex sweat sensors [28]. WMS-based systems have also been developed for continuous long-term health monitoring [11, 29].

In the last decade, with the pervasive use of Internet-connected WMSs, the scope of applications of WMS-based systems has extended far beyond health care. For example, such systems have targeted application domains as diverse as education, information security, and human-computer interaction (HCI). Park et al. [30] introduced a WMS-based teaching assistant system, called SmartKG. It collects, manages, and fuses data gathered by several wearable badges to prepare valuable feedback to the teacher. Barreto et al. [31] designed and implemented a human-computer interface, which uses EEG and electromyogram (EMG) signals gathered from the subject's head to control computer cursor movements.

Despite the emergence of numerous WMS-based systems in recent years, potential challenges associated with their design, development, and implementation are neither well-studied nor well-recognized. The rest of this section:

- provides a brief history of wearable computing devices and WMSs and discusses how their market is growing,
- explains in depth the scope of applications of WMS-based systems,
- describes the architecture of a typical WMS-based system and discusses constituent components, and the limitations of these components,

- suggests an inclusive list of desirable design goals and requirements that WMS-based systems should satisfy.

### 1.2.1 History and market growth

Wearable devices have a history that goes back longer than most people expect. The first truly wearable computer appeared in 1961, when Edward O. Thorpe and Claude Shannon created Roulette Predictor [32], a wearable computer that could be concealed in a shoe and accurately predict where the ball would land on a roulette circle. Integration of wearable sensors in wearable computing devices was done in 1981, when Polar Electro Company introduced the first wearable heart rate monitors for professional athletes [26]. After that, several companies were founded to offer various services based on WMSs. However, due to the immaturity of the sensing technology, implementation complexities, e.g., heat management, limitations of wearable sensors, e.g., small local storage, and security/privacy concerns, the majority of such companies experienced a difficult time commercializing their products, and as a result, went through bankruptcy [33].

Rapid advances in communication protocols and the miniaturization of transceivers in 1990s, along with the emergence of different WMSs in the early 2000s, transformed the market of wearable technologies. In the last decade, the rapidly-falling prices of WMSs and components used to implement WMS-based systems have changed the application landscape [34–36]. In addition, the rising market of personal smart devices, e.g., smartphones and tablets, that are powerful, ubiquitous, and less resource-limited relative to wearable sensors, has enabled a plethora of services, ranging from continuous health monitoring [11] to continuous user authentication [37]. The introduction of Apple’s App Store for the iPhone and iPod Touch in July 2008, Google’s Android Market (now called Google Play Store), and RIM’s BlackBerry

App World in 2009, enabled easy distribution of third-party applications, further boosting the WMS industry [38, 39].

Global Wearable Sensors Market [40] recently published a report that includes information from 2011 to 2016. This report indicates that the introduction of smart watches from companies like Samsung, Sony, and Nike has given a significant boost to the wearable technology market. As of 2016, North America has the highest penetration of wearable sensors since Americans tend to be early adopters of new technologies. However, Asia is expected to show the highest growth rate in a few years due to the presence of developing countries like India and China [41]. A recently-published report provided by IHS Technology [42] forecasts that the number of WMSs will rise by 7× from 67 million units in 2013 to 466 million units in 2019. Another recent report by Business Insider [43] claims that 33 million wearable devices were sold in 2015 only for health monitoring. It forecasts that this number will reach 148 million by 2019. In the years after that, such usage is expected to explode further.

### 1.2.2 Scopes of applications

In this section, we describe various applications of WMS-based systems (a summary is shown in Fig. 1.3).

#### Health care

Rapid advances in WMS-based systems are transforming and revolutionizing health care. Medical WMS-based systems are of two main types: (i) health monitoring systems that monitor the patient to prevent the occurrence of a medical condition or detect a disease at an early stage, and (ii) medical automation systems, which offer continuous treatment or rehabilitation services. Next, we describe each type.

**1. Health monitoring systems:** Prevention and early detection of medical conditions are essential for promoting wellness. Unfortunately, conventional clinical di-

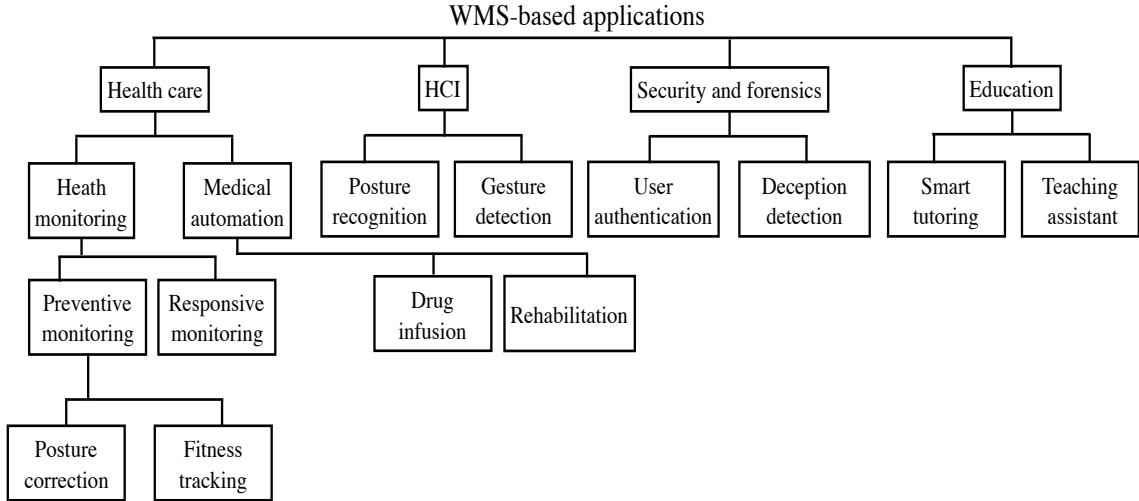


Figure 1.3: The scope of applications of WMS-based systems

agnostic practices commonly fail to detect health conditions in the early stages since diagnosis is typically performed after the emergence of major health symptoms, and previous medical data on the patient are often very sketchy. Furthermore, clinical practices are difficult to carry out in out-of-hospital environments.

In order to address the above-mentioned drawbacks of traditional clinical practices, several research studies have targeted WMS-based health monitoring systems. Such systems can be divided into two categories based on their main task: (i) preventive systems that aim to provide an approach to prevent diseases before the emergence of their symptoms, and (ii) responsive systems that attempt to detect health conditions at an early stage and provide health reports to the patient or the physician. Next, we describe each category.

**Preventive systems:** Preventive health monitoring systems provide real-time feedback to the user in an attempt to correct behaviors that might lead to adverse health conditions in the future. They promote healthy behaviors and lower the probability of serious illnesses by automatically detecting/predicting unhealthy activities and warning the user about them [44]. Posture correctors and fitness trackers are two of the most widely-known types of preventive health monitoring systems.

*Posture corrector:* A poor posture results in muscle tightening, shortening, or weakening, causing several health conditions, e.g., back pain and spinal deformity [45]. Posture correctors [46–48] monitor the user’s movements and habits and offer real-time feedback upon the detection of any posture abnormality, e.g., slouching when sitting in front of a computer display. In fact, they help the user maintain a healthy posture while performing daily activities.

*Fitness tracker:* Such trackers are in widespread use and their market is rapidly growing. Although they may use different sensing technologies, they all have a common characteristic: they non-invasively measure some types of fitness-related parameters, e.g., calories burned, heart rate, number of steps taken [49], and even sleep patterns [50]. State-of-the-art fitness trackers play a significant role in the IoT paradigm by enabling object-to-object communication, transmission of user’s data to the Cloud, and remote monitoring of user’s activities [51]. For example, a fitness tracker, which can communicate with other objects, may be able to gather data from gymnasium equipment to support aspects of fitness progress awareness, such as shopping suggestions to support the user’s fitness regime [52].

**Responsive systems:** Responsive health monitoring systems aim to detect medical conditions at an early stage by monitoring and analyzing various biomedical signals, e.g., heart rate, blood glucose, blood sugar, EEG, and ECG, over a long time period. For example, the CodeBlue project [53] examined the feasibility of using interconnected sensors for transmitting vital health signs to health care providers. Nia et al. [11] proposed an extremely energy-efficient personal health monitoring system based on eight biomedical sensors: (1) heart rate, (2) blood pressure, (3) oxygen saturation, (4) body temperature, (5) blood glucose, (6) accelerometer, (7) ECG, and (8) EEG. MobiHealth [54] offered an end-to-end mobile health platform for continuous health care monitoring.

**2. *Medical automation systems:*** Unlike health monitoring systems, medical automation systems enhance the user’s quality of life after/during the emergence of health issues. They mitigate health issues or minimize disease symptoms by actively providing essential therapy. Based on their functionality, medical automation systems can be divided into two main categories: drug infusion and rehabilitating systems.

**Drug infusion systems:** Drug infusion systems enable safe injection of pharmaceutical compounds, e.g., nutrients and medications, into the body to achieve desired therapeutic effects. Automatic drug infusion systems control the drug release profile, absorption, and distribution to enhance the treatment efficacy and safety as well as patient convenience and compliance [55]. Insulin delivery systems are one of the most commonly-used types of drug infusion systems. They continuously monitor the patient’s blood glucose level using wearable glucose sensing patches and inject a prescribed amount of insulin into the blood stream when necessary.

**Rehabilitation systems:** Such systems have attracted a lot of attention in the past two decades. They are currently used by patients after a major operation, sensory loss, stroke, severe accident, or brain injury [56]. They are also used to help patients who suffer from serious neurological conditions, e.g., Parkinson’s disease or post-stroke condition [57]. Gait and/or motor abilities analysis is often used in rehabilitation in hospitals and health care centers [58].

An example of WMS-based rehabilitation system is Valedo [59], which is a medical back-training device developed by Hocoma AG to enhance patient compliance. It gathers trunk movements using two WMSs, transfers them to a game environment, and guides the patient through exercises targeted at low back pain therapy. Another example is Stroke Rehabilitation Exerciser [60] developed by Philips Research, which coaches the patient through a sequence of exercises for motor retraining. Salarian et al. [61] proposed a method for enhancing the gait of a patient with Parkinson’s



disease. Hester et al. [62] proposed a WMS-based system to facilitate post-stroke rehabilitation.

## HCI

In our daily conversations, the existence of common contexts, i.e., implicit information that characterizes the situation of a person or place that is relevant to the conversation, helps us convey ideas to each other and react appropriately. Unfortunately, the ability to share context-dependent ideas does not transfer well to humans interacting with machines. The design of WMS-based human-computer interfaces has notably improved the richness of communications in HCI [63]. In particular, various WMS-based gesture detection and emotion recognition systems have been proposed in the literature to enhance HCI.

**1. *Gesture detection systems:*** Several applications, such as sign-language recognition and remote control of electronic devices, need to respond to simple gestures made by humans. In the last decade, many WMS-based gesture recognition mechanisms have been developed to process sensory data collected by WMSs, e.g., magnetometer [64,65], accelerometer [25,27], and gyroscopes [66], to recognize user’s gesture and enable gesture-aware HCI.

Although gestures from any part of the body can be used for interacting with a computing device, previous experimental research efforts [67] have demonstrated that finger-based gesture detection mechanisms are more successful in practice since their information entropy is much larger than that of interactions based on other human body parts. As a result, several research studies [66,68–70] have focused on developing algorithms to detect hand gestures in real-time. A promising example of WMS-based gesture detection systems is Pingu [66], a smart wearable ring that is capable of recognizing simple and tiny gestures from user’s ring finger.

**2. *Emotion recognition systems:*** Wearable technology was first used to detect emotions/feelings by Picard et al. [71]. Since then, several researchers have used different sets of WMSs to detect different emotions/feelings, e.g., stress [72, 73], depression [74], and happiness [75]). However, we humans still cannot agree on how we define certain emotions, even though we are extremely good at expressing them. This fact has made emotion recognition a technically challenging field. However, it is becoming increasingly important in HCI studies as its advantages become more apparent.

## **Information Security and Forensics**

Next, we discuss two well-known types of WMS-based systems developed in the domain of information security and forensics for deception detection and authentication.

**1. *Deception detection systems:*** The examination of the truthfulness of statements made by victims, suspects, and witnesses is of paramount importance in legal settings. Real-time WMS-based deception detection systems attempt to facilitate security screening and criminal investigation, and also augment human judgment [76]. They process sensory data collected by various types of WMSs (commonly heart rate, blood pressure, and accelerometers) to detect suspicious changes in the individual’s mental state, e.g., a rapid increase in stress level, behavior, e.g., involuntary facial movements, and physiological signals, e.g., an increase in the heart rate. For example, PokerMetrics [77] is a lie detection system that processes heart rate, skin conductance, temperature, and body movements to find out when the user is bluffing during a poker tournament. FNIRS-based polygraph [78] is another fairly accurate lie detection system that processes data collected by a wearable near-infrared spectroscope.

**2. *Authentication systems:*** Authentication refers to the process of verifying a user’s identity based on certain credentials [79]. A rapidly-growing body of literature on the usage of biometrics, i.e., measurable behavior such as frequency of

keystrokes, and biometrics, i.e., strongly-reliable biological traits such as EEG signals, for authentication has emerged in the last two decades [80–82].

Design of WMS-based authentication is an emerging research domain that is attracting increasing attention. Several research efforts have investigated the feasibility of using the data collected by WMSs as behaviometrics or biometrics. In particular, various research studies [83,84] have demonstrated that the data collected by smart watches, e.g., acceleration, orientation, and magnetic field, can be used to distinguish users from each other. Furthermore, the use of EEG [85] and ECG [86] signals, as biomedical traits with high discriminatory power for authentication, has received widespread attention. Although EEG/ECG-based authentication systems have shown promising results, they have been unable to offer a convenient method for *continuous user authentication* for two reasons. First, the size/position requirements of the sensors that capture EEG/ECG signals significantly limit their applicability [86,87]. Second, processing of EEG/ECG signals for authentication is resource-hungry [88]. A recently-proposed WMS-based authentication system, called CABA [37], has attempted to effectively address these drawbacks by using an ensemble of biomedical signals that can be continuously and non-invasively collected by WMSs.

## Education

Next, we describe how technological advances in WMSs are transforming education by opening up new opportunities for employing smart tutoring and teaching assistant systems.

**1. *Smart tutoring:*** With the rapid development of online tutoring and exponential increase in the number of massive open online course websites, many research projects have been conducted on computer-based tutoring systems, which aim to select suitable instructional strategies based on the learner’s reactions, mental conditions, emotional states, and feedback (see [89] for a survey). Moreover, there is a

strong motivation in the military community for designing adaptive computer-based tutoring systems to provide effective training in environments where human tutors are unavailable [90,91]. WMS-based tutoring systems can recognize the user's emotional condition, level of understanding, physical state, and stress level by collecting and processing sensory data, e.g., user's heart rate and blood pressure. They can also predict learning outcomes, e.g., performance and skill acquisition, and continuously adapt their teaching/training approaches to optimize learning efficiency [89].

**2. *Teaching assistant:*** WMS-based teaching assistant systems can continuously collect and process various forms of biomedical signals from students, and analyze their voices, movements, and behaviors in order to reach a conclusion about the lecturer's quality of presentation and listeners' level of satisfaction. They can facilitate the teaching process by continuously assisting the lecturer in delivering and subsequently making the learning process shorter, more efficient, more pleasant, and even entertaining. For example, Grosshauser et al. [92] have designed a WMS-based teaching assistant system that monitors movements of dancers and provides feedback to their teacher. Park et al. [30] have designed SmartKG that relies on several wearable badges to provide valuable information about kindergarten students to their teacher.

### **1.2.3 Main components of WMS-based systems**

In this section, we describe the components that constitute a typical WMS-based system, and their limitations. As shown in Fig. 1.4, a typical WMS-based system consists of three main components: WMSs, the base station, and Cloud servers. Next, we describe each.

#### **WMSs**

With continuing performance and efficiency improvements in computing and real-time signal processing, the number and variety of WMSs have increased significantly,

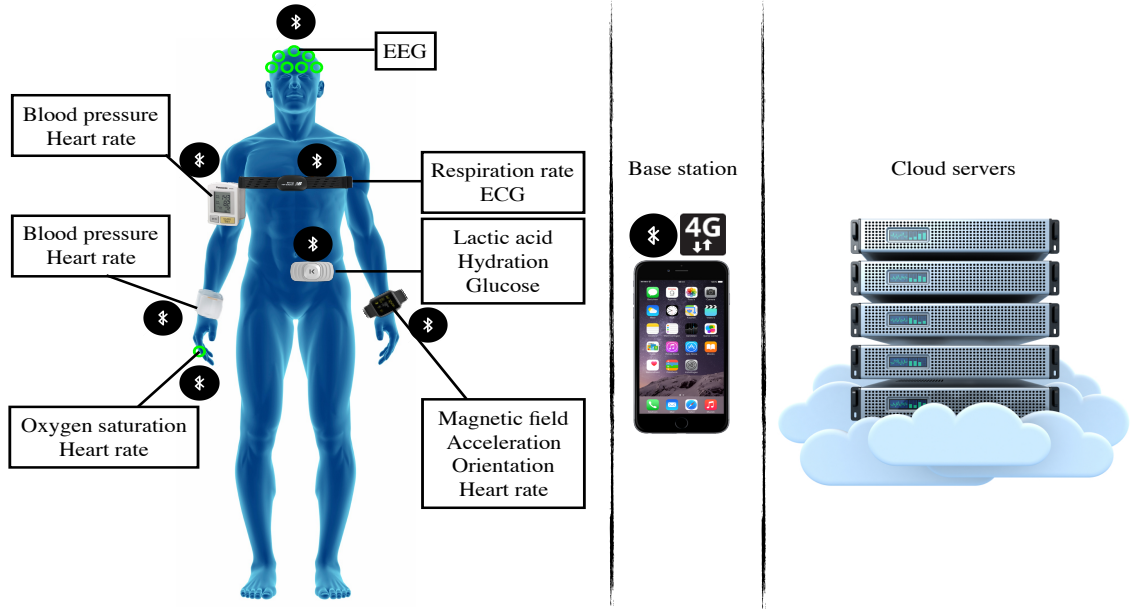


Figure 1.4: The three main components of WMS-based systems: WMSs, the base station, and Cloud servers [2].

ranging from simple pedometers to sophisticated heart-rate monitors. WMSs sense electrical, thermal, chemical, and other signals from the user’s body. The majority of these sensors, e.g., EEG and ECG, directly sense and collect biomedical signals. However, a few sensors, e.g., accelerometers, gather raw data that can be used to extract health-related information. Table 1.2 lists various commonly-used WMSs in an alphabetical order, along with a short description for each sensor.

Despite the variety of WMSs available, they share two common limitations that must be considered while designing a WMS-based system: small storage capacity and limited energy.

**1. Small storage:** Storing a large amount of data in a WMS is not feasible for two reasons. First, adding a large storage to a WMS dramatically increases its energy consumption, and as a result, significantly decreases its battery lifetime [11]. Second, the size constraints of WMSs impose specific storage constraints. The WMS size needs to be kept small to ensure user convenience.

Table 1.2: Common WMSs

Sensor	Description
Accelerometer	measures changes in the acceleration of the device caused by user's movements
Blood pressure sensor	measures systolic and diastolic blood pressures
ECG sensor	measures the electrical activity of the heart
EEG sensor	measures the electrical activity of the brain
EMG sensor	records electrical activity produced by muscles
Glucometer	measures approximate blood glucose concentration
GSR sensor	measures continuous variation in the electrical characteristics of the skin
Gyroscope	measures changes in device orientation caused by user's movements
Heart rate sensor	counts the number of heart contractions per minute
Magnetometer	specifies user's direction by examining the changes in the earth's magnetic field around the user
Microphone	records acoustic sounds generated by the body (used for respiration analysis or emotion detection)
Near-infrared spectroscope	provides neuroimaging technology to examine an aspect of brain function
Oximeter	measures the ratio of oxygen-saturated hemoglobin to the total hemoglobin count in the blood
Pedometer	counts each step a person takes by detecting the motion of the person's hands or hips
Respiration rate sensor	counts how many times the chest rises in a minute
Strain sensor	measures strain on different body parts (used to detect when the user is slouching)
Thermometer	measures an individual's body temperature

**2. Limited energy:** The small on-sensor battery with limited energy capacity is one of the most significant factors that limits the volume of data sampled and transmitted by WMSs. It is still feasible to wirelessly transmit all raw data without performing any on-sensor processing if devices are charged regularly, e.g., on an hourly basis. However, forcing the user to frequently recharge the WMSs would impose severe inconvenience. As described later in Section 2.2.1, on-sensor processing may significantly preserve battery lifetime by extracting salient information from the data and transmitting it.

The above-mentioned limitations of WMS-based systems have three direct consequences. First, the data generated by WMSs cannot be stored on them for a long period of time and should be transmitted to other devices/servers. Second, only extremely resource-efficient algorithms can be implemented on WMSs. Third, WMSs cannot usually support traditional cryptographic mechanisms, e.g., encryption, and are vulnerable to several security attacks, e.g., eavesdropping.

### **Base station**

Due to limited on-sensor resources (small storage and limited energy), the sensory data are frequently sent to an external device with more computation power. This device is referred to as the *base station*. It may range from smartphones to specialized computing devices, known as central hubs [11]. They commonly have large data storage, and powerful network connectivity through cellular, IEEE 802.11 wireless, and Bluetooth interfaces, and powerful processors [93]. Smartphones have become the dominant form of base stations since they are ubiquitous and powerful and provide all the technologies needed for numerous applications [94]. Moreover, smartphones support highly-secure encrypted transmission, which deters several potential attacks against the system [37].

The base station has its own resource constraints, though much less severe, in terms of storage and battery lifetime. Continuous processing along with wireless transmission to the Cloud may drain the base station's battery within a few hours, and as a result, cause user inconvenience. Base stations typically perform lightweight signal processing on the raw data and re-transmit a fraction or a compressed form of data to Cloud servers for further analysis and long-term storage.

## Cloud servers

Since both WMSs and base stations are resource-constrained, sensory data are commonly sent to Cloud servers for resource-hungry processing and long-term storage. Depending on the wireless technology used, the data can be sent either directly or indirectly (through a base station, such as a smartphone) to the Cloud. In addition to the huge storage capacity and high computational power that Cloud servers can provide for WMS-based applications, they facilitate access to shared resources in a pervasive manner, offering an ever-increasing number of online on-demand services. Furthermore, Cloud-based systems support remote update of software, without requiring that the patient install any software on the personal devices, thus making system maintenance quick and cost-effective. This makes Cloud-based systems a promising vehicle for bringing health care services to rural areas [95].

Despite the promise of Cloud servers in this context, utilizing them in WMS-based systems has two drawbacks. First, Cloud-based systems are highly dependent on the reliability of the Internet connection. Outage of Internet service may have serious consequences. For example, unavailability of a seizure prediction system (that tries to detect the occurrence of a seizure a few seconds before the patient's body starts shaking) may lead to a life-threatening situation. Second, the use of Cloud servers increases the response time (the time required to collect sensory data, process them, and provide a response or decision). As a result, there may be a significant deterioration of the quality of service in real-time applications.

### 1.2.4 Design goals

Although the scope of applications of WMS-based systems is quite wide, they share several common design goals. We reviewed many recent research studies on the design and development of different types of WMS-based systems and realized that, unfortunately, there is no standard inclusive list of desirable goals in the literature.



In this section, we suggest such a list. Fig. 1.5 summarizes seven general design goals that should be considered in designing WMS-based systems. Next, we present the rationale behind each goal.

**1. Accurate decisions:** WMS-based systems process the input data, e.g., an EEG

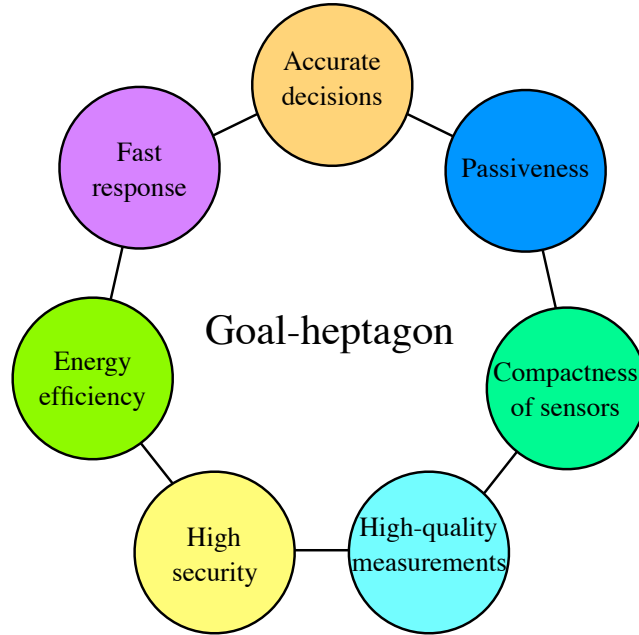


Figure 1.5: Goal-heptagon: Desiderata for WMS-based systems [2].

signal, and return decisions as output, e.g., whether a seizure is occurring or not. The quality of the service provided by a WMS-based system depends on the accuracy of decisions made by the system. For instance, a WMS-based authentication system must confidently determine if the user is authorized to use restricted resources, or a posture corrector must accurately decide whether the user’s posture is healthy.

**2. Fast response:** A short response time is a desirable design goal for the majority of systems. In order to ensure user convenience, it is obviously desirable for the system to quickly respond to user requests. Moreover, a short response time is essential for an authentication system, in which the system must quickly authenticate a legitimate user and reject an impostor [37]. Furthermore, a long response time may endanger user safety in some scenarios. For example, if an insulin pump fails to immediately

detect an emergency, e.g., hyperglycemia or hypoglycemia, and provide a response when it is necessary, the patient might suffer from life-threatening conditions [96].

**3. *Energy efficiency:*** The battery used in a WMS is typically the greatest contributor to both size and weight. As a result, WMSs typically have very limited on-sensor energy [97]. Rapid depletion of battery charge, necessitating frequent, e.g., on a hourly basis, battery replacement/recharge would deter wide adoption of the device [98]. Thus, all components embedded in WMSs and the signal processing algorithms implemented on them must be energy-efficient.

**4. *High security:*** The emergence of the IoT paradigm has magnified the negative impact of security attacks on sensor-based systems. Furthermore, the demonstration of several attacks in recent research efforts (see [1] for a survey) has led to serious security concerns and highlighted the importance of considering security requirements. To ensure system security, different security requirements must be proactively addressed. As mentioned earlier, security requirements are often broken down into three main categories: (i) confidentiality, (ii) integrity, and (iii) availability, referred to as the CIA-triad [20].

**5. *High-quality measurements:*** Undoubtedly, the quality of the decisions offered by a WMS-based system depends on the quality of sensory measurements provided by WMSs. It has been shown that user's activities may negatively impact the quality of data obtained by the WMSs, e.g., running significantly deteriorates the quality of the signal collected by EEG sensors [99]. Hence, WMSs should be designed to provide accurate and noise-robust measurements during different daily activities, especially intensely physical ones.

**6. *Compactness of sensors:*** To ensure user convenience, WMSs must be kept lightweight and as small as possible. Moreover, in many scenarios, the presence of specific WMSs, e.g., blood glucose monitor, may reveal the presence of an illness along with the current level of the illness, leading to serious privacy concerns [100].

Thus, WMSs should be designed to be compact so that the user can easily hide them.

**7. *Passiveness*:** Passiveness, i.e., minimal user involvement, is a key consideration in designing a WMS-based system. It is very desirable that WMSs be calibrated transparently to the user and sensory data be measured independently of user activities [101]. Obviously, if a wearable device, e.g., a smart watch, asks the user to calibrate internal sensors, e.g., accelerometers and magnetometers, manually, it may be quite annoying to the user [102].

### 1.3 Contributions of the thesis

To mitigate the security/privacy issues in the IoT domain while considering domain-specific limitations (e.g., limited energy and small storage capacity) of various components utilized in IoT-based systems, this thesis provides low-energy solutions that make data encryption practical for resource-constrained sensors (e.g., WMSs). Furthermore, in order to shed light on new domain-specific security/privacy issues associated with IoT-based systems, two novel security attacks are introduced in this thesis. Moreover, a novel IoT-enabled continuous authentication system is presented, which aims to address the security issues and weaknesses of previously-proposed authentication systems. Our main contributions can be summarized as follows:

1. The thesis first targets health monitoring systems, one of the most widely-known types of IoT-based systems that are envisioned as key to enabling a holistic approach to health care. It describes different solutions for reducing the total energy consumption of different implantable and wearable medical devices (IWMDs) utilized in continuous health monitoring systems. The proposed solutions can significantly increase the battery lifetimes of different IWMDs while offering spare energy for encrypting medical data before transmitting them.

2. The thesis introduces OpSecure, an optical secure communication channel between an implantable medical device (IMD) and an external device, e.g., a smartphone. OpSecure enables an intrinsically user-perceptible unidirectional data transmission, suitable for physically-secure communication with minimal size and energy overheads. Based on OpSecure, we design and implement two protocols: (i) a low-power wakeup protocol that is resilient against remote battery draining attacks, and (ii) a secure key exchange protocol to share the encryption key between the IMD and the external device. The proposed protocols complement lightweight symmetric encryption mechanisms, so that common security attacks against insecure communication channels can be prevented.
3. The thesis shows how security/privacy attacks against health monitoring systems extend far beyond wireless communication to/from IWMDs, and explains why encryption cannot always provide a comprehensive solution for eliminating security/privacy attacks on IWMDs. In particular, it describes the possibility of privacy attacks that target physiological information leakage, i.e., signals that continuously emanate from the human body due to the normal functioning of its organs. Furthermore, it discusses several novel attacks on privacy by leveraging information leaked from them during their normal operation.
4. The thesis then introduces a generic security attack that is applicable to a variety of cyber-physical systems (CPSs), i.e., systems with integrated physical and processing capabilities that can interact with humans and the environment. These attacks are called dedicated intelligent security attacks against sensor-triggered emergency responses (DISASTER). DISASTER targets safety mechanisms deployed in automation/monitoring CPSs and exploits design flaws and security weaknesses of such mechanisms to trigger emergency responses even in the absence of a real emergency. In addition to introducing DISASTER, it

describes the serious consequences of such attacks, and demonstrates the feasibility of launching DISASTER against the two most widely-used sensor-based systems: residential and industrial automation/monitoring systems. Moreover, it provides several countermeasures that can potentially prevent DISASTER and discusses their advantages and drawbacks.

5. Finally, the thesis presents continuous authentication based on biological aura (CABA), a novel user-transparent system for continuous authentication based on information that is already gathered by WMSs for diagnostic and therapeutic purposes. The presented continuous authentication system can offer a promising alternative to one-time knowledge-based authentication systems (e.g., password-/pattern-based authentication systems) and potentially be used to protect personal computing devices and servers, software applications, and restricted physical spaces.

## 1.4 Thesis outline

The rest of this thesis is organized as follows. Chapter 2 discusses related work. Chapter 3 quantifies the energy and storage requirements of continuous personal health monitoring systems and presents several schemes to reduce the overheads of wirelessly transmitting, storing, and encrypting/authenticating the data. Chapter 4 discusses OpSecure and two protocols that can be used in conjunction with symmetric encryption to protect the wireless channel between the IMD and an external device from different security attacks. Chapter 5 describes the concept of physiological information leakage and how such leakage can be exploited by attackers even if the communication channels are encrypted. Chapter 6 introduces DISASTER and describes its consequences. Moreover, it suggests several countermeasures to mitigate such attacks. Chapter 7 presents CABA, describes its various applications, and

discusses how it can be extended to user identification and adaptive access control authorization. Chapter 8 concludes the thesis and presents ideas for future research.

# Chapter 2

## Related Work

In this chapter, we discuss related work and provide background for several key concepts used in this thesis. In Section 2.1, we summarize different attacks and threats on the edge-side layer of IoT along with their countermeasures. In Section 2.2, we describe several research directions related to the domain of WMSs.

### **2.1 Vulnerabilities of IoT and their countermeasures**

In this section, we discuss different attacks and threats on the edge-side layer of IoT and describe possible countermeasures against them.

#### **2.1.1 Known vulnerabilities**

Next, we provide an in-depth analysis of possible attacks and vulnerabilities at each level of the edge-side layer (edge nodes, communication, and edge computing). Fig. 2.1 summarizes several attacks and their countermeasures that are discussed in this section. We describe the left side of this figure (attacks) first. The security requirements and their abbreviations that are used in Fig. 2.1 are given in Table 1.1.

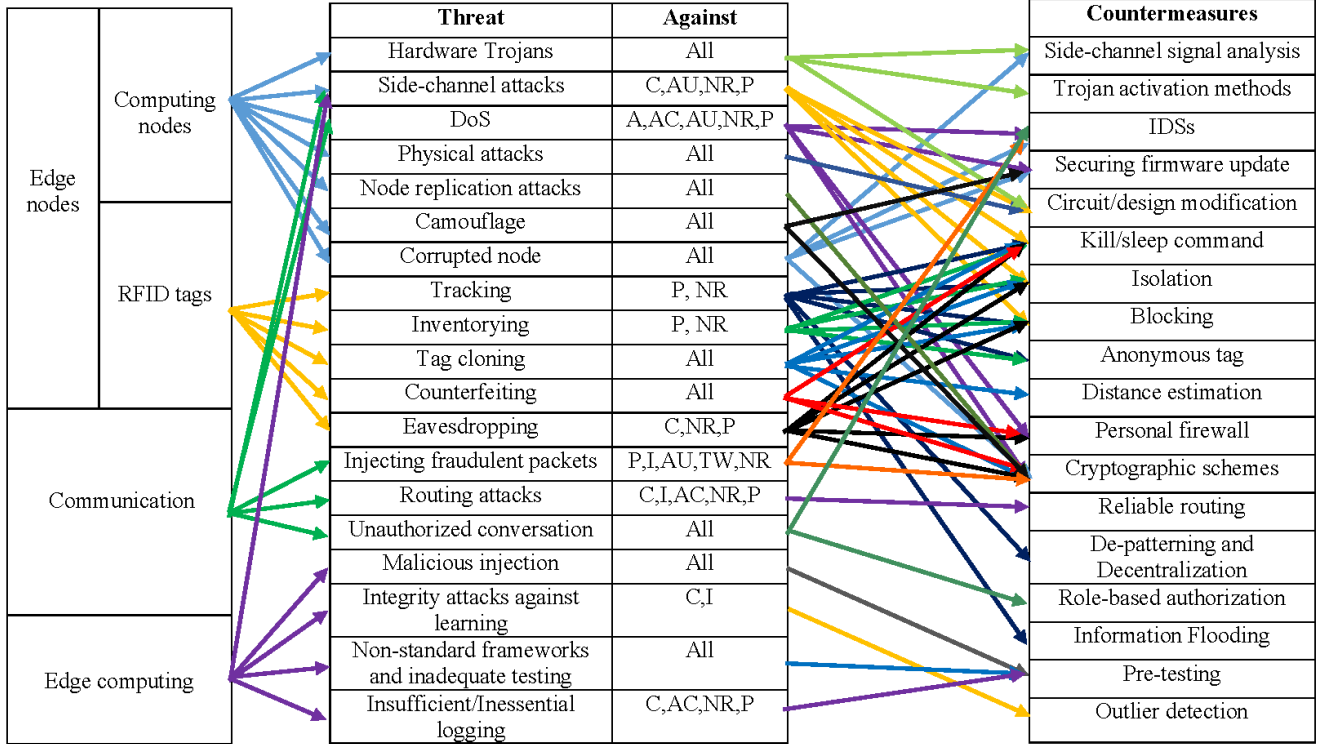


Figure 2.1: Summary of attacks and countermeasures [1]

## Edge nodes

Next, we discuss various attacks against the first level of the reference model that includes computing nodes and RFID tags.

**1. Computing nodes:** We begin with attacks against the edge computing nodes, e.g., RFID readers, sensor nodes, and compact controlling nodes.

**Hardware Trojan:** Hardware Trojans have emerged as a major security concern for integrated circuits [103–107]. Hardware Trojan is a malicious modification of an integrated circuit, which enables the attacker to use the circuit or to exploit its functionality to obtain access to data or software running on the integrated circuits (ICs) [108]. In order to insert a hardware Trojan in the original circuitry, the attacker maliciously alters the design before/during fabrication and specifies a triggering mechanism that activates the malicious behavior of the Trojan [103]. Trojans are



generally divided into two categories based on their triggering mechanisms [107,108]: (i) externally-activated Trojans, which can be triggered by an antenna or a sensor that can interact with the outside world, and (ii) internally-activated Trojans that are activated after a certain condition is met inside the integrated circuit, e.g., a Trojan that wakes up after a specific timespan when it receives a triggering signal from a countdown circuitry added by the attacker.

**Non-network side-channel attacks:** Each node may reveal critical information under normal operation, even when not using any wireless communication to transmit data. For example, the electromagnetic (EM) signature, i.e., the EM waves emitted by the node, can provide valuable information about the status of the device. The declassification of TEMPEST documents [109] in 2007, and the recent publications of some EM-based attacks [110–112] have started to develop the idea of non-network side-channel threats. For example, in a recent work, researchers were able to demonstrate how the acoustic/EM signals leaked from a medical device can provide valuable information about the patient or the device [112]. As mentioned in that work, detection of the existence of known signals or protocols may endanger the safety of the user, e.g., if the user has a device that is very expensive. Moreover, this type of attack may lead to a serious privacy issue in medical systems. For example, consider a subject who wears a medical device indicating a certain medical condition that carries a social stigma. Detecting the presence of this device can embarrass the patient. In addition, specific side-channel information from the devices may provide significant information about the individual’s health condition, e.g., glucose level, blood pressure, etc.

**Denial of Service (DoS) attacks:** There are three well-known types of DoS attacks against edge computing nodes: battery draining, sleep deprivation, and outage attacks.

1. *Battery draining:* Due to size constraints, nodes usually have to carry small

batteries with very limited energy capacity. This has made battery-draining attacks a very powerful attack that may indirectly lead to serious consequences, such as a node outage or a failure to report an emergency. For example, if an attacker can find a way to deplete the battery of a smoke detector, he will be able to disable the fire detection system [113]. Such attacks could destroy a network if recharging the nodes is difficult [114]. An example of a battery-draining attack is when an attacker sends tons of random packets to a node and forces the node to run its checking mechanisms, e.g., authentication mechanism. Several battery-draining attacks have been discussed in the literature [115–118].

*2. Sleep deprivation:* Sleep deprivation is a specific type of DoS attack in which the victim is a battery-powered node with a limited energy capacity. In this type of attack, the attacker attempts to send an undesired set of requests that seem to be legitimate. Therefore, detection of this type of attack is much harder than that of a simple battery-draining attack. The idea of sleep deprivation was first described by Stajano [119]. The research effort by Martin et al. is one of the first publications to closely examine the impact of sleep deprivation attacks on energy-constrained devices [115].

*3. Outage attacks:* Edge node outage occurs when an edge device stops performing its normal operation [120]. In some cases, a set of devices or an administrator device may stop functioning. Outage may be a result of an unintended error in the manufacturing process, battery draining, sleep deprivation, code injection or unauthorized physical access to the node. One of the most famous examples of outage attacks is injecting Stuxnet [121] into Iran’s nuclear process control program. Stuxnet manipulates the industrial process control sensor signals such that the infected system loses its ability to detect abnormal behavior. Therefore, the system does not shut down even in an emergency situation [121, 122].

**Physical attacks/tampering:** Edge devices operate in hostile environments in

which physical access to the devices may be possible, thus making them highly vulnerable to hardware/software attacks. The attacker, with a physical access to the device, may extract valuable cryptographic information, tamper with the circuit, modify programming, or change the operating system [123–127]. Physical attacks against the edge nodes may cause permanent destruction. Therefore, their main purpose is to extract information for future use, e.g., find the fixed shared key. Such a well-known recent attack was on the Nest thermostat [127], in which the attacker replaces the default firmware with a malicious one. This attack enables the attacker to control the thermostat, even when he no longer has physical access to the device.

**Node replication attacks:** In such an attack, the attacker adds a new node, e.g., a malicious one, to an existing set of nodes by replicating one node’s identification number. This attack can lead to a significant reduction in network performance. Moreover, the attacker can easily corrupt or misdirect packets that arrive at the replica [128]. This attack usually causes severe damage to the system by enabling the attacker to obtain required access to extract cryptographic shared keys [129]. Moreover, node replicas may revoke authorized nodes by executing node-revocation protocols [128, 130].

**Camouflage:** In this type of attack, the attacker inserts a counterfeit edge node or attacks an authorized node in order to hide at the edge level. Afterwards, the modified/counterfeit node can operate as a normal node to obtain, process, send, or redirect packets [129, 131]. Moreover, such a node can function in a passive mode in which it only conducts traffic analysis.

**Corrupted/malicious node:** The main goal of corrupting nodes is to gain unauthorized access to the network they belong to. Malicious nodes injected into a network can obtain access to other nodes, possibly controlling the network on behalf of the attacker [129]. A malicious node can also be used by the attacker to inject false data into the system or prevent delivery of true messages [131].

**2. RFID tags:** Next, we discuss the attacks against RFID tags.

**Tracking:** Covert reading of RFID tags is a significant threat. Unfortunately, almost all such tags provide a unique identifier. As a result, a nearby unauthorized reader can easily and effectively read a tag that is attached to a product or an individual. Such a reading provides very strong tracking information [132]. In the simplest form of the attack, an attacker uses a large number of RFID readers to read these fixed identifiers. The threat grows and becomes more important when a tag identifier is combined with personal information, e.g., credit/loyalty card number and personal profile [133].

**Inventorying:** There are certain types of tags that carry valuable information about the products they are attached to. In particular, electronic product code (EPC) tags have two custom fields: a manufacturer code and a product code. As a result, an individual who has an EPC tag is subject to inventorying [134], i.e., a tag reader can examine what products the individual has. This threat leads to serious privacy concerns. For example, the attacker might recognize what types of medical device, e.g., an insulin pump, a patient is wearing and, therefore, what illnesses, e.g., diabetes, he suffers from.

**Physical attacks/tampering:** This type of attack can be launched when the attacker has full physical access to a tag. In this attack, the tags can be physically manipulated and modified in a laboratory setup [135]. There are several known physical attacks against RFIDs. Among them are probe attacks, material removal, circuit manipulation, and clock glitching [136]. These attacks are used for extracting information from the tag, or modifying the tag for counterfeiting.

**Tag cloning:** Tag cloning (also referred to as spoofing) and impersonation of RFID tags could be very profitable to hackers, and extremely dangerous for the company's reputation. Potential damage can be amplified through a high level of automation

[137]. An attacker may use tag cloning to access restricted areas, bank accounts, or sensitive information.

**Counterfeiting:** In counterfeiting, the attacker modifies the identity of an item, typically by means of tag manipulation. Generally, the attacker needs less information to launch counterfeiting attacks relative to spoofing attacks. In these attacks, a tag is partially manipulated. Westhues describes how an RF tape-recorder can be constructed to read commercial proximity cards and partially simulate their signals to bypass building security systems [138].

**DoS attacks:** In DoS attacks, the RF channels are jammed such that the tags cannot be read by the tag readers and, as a result, the intended services based on the RFID tags become unavailable. For example, an attacker can lock down a whole building by jamming all the RFID-based doors. Additional vulnerabilities of RFID authentication protocols to DoS attack have been discussed in [139].

**Eavesdropping:** In this attack, the main goal of the attacker is to intercept, read, and save messages for future analysis. The intercepted data can be used as an input to other attacks, such as tag cloning. The concept of eavesdropping attacks against RFIDs is not new and is frequently mentioned in the literature. Recent reports by the National Institute of Standards and Technology [140] and the Department of Homeland Security [141], in addition to several published surveys, e.g. [134, 135, 142], all mention risks of eavesdropping in the RFID environment. In particular, several practical attack scenarios and their experimental setups have been discussed in [142].

**Side-channel attacks:** Such attacks use state-of-the-art tools to intercept and process communications in order to extract information from various patterns, even when the messages are encrypted. For example, if an attacker reads the tags at the entrance of a building, he can guess the number of individuals in the building at any moment by counting the number of communications. Over-the-air timing attacks against RFID tags and their efficacy are open research problems [134]. Carluccio

et al. have described the use of EM emanations to launch a power-analysis attack against RFIDs [143].

## **Communication**

Next, attacks against the communication level of the IoT reference model are discussed.

**Eavesdropping:** At the communication level, eavesdropping (also called sniffing) refers to intentionally listening to private conversations over the communication links [144]. It can provide invaluable information to the attacker when the data are unencrypted. In this situation, usernames and/or passwords are often easy to extract. When packets also carry access control information, such as node configuration, shared network password, and node identifiers, eavesdropping can provide critical information. The attacker can use and process this captured information to design other tailored attacks. For example, if an attacker can successfully extract the information that is required to add a new node to the set of authorized nodes, he will easily be able to add a malicious node to the system.

**Side-channel attacks:** Although side-channel attacks are not easy-to-implement, they are powerful attacks against encryption. They pose a serious threat to the security and reliability of cryptographic implementations. As mentioned earlier, side-channel attacks can also be launched at the edge node level. In contrast to the attack at the edge node level, the side-channel attacks at the communication level are usually non-invasive. They only extract information that is often unintentionally leaked. Typical examples of unintentional information leakage are time between two consecutive packets, frequency band of communications, and communication modulation. An important characteristic of non-invasive attacks is that they are undetectable, and as a result, there is no easy defense against them except to minimize leakage or else add noise to the leaked information.

**DoS attacks:** The most common and well-known DoS attack at the communication level is a standard attack that jams the transmission of radio signals. Two types of active jamming attacks have been defined in the literature [145,146]: (i) continuous jamming that involves complete jamming of all transmissions, and (ii) intermittent (also called non-continuous) jamming in which jamming is periodic and, as a result, the nodes can send/receive packets periodically. While the goal of constant jamming is to block all transmissions, with intermittent jamming, the attacker intends to lower the performance of time-sensitive systems. Consider a fire detection system that can detect unusual changes in the level of gases in the environment and calls the fire department in case of an emergency. An attacker can easily make the system unreliable by intermittently jamming node-to-node and node-to-base transmissions. In this scenario, the system will become out-of-service if the attacker uses constant jamming. Several research efforts have examined the possibility and effectiveness of launching DoS attacks against various transmission protocols, including Bluetooth [147], ZigBee [148], and 6LowPan [149]. In addition to active jamming attacks, the attacker can launch DoS against communication using malicious nodes or routers. The attacker may insert a node/router that intentionally violates the communication protocol in order to generate collisions or jam the communications [129]. A malicious router/node may also refuse to route messages or attempt to misdirect them. This could be done intermittently or constantly. Constant DoS attacks are usually easy to detect, whereas detection of intermittent ones requires accurate and efficient monitors.

**Injecting fraudulent packets:** An attacker can inject fraudulent packets into communication links using three different attack methods: (i) insertion, (ii) manipulation, and (iii) replication (also called replay) [129]. In insertion scenarios, the attacker inserts new packets in network communication. In other words, an insertion attack has the ability to generate and send malicious packets that seem legitimate. Manipulation attacks involve capturing the packet, and then modifying, e.g., updating header

information, checksum, and data, and sending the manipulated packet. In replication attacks, the attacker captures the packets that have been previously exchanged between two things in order to replay the same packets. Generally, a stateless system, which does not keep track of previous packets or previous state of the system, is quite vulnerable to replay attacks.

**Routing attacks:** Attacks that affect how messages are routed are called routing attacks. An attacker may use such attacks to spoof, redirect, misdirect, or drop the packets at the communication level. The simplest type of routing attack is an altering attack in which the attacker changes the routing information, e.g., by generating routing loops or false error messages. In addition to altering attacks, several other serious attacks have been proposed, e.g., Black Hole [150,151], Gray Hole [151], Worm Hole [152], Hello Flood [153,154], and Sybil [155]. We briefly describe them next.

1. *Black Hole:* A Black Hole attack is launched by using a malicious node, which attracts all the traffic in the network by advertising that it has the shortest path to the destination in the network. As a result, all packets are sent to the malicious node, and the attacker can process the packets or simply drop them.

2. *Gray Hole:* A Gray Hole attack is a variation of Black Hole attack in which the nodes selectively drop some packets.

3. *Worm Hole:* A Worm Hole attack is a severe attack that can be launched even when authenticity and confidentiality are guaranteed in all communications. In this attack, an attacker first records packets at one location in the network and then tunnels them to a different location.

4. *Hello Flood:* A Hello Flood attack is based on the fact that a node must broadcast “HELLO PACKETS” to show its presence to neighbors. The receiving nodes may assume that they are within the communication range of the sender. In this attack, an attacker uses a malicious node with high transmission power to send “HELLO PACKETS” to every other node in the network and claim to be their neighbor.



5. *Sybil*: In a Sybil attack, the attacker adds/uses Sybil nodes, which are nodes with fake identities. Sybil nodes can out-vote honest nodes in the system.

**Unauthorized conversation:** Every edge node needs to communicate with other nodes in order to share data or access their data. However, each node should only talk to a subset of nodes that need its data. This is an essential requirement for every IoT system, in particular, ones consisting of both insecure and secure nodes. For example, in a smart home scenario, the thermostat requires the smoke detector's data in order to shut down the heating system in an emergency situation. However, if the insecure smoke detector can share (get) information with (from) every other node, an attacker might be able to control the whole home automation system by hacking the smoker detector.

### **Edge computing level**

Edge (fog) computing is an emerging technology. Thus, its vulnerabilities have not yet been adequately explored. The few research efforts that address attacks on edge computing mainly focus on possible threats to sensor networks [156–158]. Next, we discuss and suggest some attack scenarios against an edge computing based scheme. Although some of these attacks were designed to target conventional systems and networks, they are also applicable to the edge computing based systems.

**Malicious injection:** Insufficient validation of the input may enable malicious input injection. An attacker could inject a malicious input that causes the service providers to perform operations on behalf of the attacker. For example, an attacker may add an unauthorized component to one of the levels below (communication or edge node levels) that is capable of injecting malicious inputs into the servers. Afterwards, the attacker might be able to steal data, compromise database integrity, or bypass authentication. Standard database error messages returned by a database may also assist the attacker. In situations where the attacker has no knowledge of the database's

tables, forcing an exception may reveal more details about each table and the names of its fields [159].

**Integrity attacks against machine learning:** Two types of attacks can be launched against machine learning methods that are used in IoT systems: causative and exploratory [160]. In causative attacks, the attacker changes the training process by manipulating the training dataset, whereas in exploratory attacks, he exploits vulnerabilities without altering the training process. Recent research has introduced a new type of causative attack, called the poisoning attack [161–163]. In a poisoning attack, the attacker adds precisely-selected invalid data points to the training dataset. In an edge computing based system, an attacker might be able to launch this attack against the learning algorithm by directly accessing the server or computing nodes, or he might be able to add malicious data to the dataset by adding a sufficient number of malicious nodes to lower levels of the IoT model. The main motivation is to cause the classification algorithm to deviate from learning a valid model by manipulating the dataset.

**Side-channel attacks:** Earlier, we mentioned several types of side-channel attacks against the components at the edge node and communication levels. In addition, an attacker might use the information leaked from additional components, e.g., service providers and servers, to launch side-channel attacks. For example, a service, which generates verbose fault warnings, provides a useful tool for designers and developers. However, the same warnings can provide extravagant information in operational environments.

**Non-standard frameworks and inadequate testing:** Non-standard coding flaws can give rise to serious privacy and security concerns. Moreover, since the nodes typically need to connect to intermediate servers, the consequences of a compromise might be amplified. The development of an edge computing based system is a sophisticated process because it requires combining heterogeneous resources and devices

that are often made by different manufacturers [164]. In addition, there is neither a generally-accepted framework for the implementation of edge computing based systems nor a standard set of policies. As a result, several privacy and security flaws of these systems may remain undetected.

**Insufficient/inessential logging:** Logging is a nice approach for detecting an intrusion or a hacking attempt. Developers should log events such as successful/unsuccessful authentication attempts, successful/unsuccessful authorization attempts, and application errors. The edge computing based systems may be damaged as a result of insufficient logging [165]. It is also recommended that the log files be encrypted.

### 2.1.2 Existing countermeasures

Here, the right side of Fig. 2.1 that consists of several countermeasures is discussed. Next, we describe each defense in a level-by-level fashion.

#### Solutions for security issues in edge nodes

First, we describe countermeasures for addressing attacks against the edge nodes.

**1. Computing nodes:** We start with solutions for attacks against computing nodes.

**Side-channel analysis:** Side-channel signal analysis provides an effective approach for the detection of both hardware Trojans and malicious firmware/software installed on a device.

*1. Trojan detection:* Side-channel signals, including timing [108, 166, 167], power [168–170], and spatial temperature [168, 171] can be used for Trojan detection. The presence of a Trojan in a circuit commonly affects power and/or delay characteristics of wires and gates in the circuit, and alters heat distribution on the silicon IC. In order to detect a hardware Trojan, side-channel signal-based Trojan detection mechanisms compare physical characteristics and/or the heat distribution map of a suspicious

IC to the ones of a Trojan-free reference IC. Power-based analyses offer an activity monitoring method that can be utilized to detect suspicious activities within the IC, enabling detection of Trojans. Timing-based methods enable the detection of Trojans by testing the IC using efficient delay tests, which are sensitive to small changes in the circuit delay along the affected paths and can differentiate Trojans from process variations. Spatial temperature-based mechanisms rely on infrared imaging techniques, which provide thermal maps of ICs. Silicon is transparent in the infrared spectral region and this transparency enables us to obtain maps of thermal infrared emissions using infrared imaging techniques [171].

*2. Malicious firmware/software detection:* The effectiveness of side-channel signal analysis in detecting malicious firmware/software installed on a device has been shown by several previous research efforts [172–176]. As mentioned earlier in Section IV, side-channel signals can reveal valuable information about the device’s operation. Similar to the Trojan detection mechanism, malware detection methods can process side-channel signals to detect abnormal behaviors of the device, e.g., a significant increase in its power consumption, which are the results of a malware installed on the device.

**Trojan activation:** Trojan activation strategies aim to partially/fully activate the Trojan circuitry to facilitate Trojan detection. Several Trojan activation approaches have been proposed in the last decade [108, 177, 178]. The common goal of such strategies is to magnify and detect the disparity between the behavior, outputs, or side-channel leakages of a Trojan-free circuit and the ones of a Trojan-inserted circuit. For example, Chakraborty et al. proposed MERO [179], an efficient methodology to derive a compact set of test patterns (minimizing test time and cost), while maximizing the Trojan detection coverage. MERO can increase the detection sensitivity of many side-channel Trojan detection. The basic concept is to detect low probability conditions at the internal nodes, select candidate Trojans triggerable by a subset of

these rare conditions, and then derive an optimal set of vectors that can trigger each of the selected low probability nodes.

**Policy-based mechanisms and intrusion detection systems (IDSs):** Policy-based approaches are promising mechanisms for solving security and privacy problems at this IoT level. Violation of essential policies can be detected continuously by introducing an IDS [129]. An IDS ensures that general rules are not broken. It provides a reliable approach to defend against battery-draining and sleep deprivation attacks by detecting unusual requests to the node. Several recent and ongoing research efforts provide efficient IDS designs for monitoring the edge nodes and detecting potential threats [180–184].

**Circuit modification:** Changing the circuit is one of the most effective defenses against physical, side-channel, and Trojan attacks. In the following, for each of these attacks, we briefly discuss how specific circuit changes and modifications may address/prevent the attack.

1. *Tamper proofing and self-destruction:* Nodes may be integrated with physical hardware that enhances protection against physical attacks. For example, to protect against tampering of sensors, several mechanical/electrical tamper-proofing methods for designing the physical packages of the nodes have been proposed and have traditionally been used in home automation sensors, e.g., smoke detectors. Moreover, using self-destruction mechanisms provides an alternative approach to defend against physical attacks [185].

2. *Minimizing information leakage:* There are also some well-known approaches for addressing side-channel attacks including, but not limited to, adding randomized delay [143] or intentionally-generated noise [186], balancing Hamming weights [187], using constant execution path code [187], improving the cache architecture [188], and shielding [112].

3. *Integrating physically unclonable function (PUF) into the circuitry:* A PUF is

a noisy function embedded into an integrated circuit [189]. When queried with a challenge  $x$ , a PUF generates a response  $y$  that depends on both  $x$  and the unique intrinsic physical properties of the device [190,191]. PUFs are assumed to be physically unclonable, unpredictable, and tamper-evident. PUFs enable unique device identification and authentication [190,192], and offer Trojan detection mechanisms [108]. Any unintended modification of the circuit physical layout changes the circuit parasitic parameters that can be detected by Trojan detection methods.

**Securing firmware update:** Each firmware update can be launched remotely or directly. In the case of remote firmware update, the base or server broadcasts a command (CMD) to announce that there is a new version of firmware available. Then, a node with the new firmware broadcasts an advertisement (ADV) to neighboring nodes. The nodes that are willing to update their firmware and have also received ADV compare the new version with their existing version, and send requests (REQ) if they need an update. Eventually, the advertiser starts sending data to the requesters. Providing a secure method for remotely updating the firmware requires authentication of CMD, ADV, REQ, and data packets. Moreover, risks posed by DoS attacks during each step of the protocol should be considered [193]. In addition to remote firmware updates, some nodes support direct updates of the firmware, e.g., using a USB cable. In this case, the integrity of the firmware should be checked, and the user, who tries to update the firmware, should be authenticated, because a lack of sufficient integrity check mechanisms may enable an attacker to replace legitimate device firmware with a malicious one [127].

**2. RFID tags:** Next, we describe solutions and suggestions for addressing attacks against RFID tags.

**Kill/sleep command:** A kill scenario is built into the manufacturing process of RFID tags. An RFID tag has a unique PIN, e.g., a 32-bit password. Upon receiving the correct PIN from the RFID reader, the tag can be killed, i.e., the tag will not be

able to transmit any further information after receiving this command [135]. There is an alternative approach called a sleep command that puts the tags to sleep, i.e., makes them inactive for a period of time [134]. Although these ideas seem simple at first glance, designing and implementing secure and effective PIN management schemes need sophisticated techniques.

**Isolation:** A very effective way of protecting the privacy of tags is to isolate them from all EM waves. One way is to build and use isolation rooms. However, building such rooms is usually very expensive. An alternative approach is to use an isolation container that is usually made of a metal mesh [134]. This container, which can block EM waves of certain frequencies, is called a Faraday cage [194]. Another approach is to jam all nearby radio channels using an active RF jammer which continuously interrupts specific RF channels.

**Blocking:** Juels et al. proposed a protection scheme called blocking [132]. It adds a modifiable bit to the tag that is called a privacy bit. A ‘0’ privacy bit indicates that public scanning is allowed for the tag, whereas a ‘1’ bit marks the tag as private. This scheme requires a certain type of tag (called blocker tag), which is a special RFID tag that prevents unintended scanning. However, the idea of using blocker tags has two main limitations: (i) it requires the use of a modified version of RFID tags, and (ii) unreliable transmission of the tags may easily lead to privacy failure even when the blocking scheme is implemented. Another blocking approach, called soft blocking, has been proposed in [195]. It relies on auditing of reader configurations to enforce a set of policies that is defined in software. This set guarantees that readers can only read public tags. Then, a monitoring device can passively examine if a reader is violating tag policies.

**Anonymous tag:** A novel idea based on look-up table mapping has been proposed by Kinoshita [196]. The key contribution of his work is a scheme to store a mapping between an anonymous ID and a real ID of each tag in such a way that an attacker

cannot find the mapping algorithm to recover the real ID from the anonymous one. The mapping may represent a key encryption algorithm or a random value mapped to the real ID. Note that although the anonymous ID emitted by an RFID tag has no intrinsic valuable information, it can still enable tracking as long as the ID is fixed over time [135]. In order to address the tracking problem, the anonymous ID should be re-issued frequently.

**Distance estimation:** Use of signal-to-noise ratio as a metric to determine the distance between a reader and a tag is proposed in [134]. For the first time, Fishkin et al. claim that it is possible to derive a metric to estimate the distance of a reader that tries to read the tag information. This enables the tag to only provide distance-based information. For example, the tag might release general information, e.g., the product type, when scanned at 10 meters distance, but release its unique identifier at less than 1 meter distance.

**Personal firewall:** A personal RFID firewall [197] examines all readers' requests to tags. The firewall can be assumed to be implemented in a device that supports high computation needs and provides enough storage capacity, e.g., a cellphone. The firewall enables the setting of sophisticated policies. For example, "my tag should not release my personal information when I am not within 50 meters of my work place".

**Cryptographic schemes:** Three types of cryptographic schemes are widely discussed in the previous literature to address the security attacks against RFID tags:

1. *Encryption:* Full encryption usually requires significant hardware. Therefore, its implementation in RFID tags has not been feasible due to the need for the tags to be low-cost (a few cents). Feldhofer [198] proposed an authentication mechanism based on the Advanced Encryption Standard (AES). However, for a standard implementation of AES, 20-30K gates are typically needed [199], whereas RFID tags can only store hundreds of bits and support 5-10K logic gates. The limitations arising from gate count and cost suggest that the tag can only devote 250-3500 gates to the



security mechanism. The traditional implementation of AES was not appropriate until Jung et al. proposed a novel implementation of AES that requires only 3595 logical gates [200]. However, no fully-developed version of AES has been implemented in any RFID tag.

*2. Hash-based schemes:* Such schemes are widely used for addressing security issues in the RFID technology. Recent research on hash functions can be found in [201–205]. A simple security mechanism based on hash functions is proposed in [133]. In this work, two states are defined for each tag: (i) locked state in which a tag responds to all queries with its hashed key, and (ii) unlocked state in which the tag carries out its normal operation. To unlock a tag, the reader sends a request, including the hashed key, to a back-end database and waits to get the key. After getting the key, the reader sends the key to the locked tag. Then, the tag changes its state to unlocked. Although this significantly improves RFID security, the problem of tracking still remains. To address this issue, Weis et al. [133] propose a more sophisticated scheme, in which the hashed key is changed in a manner that is unpredictable.

*3. Lightweight cryptographic protocols:* In order to address the security and privacy issues of RFID tags by taking into account their cost requirements, several lightweight cryptographic protocols have been suggested. For example, Peris et al. propose a minimalist lightweight mutual authentication protocol for low-cost RFID tags [199]. They claim that their method provides an adequate security level for certain applications, and can be implemented with only slightly more than 300 gates, which is quite acceptable even for the most limited RFID tags. Moreover, a simple scheme for mutual authentication between tags and readers is proposed by Molnar et al. [206]. Their protocol uses a shared secret and a pseudorandom function to protect the messages exchanged between the tag and the reader. Another example is extremely-lightweight challenge-response authentication protocols described in [207]. These protocols can be used in authenticating tags, but can be broken by a powerful

adversary [135].

**Circuit modification:** In addition to the previously-mentioned applications of PUF (device identification/authentication and hardware Trojan detection), several research efforts have proposed different anti-counterfeiting mechanisms to prevent RFID tag cloning by integrating PUFs into RFID tags [208–211]. For example, consider an authentication mechanism that aims to identify the user based on his RFID tag. It can generate a set of challenge-response pairs for each tag during the enrollment phase and store it in a database. At a later point in time, during verification, it can compare the response provided by the user’s PUF-based RFID tag for a chosen challenge from the database with the corresponding response in the database [210, 211].

### **Solutions for security issues in communication**

Next, we discuss solutions for addressing the security issues that exist at the communication level of the reference model.

**Reliable routing:** An essential characteristic of IoT networks that complicates implementation of secure routing protocols is that intermediate nodes or servers might require direct access to message content before forwarding it. As mentioned earlier, several valid attacks against routing have been proposed in the literature. Karlof et al. have addressed most major attack scenarios [212]. They provide the first detailed security analysis of major routing protocols and practical attacks against them, along with countermeasures. Various other research efforts have also tried to address security and privacy concerns in routing [213–216].

**IDS:** IDS is essentially needed at the communication level as a second line of defense to monitor network operations and communication links, and raise an alert in case of any anomaly, e.g., when a pre-defined policy is ignored. Traditional IDS approaches [183, 217, 218] are usually customized for WSNs or for the traditional Internet. However, few recent IDS proposals address the security and privacy concerns

of IoT directly. SVELTE [219] is one of the first IDSs designed to meet the requirements of the IPv6-connected nodes of IoT. It is capable of detecting routing attacks, such as spoofed or altered information, and Black Hole attack. Another intrusion detection method for the IoT has been proposed in [220].

**Cryptographic schemes:** Using cryptographic schemes, e.g., strong encryption, to secure communication protocols is one of the most effective defenses against a variety of attacks, including eavesdropping and simple routing attacks, at the communication level. Several encryption methods have been proposed to address security issues in communication [221, 222]. The encryption-decryption techniques, developed for traditional wired networks, are not directly applicable to most IoT components, in particular, to small battery-powered edge nodes. Edge nodes are usually tiny sensors that have limited battery capacity, processing power, and memory. Using encryption increases memory usage, energy consumption, delay, and packet loss [223]. Variants of AES have yielded promising results for providing secure communication in IoT. Moreover, different lightweight encryption methods have been proposed, e.g., CLEFIA [224] and PRESENT [225]. Unfortunately, at this time, there are no promising public key encryption methods that provide enough security while meeting lightweight requirements [223].

**De-patterning and decentralization:** De-patterning and decentralization are two of the major methods proposed to provide anonymity and defense against side-channel attacks. There is always a trade-off between anonymity and the need to share information. De-patterning data transmissions can protect the system against side-channel attacks, e.g., traffic analysis, by inserting fake packets that can significantly alter the traffic pattern, when required. An alternative method for ensuring anonymity is distribution of sensitive data through a spanning tree such that no node has a complete view of the original data. This method is called decentralization [226].

**Role-based authorization:** In order to prevent a response to requests by intruders or malicious nodes in the system, a role-based authorization system verifies if a component, e.g., edge node, service provider, or router, can access, share, or modify the information. Moreover, for every communication, the authorization system should check whether the two parties involved in the action have been validated and have required authority [227].

**Information flooding:** Ozturk et al. propose flooding based anti-traffic analysis mechanisms to prevent an external attacker from tracking the location of a data source, since that information may release the location of things [228]. They have proposed three different approaches to flooding: (i) baseline, (ii) probabilistic, and (iii) phantom. In baseline flooding, every node in the network forwards a packet once and only once. In probabilistic flooding, only a subset of nodes within the entire network contributes to data forwarding and the others discard the messages they receive. In phantom flooding, when the source sends a message, the message unicasts in a random fashion (referred to as a random walk phase). Then, the message is flooded using the baseline flooding technique (referred to as the flooding phase).

### **Solutions for security issues at the edge computing level**

Next, we describe countermeasures and solutions for addressing the security attacks and issues at the edge computing level.

**Pre-testing:** Testing of updates and design implementations is important before they can be used in a critical system [229]. The behavior of the whole system and its components, e.g., routers, edge nodes, servers, etc., should be closely examined by feeding different inputs to the system and monitoring the outputs. In particular, pre-testing attempts to identify the set of possible attack scenarios and simulate these scenarios to see how the system responds [230]. It also specifies what information should be logged and what information is too sensitive to be stored. In addition, the

input files should be closely examined to prevent the danger of malicious injection. For example, the attacker should not be able to execute any command by injecting it into the input files.

**Outlier detection:** The common goal of almost all defenses against integrity attacks on machine learning methods is to reduce the influence of adding invalid data points to the result. These invalid data points are deemed outliers in the training set. Rubinstein et al. have designed a defense framework against poisoning attacks based on robust statistics to alleviate the effect of poisoning [231]. In addition, a bagging defense against such integrity attacks has been proposed by Biggio et al. [232]. They examine the effectiveness of using bagging, i.e., a machine learning method that generates multiple versions of a predictor and utilizes them to get an aggregated predictor by getting averages over the versions or using a plurality vote [233], in reducing the influence of outlying observations on training data. Mozaffari-Kermani et al. have presented several countermeasures against poisoning attacks in the area of healthcare [234]. They have evaluated the effectiveness of their schemes and identified the machine learning algorithms that are easiest to defend.

**IDS:** IDSs can detect the existence of a malicious node that tries to inject invalid information into the system or violate the policies. Several recent research efforts have proposed IDS based methods to address the injection issue [235–238]. For example, Son et al. describe the design and implementation of DIGLOSSIA [235], a new tool that precisely and efficiently detects code injection attacks on servers.

## 2.2 Emerging research directions in the domain of WMS-based systems

As described in Chapter 1, with the pervasive use of Internet-connected WMSs, the scope of applications of WMS-based systems has extended far beyond what has been

traditionally imagined. In this section, we describe several research directions that are closely related to the domain of WMSs and discuss how previous research studies have attempted to facilitate the design and development of WMS-based systems. In particular, we briefly discuss the related research work present at the intersection of WMS and the following research areas: (i) design of low-power sensors, (ii) minimally-invasive capture methods, (iii) security and privacy, (iv) calibration and noise cancellation, and (v) big data.

### **2.2.1 Design of low-power sensors**

The on-sensor energy has three major consumers: (i) sampling, (ii) transmission, and (iii) on-sensor computation [11]. Thus, for each WMS, the energy consumption of one or a combination of these consumers should be reduced to enhance its battery lifetime. Next, we summarize what solutions previous studies have proposed to reduce the energy consumption of each of these energy consumers.

#### **Sampling**

The sampling energy is mainly the energy consumed by the analog-to-digital converter (ADC). The total energy consumption of an ADC can be divided into: (i) I/O energy, (ii) reference energy, (iii) sample-and-hold energy, (iv) ADC core energy, and (v) input energy [239]. However, separate calculations of these values is difficult. Hence, the total on-chip ADC energy consumption per sample (EADC) is commonly reported in the literature. In order to enhance ADC energy efficiency, several architectures have been proposed in the last two decades, including but not limited to, asynchronous [240], cyclic [241], and delta-sigma [242] (see [239] for a survey). As extensively discussed in [11], with recent advances in the design and development of ADCs, the sampling energy consumption of a WMS has become negligible in comparison to its total energy consumption.

## **Transmission protocols**

A key consideration in the design of a WMS is the communication technology (radio and protocol) used to connect the WMSs with the base station. Several transmission protocols have been implemented on low-power wireless chipsets to enable energy-efficient data transmission. These protocols include, but are not limited to, ANT/ANT+ [243], ZigBee [244], Bluetooth Low Energy (BLE) [245], and Nike+ [246]. Among them, three protocols have become dominant in the market: ANT, ZigBee, and BLE. Dementyev et al. [247] analyzed the power consumption of these protocols. They found that BLE typically achieves the lowest power consumption, followed by ZigBee and ANT. BLE has become a promising solution for short-range transmissions between WMSs and the base station since it benefits from the widespread use of Bluetooth circuitry integrated in smartphones. In addition to energy-efficient transmission, new protocols commonly offer lightweight strong encryption, e.g., a modified form of AES [221], to provide confidentiality as well as per-packet authentication and integrity. This prevents several security attacks, e.g., eavesdropping and integrity attacks, against WMS-based systems.

## **On-sensor computation**

The required signal processing varies significantly from one application to another. In most applications, sensors perform lightweight signal processing on the data, e.g., compression, using on-sensor resources and then transmit the processed data to the base station for further processing, e.g., indexing and machine learning. Due to limited on-sensor resources, on-sensor computation, with attendant energy overhead, can be avoided for applications in which the sampling rate of biomedical signals is low, e.g., monitoring the patient's body temperature [11]. However, in some applications, on-sensor computation is beneficial and preferred over off-sensor computation due to one of the following reasons [248,249]. First, on-sensor computation may significantly

reduce the transmission energy (and as a result the total energy consumption of the device) even though it imposes extra energy consumption for computation. For example, if an EEG sensor can detect abnormal changes in the data, it only needs to transmit a small fraction of the data that includes those changes. Second, for some applications, in particular mission-critical applications, the communication delay or the possibility of unavailability of the Cloud or Internet may not be tolerable.

Next, we briefly discuss three commonly-used types of on-sensor algorithms.

**1. Aggregation:** In practice, a WMS does not usually need to transmit data as fast as it collects them. Hence, it can first aggregate multiple sensory measurements in one packet and only then transmit the packet. In this scenario, the total number of bits transmitted remains the same. However, the average number of transmitted packets over a fixed time period is reduced due to the aggregation. This can significantly reduce the transmission energy of WMSs [250]. The number of samples that can be aggregated in a single packet varies from one device to another based on its resolution, and is specified based on what is a tolerable response time [11].

**2. Compression:** Compression algorithms reduce the number of bits needed to represent data. On-sensor compression is commonly utilized to decrease transmission energy by reducing the total number of transmitted bits [251]. It can also save on-sensor storage by dropping non-essential information from the raw data [252]. For example, compressive sensing [253] offers a promising signal compression technique for acquiring and reconstructing a continuous signal by exploiting the sparsity of the signal to recover it from far fewer samples than required by the Shannon-Nyquist sampling theorem. Compressive sensing is recommended as a promising on-sensor compression technique in several recent research studies on WMSs [254, 255]. It significantly reduces the number of bits required to represent a signal and, at the same time, enables energy-efficient feature extraction and classification in the compressed domain [254].



**3. *Lightweight classification:*** Classification is defined as the problem of identifying to which category from a given set a new observation belongs. In a typical classification problem, a feature extraction procedure first extracts a set of features from the raw data. Then, a learning algorithm (also called classifier) trains a model based on a training set of data containing observations whose category membership is known. After training, the classifier infers the category of new observations using the trained model and the features extracted from the new data samples. As a resource-limited device, a WMS may consume a considerable percentage of its energy to extract features and classify data samples. In order to reduce the energy required for inference, both feature extraction and classification must be energy-efficient. Compressive sensing-based feature extraction and classification [254] can significantly reduce the number of features that need to be processed, while maintaining high accuracy. Simple classifiers, e.g., decision trees [256] and perceptrons [257], enable lightweight classification when the use of traditional classification methods, e.g., support vector machine [258], which need more computational power and storage, is not tolerable. A few recent research studies have proposed application-specific classification algorithms, e.g., seizure detection based on EEG signals [259], arrhythmia detection based on ECG signals [260], and physical activity classification based on acceleration data [27, 261].

### **2.2.2 Minimally-invasive capture methods**

As mentioned in Section 1.2.4, passiveness is one of the key design goals of a WMS-based system. In order to ensure passiveness, WMSs should exploit minimally-invasive capture methods. Prior to the emergence of WMSs, such methods were developed to enhance user convenience for in-hospital settings. For example, EEG capture was invented by Berger in 1924 [262]. The emergence of WMSs has magnified the need for such methods. As a result, several novel sensing approaches, e.g.,

for glucose sensing [263, 264] and sweat analysis [28, 265], have been developed for wearable watches and patches. They can non-invasively analyze on-skin chemical substances and minimize/eliminate the need for incisions or surgery. For example, Gao et al. [28] have proposed a wearable sweat-analyzing patch that selectively measures sweat metabolites, e.g., glucose and lactate, and electrolytes, e.g., sodium and potassium ions, from on-skin liquids. Designing novel minimally-invasive methods for gathering biomedical data using wearable technology is an ongoing research direction that has attracted significant attention in recent years.

### **2.2.3 Security and privacy**

The pervasive use of WMSs along with the emergence of the IoT paradigm during the last decade have led to several threats and attacks against the security of WMS-based systems and the privacy of individuals [1]. Next, we describe such threats/attacks along with their most well-known countermeasures.

#### **Security threats and attacks**

Unfortunately, the security threats against WMS-based systems are not well-recognized. This has made WMSs targets for a multitude of adversaries, such as cybercriminals, occasional hackers, hacktivists, government, and anyone interested in accessing the sensitive information gathered, stored, or handled by WMS-based systems, e.g., health conditions or details of a prescribed therapy.

As described in Section 1.2.3, a WMS-based system commonly consists of three main components: WMSs, base station, and Cloud servers. Possible security attacks against each of these components should be recognized and studied in depth in order to address attacks/threats against the whole system. Many well-known types of security attacks against the components/objects commonly used in IoT-based systems are summarized in [1]. Since the majority of WMSs are connected to the Internet

(either directly or through a smartphone), almost all such attacks are also applicable to WMS-based systems. Subashini et al. [266] describe various security attacks against the Cloud. These attacks/challenges include, but are not limited to, web application vulnerabilities such as Structured Query Language (SQL) injection, authorization/access control, integrity attacks, and eavesdropping. Moreover, many survey articles [267–269] summarize security attacks against wireless sensor networks (WSNs) that are also applicable to WMS-based systems.

Among previously-proposed attacks against WMS-based systems, the most well-known ones are: (i) eavesdropping on the communication channel to record unencrypted packets (an attack against confidentiality), and (ii) injection of illegitimate packets into the communication channel by reverse engineering the communication protocol (an attack against integrity). Encryption is the most effective approach for preventing these attacks. However, traditional encryption mechanisms are not suitable for WMSs due to on-sensor resource constraints. In order to reduce the resource overheads of encryption, several lightweight encryption mechanisms [270, 271] have been proposed in recent studies. Unfortunately, finding a practical low-power key exchange mechanism to securely share the encryption key is still a challenge, but with some solutions on the horizon [272].

### **Privacy concerns**

With the exponential increase in the number of WMS-based systems, ensuring user privacy is becoming a significant challenge. Smart wearable devices, e.g., smart watches, are equipped with many compact built-in WMSs, e.g., accelerometers and heart rate sensors, and powerful communication capabilities in order to offer a large number of services. They collect, process, and store several types of private user-related data.

Several recent research efforts have demonstrated how WMS-based systems may intentionally/unintentionally reveal the personal or corporate secrets of the user [273–275]. For example, Wang et al. [273] demonstrate the feasibility of extracting the user’s password by processing data gathered by the smart watch. The use of encryption may reduce leakage of private information by protecting the communication channel.

#### **2.2.4 Calibration and noise cancellation**

The negative impact of various disturbances on the data collected by WMSs has been extensively discussed in recent research. In particular, it has been shown that environmental noise [276, 277], user movement [278, 279], and changes in sensor locations [12, 280, 281] can impact sensory measurements significantly. For example, Salehizadeh et al. [278] discuss how sudden user movements can negatively impact pulse oximetry measurements, thus leading to inaccurate readings and even loss of signal. Alinia et al. [12] demonstrate that a change in the location of an accelerometer can impact the quality of sensory readings.

The above examples demonstrate that the various sources of noise should be taken into account while designing WMSs, and each sensor should be calibrated to ensure reliability and validity of measurements [12]. Several noise cancellation and filtering techniques, e.g., for ECG [282] and EEG [283], have been proposed to mitigate the impact of noise. Furthermore, various user-independent and user-oriented calibration algorithms have been developed to calibrate different sensors, e.g., accelerometer [102, 284], magnetometer [285], and gyroscope [286]. Prior to a measurement, a user-independent (user-oriented) calibration algorithm calibrates the sensor without (with) the user’s involvement based on the data gathered by the sensor itself and other sensors embedded in the system. However, there is still a significant gap between the quality of measurements provided by wearable sensors and that of in-hospital moni-

toring devices. Unlike the in-hospital environment in which the user remains almost stationary, the user’s position frequently changes during various daily activities. This makes the design of high-precision WMSs, which can provide high-quality measurements comparable to in-hospital equipment, a very complex task.

### 2.2.5 Big data

WMSs have the potential to generate big datasets over a short period of time. For example, a typical wearable EEG sensor generates over 120 MB of data per day [11]. With improvements in battery, sensor, and storage technologies, even more data might be generated by WMSs. Processing such large datasets is a complex task due to the following reasons.

1. Data heterogeneity: Different WMSs collect different types of signals [287]. Moreover, due to on-sensor resource constraints, the data may not necessarily be acquired continuously or even at a fixed sampling rate, adding to the heterogeneity of data [288].
2. Noisy measurements: As mentioned earlier, there are numerous sources of noise and disturbances that can corrupt the raw data or deteriorate their quality. In addition, the dataset might have several hours of data missing, when the user is not wearing one or multiple WMSs [289].
3. Inconsistency in data representation: Two devices containing the same sensors may offer very different types of raw data, e.g., older activity monitors generate a proprietary measure called an activity count, i.e., how often the acceleration magnitude exceeds some preset threshold, whereas newer ones commonly provide raw acceleration data [288]. Often, researchers and the industry use their own (often proprietary) data types and standards to report raw data.

Previous WMS-related research on big data has mainly focused on extracting valuable information from big datasets generated by WMSs. Three of the most well-known research areas that aim to address the above challenges in processing large datasets are: (i) big data analytics, (ii) standardization, and (iii) data cleaning.

### **Big data analytics**

This entails developing new methods and technologies to analyze big datasets, enabling a variety of services. The aim is to provide fast and efficient algorithms to extract valuable information and trends embedded in the large datasets generated by WMSs. Sensory data encode aspects of human movement, but simultaneously, and at a higher level of abstraction, sleep patterns, physical strength, and mobility, and even complex aspects of physical/mental health [290]. The complex relationships and correlations present in big datasets might facilitate noise detection, and as a result, enable the negative impact of the noise artifacts to be mitigated [288].

### **Standardization**

Standardizing how wearable sensor datasets are stored and transferred can enable simultaneous processing of datasets from multiple locations around the globe. A naive solution may be as follows: all devices should record and transmit raw signal data in a standard format and sample rate without any on-board preprocessing [288]. However, this is currently not a universally-practicable solution, mainly because battery restrictions for some applications, e.g., arrhythmia detection, necessitate preprocessing of data on the device [11, 291]. Furthermore, different applications inherently require different sample rates due to the nature of signals being monitored [11]. Thus, if standards mandate sample rates and filter settings, the rules should be application-specific.

## **Cleaning**

One of the first steps in data processing is data cleaning. This is the process of identifying and fixing data errors [292]. Errors can be discovered in datasets by: (i) detecting violations of predefined integrity rules, (ii) finding inconsistent patterns in data, (iii) locating data duplicates, and (iv) searching for outlier values (see [293] for a survey). A few innovative systems, e.g., NADEEF [294] and Bigdancing [295], provide end-to-end solutions to data cleaning. However, there is still a lack of end-to-end off-the-shelf efficient systems for data cleaning [292].

### **2.2.6 Cloud computing**

As discussed in Section 1.2.3, a large number of WMS-based systems rely on Cloud servers. Despite the promise of the Cloud in this context (access to shared resources in a pervasive manner, large storage capacity, and high computational power), there are several challenges that need to be addressed for on-Cloud WMS-based services (see [296–299] for survey articles). We briefly summarize them next.

#### **Availability/reliability**

Many researchers have investigated the negative consequences of Cloud failure [300, 301]. Frequent failures of Cloud servers have serious consequences, e.g., increased energy consumption [302], propagated service disruptions [303], and, more importantly, adverse impact on the reputation of the provider [304]. In order to offer a smooth and continuous service, Cloud providers use redundancy techniques [305] (that back up data and store them in multiple data centers geographically spread across the world). As a result, the average system demand is several times smaller than server capacity, imposing significant costs on the provider. To alleviate this burden, an availability-tuning mechanism [306] has been suggested. It allows the customers to express their true availability needs and be charged accordingly.

## **Access control**

The Cloud environment introduces new challenges on access control due to large scale, multi-tenancy (a software architecture in which a single instance of an application runs on a server and serves multiple groups of users), and host variability within the Cloud [307]. In particular, multi-tenancy imposes new requirements on access control as intra-Cloud communication (provider-user and user-user) becomes popular [308]. Recent research efforts have been targeted at new access control techniques [308–310], specifically designed for the Cloud. Masood et al. summarize and compare the majority of newly-proposed Cloud-specific access control methods in [311].

## **Standardization and portability**

Standardization of an efficient user interface is essential for ensuring user convenience. Web interfaces enable the user to access and analyze data on personal devices, e.g., a smartphone. Unfortunately, such web interfaces commonly impose a significant overhead because they are not specifically designed for smartphones or mobile devices [312]. In addition to standardizing the user interface, standardization of data formats is also essential to enable user-friendly services. If a Cloud provider stores data in its own proprietary format, users cannot easily move their data to other vendors [313].

## **Bandwidth limitation**

This is one of the fundamental challenges that needs to be handled in on-Cloud WMS-based systems when the number of users increases drastically, in particular for applications that need frequent data upload/download. Managing bandwidth allocation in a gigantic infrastructure, such as the Cloud that consists of several heterogeneous entities and millions of users, is very difficult. Some recent research efforts [314,315] propose efficient bandwidth allocation methods for Cloud infrastructures. For example, Wei et al. propose an allocation based on game theory [315].



# Chapter 3

## Energy-Efficient Long-term Continuous Personal Health Monitoring

Continuous health monitoring using wireless body-area networks of implantable and wearable medical devices (IWMDs) is envisioned as a transformative approach to health care. Rapid advances in biomedical sensors, low-power electronics, and wireless communications have brought this vision to the verge of reality. However, key challenges still remain to be addressed. The constrained sizes of IWMDs imply that they are designed with very limited processing, storage, and battery capacities. Therefore, there is a very strong need for efficiency in data collection, analysis, storage, and communication.

In this chapter, we first quantify the energy and storage requirements of a continuous personal health monitoring system that uses eight biomedical sensors: (1) heart rate, (2) blood pressure, (3) oxygen saturation, (4) body temperature, (5) blood glucose, (6) accelerometer, (7) electrocardiogram (ECG), and (8) electroencephalogram (EEG). Our analysis suggests that there exists a significant gap between the energy

and storage requirements for long-term continuous monitoring and the capabilities of current devices.

To enable energy-efficient continuous health monitoring, we propose schemes for sample aggregation, anomaly-driven transmission, and compressive sensing to reduce the overheads of wirelessly transmitting, storing, and encrypting/authenticating the data. We evaluate these techniques and demonstrate that they result in two to three orders-of-magnitude improvements in energy and storage requirements, and can help realize the potential of long-term continuous health monitoring [11].

### **3.1 Introduction**

Rapid technological advances in biomedical sensing and signal processing, low-power electronics, and wireless networking are transforming and revolutionizing health care. Prevention and early detection of disease are increasingly viewed as critical to promoting wellness rather than just treating illness. In particular, continuous long-term health monitoring, where various physiological signals are captured, analyzed, and stored for future use, is envisioned as key to enabling a proactive and holistic approach to health care.

Several trends in computing and communications technology have converged to advance continuous health monitoring from a distant vision to the verge of practical feasibility. Foremost among these is the evolution of IWMDs. Traditionally, medical monitoring systems, such as ECG and EEG monitors, have been used to simply gather raw data, with signal processing and data analysis being performed offline. However, with the continuing performance and energy efficiency improvements in computing, real-time signal processing has become possible. In the last decade, the number and variety of IWMDs have increased significantly, ranging from simple wearable activity and heart-rate monitors to sophisticated implantable sensors. Moreover, advances in

low-power wireless communications enable radios to be integrated into even the most energy- and size-constrained devices. This has led to the possibility of composing IWMDs into wireless body-area networks (WBANs) [316, 317].

WBANs are opening up new opportunities for continuous health monitoring and proactive health care [318]. A typical WBAN for health monitoring consists of (i) implantable and wearable sensors, which are attached to the body or even implanted under the skin to measure vital signs and body signals, e.g., body temperature, heart-beat, blood pressure, etc. and (ii) external devices (which could be smartphones) that act as base stations to collect, store, display, and analyze the data.

Many recent and ongoing research efforts have addressed the design and deployment of WBANs. The CodeBlue project [53] focused on designing wireless sensor networks for medical applications. It included an ad-hoc network to transmit vital health signs to health care providers. Otto et al. [319] designed a system architecture to address various challenges posed by the need for reliable communication within the WBAN, and between the WBAN and a medical server. The MobiHealth project [320] offered an end-to-end mobile health platform for health care monitoring. Different sensors, attached to a MobiHealth patient, enabled constant monitoring and transmission of vital signals. They considered security, reliability of communication resources, and quality of service (QoS) guarantees.

Notwithstanding advances in IWMDs and WBANs, some key technical challenges need to be addressed in order to enable long-term continuous health monitoring. Due to size constraints and the inconvenience or infeasibility of battery replacement, IWMDs need to be highly energy-efficient. IWMDs as well as the external devices that aggregate the monitored data have limited storage capacity. Finally, health care applications also impose strict requirements for privacy, security, and reliability [317].

This chapter aims to address the challenging question of *whether it is feasible to energy- and storage-efficiently provide long-term continuous health monitoring based on state-of-the-art technology*. In this chapter:

- We first discuss the traditionally used sense-and-transmit monitoring scheme to establish a baseline for our analyses. We evaluate a system that consists of eight biomedical sensors: (1) heart rate, (2) blood pressure, (3) oxygen saturation, (4) body temperature, (5) blood glucose, (6) accelerometer, (7) ECG, and (8) EEG.
- We present analytical models that can be used to estimate the energy and storage requirements for these biomedical sensors. Our analysis suggests a significant gap between the energy and storage requirements for long-term continuous monitoring and the capabilities of current devices.
- To address the aforementioned gaps in health monitoring, we propose and evaluate three schemes to reduce the overheads of sensing, storing, and wirelessly transmitting the data:
  1. First, we explore a simple scheme based on aggregation of samples to amortize the communication protocol overheads and reduce the number of transmissions.
  2. Second, we explore anomaly-driven transmission in which the sensors perform on-sensor signal processing to identify time intervals of interest, and only transmit/store data from these intervals.
  3. Finally, we explore the concept of compressive sensing (CS) [321], together with a newly developed approach for computation on compressively-sensed data [254, 322], to drastically reduce energy and storage.

- We demonstrate that the proposed schemes can potentially result in two to three orders-of-magnitude reduction in energy and storage requirements, and therefore may be instrumental in enabling continuous long-term health monitoring.
- We compare all proposed schemes and discuss how a continuous long-term health monitoring system should be configured based on patients' needs and physicians' recommendations.

The rest of the chapter is organized as follows. Section 3.2 describes different components, which form a WBAN and the communication protocols that can be used to connect them together. Section 3.3 describes the baseline continuous health monitoring scheme. Section 3.4 presents our analytical models and an analysis of the energy and storage requirements for the baseline WBAN using these models. Section 3.5 describes the proposed schemes that include sample aggregation, anomaly-driven sampling, and CS-based computation, and evaluates their energy impact. Section 3.6 evaluates the impact of the proposed schemes on storage requirements. Section 3.7 compares different schemes and summarizes the medical considerations in configuration and optimization of different sensors. Finally, Section 3.8 concludes the chapter.

## **3.2 Different components of a general-purpose health monitoring system**

In this section, we first describe two fundamental components that form a medical WBAN, namely biomedical sensors and the base station. Second, we discuss the communication protocols, which can be used to connect them together.

### 3.2.1 Health monitoring with networked wireless biomedical sensors

Biomedical sensors have been used for health monitoring for a long time [323]. They sense electrical, thermal, optical, chemical, and other signals to extract information that are indicative of a patient's health condition. Examples of such sensors include oxygen saturation, glucose, blood pressure, heart rate, ECG, EEG, and several forms of imaging.

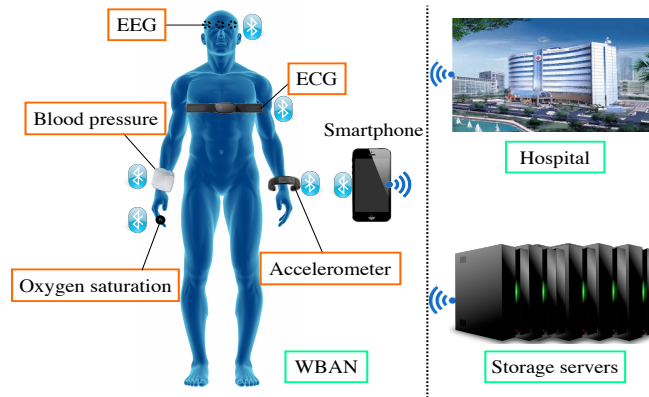


Figure 3.1: A personal health care system.

In addition to the biomedical sensors, an important component of a WBAN, as shown in Fig. 3.1, is the base station or hub, a more capable device that aggregates data from the biomedical sensors, visualizes health data for the patient, performs simple analytics, and communicates the health data to remote health providers or health databases. The base station, which could be a customized device or a commodity mobile device such as a smartphone, contains a more capable processor, data storage, and one or more wide-area network interfaces.

### 3.2.2 Communication protocol

A key consideration in the design of a WBAN is the communication technology (radio and protocol) used to connect the medical sensors with the base station. Energy efficiency, security, and interoperability are some of the key factors that must be considered in this context.

Dementyev et al. analyzed the power consumption characteristics of three popular emerging standards – ANT, ZigBee, and BLE – in a duty-cycled sensor node scenario [247]. They found that BLE achieves the lowest power consumption, followed by ZigBee and ANT. Most of the power consumption differences can be attributed to the time taken for a sensor to reconnect to the base station after waking up and the efficiency of the sleep mode used between transmissions of successive packets. In addition to low power consumption, BLE provides several other advantages for continuous health monitoring:

1. Smartphones have become dominant over other forms of base stations for potential use in the health monitoring system. BLE benefits from the widespread use of Bluetooth technology since BLE can be easily integrated into classical Bluetooth circuitry, and almost all new smartphones support BLE.
2. BLE is optimized for use in devices that need to communicate small packets wirelessly.
3. BLE is optimized to provide a low-rate ( $< 270 \text{ kb/s}$ ) wireless data transfer. As shown later, the maximum transmission rate of all sensors is much less than  $270 \text{ kb/s}$ .
4. BLE provides a long transmission range (more than  $100 \text{ m}$ ) that enhances user convenience.

5. Due to the privacy and safety concerns in medical systems, security is a key consideration in WBAN design. BLE supports strong encryption (Advanced Encryption Standard) to provide confidentiality as well as per-packet authentication and integrity.

Thus, in our work, we use BLE for short-range transmissions between medical sensors and the base station.

### **3.3 Baseline continuous health monitoring system**

In this section, we first describe our baseline WBAN targeted at long-term continuous health monitoring that consists of eight sensors. Then, we discuss its energy and storage requirements.

#### **3.3.1 Baseline WBAN**

As mentioned earlier, we use eight biomedical sensors in the WBAN. In the baseline WBAN, each sensor node gathers raw data at a specific sampling frequency related to its application. Then, the node generates a BLE packet using a single sample and sends the raw data to the base station for further analysis. In this scheme, each sensor transmits the sample as soon as it is gathered, and the base station is responsible for processing. In order to implement the WBAN, first, it is required to specify the sampling rate for each sensor. This rate must be chosen in such a way that the requirements of different applications are met. The rates vary significantly from one sensor to another. Moreover, the same sensor may need to have different sampling rates in different applications [324]. We have investigated the range of possible sampling rates for each sensor by reviewing the medical literature published between 1997 and 2014. Next, we provide these ranges for various sensors.



- **Heart rate:** The heart rate is commonly sampled at 6-8  $Hz$  frequency. For example, this sampling rate is currently used in fetal heart rate monitors [325]. While the typical human heart rate is 65-82 beats per minute ( $bpm$ ), the rate can sometimes exceed 180  $bpm$ . These considerations suggest a sampling rate of 2-8  $Hz$  [326].
- **Blood pressure:** During a typical ambulatory blood pressure monitoring session, the blood pressure is commonly measured every 15 to 30 minutes over a 24-hour period [327]. In some cases (e.g., occurrence of a hemorrhage), the blood pressure should be sampled at a much higher frequency. For example, Adibuzaman et al. have investigated the use of a blood pressure waveform sampled at 100  $Hz$  to monitor physiological system variations during a hemorrhage [328].
- **Oxygen saturation:** The sampling rate of continuously-monitored oxygen saturation is suggested to be in the 0.001  $Hz$  to 2.00  $Hz$  range [324, 329, 330]. For example, Evans et al. use measurements at 5-min intervals (sampling rate of 0.003  $Hz$ ) to monitor critically ill, mechanically ventilated adult patients during intrahospital transport [329].
- **Temperature:** The body temperature normally fluctuates over the day. Continuous monitoring of these small fluctuations is suggested by different researchers for a variety of applications [324, 331]. For example, Simon et al. suggest measurements at 10-min intervals to determine the influence of circadian rhythmicity and sleep on 24-hour leptin variations [331]. However, some applications require a higher sampling rate (e.g., 1  $Hz$ ) [324]. Thus, we assume the sampling rate of the body temperature sensor to be in the 0.001  $Hz$  to 1  $Hz$  range.
- **Blood sugar:** Blood sugar measurements every 5 to 15 minutes are used in a variety of medical applications [324, 332]. However, some applications, such

as continuous glucose monitoring to detect a sudden rise or drop in the glucose level of diabetics, require a higher sampling rate ( $\sim 100 \text{ Hz}$ ) [324].

- **Accelerometer:** An accelerometer is widely used for physical activity detection. Its sampling rate typically lies in the  $30 \text{ Hz}$  to  $400 \text{ Hz}$  range. However, a lower sampling rate (e.g., down to  $2 \text{ Hz}$ ) might be enough for some applications [324, 333–335].
- **ECG:** Determining the frequency content of an ECG signal by investigating its frequency spectrum is usually difficult because it is hard to distinguish between frequency components of signal and noise. Berson et al. record over-sampled ECG signals and then apply different low-pass filters to them [336]. They describe the effect of filtering on amplitude variations, concluding that at least a sampling frequency of  $50\text{-}100 \text{ Hz}$  is necessary to prevent amplitude errors. Moreover, Simon et al. demonstrated that a  $1000 \text{ Hz}$  sampling rate is enough for the majority of ECG-based applications [337]. We consider ECG sampling rates in the  $100\text{-}1000 \text{ Hz}$  range.
- **EEG:** Traditionally, the range of EEG frequencies that was accepted to be clinically relevant was in/below the gamma band ( $40\text{-}100 \text{ Hz}$ ). However, filtering of the EEG signal at around  $70 \text{ Hz}$  and using at least a  $200 \text{ Hz}$  sampling rate are commonly suggested by medical literature [338]. Moreover, recent studies have shown that EEG signals may also have physiological relevance in high-frequency bands (e.g.,  $100\text{-}500 \text{ Hz}$ ) [338, 339]. Based on the above discussion, we consider EEG sampling rates in the  $100\text{-}1000 \text{ Hz}$  range.

Next, we consider the sampling resolution of each sensor, where resolution is defined as the number of bits required for representing a sample. We reviewed several recent publications in the biomedical literature to obtain these resolutions.

- **Heart rate:** An accurate and compact low-power heart rate sensor for home-based health care monitoring is described and implemented in [340]. It shows that a resolution of 10 bits is appropriate for providing an accurate measurement of the heart rate.
- **Blood pressure:** We consider 16 bits of resolution for blood pressure samples, which is commonly used in commercial blood pressure monitoring devices [324].
- **Oxygen saturation:** We consider 8 bits of resolution for oxygen saturation based on the data reported in [341, 342].
- **Temperature:** The body temperature varies within the 35 to 42°C range. An 8-bit resolution is sufficient for body temperature sampling.
- **Blood sugar:** Measurements of blood sugar are based on color reflectance. The meter quantifies the color change and generates a numerical value that represents the concentration of glucose. A 16-bit resolution has been shown to be adequate for blood sugar monitoring devices [343].
- **Accelerometer:** We consider 12-bit resolution, which has been used in a variety of wearable accelerometer applications and commercial devices [324, 333, 344].
- **ECG:** Ultra low-power ECG sensors, which are commonly used in long-term monitoring, support 8 or 12 bits of resolution [345–347]. A resolution of 8 bits may result in a small but noticeable quantization error. Researchers have shown that greater than 8 bits of resolution will meet ECG requirements [348]. Therefore, we assume a resolution of 12 bits.
- **EEG:** Several low-power wearable EEG sensors [349, 350] use 10- or 12-bit analog-to-digital converter (ADC) units. The recording should represent sam-

ples down to  $0.5 \mu V$  and up to plus/minus several millivolts. We consider a 12-bit resolution.

Table 3.1 summarizes information on sensors, their resolution and sampling rate, and the maximum wireless data transmission rate.

Table 3.1: Resolution, sampling rate, and maximum transmission rate

Sensor	Resolution (bits/sample)	Sampling rate (Hz)	Maximum transmission rate (bits/s)
Heart rate	10	2-8	80
Blood pressure	16	0.001-100	1600
Oxygen saturation	8	0.001-2	16
Temperature	8	0.001-1	8
Blood sugar	16	0.001-100	1600
Accelerometer	12	2-400	4800
ECG	12	100-1000	12000
EEG	12	100-1000	12000

### 3.3.2 Energy and storage requirements

Next, we discuss energy and storage requirements for a continuous health monitoring system.

Energy consumption can be divided into three categories: sampling, data transmission, and data analysis [351]. Wireless data transmission is usually the major energy-consumer. The available energy in each sensor node is often quite limited. The battery used in the node is typically the largest contributor in terms of both size and weight. Battery lifetime is a very important consideration in biomedical sensors. In particular, battery replacement of implanted sensors may require surgery and, hence, impose cost and health penalties [318]. Thus, biomedical sensors often need to maintain their functionality for months or even years without the need for a battery change. For instance, an implanted pacemaker requires a battery lifetime of at least five years. Furthermore, during communication, biomedical sensors generate

heat that may be absorbed in nearby tissue, with possible harmful effects. Hence, the energy consumption should also be minimized from this perspective [318].

Moreover, a WBAN imposes specific storage requirements. Although WBANs facilitate health monitoring and early detection of health problems, physicians usually want access to raw data so that they can independently verify the accuracy of on-sensor processing. Thus, it is important to enable medical personnel to access all or at least important chunks of raw data. However, storing the raw data in the sensor nodes is not feasible for two main reasons. First, IWMD sizes need to be kept small to facilitate patient mobility. Second, adding a large storage to a sensor increases its energy consumption drastically, and as a result, battery lifetime decreases dramatically. Therefore, we may think of storing the data in the base station. However, the base station (e.g., a smartphone) may have its own resource constraints, though much less severe, in terms of storage and battery lifetime. In addition, in order to provide data backup, we may want to periodically send stored data from the base station to storage servers. Therefore, the costs of long-term storage using reliable storage services (e.g., Amazon S3 [352]) should also be considered. Thus, it is important to minimize storage requirements for long-term health monitoring while maintaining adequate information for future reference.

### **3.4 Analytical models for the evaluation of WBAN's energy and storage requirements**

In this section, we first describe the analytical models that we use to abstract the essential characteristics of the continuous health monitoring system. Then, we use the model to evaluate the baseline IWMDs.

### 3.4.1 Analytical models

Analytical models can be used to predict system requirements. They are much more efficient than performing simulation. Next, we describe the models used to quantify the energy consumption and storage requirements of the continuous health monitoring system. Table 3.2 provides the list of variables used in our models.

Table 3.2: Variables, unit, and description

Variable	Unit	Description
$E_{total}$	$J/day$	Total energy consumption of a biomedical sensor
$E_s$	$J/day$	Energy consumption of sampling
$E_t$	$J/day$	Energy consumption of transmission
$E_c$	$J/day$	Energy consumption of computation
$E_{ADC}$	$J/sample$	Energy consumption of sampling per sample
$f_t$	$Hz$	Transmission frequency
$f_s$	$Hz$	Sampling frequency
$N$	–	Sampling resolution
$S$	$1/day$	#samples per day
$C$	$1/day$	#transmissions per day
$P_{send}$	$W$	Average power consumption in the sending mode
$P_{standby}$	$W$	Average power consumption in the standby mode
$I_{send}$	$A$	Average drained current in the sending mode
$I_{standby}$	$A$	Average drained current in the standby mode
$T_{send}$	$s$	Sending time
$T_{standby}$	$s$	Standby time
$V_{supply}$	$V$	Supply voltage
$SR$	$B/year$	Required amount of storage in a year

#### Energy consumption

As mentioned earlier in Section 3.3, energy consumption of a sensor has three major components: sampling, transmission, and on-sensor computation. Therefore, we assume that total energy consumption of the sensor ( $E_{total}$ ) can be written as:

$$E_{total} = E_s + E_t + E_c \quad (3.1)$$

## 1. Sampling energy

Next, we discuss the sampling energy that is consumed by the ADC chip. The total energy consumption of an ADC chip can be divided into: (i) I/O energy, (ii) reference energy, (iii) sample-and-hold energy, (iv) ADC core energy, and (v) input energy [239]. However, separate calculation of these values is difficult. Thus, we use the actual values of the total on-chip ADC energy consumption per sample ( $E_{ADC}$ ) reported in [239]. It summarizes the experimental results from more than 1400 scientific papers published between 1974 and 2010. Fig. 3.2 shows the scatter plot of the reported  $E_{ADC}$  in each of these papers vs. the effective number of bits (ENOB), where ENOB is defined as:

$$ENOB = \frac{SNR - 1.76}{6.02}, SNR = \frac{P_{signal}}{P_{noise}} \quad (3.2)$$

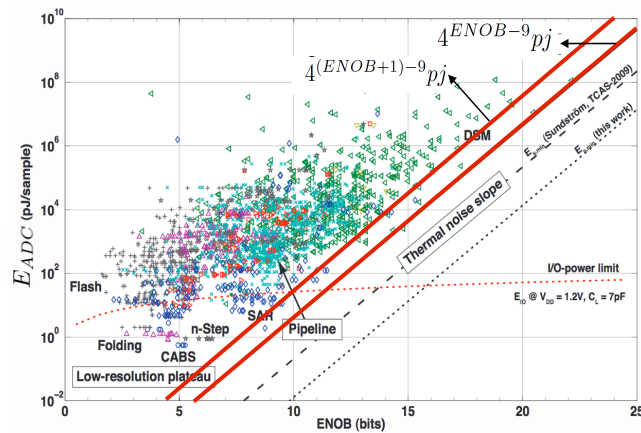


Figure 3.2: Scatter plot of the reported  $E_{ADC}$  vs. ENOB bits for different ADC architectures: asynchronous ( $\circ$ ), cyclic ( $\square$ ), delta-sigma ( $\triangleleft$ ), flash (+), folding ( $\triangle$ ), pipeline ( $\times$ ), successive approximation ( $\diamond$ ), subranging ( $\triangleright$ ), n-Slope ( $*$ ), n-Step ( $*$ ), and other ( $\nabla$ )

ENOB is always less than the resolution for all ADC chips. In particular, for medium-resolution ADCs ( $8 \leq N \leq 16$ ) that are used in biomedical sensors,  $ENOB \leq N-1$  provides a better boundary for the ENOB. For example, Verma et al. presented a

low-power 12-bit resolution ADC for WSNs [353]. The ENOB of this ADC is reported to be 10.55 bits.

As shown in Fig. 3.2, the  $E_{ADC}$  of modern medium-resolution ADCs is within the  $4^{ENOB-9} pJ$  to  $4^{(ENOB+1)-9} pJ$  range. Therefore, the sampling energy consumption per day ( $E_s$ ) can be upper-bounded as follows:

$$E_s = E_{ADC} * S \quad (3.3)$$

$$E_{ADC} < 4^{(ENOB+1)-9} pJ \leq 4^{(N-9)} pJ, \quad (3.4)$$

$$S = f_s \left( \frac{1}{s} \right) * 60 \left( \frac{s}{min} \right) * 60 \left( \frac{min}{hr} \right) * 24 \left( \frac{hr}{day} \right) \quad (3.5)$$

$$\implies E_s < f_s \left( \frac{1}{s} \right) * 60 \left( \frac{s}{min} \right) * 60 \left( \frac{min}{hr} \right) * 24 \left( \frac{hr}{day} \right) * 4^{(N-9)} pJ \quad (3.6)$$

Table 3.3 shows the upper-bound values of  $E_s$  for all the sensors. As discussed later,  $E_s$  values for all sensors are negligible in comparison to their total energy consumption. Hence, we can safely assume that  $E_{total} \approx E_t + E_c$ .

Table 3.3: Upper-bound values of  $E_s$

Sensor	$E_s$ (J/day)
Heart rate	2 e-6
Blood pressure	1 e-1
Oxygen saturation	4 e-8
Temperature	4 e-8
Blood sugar	1 e-1
Accelerometer	2 e-3
ECG	5 e-3
EEG	5 e-3

## 2. Transmission energy

In our experiments, we used the Texas Instruments CC2541 Development Kit as the BLE transmission device. To provide a quantitative comparison, we experimentally measured the energy consumption of the transmission chip in a cyclic scenario.



In a cyclic transmission, the transmitter takes  $T_{send}$  seconds to send the data to the base station and then enters a standby phase for  $T_{standby}$  seconds. Hence, the average energy consumption of transmission can be calculated as follows:

$$E_t = (T_{send} * P_{send} + T_{standby} * P_{standby}) * C \quad (3.7)$$

$$C = f_t \left( \frac{1}{s} \right) * 60 \left( \frac{s}{min} \right) * 60 \left( \frac{min}{hr} \right) * 24 \left( \frac{hr}{day} \right) \quad (3.8)$$

$T_{send}$  is a fixed value and measured as 2.6 milliseconds for a single packet transmission.  $T_{standby}$  depends on the transmission frequency ( $f_t$ ):

$$T_{standby} = \frac{1}{f_t} - T_{send} \quad (3.9)$$

$P_{send}$  and  $P_{standby}$  can be obtained by measuring the current drained from the battery with supply voltage  $V_{supply}$ . We calculated the average power consumption for a single packet transmission using a standard oscilloscope.  $P_{send}$  and  $P_{standby}$  were found to be 30.5 mW and 2.5  $\mu$ W, respectively, where  $V_{supply}$  is set to 2.5 V. In order to measure the power consumption of a single packet transmission, we also considered different packet sizes (varying from 1 B to 20 B). Our experimental results show that variations in transmission energy of a single packet are negligible when the packet size changes from 1 B to 20 B. However, since  $P_{send} \gg P_{standby}$ , a higher transmission rate obviously leads to a higher energy consumption.

### **3. Computation energy**

Computation energy varies significantly from one biomedical application to another. In most applications, the computation energy can be divided into feature extraction energy and classification energy. Since a feature extraction function can be converted into matrix form, the feature extraction energy can be estimated as the energy consumption of a matrix multiplication function. The classification energy can be estimated based on the reported values of classification energy per vector for

various methods. However, obtaining a general model for computation energy is difficult because of its dependence on the application. In this work, when we consider on-sensor computation energy, we use the values reported in [254, 322].

### Storage requirement

Next, we provide an analytical model for estimating the amount of required storage for one-year storage of raw medical data. When there is no on-sensor computation, this only depends on the sampling frequency ( $f_s$ ) and sampling resolution ( $N$ ):

$$SR = f_s \left( \frac{1}{s} \right) * N(\text{bits}) * \left( \frac{1B}{8\text{bits}} \right) * 31536000 \left( \frac{s}{\text{year}} \right) \quad (3.10)$$

However, simple on-sensor computation can significantly decrease the amount of required storage. For example, if the computation method can efficiently detect points of interest from the raw data, we may only need to store those specific points for further analysis. Moreover, on-sensor data compression, e.g., in CS-based applications, can also decrease the number of transmitted bits from the sensor to the base station by compressing the raw data before transmission.

### 3.4.2 Evaluation of the baseline WBAN

Next, we evaluate the energy consumption and storage requirement for the baseline scheme, described in Section 3.3, using the models described above.

#### Evaluation of the energy consumption

Since each sensor has its own sampling rate and resolution, its energy consumption differs from that of others. Table 3.4 shows the minimum and maximum amounts of

energy consumption for different devices in this baseline scenario. They correspond to the minimum and maximum sampling rates, respectively. Table 3.5 shows the battery lifetime of each sensor. The minimum/maximum battery lifetimes are reported assuming that each sensor node uses a regular coin cell battery (CR2032). A regular coin cell battery is commonly used in biomedical sensors. Not surprisingly, ECG and EEG sensors are seen to consume the most amount of energy. Thus, these sensors are the main obstacles to providing long-term health monitoring.

Table 3.4: Minimum and maximum values of total energy consumption

Sensor	Minimum (J/day)	Maximum (J/day)
Heart rate	13.99	55.23
Blood pressure	0.26	686.88
Oxygen saturation	0.26	14.00
Temperature	0.26	7.13
Blood sugar	0.26	686.88
Accelerometer	14.00	2747.52
ECG	686.88	6868.80
EEG	686.88	6868.80

Table 3.5: Minimum and maximum battery lifetimes of different sensors

Sensor	Minimum (days)	Maximum (days)
Heart rate	48.8	192.90
Blood pressure	3.93	10125.69
Oxygen saturation	192.86	10125.69
Temperature	378.68	10125.69
Blood sugar	3.93	10125.69
Accelerometer	0.98	192.86
ECG	0.39	3.93
EEG	0.39	3.93

### Evaluation of the storage requirement

Next, we evaluate the baseline system from the storage perspective. We readily realize the baseline transmission scheme requires a significant amount of storage.

Table 3.6 shows the minimum and maximum amounts of storage required for long-term health monitoring in this system. The minimum (maximum) value corresponds to the minimum (maximum) sampling frequency. Since EEG and ECG signals require the largest amount of storage, we mainly target these signals for storage reduction.

Table 3.6: Minimum and maximum storage required for long-term storage

Sensor	Minimum (MB/yr)	Maximum (GB/yr)
Heart rate	75.18	0.29
Blood pressure	0.07	5.87
Oxygen saturation	0.03	0.06
Temperature	0.03	0.03
Blood sugar	0.07	5.87
Accelerometer	90.23	17.62
ECG	4511.26	44.06
EEG	4511.26	44.06

### 3.5 Improving the energy efficiency of continuous health monitoring

In this section, we first propose three schemes for signal processing and transmission that can be used in a WBAN. Then, we evaluate and compare these schemes from the energy perspective. We divide the sensors into two different categories based on their transmission rate: low-sample-rate sensors (heart rate, blood pressure, oxygen saturation, temperature, blood sugar, accelerometer) and high-sample-rate sensors (EEG and ECG). Then, we use the following three schemes to reduce the energy consumption of each node.

- We accumulate multiple samples in one packet before transmitting the raw data in order to decrease the number of transmitted packets. The base station is responsible for processing and storage of the raw data. This approach is applicable to both high-sample-rate and low-sample-rate sensors.

- We process the data in high-sample-rate sensors (EEG and ECG) using traditional signal processing methods. Then, we transfer just a fraction of the raw data from the sensor node for storage in the base station based on the result of computation.
- We suggest using CS-based computation in high-sample-rate sensor nodes before data transmission. Again, we just transfer a small fraction of the raw data from the sensor node for storage in the base station based on the result of on-sensor computation.

Although on-sensor computation leads to some extra computational energy consumption, it reduces transmission energy consumption significantly due to the reduction in the amount of data transmitted. This is especially true when the transmission rate of a sensor is very high and important events (e.g., seizure, heart attack) are rare. However, in the case of low-sample-rate sensors, the decrease in transmission energy does not offset the increase in computational energy. Therefore, we do not employ any on-sensor computation for low-sample-rate sensors.

Each scheme is discussed in the following subsections and compared against the baseline scheme. We estimated the minimum/maximum energy consumption of each sensor in different scenarios, and based on that, we computed the minimum/maximum battery lifetime.

### 3.5.1 Sample aggregation

In practice, we do not usually need to transmit the data as fast as we gather them. Thus, we could first accumulate multiple samples (up to  $20 B$ ) in one packet and only then transmit the packet. The total number of bits transmitted remains the same. However, the average number of transmitted packets per second is reduced due to the accumulation. The number of samples that can be accumulated in a single

packet varies from one device to another based on its resolution. In addition, the data processing algorithm in the base station might have been optimized with a specific number of required samples in mind. Therefore, the number of samples per packet may need to be varied between 1 and the maximum number. For the devices being evaluated, Table 3.7 shows the maximum number of samples that can be gathered into a single packet.

Table 3.7: Maximum number of samples in one packet

Sensor	#Samples
Heart rate	16
Blood pressure	10
Oxygen saturation	20
Temperature	20
Blood sugar	10
Accelerometer	13
EKG	13
EEG	13

In order to calculate the total energy consumption of a sensor, we also need to consider the storage energy required for storing multiple packets before transmission. To store 20  $B$ , which is the maximum number of bytes that can be sent in a single transmission, we consider the energy consumption of a 160-cell buffer. This storage energy remains fixed for the maximum and minimum transmission rates. However, the maximum (minimum) energy consumption is calculated as the energy consumption of transmission using the maximum (minimum) rate plus the energy consumed by the 160-cell buffer. Using the SRAM cell energy reported for the 90  $nm$  technology node in [354], we calculate the minimum and maximum energy consumption of each device, as shown in Table 3.8. The minimum and maximum battery lifetimes of each sensor are shown in Table 3.9. Relative to the baseline, this method provides up to 13.58 $\times$  reduction in maximum energy consumption for low-sample-rate sensors.

The maximum and minimum energy consumptions of high-sample-rate sensors are reduced by 12.98× and 12.83×, respectively.

Table 3.8: Minimum and maximum values of total energy consumption while using the sample aggregation scheme

Sensor	Minimum (J/day)	Maximum (J/day)
Heart rate	1.50	4.07
Blood pressure	0.65	69.38
Oxygen saturation	0.65	1.33
Temperature	0.64	0.98
Blood sugar	0.65	69.38
Accelerometer	1.70	212.13
ECG	53.52	529.36
EEG	53.52	529.36

Table 3.9: Minimum and maximum battery lifetimes of different sensors while using sample aggregation scheme

Sensor	Minimum (days)	Maximum (days)
Heart rate	663.39	1800
Blood pressure	38.92	4153.85
Oxygen saturation	2030.08	4153.85
Temperature	2715.10	4218.75
Blood Sugar	38.92	4153.85
Accelerometer	12.73	1588.24
ECG	5.10	50.45
EEG	5.10	50.45

### 3.5.2 Anomaly-driven transmission

Next, we evaluate a process-and-transmit scheme that is more appropriate for high-sample-rate sensors (ECG and EEG), which consume significant amounts of energy. If we first process raw data in the sensor nodes themselves and then just transmit some small chunks of data based on the processing results, we can reduce the transmission rate significantly. In this scenario, whenever we detect an abnormal activity, we are required to transmit the raw data corresponding to the abnormal event, in order to

facilitate offline evaluation of the data. The computational energy in each sensor node and data transmission rate directly depend on the intended application. We evaluated seizure detection and arrhythmia detection as applications for EEG and ECG sensors, respectively. The traditional computation that we have considered for seizure/arrhythmia detection is as follows. First, we sample the signal at the Nyquist sampling rate. Second, we use a feature extraction algorithm (spectral energy analysis for EEG and Wavelet transform for ECG) to extract the important feature of the signal and build a feature vector. Third, we classify the feature vectors using a binary classifier [254, 322, 355–357].

Let us consider an EEG sensor first. We assume signal processing in this sensor is based on a traditional algorithm for seizure detection, as described in [254, 322]. The frequency of epileptic seizures varies from person to person. In some cases, seizures may even be separated by years. On the other extreme, seizures might occur every day. Williamson et al. [358] studied 90 patients and reported the mean seizure frequency and mean duration to be 4.7 per month (range: 3 to 9 per month) and 3.8 minutes (range: 1 to 20 minutes), respectively. Based on their result, if the EEG sensor just transmits the small fraction of data corresponding to seizures, the sensor needs to transmit information over a duration of 17.8 minutes per month, on an average. Table 3.10 shows the average total energy consumption of the EEG sensor when we use the traditional signal processing method described in [254, 322] and only transmit important chunks of data whenever an abnormality is detected. The minimum (maximum) value corresponds to the minimum (maximum) sampling frequency. In this scheme, the processing module consumes the major part of energy. Relative to the baseline, it provides up to  $177\times$  reduction in total energy consumption for the EEG sensor. Table 3.11 shows the minimum and maximum battery lifetimes of the EEG sensor in this scheme.



Next, we consider ECG sensors, and assume that the signal processing method is the traditional computation method for arrhythmia detection, as discussed in [322]. Unlike seizure, the frequency of occurrence of arrhythmia varies significantly. There are different types of arrhythmia: each may lead to intermittent or consistent symptoms. Therefore, it is difficult to predict the frequency of occurrence for arrhythmia. Fig. 3.3 shows the total energy consumption and battery lifetime of the ECG sensor with respect to frequency of occurrence of arrhythmia in a day, respectively. We assume that after detecting an abnormal event, the sensor transmits the information of a standard one-minute ECG strip to the base station.

Table 3.10: Average total energy consumption of the EEG sensor for the anomaly-driven method

Sensor	Minimum (J/day)	Maximum (J/day)
EEG	36.27	38.83

Table 3.11: Average battery lifetimes for the EEG sensor for the anomaly-driven method

Sensor	Minimum (days)	Maximum (days)
EEG	69.53	74.44

### 3.5.3 CS-based computation and transmission

As the third scheme, we evaluate an approach for computation and data transmission that can reduce the energy consumption of EEG and ECG sensors significantly. As mentioned earlier, since the total energy consumption of EEG and ECG sensors is very high due to their high data transmission rates, if we can process the raw data in these sensors and transmit only small chunks of data upon the occurrence of an abnormal event, the transmission energy may be reduced significantly. However, now the computation energy becomes the major energy bottleneck. Hence, we try to reduce it through CS-based computation. First, we briefly describe CS.

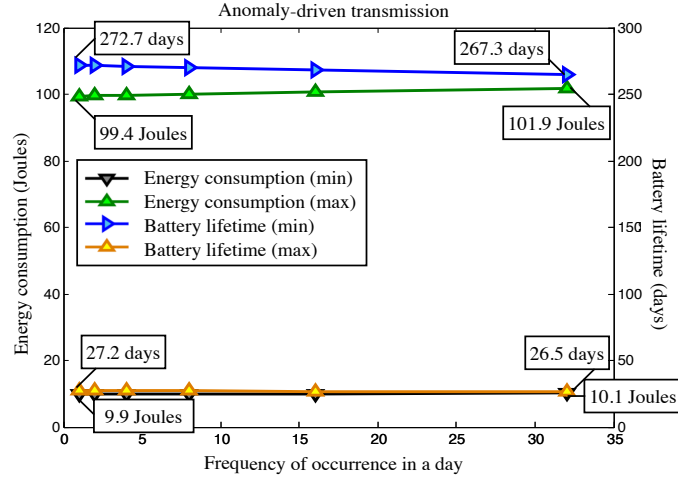


Figure 3.3: Energy consumption and battery lifetime of the ECG sensor for the anomaly-driven method with respect to frequency of occurrence of arrhythmia in a day.

CS (also called compressive sampling or sparse sampling) is a signal processing approach for efficiently sampling and reconstructing a signal [321]. The common goal of various signal processing approaches is to reconstruct a signal from a finite number of measurements. Without any prior knowledge or assumptions about the signal, this task is not feasible due to the fact that there is no way to reconstruct an arbitrary signal in an interval in which it is not measured. However, under certain conditions and assumptions, the signal can be reconstructed using a finite number of samples. In the CS approach, a signal can be recovered from far fewer samples than required by Nyquist sampling. Recovering a signal using the CS approach relies on two fundamental principles: sparsity and incoherence.

1. Sparsity: This requires that the signal be sparse in some domain (i.e., the signal's representation in some domain should have many coefficients close to or equal to zero) [359, 360]. CS can be used to compress an  $N$ -sample signal  $X$  that is sparse in a secondary basis  $\Psi$ . Previous research has shown that ECG and EEG signals are sparse enough in the Wavelet transform space [361] and Gabor space [362–364], respectively.

- Incoherence: This indicates that unlike the signal of interest, the sampling/sensing waveforms have an extremely dense representation in the transformed domain.

The main limitation of the classical CS approach is as follows. Although the signal can be recovered using only a few samples, the traditional signal processing methods are not designed to process the compressed form of the signal. Therefore, the signal needs to be reconstructed before processing by the traditional signal processing methods. Unfortunately, reconstruction of a signal from its compressed representation is an energy-intensive task and cannot be performed on sensors due to their energy constraints. In WBANs, it is often necessary to process the data sampled by the biomedical sensors, e.g., to detect anomalies or compute statistics of interest. In this work, we evaluate a modified version of the classical CS approach that enables ECG and EEG signals to be processed on the sensor without being reconstructed (Fig. 3.4). The need for reconstruction can be circumvented by performing signal processing computations directly in the CS domain. Shoaib et al. have developed precisely such a method [254, 322], and demonstrated applications to various biomedical signals. This method reduces the computation energy significantly because much fewer data samples need to be processed. Generally, this method consists of three steps:

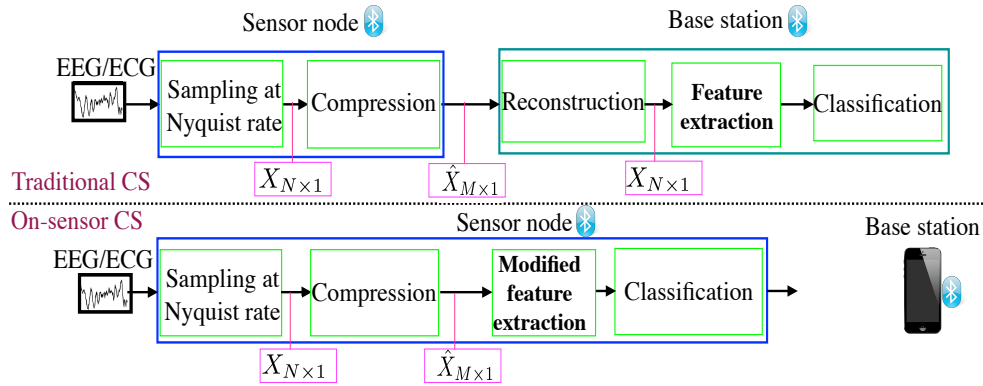


Figure 3.4: Traditional CS vs. on-sensor CS-based computation.

1. First, we compress the signal of interest using a low-rank random projection matrix. If we can represent the signal ( $X$ ) as  $\Psi * s$ , where  $s$  is a vector of  $K$ -sparse coefficients, a low-rank random matrix  $\Phi$  can be found to transform  $X$  to a set of  $M$  samples where  $O(K \log(N/K)) < M \ll N$ . We can then use the following equation for obtaining the compressed samples (denoted by  $\hat{X}$ ):

$$\hat{X}_{M \times 1} = \Phi_{M \times N} \times X_{N \times 1} \quad (3.11)$$

2. Second, we generate a feature extraction operation in the CS domain ( $\hat{H}$ ) from its equivalent in the Nyquist domain ( $H$ ) by minimizing the error in the inner product between feature vectors. For any feature extraction method, which can be represented by matrix  $H$ , we can derive an equivalent  $\hat{H}$  matrix in the CS domain [254, 322].
3. Third, we compute  $\hat{Y} = \hat{H} \times \hat{X}$  and provide  $\hat{Y}$  to the classification process.

The compression ratio is given by  $\alpha = N/M$ . It denotes the amount of compression obtained by the projection. Because CS leads to a drastic reduction in the number of samples, it has the potential for reducing the energy consumption of various sensors, including biomedical sensors. Direct computation on compressively-sensed data enables classification to be performed on the sensor node with one to two orders of magnitude energy reduction. We exploit this method for long-term continuous health monitoring.

In order to choose a reasonable compression ratio ( $\alpha$ ), we first need to compare the outcomes of the CS-based method for different compression ratios. Next, we discuss sensitivity (also called recall) and number of false alarms per hour (FA/h) for different compression ratios. Sensitivity represents the true positive rate. It measures

the percentage of actual positives that are correctly identified, such as the percentage of seizure conditions that are correctly classified as seizure. FA/h is the number of false positive outcomes in an hour of detection. Such an outcome is an error in classification since a test result indicates the presence of a medical condition that is not actually present.

Fig. 3.5 shows the sensitivity and FA/h for seizure detection with respect to different compression ratios. A compression ratio  $\alpha$  of  $8\times$  is seen to maintain sensitivity and FA/h for seizure classification. Moreover, an  $8\times$  compression ratio also exhibits similar results for arrhythmia detection [254, 322]. Thus, we assume this ratio for deriving the next set of results.

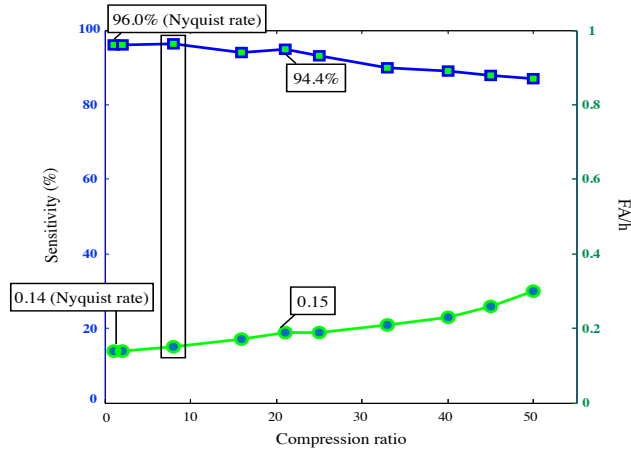


Figure 3.5: Sensitivity and FA/h of seizure detection classification with respect to compression ratio. Sensitivity and FA/h CS-based method using  $\alpha = 8\times$  are almost equal to the sensitivity and FA/h of the traditional method using Nyquist sampling ( $\alpha = 1\times$ ).

Next, we examine the EEG sensor in the context of seizure detection. Using the CS-based algorithm for seizure detection, the average value of total energy consumption of the EEG sensor (Table 3.12) is much less than that of the anomaly-driven signal processing method (Table 3.10). Relative to the baseline, the total energy consumption of the EEG sensor is reduced by up to  $724\times$  in this scheme. Table 3.13 shows the battery lifetime of the EEG sensor, which improves by a similar ratio.

Next, we examine an ECG sensor in the context of arrhythmia detection. Fig. 3.6 shows the total energy consumption and battery lifetime of the ECG sensor with respect to the frequency of occurrence of arrhythmia in a day. Similar to the previous scheme, we assumed that after detecting an arrhythmia, the ECG sensor transmits the information of a standard one-minute ECG strip to the base station.

Table 3.12: Average total energy consumption of the EEG sensor for CS-based computation

Sensor	Minimum (J/day)	Maximum (J/day)
EEG	6.93	9.50

Table 3.13: Average battery lifetimes of the EEG sensor for CS-based computation

Sensor	Minimum (days)	Maximum (days)
EEG	284.43	389.45

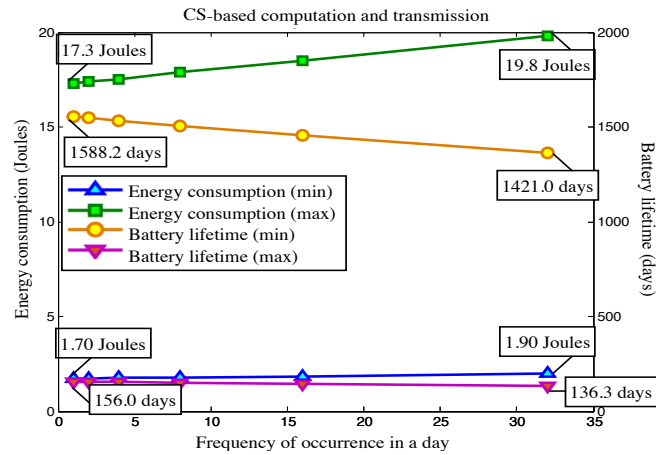


Figure 3.6: Energy consumption and battery lifetime of the ECG sensor for the CS-based method with respect to frequency of occurrence of arrhythmia in a day.

### 3.5.4 Summary of proposed schemes

Next, we summarize the results.

Fig. 3.7 shows the energy reduction in each sensor for the sample aggregation scheme. The energy reduction is an order of magnitude relative to the baseline.

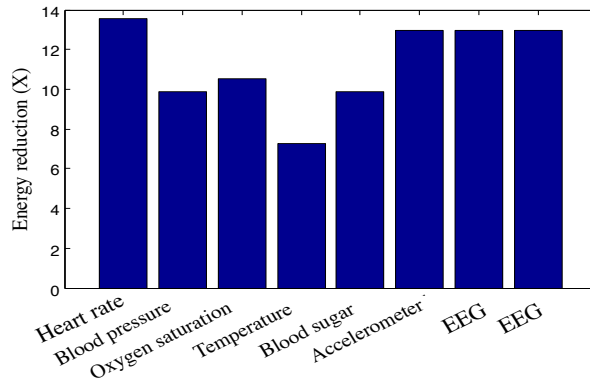


Figure 3.7: Energy reduction in each sensor when the sensor accumulates multiple samples in one packet. Raw data are assumed to be gathered at the maximum frequency.

Fig. 3.8 shows the energy reduction in EEG and ECG sensors when the maximum sampling frequency is employed. The CS-based approach can be seen to result in two to three orders of magnitude energy reduction relative to the baseline.

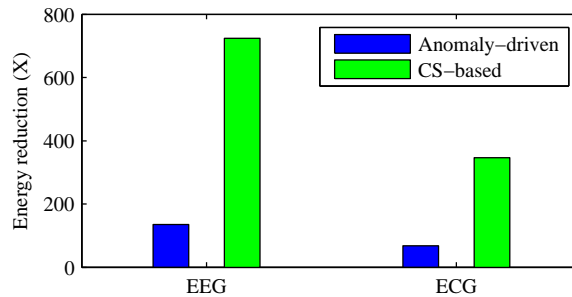


Figure 3.8: Energy reduction in EEG and ECG sensors. The number of arrhythmia events in a day is assumed to be 32, and raw data are assumed to be gathered at the maximum frequency.

### 3.6 Storage requirements

We have described three schemes for decreasing the energy consumption of sensors: (i) sample aggregation, (ii) anomaly-driven, and (iii) CS-based computation in the node. The first scheme cannot reduce the amount of required storage because we just accumulate multiple packets in order to reduce the number of transmissions, but we

still transmit all the data. However, if we can process the raw data in the sensor nodes and just transmit a chunk of raw data that is essential for future analysis, we would be able to reduce the amount of required storage significantly.

When anomaly-driven or CS-based signal processing is done on the sensor node, the sensor node samples, processes, and then transmits the data based on the result of processing. However, in the case of CS-based computation, the data can be transmitted in compressed form and reconstructed in the base station or server for further processing if needed.

Let us consider EEG sensors first. Based on the results in [358], we assume the mean seizure frequency and mean seizure duration to be 4.7 per month and 3.8 minutes, respectively. Therefore, as mentioned earlier, the EEG sensor needs to transmit information for a duration of 17.8 minutes per month, on an average. Table 3.14 shows the average amount of storage required for storing the raw data in the two schemes for seizure detection based on EEG signal analysis. In this table, the minimum (maximum) value corresponds to the minimum (maximum) sampling frequency. The anomaly-driven scheme can be seen to reduce the amount of storage required for storing these signals by 2418 $\times$ . The CS-based scheme provides another 8 $\times$  reduction on top of this.

As mentioned earlier, unlike seizures, the frequency with which arrhythmia occurs may vary significantly. In order to provide a quantitative analysis for storage requirements in the case of arrhythmia detection, we assume that, after each detection, the sensor transmits the information of a standard one-minute ECG strip to the base station. Fig. 3.9 shows the amount of required storage for the anomaly-driven and CS-based schemes with respect to the frequency of occurrence. Again, we observe the significant advantage of the CS-based scheme.



Table 3.14: Average storage required for long-term storage of processed data

Sensor	Minimum (MB/yr)	Maximum (MB/yr)
EEG (Anomaly)	1.87	18.65
EEG (Compressed)	0.23	2.33

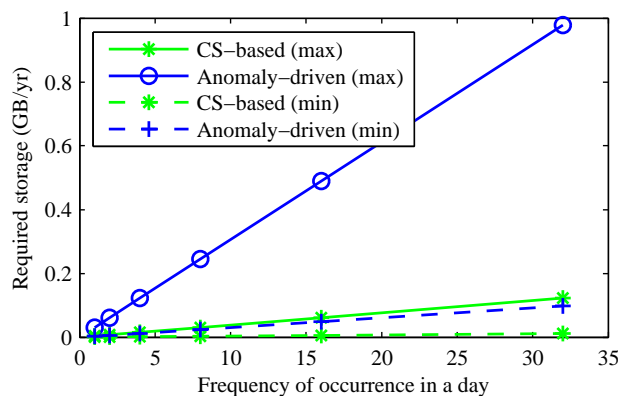


Figure 3.9: The amount of storage required for storing important chunks of ECG signals based on the results of computation.

## 3.7 Choosing the appropriate scheme and hardware platform

In this section, we first compare the different schemes we presented, and discuss how the appropriate scheme can be chosen for each sensor. Second, we discuss two different types of hardware platforms: application-specific integrated circuit (ASIC) and general-purpose commercial products. We describe the potential benefits of using ASIC hardware.

### 3.7.1 The appropriate scheme for each sensor

Each scheme has its own advantages and disadvantages. For example, sample aggregation decreases energy consumption at the cost of increased latency. Schemes that use on-sensor computation can significantly increase battery lifetime, however, provide less raw data to the physicians.

Choosing an appropriate scheme for each sensor depends on medical considerations such as tolerable latency and patient's condition. Next, we discuss different considerations that should be taken into account by designers, in addition to the battery lifetime and storage requirement.

**Latency:** Latency is the time interval between the occurrence of an anomaly and the response that is provided by medical devices, physicians or medical personnel. Tolerable latency depends on the patient's condition.

- *Example 1:* Consider a continuous health monitoring system that is used to monitor a healthy subject who does not have any history of a serious illness. The system can be configured for this subject to provide routine medical check by collecting and sending medical information to physicians or hospitals at long intervals (e.g., once a day). In fact, latency is not an important factor in this case, and the sensor can be configured to minimize the energy and storage requirements. For example, we can use the CS-based computation method for both EEG and ECG sensors and use the aggregation method for other low-frequency sensors (e.g., temperature) to maximize the battery lifetime of all sensors.
- *Example 2:* Consider a continuous health monitoring system that is used to monitor a subject who has previously been diagnosed with high blood glucose. As a result, any rapid rise in blood glucose should be detected and addressed immediately. In such a scenario, the latency that might be added by using sample aggregation for blood glucose levels may not be acceptable.

Among all the discussed schemes, sample aggregation is the only one that may lead to a non-negligible increase in latency. Therefore, the number of samples that can be aggregated in one packet before transmission can be limited by the latency that can be tolerated.

Table 3.15: Comparison of different schemes

Scheme	Latency	Amount of raw data transmitted	Extensibility
Baseline	Low	All raw data	High
Sample aggregation	Varies	All raw data	High
Anomaly-driven	Low	A portion of collected data	Low
CS-based	Low	A portion of compressed data	Low

**2. Amount of raw medical data transmitted:** Physicians may want to examine raw medical data over a specific time period to verify on-sensor computation. The amount of raw information that needs to be transmitted and stored for further analysis varies from one device to another. It also depends on the medical condition of the patient.

Schemes that use on-sensor computation (anomaly-driven transmission and CS-based computation and transmission) only transfer a small portion of raw data containing important information about the occurrence of the anomaly. However, if more medical information is required to be transferred to the base station, the designers should use the other schemes or send more raw data (e.g., over an hour of measurements) after detecting an anomaly.

**3. Extensibility:** This is a design consideration where the implementation takes future modifications of the algorithms into consideration. High extensibility implies that applications of a biomedical sensor can be extended in the future with a minimum level of effort. Generally, schemes that rely on on-sensor computation are less extensible in comparison to schemes that transfer raw data to the base station due to the fact that they are designed to minimize the energy consumption and the amount of required storage in certain applications (e.g., arrhythmia detection). Therefore, if a physician wants to change the computation algorithm of the medical device, another device should be designed and used, or at least the device’s firmware should be updated each time.

Table 3.15 compares various schemes.

Potentially, different schemes can be used in the health monitoring system for different sensors. Since the sensors are located on different parts of the body, they cannot share on-sensor resources (e.g., the battery). Thus, their battery lifetimes are independent.

We can also use a combination of schemes even in just one sensor. For example, we can combine one of the schemes that uses on-sensor computation (anomaly-driven or CS-based) with the sample aggregation scheme to reduce total energy consumption even more. However, since in anomaly-driven and CS-based schemes, the computation energy is dominant and the transmission energy is only a small fraction of total energy consumption, the addition of the sample aggregation scheme will not provide a significant energy reduction.

### **3.7.2 The hardware platform**

An appropriate hardware platform can be chosen from various general-purpose commercial products or else designed as ASIC hardware. General-purpose commercial products enable the designers to implement an algorithm or prototype of a biomedical sensor quickly. However, they are not optimized for the specific application. Anomaly-driven and CS-based schemes use some algorithms to process the raw data on the EEG or ECG sensor nodes before transmission. An ASIC could be designed for these algorithms. In particular, in our computation schemes, the on-sensor computation algorithm uses a support vector machine as a classifier to detect anomalies (arrhythmia and seizure). Specialized processors and architectures that enable efficient handling of data structures used by the classifier could reduce computation energy even further [365–371]. Further energy reduction can be achieved through supply voltage scaling. The total energy is determined primarily by the sum of dynamic (active-switching) energy and the static (leakage) energy. However, reduction in active-switching energy due to supply voltage scaling is opposed by an increase

in leakage energy. Therefore, there is an optimal supply voltage at which the circuit attains its minimum energy consumption and still work reliably. This could be addressed in an ASIC. However, such an ASIC may not be desirable from a cost perspective and does not improve transmission energy.

## 3.8 Chapter summary

In this chapter, we discussed a secure energy-efficient system for long-term continuous health monitoring. We discussed and evaluated various schemes with the help of eight biomedical sensors that would typically be part of a WBAN. We also evaluated the storage requirements for long-term analysis and storage.

Among the four schemes we evaluated (including the baseline scheme), we showed that the CS-based scheme provides the most computational energy savings (e.g., up to 724× for ECG sensors) because it needs to process much fewer signal samples. For low-sample-rate sensors, we can achieve significant energy savings by simply accumulating the raw data before transmitting them to the base station.

In addition, the CS-based scheme also allows us to reduce the storage requirements significantly. For example, for an EEG sensor based seizure detection application, we achieve total storage savings of up to 19344×. The results indicate that long-term continuous health monitoring is indeed feasible from both energy and storage points of view.

Finally, we compared all proposed schemes and discussed how a continuous long-term health monitoring system should be configured based on patients' needs and physicians' recommendations.

## Chapter 4

# OpSecure: A Secure Optical Communication Channel for Implantable Medical Devices

Implantable medical devices (IMDs) are opening up new opportunities for holistic health care by enabling continuous monitoring and treatment of various medical conditions, leading to an ever-improving quality of life for patients. Integration of radio frequency (RF) modules in IMDs has provided wireless connectivity and facilitated access to on-device data and post-deployment tuning of essential therapy. However, this has also made IMDs susceptible to various security attacks. Several lightweight encryption mechanisms have been developed to prevent well-known attacks, e.g., integrity attacks that send malicious commands to the device, on IMDs. However, lack of a secure key exchange protocol (that enables the exchange of the encryption key while maintaining its confidentiality) and the immaturity of already-in-use wakeup protocols (that are used to turn on the RF module before an authorized data transmission) are two fundamental challenges that must be addressed to ensure the security of wireless-enabled IMDs.

In this chapter, we introduce OpSecure, an optical secure communication channel between an IMD and an external device, e.g., a smartphone. OpSecure enables an intrinsically user-perceptible unidirectional data transmission, suitable for physically-secure communication with minimal size and energy overheads. Based on OpSecure, we design and implement two protocols: (i) a low-power wakeup protocol that is resilient against remote battery draining attacks, and (ii) a secure key exchange protocol to share the encryption key between the IMD and the external device. We investigate the two protocols using a human body model [372].

## 4.1 Introduction

IMDs are revolutionizing health care by offering continuous monitoring, diagnosis, and essential therapies for a variety of medical conditions. IMDs can capture, process, and store various types of physiological signals, and are envisioned as the key to enabling a holistic approach to health care [11]. Rapid technological advances in wireless communication, sensing, signal processing, and low-power electronics are transforming the design and development of IMDs. State-of-the-art IMDs, e.g., pacemakers and implantable drug infusion systems, commonly support short-range wireless connectivity, which enables remote diagnosis and/or monitoring of chronic disorders and post-deployment therapy adjustment [19]. Moreover, wireless connectivity allows health care professionals to non-intrusively monitor the device status, e.g., physicians can gauge the device battery level without performing any surgery.

Despite the numerous services that wireless connectivity offers, it may make an IMD susceptible to various security attacks. Previous research efforts [18,19,112,272,373,374] have demonstrated how wireless connectivity may be a security loophole that can be exploited by an attacker. For example, Halperin et al. [19] show how an attacker can exploit the security susceptibilities of the wireless protocol utilized in

an implantable cardioverter defibrillator (ICD) to perform a battery draining attack against the device. This is an attack that aims to deplete the device battery by frequently activating/using the RF module. Moreover, they show that it is feasible to exploit these susceptibilities to change on-device data or the current operation of the device. Gollakota et al. [373] explain how an adversary can eavesdrop on an insecure communication channel between an IMD and its associated external device to extract sensitive information about the patient.

To prevent battery draining attacks, an attack-resilient wakeup protocol, which activates the RF module before every authorized communication, must be used. Today's IMDs often employ a magnetic switch, which turns on their RF module in the presence of an external magnet. Unfortunately, it has been shown that magnetic switches cannot prevent battery draining attacks since they can be easily activated by an attacker (without the presence of a nearby magnet) if a magnetic field of sufficient strength is applied [19, 375].

In order to secure the RF wireless channel between the IMD and the external device and avert the risk of eavesdropping on the channel, the use of cryptographic techniques, e.g., data encryption, has been suggested [17, 376]. However, traditional cryptographic techniques are not suitable for IMDs due to limited on-device resources, e.g., limited storage and battery energy. For example, asymmetric encryption mechanisms are not applicable to resource-constrained IMDs since they would significantly decrease the IMD battery lifetime [376, 377]. Several lightweight symmetric encryption mechanisms have been proposed in the last decade to ensure the security of communication protocols utilized in IMDs (see [378] for a survey). While symmetric cryptography may offer a secure lightweight solution, it is greatly dependent on a secure key exchange protocol. Such a protocol enables sharing of the encryption key between the IMD and the external device. As extensively described later in Section 4.2.2, previously-proposed key exchange protocols have various shortcomings



since *they either add significant overheads to the IMD or are susceptible to remote eavesdropping.*

In this chapter, we present practical key exchange and wakeup protocols, which complement lightweight symmetric encryption mechanisms, to thwart common security attacks against insecure communication channels. We introduce a secure optical communication channel, which we call OpSecure. We discuss the design and implementation of a low-power wakeup protocol and a secure key exchange protocol based on OpSecure. Our main contributions can be summarized as follows:

1. We introduce OpSecure, an optical secure unidirectional (from the external device to the IMD) communication channel.
2. We present an attack-resilient low-power wakeup protocol for IMDs based on OpSecure.
3. We propose a secure key exchange protocol, which enables sharing of the encryption key between IMDs and their associated external devices.
4. We discuss the design and implementation of a prototype IMD platform that supports the proposed protocols and present evaluation results for the prototype.

The remainder of this chapter is organized as follows. In Section 4.2, we explain why wakeup and key exchange protocols are essential for IMDs and briefly discuss the shortcomings of previously-proposed protocols. We present OpSecure and summarize its advantages in Section 4.3. We also propose a wakeup protocol and a key exchange protocol based on OpSecure. In Section 4.4, we describe our prototype and experimental setup. We evaluate the prototype implementation that supports both the proposed protocols (wakeup and key exchange) in Section 4.5. Finally, we conclude in Section 4.6.

## 4.2 Problem definition

In this section, we first explain the role of wakeup and key exchange protocols in providing secure communication for IMDs. Then, we present a brief overview of prior related work on these protocols and summarize their shortcomings.

### 4.2.1 Wakeup and key exchange protocols

As mentioned earlier, the IMD and its associated external device commonly have an RF channel that is used for bidirectional data communication. We assume that both devices are capable of using symmetric encryption for protecting the data sent over the RF channel. The overall system architecture that we target is illustrated in Fig. 4.1.

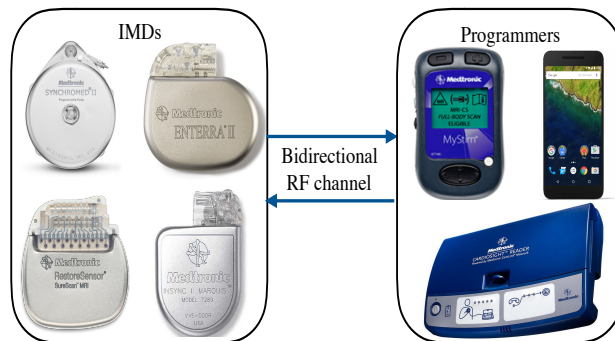


Figure 4.1: Overall system architecture: IMD and external device have a bidirectional RF channel that supports symmetric encryption, e.g., Bluetooth Low Energy.

Due to severe on-sensor energy constraints, the RF module must be enabled only when absolutely needed, e.g., when an authorized physician wants to access on-device data. Thus, prior to each data transmission, the RF module should be activated using a pre-defined wakeup protocol. This protocol must satisfy two main design requirements. First, it must be resilient against battery draining attacks so that an attacker cannot activate the RF module. Second, it should add negligible size and energy overheads to the device.

After enabling the RF module by the wakeup protocol, data can be transmitted over the bidirectional communication channel that supports symmetric encryption. Since symmetric encryption is based on an encryption key, an exchange protocol must be used to securely exchange the encryption key between the IMD and the external device. Every practical key exchange protocol must satisfy the following design requirements. First, it must guarantee the confidentiality of the encryption key and be resilient to remote eavesdropping. Second, its size and energy overheads must be minimal. Third, it must ensure that health care professionals can access and control the IMD without a notable delay in an emergency situation in which the patient needs immediate medical assistance.

### **4.2.2 Related work**

Next, we summarize previous research efforts on both wakeup and key exchange protocols and highlight their shortcomings.

#### **Wakeup protocols**

As mentioned earlier, a magnetic switch is commonly integrated into today's IMDs to turn on the RF module when needed. However, magnetic switches are vulnerable to battery draining attacks since they can be remotely activated [19]. A few wakeup protocols have recently been presented in the academic literature. For example, the wakeup protocol presented by Halperin et al. [19] relies on an authentication technique in which the IMD harvests the RF energy supplied by the external device itself. The RF module is powered by the battery only after the external device is authenticated. However, the RF energy harvesting subsystem needs an antenna, which imposes a significant size overhead on the IMD. Kim et al. [272] suggest a wakeup scheme in which the IMD activates the RF module when it detects the vibration generated by an external electrical motor. Their scheme adds minimal size and energy

overheads to the IMD since it only needs the addition of a low-power accelerometer to the IMD. However, in practice, the patient’s regular activities, e.g., running, may unintentionally and frequently turn on the RF module, and as a result, deplete the device battery.

### **Key exchange protocols**

The use of a pre-defined password, which is stored on the device and known to the user, is a longstanding tradition in the security community. However, a key exchange approach that needs active user involvement, e.g., asking the user to remember a password and give it to authorized physicians upon request, is not suitable for IMDs since the user may not be able to cooperate with health care professionals in an emergency, e.g., when the patient is unconscious. In order to minimize user involvement, previous research studies have proposed several user-independent key exchange protocols. Next, we summarize them and discuss their shortcomings.

**1. *Ultraviolet tattoos:*** Schechter [379] presented a scheme in which a fixed user-selected human-readable key is tattooed directly on the patient’s body using ultraviolet ink. In this protocol, all devices that need to communicate with the IMD must be equipped with a small, reliable, and inexpensive ultraviolet light-emitting diode and an input mechanism for key entry. This tattoo-based approach has two limitations. First, the design requires the patient to agree to acquire a tattoo, which significantly limits its applicability [380]. Second, if the password becomes compromised, access by the attacker cannot be prevented easily since the password cannot be changed in a user-convenient manner.

**2. *Physiological signal-based key generation:*** A few physiological signal-based key generation protocols have been proposed [381–383], which can be used to generate a shared key for the IMD and the external device from synchronized readings of physiological signals, such as an electrocardiogram (ECG). Unfortunately, the robust-

ness and security properties of keys generated using such techniques have not been well-established [272].

**3. Using an acoustic side channel:** Halperin et al. presented a key exchange protocol based on acoustic side channels in [19]. Unfortunately, their protocol is susceptible to remote acoustic eavesdropping attacks [384] and, as a result, does not offer a secure key exchange protocol. Moreover, it is not reliable in noisy environments since they utilized a carrier frequency within the audible range. Furthermore, it imposes a significant size overhead [272].

**4. Using a vibration side channel:** Kim et al. [272] proposed a key exchange protocol that relies on a vibration side channel, i.e., a channel in which the transmitter is a vibration motor, and the receiver is an accelerometer embedded in the IMD. This protocol requires negligible size and energy overheads. However, it has two shortcomings. First, since electrical motors generate capturable electromagnetic and acoustic waves during their normal operation [112], an adversary might be able to extract the key from signals leaked from the vibration motor. Second, since the method uses an accelerometer to detect vibrations, regular physical activities, e.g., running, may be interpreted as key transmission. This can reduce the battery lifetime of the IMD since the device needs to listen to the communication channel even when there is no actual transmission.

In this chapter, we aim to address the above-mentioned shortcomings of previously-proposed protocols, *in particular size/energy overheads and vulnerability to eavesdropping*, through a simple low-power, yet secure key exchange protocol using *visible light*.

## 4.3 The proposed channel and protocols

In this section, we first describe OpSecure and highlight its advantages. Then, we discuss the two proposed protocols that are based on OpSecure.

### 4.3.1 OpSecure: The proposed channel

Optical data transmission (also called light-based wireless communication) is a well-known communication type that has attracted increasing attention in recent years due to its potential to offer high-speed wireless communication (as a complement or an alternative to WiFi) for a variety of portable devices, e.g., smartphones and laptops. Previous research studies [385,386] demonstrate that optical communication channels can enable high-rate data transmission (the transmission rate can vary from several hundred *Mb/s* to a few *Gb/s*). In an optical channel, data packets flow from a light source (transmitter) to a light sensor (receiver). Therefore, to establish a bidirectional communication channel between two devices, both devices must have a light source and a light sensor.

There is a basic domain-specific challenge that must be addressed when developing an optical communication scheme for IMDs: integration of light sources into IMDs imposes significant size and energy overheads on these resource-constrained devices. Hence, it is not feasible to transmit data from an IMD to an external device via an optical channel even though such a channel can potentially enable two-way communication. Unlike light sources, state-of-the-art already-in-market light sensors are sufficiently compact and energy-efficient to be embedded in IMDs. Therefore, a one-way communication channel, which transmits data from the external device to the IMD, can be implemented with minimal size and energy overheads. We implement such a channel and call it OpSecure.

OpSecure is intrinsically secure due to its close proximity requirement and high user perceptibility. Visible light attenuates fast in the body and, hence, can only be captured within a very close range. As demonstrated later in Section 4.5, if the light source is in contact with the body and directed at the IMD, it can penetrate deep enough into the body to reach the IMD. However, a passive adversary cannot eavesdrop on OpSecure without an eavesdropping device attached to the body, which is very likely to be noticed by the patient.

As illustrated in Fig. 4.1, the external device may vary from specialized IMD programmers, i.e., external devices that are specifically designed to query the IMD data or send commands to the IMD, to general-purpose portable devices, e.g., smartphones. As in the case of vibration-based key exchange [272], we implement our prototype using a smartphone used as the external device (see Fig. 4.2). This has three advantages. First, the component that we need in the external device for establishing OpSecure is already present in smartphones (the flashlight can be used as a light source). Second, smartphones have become the dominant form of base stations for a large number of medical devices since they are ubiquitous and powerful, and provide various technologies needed for numerous applications [94]. As a result, they can be used as a base station for collecting and processing several types of physiological data (including data collected by IMDs) [11]. Third, smartphones can easily support highly-secure encrypted transmission, which deters several potential attacks against the IMD [37].

However, note that OpSecure can also be implemented on other devices that are used to communicate with the IMD with minimal overheads if they can be equipped with a small light source and an input mechanism for key entry.



Figure 4.2: The IMD (pacemaker) has an embedded light sensor, and the smartphone flashlight acts as a light source.

### 4.3.2 The proposed protocols

Next, we describe both the wakeup and key exchange protocols that we have developed based on OpSecure.

#### Wakeup protocol

As mentioned earlier, when the light source is in contact with the human body, visible light can penetrate deep enough into the body to reach the IMD. However, it attenuates very fast in the body. We exploit this fundamental characteristic of visible light to develop a wakeup protocol that works as follows. The smartphone fully turns on its flashlight and the IMD wakes up periodically to check if a light source is on the body, i.e., it checks if the intensity of the light received by the IMD is above a pre-defined threshold. *The presence of an on-body light source* that points to the IMD is interpreted as the presence of a trusted external device.

As shown later in Section 4.5, the proposed wakeup protocol adds minimal size and energy overheads to the device. Unlike a majority of previously-proposed protocols, it also provides immunity against battery draining attacks. In fact, an attacker, who



wants to wake up the RF module, needs to attach a light source to the patient’s body at a location close to the IMD. Such an action can be easily detected by the patient.

### Key exchange protocol

Assuming the IMD and the external device use a bidirectional RF communication protocol that supports symmetric encryption, our protocol can be used to transmit a randomly-generated key from the smartphone to the IMD. For each key exchange:

**Step 1:** The smartphone first generates a random key  $K \in \{0,1\}^N = k_1k_2\dots k_N$  of length  $N$ , and prepares a key packet as  $Key_{packet} = Pre||K||Post$ , where  $Pre$  and  $Post$  are two fixed binary sequences that are concatenated with the key to mark the beginning and end of a key packet.

**Step 2:** The physician places the smartphone on the patient’s body so that its flashlight is directed at the light sensor of the IMD (IMDs commonly have a fixed location and can be easily detected by the physician).

**Step 3:** The external device uses on-off keying (OOK) modulation to transmit  $Key_{packet}$ : the flashlight is turned on (off) for a fixed period of time ( $T_{step}$ ) to transmit bit “1” (“0”). *Algorithm 1* shows a simplified pseudo-code for this step. It first computes  $T_{step} = \frac{1000}{R}$  ms, where  $R$  is the transmission rate given by the user. Then, it calls the *keySegmentation* procedure, which divides  $Key_{packet}$  into smaller segments such that each segment only consists of all “1”s or all “0”s. The *keySegmentation* procedure outputs an array of integer numbers ( $segments[]$ ) so that: (i) the absolute value of each element in the array represents the length (the number of bits) of each of the above-mentioned segments, and (ii) the sign of the element shows whether bits of the segment are all “1”s or all “0”s, i.e., if all bits in the  $i$ th segment are “1”,  $segments[i] > 0$ , otherwise,  $segments[i] < 0$  (see Fig. 4.3 for an example). Finally, *Algorithm 1* turns on/off the flashlight with respect to the absolute values of the

elements of  $segments[]$  and  $T_{step}$ , i.e.,  $Abs(segment) * T_{step}$  determines how long the flashlight must be kept on/off.

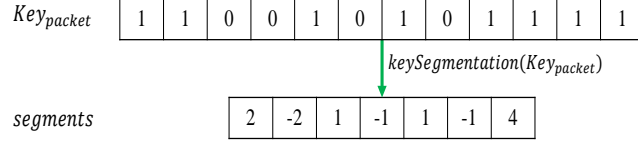


Figure 4.3:  $keySegmentation$  outputs  $segments[]$  given  $Key_{packet}$ .

*Algorithm 1: flashlightControl procedure*

---

Given: The key packet ( $Key_{packet}$ ) and transmission rate ( $R$ )

---

1.  $T_{step} \leftarrow 1000/R$
  2.  $segments[] \leftarrow keySegmentation(Key_{packet})$
  3. For each segment in  $segments[]$
  4.    If( $segment > 0$ )
  5.         $turnTheLightOn(Abs(segment) * T_{step})$
  6.    else
  7.         $turnTheLightOff(Abs(segment) * T_{step})$
  8.    end
  9. end
- 

**Step 4:** The IMD demodulates the received visible light and recovers  $Key_{packet}$ . Then, it extracts  $K$  from  $Key_{packet}$  by removing  $Pre$  and  $Post$ . Thereafter, it encrypts a fixed pre-defined confirmation message  $M_{confirm}$  using  $K$  and transmits this message  $C = ENC(M_{confirm}, K)$  to the smartphone.

**Step 5:** The smartphone checks if it can successfully decrypt the received message  $C$  using  $K$ , i.e., if  $DEC(C, K) = M_{confirm}$ . If the message can be successfully de-

encrypted, the smartphone knows that the IMD received the key  $K$  correctly, and then subsequent RF data transmissions are encrypted using key  $K$ .

In addition to key exchange, the above-mentioned protocol (the first three steps) can be used to transmit data/commands from the smartphone to the IMD without using the RF module. For example, a predefined stream of bits can be reserved for the shutdown command, i.e., a command that entirely disables the device, and sent using this protocol when needed. Note that the IMD cannot provide any feedback via OpSecure since the channel is unidirectional. However, modern IMDs commonly have an embedded beeping component that warn the patient in different scenarios, e.g., when the RF module is activated [19] or when the device’s battery level is low [387]. Such a component can be also used to provide feedback when the IMD receives a predefined message over OpSecure, e.g., the beeping component can generate three beeps when the IMD receives the shutdown command via OpSecure.

## **4.4 The prototype implementation and body model**

In this section, we first describe the wireless-enabled IMD that we implemented and the smartphone application that we developed. Then, we describe the human body model, which we used to evaluate the prototype implementation.

### **4.4.1 Prototype implementation**

As mentioned earlier, OpSecure establishes a unidirectional communication channel between the IMD and the external device. We implemented a wireless-enabled IMD prototype based on ATmega168V [388] (a low-power microprocessor from Atmel), TEMT6000 [389] (an ambient light sensor from Vishay Semiconductors), and RFD77101 [390] (a Bluetooth Low Energy module from Simblee). The prototype

does not offer any health monitoring/therapeutic operations. Indeed, it only implements the two proposed protocols. TEMT6000 enables OpSecure by receiving visible light generated by the user’s smartphone, and RFD77101 provides the bidirectional RF communication that can be secured using a symmetric encryption mechanism for which the key can be exchanged over OpSecure. We also developed an Android application that can be used to either wake the IMD up or generate and transmit a random key to the IMD using the smartphone flashlight. The application allows the user to set the key length ( $N$ ) and transmission rate ( $R$ ). Fig. 4.4 illustrates the application and the prototype. It also demonstrates how the application turns the flashlight on/off to transmit the key. For the key exchange example shown in Fig. 4.4, the transmission rate and key length are set to 20  $b/s$  and 4  $b$  (in practice, the  $N$  used would be much higher, e.g., 64  $b$ ), respectively. Thus, the smartphone needs  $T_{step} = \frac{1000}{4} = 50 \text{ ms}$  for transmitting a single bit. In this implementation, the application uses two 4-bit sequences (“1100” and “1111”) to mark the beginning and end of the key.

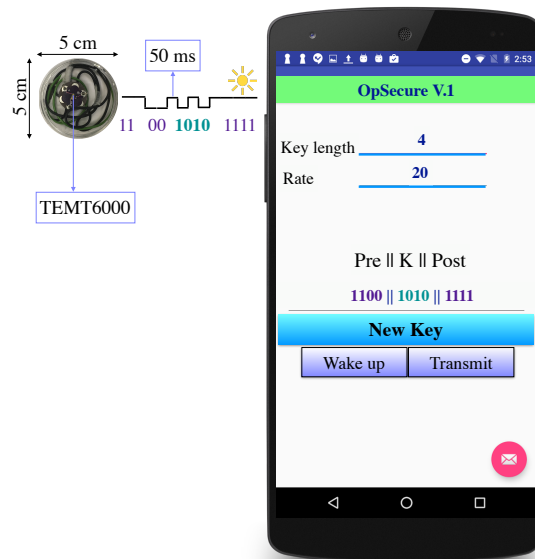


Figure 4.4: The smartphone generates a 4-bit key and transmits the key over OpSecure. The application allows the user to control both the key length ( $N$ ) and transmission rate ( $R$ ).

We evaluated our protocols using three different smartphones: Nexus 5s, Nexus 6, and MotoX.

#### 4.4.2 The bacon-beef body model

The bacon-beef model for the human body has been previously used in several research studies [19, 272, 373]. Although this model may not fully represent all the characteristics of the human body, it has been accepted as a valid testing methodology by researchers working on IMDs [391] due to the difficulties associated with more realistic experiments, e.g., laws that permit and control the use of animals for scientific experimentation. The bacon-beef body model consists of a thin layer of bacon on a thick layer of 85% lean ground beef (Fig. 4.5). In our experiments, the IMD prototype is placed between the bacon and the ground beef, which reflects the typical placement of ICDs [19]. The smartphone is placed on top of the bacon layer above a transparent plastic sealing.

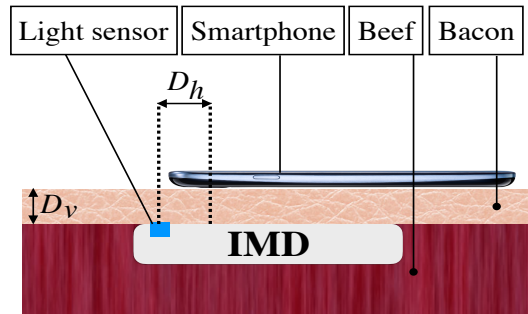


Figure 4.5: Experimental setup: The smartphone is placed on top of the bacon layer above a transparent plastic sealing.

### 4.5 Evaluation of the proposed protocols

In this section, we present evaluation results for the prototype implementation. In particular, we evaluate the transmission range (how far the smartphone can be placed

from the IMD and have the visible light still reach it), wakeup/exchange time (the time needed by the wakeup/exchange protocol), protocol overheads (size and energy), and their security.

#### 4.5.1 Transmission range

We evaluated the prototype using the bacon-beef model for the human body. We varied both the vertical distance and horizontal distance between the IMD and the smartphone (shown as  $D_v$  and  $D_h$  in Fig. 4.5, respectively) to evaluate the vertical and horizontal transmission range (maximum  $D_v$  and  $D_h$  at which the visible light can still reach the IMD). We found that both maximum  $D_v$  and  $D_h$  are independent of the key length and transmission rate. They mainly depend on the maximum light intensity that the flashlight has to offer. For the three smartphones we used in our experiments (Nexus 5s, Nexus 6, and MotoX), the maximum light intensity generated by their flashlights is almost the same. Indeed, for all three smartphones, the maximum vertical (horizontal) transmission range was about 2 *cm* (1.5 *cm*). Thus, if the physician places the smartphone on the patient’s body and keeps the smartphone within 1.5 *cm* of the IMD’s light sensor ( $D_h < 1.5$  *cm*), the visible light can easily reach a depth of 1 *cm* (the typical  $D_v$  for IMDs such as ICDs [19]). The IMD location is fixed and easily recognizable by inspecting the patient’s skin under which the IMD is implanted. Therefore, ensuring  $D_h < 1.5$  *cm* would be straightforward for a physician.

#### 4.5.2 Transmission quality

We transmitted 100 different keys from each of the three smartphones to the IMD, with each smartphone placed within the horizontal transmission range of OpSecure ( $D_h < 1.5$  *cm*), and with the IMD under a 2 *cm* layer of bacon (2 *cm* is the vertical transmission range). We found that all keys were transmitted over OpSecure without

any error. Therefore, the bit error rate (the number of received bits that have been altered due to noise, interference, distortion, etc.) was zero in all these transmissions. In order to evaluate the effect of ambient noise (e.g., other light sources in the environment such as sunlight or a car’s headlight) on transmission quality, we placed a powerful (3000-lumen) light source at a close distance (1  $m$ ) from the IMD. We noticed that the intensity of the visible light received by the IMD remained almost the same in the presence of the external light source. Indeed, the external light source did not negatively impact the quality of transmission at all.

### 4.5.3 Wakeup/exchange time

Next, we evaluated the wakeup time (the time that the wakeup protocol takes to detect the presence of the external device and turn on the RF module) and the exchange time (how long the key exchange protocol takes to exchange the encryption key).

**Wakeup time:** As mentioned in Section 4.3, the wakeup protocol periodically places the light sensor in the full operating mode, in which the sensor samples the light intensity, to check if the smartphone flashlight is present. The wakeup time depends on two parameters: (i) how long the light sensor is in the full operating mode ( $T_{operation}$ ), and (ii) how long the light sensor remains in the standby mode ( $T_{standby}$ ) in which the sensor is disabled.  $T_{operation}$  and  $T_{standby}$  should be set with regard to the maximum tolerable wakeup time and energy consumption of the wakeup protocol. For example, if we set  $T_{standby} = 1.8\ s$  and  $T_{operation} = 0.2\ s$ , the IMD turns on the light sensor for 0.2  $s$  and then disables it for 1.8  $s$ . In this case, the worst-case wake up time will be  $T_{standby} + T_{operation} = 2\ s$ . As described later in Section 4.5.4, the worst-case wakeup time can be traded off against energy consumption by varying either  $T_{standby}$  or  $T_{operation}$ .

**Exchange time:** The exchange time can be readily calculated as  $T_{EX} = N/R$ , where  $N$  and  $R$  are the key length and transmission rate, respectively.  $N$  depends on the encryption mechanism and is commonly 64  $b$  or 128  $b$ . The transmission rate generally depends on two parameters: (i) the blinking frequency of the light source, i.e., how fast the light source can be turned on and off, and (ii) how fast the light sensor can sample the visible light. In our experiments, the maximum blinking frequency offered by the smartphones was within a 20-30  $Hz$  range, and the light sensor was able to sample visible light with a sampling rate of a few hundred  $Hz$  (a sampling rate of 60  $Hz$  is sufficient to recover the key when the blinking frequency is 30  $Hz$ ). Therefore, the maximum blinking frequency of the smartphone flashlight limited the transmission rate. In fact, the maximum transmission rate was within the range of 20  $b/s$  (for MotoX) to 30  $b/s$  (for Nexus 6). As a result, the minimum time needed for exchanging a packet, that includes a key of length 64  $b$  (128  $b$ ) and both  $Pre$  and  $Post$ , was within the range of 2.4  $s$  to 3.6  $s$  (4.5  $s$  to 6.8  $s$ ).

Note that different smartphones may offer different maximum transmission rates. However, the IMD does not need to know the transmission rate  $R$  beforehand since  $R$  can be computed based on the binary sequence  $Pre$ , which is known to the IMD. In our prototype implementation, where the first two bits of  $Pre$  are always “11” (as mentioned in Section 4.4,  $Pre$ =“1100”),  $R$  can be computed as follows:  $R = \frac{1000}{T_{step}} ms$ , where  $\frac{1000}{T_{step}} ms$  is half of the duration of the time frame in which the IMD observes the  $Pre$  sequence.

#### 4.5.4 Size and energy overheads

Next, we examine the size and energy overheads that the proposed protocols add to the IMD.

Light sensors commonly consist of a phototransistor in series with a small resistor that converts received light to a voltage. Light sensors typically also have an analog-



to-digital converter (ADC) that converts this voltage to a digital number. Therefore, a light sensor consists of simple circuitry that can be implemented in a very small area. In order to save more area on the chip, manufacturers may also use an ADC already incorporated into the IMD and just add a phototransistor/resistor. In both cases, the size overhead is negligible.

The energy overhead is the additional energy consumed by the light sensor, which is added to the IMD to enable transmission over OpSecure. The energy consumption of a light sensor (even one with a built-in ADC) is typically very small, and thus results in negligible energy overhead on the IMD. We investigate the energy overheads for each protocol using a realistic example next.

Consider a typical ICD with a 1.5-Ah battery and 90-month lifetime (it consumes about 23.14  $\mu A$  current on an average). We can either use a light sensor with a built-in ADC such as MAX44007 [388] or a light sensor without an ADC such as TEMT6000 [389] (used in our prototype). Next, we discuss the energy overheads of wakeup and key exchange protocols for the ICD in both cases.

**Wakeup protocol:** We configure the IMD so that the light sensor is in the full operating mode for  $T_{operation} = 0.2$  s after being in the standby mode for  $T_{standby} = 1.8$  s. Thus, the light sensor only spends 10% of the time in the full operating mode. MAX44007 drains 0.65  $\mu A$  (100 pA) from the battery in the full operating (standby) mode, thus draining 65.09 nA on an average. In this case, the energy overhead of the wakeup protocol is less than 0.3% of the total energy consumption. If we use TEMT6000, the phototransistor in series with the resistor and the built-in ADC, when operating in the full operating mode, drain a few nA [389] and tens of nA [11] from the battery, respectively. Therefore, their energy overheads are negligible in comparison to the total energy consumption of the ICD. Reducing  $\frac{T_{operation}}{T_{operation}+T_{standby}}$  makes the energy overhead even smaller.

**Key exchange protocol:** After waking up the RF module, the physician can use the smartphone to initiate the key exchange procedure in which the IMD configures the light sensor to sense in the full operating mode for a few seconds. However, key exchange is a very rare event for two reasons. First, a key that is exchanged once can typically be used for a long period of time unless the user suspects that the key is compromised. Second, the communication between the IMD and the external device is very sporadic (e.g., the number of transmissions varies from a few times per day to a few times per year). Thus, even if the external device transmits a new key for each communication session, the timeframe in which the light sensor operates in the full operating mode to exchange the key is negligible in comparison to the device lifetime. Consequently, the key exchange protocol adds almost-zero overhead to the IMD.

#### 4.5.5 Security analysis

In this section, we evaluate the feasibility of two types of security attacks on OpSecure.

**Eavesdropping:** We investigated the possibility of both near-IMD and remote eavesdropping attacks.

We first placed the smartphone on the chest of a human subject and placed a light sensor close to the smartphone to measure the light intensity on the body surface at varying distances from the smartphone flashlight. As expected, the visible light attenuated very fast and the light sensor was not able to detect the light from the flashlight as the distance between them became greater than 2 *cm*. Thus, an eavesdropping device to pick up the light and extract the key would need to be placed on the body surface within 2 *cm* of the IMD, which is not likely to be feasible since the patient can easily detect such a device.

We next investigated the feasibility of launching remote eavesdropping (without an on-body sensor). We noticed that the smartphone flashlight creates a red circular area on the user's chest when it is on. We investigated if an attacker may be able to

use a camera to capture a video from the user’s chest and process the video to extract the key. In order to examine the feasibility of such an attack, we asked a subject to hold the smartphone over his chest and use his right hand to cover the smartphone. Then, we placed a 12-megapixel camera at a distance of 1  $m$  (a reasonable distance for remote eavesdropping) from the user’s chest, and captured two sets of videos in a dark room: four videos when the smartphone flashlight was on and four when the flashlight was off. The videos were captured in the dark room to simulate the worst-case scenario since in a dark environment the effect of ambient light sources is minimized and, as a result, the red spot created by the flashlight becomes more visible. We extracted 1000 frames from each video. For each video in the first set, we compared all of its frames to the ones of all videos in the second set using the concept of RGB Euclidean distance [392]. This is a metric that represents the color difference between two frames. For each video in the first set, the RGB Euclidean distances between its frames and the frames of other videos in the first set were similar to distances between its frames and the frames of videos in the second set, i.e., the videos in the first set were not distinguishable from the videos in the second set. This indicates that the attacker cannot detect the red spot created by the smartphone flashlight when the smartphone is placed on the user’s chest and the user covers the smartphone by his hand. Thus, in this scenario, the attacker cannot distinguish bit “1” from “0” when the key exchange protocol is sending the key.

**Key injection:** As mentioned earlier, the horizontal transmission range is about 1.5  $cm$  and the physician should keep the smartphone within this range to transfer the key to the IMD. Due to this proximity requirement, the attacker cannot place an unauthorized smartphone on the patient’s body within the horizontal transmission range without raising suspicion. Moreover, as mentioned in Section 4.5.2, the presence of an external powerful light source, which is not attached to the body, does not affect

the intensity of the light received by the in-body light sensor. This significantly limits the attacker’s ability to inject data (such as his encryption key) into OpSecure.

To sum up, the attacker can neither attach a device to the patient’s body without raising suspicions nor remotely attack the device.

### 4.5.6 Summary of evaluations

Table 4.1 summarizes the results of our analyses.

Table 4.1: Summary of evaluations

Horizontal transmission range ( $D_h$ )	1.5 <i>cm</i>
Vertical transmission range ( $D_v$ )	2 <i>cm</i>
Bit error rate	0
Wakeup time	a few seconds
Key exchange time	2.4 <i>s</i> to 3.6 <i>s</i> (key of length 64 <i>b</i> ) 4.5 <i>s</i> to 6.8 <i>s</i> (key of length 128 <i>b</i> )
Size overhead	negligible
Energy overhead	less than 0.3%
Security guarantees	prevents eavesdropping and key injection

## 4.6 Chapter summary

In this chapter, we described why attack-resilient wakeup and secure key exchange protocols are essential for establishing a secure RF-based communication link between the IMD and the external device. We discussed the shortcomings of previously-proposed protocols. We presented OpSecure, an optical secure communication channel between an IMD and an external device, e.g., smartphone, that enables an intrinsically short-range, user-perceptible one-way data transmission (from the external device to the IMD). Based on OpSecure, we proposed a wakeup and a key exchange protocol. In order to evaluate the proposed protocols, we implemented an IMD prototype and developed an Android application that can be used to wake up the IMD

and transmit the encryption key from the smartphone to the IMD. We evaluated our prototype implementation using a human body model. The experimental results demonstrated that OpSecure can be used to implement both wakeup and key exchange protocols for IMDs with minimal size and energy overheads.

# Chapter 5

## Physiological Information Leakage

Information security has become an important concern in healthcare systems, owing to the increasing prevalence of medical devices and the growing use of wearable and mobile computing platforms for health and lifestyle monitoring. Previous work in the area of health information security has largely focused on attacks on the wireless communication channel of medical devices, or on health data stored in online databases.

In this chapter, we pursue an entirely different angle to health information security, motivated by the insight that the human body itself is a rich source (acoustic, visual, and electromagnetic) of data. We propose a new class of information security attacks that exploit *physiological information leakage*, i.e., various forms of information that naturally leak from the human body, to compromise privacy. As an example, we demonstrate attacks that exploit acoustic leakage from the heart and lungs.

The medical devices deployed within or on our bodies also add to natural sources of physiological information leakage, thereby increasing opportunities for attackers. Unlike previous attacks on medical devices, which target the wireless communication to/from them, we propose privacy attacks that exploit information leaked by the very operation of these devices. As an example, we demonstrate how the acoustic leakage

from an insulin pump can reveal important information about its operation, such as the duration and dosage of insulin injection. Moreover, we show how an adversary can estimate blood pressure (BP) by capturing and processing the electromagnetic radiation of an ambulatory BP monitoring device [112].

## 5.1 Introduction

Implantable and wearable medical devices (IWMDs) promise to transform healthcare, by enabling diagnosis, monitoring, and therapy for a wide range of medical conditions and by facilitating improved and healthier lifestyles. Rapid advances in electronic devices are revolutionizing the capabilities of IWMDs [17]. New generations of IWMDs feature increased functional complexity, programmability, and wireless connectivity to body-area networks (BANs). Standardized communication protocols, such as Bluetooth [393] and ZigBee [244], are opening up new opportunities for providing low-power and reliable communication to IWMDs. These features facilitate convenient collection of medical data and personalized tuning of therapy through communication between different IWMDs and an external device (e.g., smartphone or clinical diagnostic equipment).

Advances in IWMDs have, unfortunately, also greatly increased the possibility of security attacks against them. Many recent research efforts have addressed the possibility of exploiting the wireless communication of IWMDs to compromise patients' privacy, or to send malicious commands that can cause unintended behavior. For example, Halperin et al. showed that the unencrypted wireless channel of a pacemaker can be exploited to compromise the confidentiality of data or to send unauthorized commands that cause the pacemaker to deliver therapy even when it was not needed [19]. Subsequently, a successful attack on an insulin pump, exploiting the wireless channel between the device and remote controller, was shown in [18]. By

reverse-engineering the customized radio communication and interpreting the unencrypted packets sent from a remote controller to an insulin pump, the attacker can launch radio attacks to inject insulin into the patient’s body beyond the dosage regimen. Finally, attacks that drain the battery of IWMDs by sending packets that fail authentication have also been proposed [19].

In this chapter, we demonstrate that medical privacy concerns extend far beyond the wireless communication to/from IWMDs. We make two main contributions. First, we describe the possibility of privacy attacks that target *physiological information leakage*, i.e., signals that continuously emanate from the human body due to the normal functioning of its organs. These attacks are a concern even when there is no medical device present, and hence have a much wider scope.

As our second contribution, we target IWMDs. We propose several novel attacks on privacy by leveraging information leaked from them during their normal operation. We demonstrate attacks on two medical devices based on acoustic and electromagnetic (EM) leakage from them. Moreover, we investigate a novel metadata-based attack that extracts critical health-related information by monitoring the communication channel, although the data may be completely encrypted. We note that the proposed attacks are applicable even when medical devices have no wireless communication, or when the wireless communication is encrypted, unlike previous attacks that compromise unencrypted wireless channels [18, 19].

The rest of the chapter is organized as follows. Section 5.2 describes the threat model. Section 5.3 discusses the sources and various types of physiological information leakage. Section 5.4 describes how we capture different types of leaked physiological signals. Section 5.5 presents our bevy of proposed privacy attacks. Section 5.6 suggests some countermeasures against the attacks, and Section 5.7 concludes the chapter.



## 5.2 Threat model

In this section, we first describe potential adversaries. Then, we describe potential risks that may arise from loss of privacy.

### 5.2.1 Adversary

We consider an adversary to be any potentially untrusted person who has a short-term physical proximity to the patient. The proposed attacks, while not impossible, may be difficult to deploy in a secure location such as the patient's home or a medical facility such as a hospital. However, none of our attacks require access to specialized medical equipment such as the ones used in hospitals. We also assume that long-term physical access to the patient or monitoring of the patient, e.g., using a camera that continuously monitors the subject's activities, is not feasible. In our attack scenarios, the adversary gains the required physical access to the patient in any public location. Crowded places, such as train stations, bus stops, and shopping malls, may provide opportunities for the adversary to come closer to the subject, while hiding the required equipment. A potential adversary might be an employer who intends to discriminate against a chronically-ill patient, a criminal group seeking to sell valuable medical information to the highest bidder [100], a private investigator who has been hired to spy on the subject, or a political operative who wants to expose the medical condition of the subject for political advantage.

### 5.2.2 Potential risks

The patient's physiological signals may be exploited in various ways. We describe some of the consequences of such information leakage next.

- 1. *Job/insurance loss*:** Revelation of medical conditions may negatively impact a person's employment prospects or make it more difficult for him to obtain insurance.

Leakage of this sensitive information from the human body or IWMDs, such as the presence of a serious illness, level of the illness, exposure of a condition that may carry social stigma, and exposure of physical, emotional or mental conditions would naturally raise serious privacy concerns.

**2. *Unauthorized interviews:*** An unauthorized interviewer may be able to combine lie detection (also called deception detection) questioning methods with the privacy attack techniques proposed in this chapter to ascertain the truth or falsehood of responses given by the subject, without his consent. Several researchers have investigated variations in vital health signals, such as the respiratory rate and heart rate, in the presence of acute emotional stress (e.g., when the person is lying) or a mental problem [394–396]. For instance, Sung et al. have demonstrated changes in the heart and respiratory rates in live poker game scenarios [77].

**3. *Indirect consequences:*** Although disclosure of medical information using the proposed privacy attacks might not be directly lethal, unlike attacks on the integrity of the medical device [18,19], it may lead to a subsequent tailored integrity attack. For instance, as described later, extracting medical device information, model, type, and configuration from the device using EM leakage may provide enough information to an adversary to design a more effective integrity attack using the extracted parameters. Moreover, detection of usage of certain medical devices by adversaries may endanger the safety of the patient, e.g., if the device is very expensive and attracts theft, or embarrass the subject if the medical condition carries a social stigma [100].

### 5.3 Information leakage

In this section, we discuss the possible sources of information leakage, followed by brief descriptions of different types of signal leakages addressed in this chapter.

### 5.3.1 Leakage sources

We consider two sources of information leakage: (i) human body and (ii) IWMDs. Each source continuously leaks information through different types of signals.

Several organs in our body generate biomedical signals. Some of these signals can be remotely captured and analyzed. For example, our lungs generate an acoustic wave called *respiration sound*, which can be captured by a microphone.

In addition to body organs, IWMDs may also reveal critical health information under normal operation even when not using any wireless communication to transmit data. For example, the electrical motor of an insulin pump generates an acoustic signal when injecting insulin. As described later in Section 5.5, performing simple signal processing on this acoustic signal can reveal the prescribed insulin dose.

### 5.3.2 Leakage types

In general, leaked physiological signals can be divided into two types: (i) acoustic and (ii) EM signals. Fig. 5.1 demonstrates the sources of leakage, as well as the different types of signals that we consider in this chapter. Body organs, such as heart and lungs, produce an acoustic signal that can be captured remotely and analyzed. IWMDs, such as an insulin pump or BP monitor, may also generate acoustic and EM signals during their normal operation even if they are not transmitting any data. The following subsections describe these signals in detail.

#### **Body-related information**

The human body consists of several continuously-operating organs. Various acoustic and EM signals are generated as a result. The majority of these signals are too weak to be captured without physical contact or may be absorbed by other organs before emanating from the body. For example, electrical activities originating from nerves carry real-time information about health status. The two commonly-used methods for

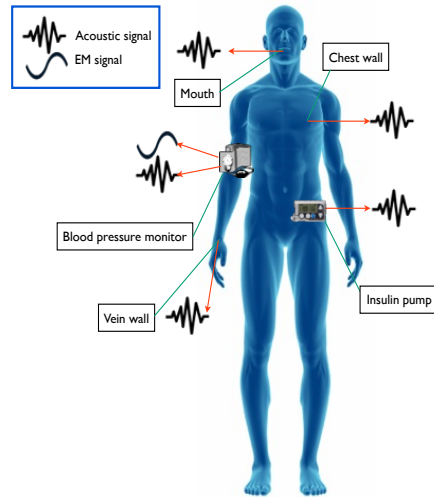


Figure 5.1: Sources of leakage and different types of signals that are continuously leaking from the human body and IWMDs.

measuring these signals are electroencephalography (EEG) and electrocardiography (ECG). The amplitudes of EEG and ECG signals vary from tens of microvolts to few millivolts. The frequencies of most of these signals are below  $40\text{ Hz}$  [397]. Another example is the acoustic signal generated by blood circulating through internal organs. However, this is absorbed by the surrounding muscles and tissues.

If an EM or acoustic signal generated by an organ emanates from the human body, it may be captured and analyzed to reveal health-related information. For example, one such signal is the respiration sound that is generated by chest vibration and airflow through the mouth. Next, we discuss different types of signals that might leak from the human body during normal operation.

***Acoustic signals emanating from the human body:*** Some of the body organs generate acoustic signals during their normal operation. In this chapter, we examine the feasibility of capturing such naturally-occurring acoustic signals from a distance to reveal confidential health information of a person. Specifically, we show how capturing acoustic signals generated by two organs, heart and lungs, can reveal critical information.

As discussed later in Section 5.5, a simple signal processing algorithm enables us to count the number of peaks in the raw heart sound signal and thus compute the heart rate. The heart rate may be an indicator of several critical illnesses [398] or a sudden emotional stress. For example, when a person lies, his heart rate gets elevated above the normal [399]. Therefore, if an adversary can monitor the heart rate remotely, he may even be able to assess whether the person is telling the truth.

Respiratory sounds also reveal valuable information about the health condition of an individual. The process of recording respiratory sounds and analyzing them is referred to as computerized respiratory sound analysis [400]; it provides crucial information on respiratory dysfunction, and changes in the respiratory characteristics (e.g., duration, timing).

***EM signals emanating from the human body:*** The human body continuously emits infrared radiation that carries health information. These raw data can be captured and processed by an attacker at a distance.

The use of thermal images has increased dramatically in the medical applications during the last decade. Thermal imaging cameras highlight warm objects against cooler backgrounds. As a result, the human body is easily visible in the environment. Moreover, some physiological variations in the human body can also be detected with thermal imaging techniques employed in medical diagnostic procedures. Several research projects on thermal imaging have been discussed in the medical literature. Using these methods [401–403], an eavesdropper can easily reveal the health status of a person. For example, in [401], Arora et al. showed the effectiveness of detecting breast cancer using digital infrared thermal imaging. The possibility of fever detection using thermal imaging techniques is described in [402].

## **IWMD-related information**

As mentioned earlier, IWMDs are used for monitoring and therapeutic purposes. An IWMD may leak health-related data or metadata that compromise the patient's privacy. We describe next how IWMDs can leak information through acoustic and EM signals.

***Acoustic signals emanating from IWMDs:*** First, we describe acoustic leakage from IWMDs. Acoustic waves propagate through a transmission medium using adiabatic compression and decompression. These waves are generated by a source. The source vibrates the medium, leading to propagation of vibrations from the source.

Electronic devices with microelectromechanical parts generate unintentional acoustic signals during normal operation. Some recent research efforts have demonstrated the feasibility of revealing critical information by interpreting acoustic emanations from peripheral computer devices. For example, researchers have shown that acoustic emanations from matrix printers carry substantial information about the printed text [404]. Moreover, Zhuang et al. have demonstrated the feasibility of recovering keystrokes typed on a keyboard from a sound recording of the user typing [405].

In this chapter, we demonstrate how acoustic signals generated by an IWMD (e.g., an insulin pump) may carry significant information about the patient's health status and the functioning of the medical device.

***EM signals emanating from IWMDs:*** We divide the EM radiations into two classes: (i) unintentionally-generated and (ii) intentionally-generated. Generally, an electronic equipment may emit unintentional EM signals that can be used as side-channel information, allowing eavesdroppers to reconstruct processed data at a distance [406]. This has been a concern in the design of military hardware for over half a century [407]. IWMDs can also unintentionally generate EM signals while performing their regular tasks. These signals may reveal critical information about the status of

Table 5.1: Sources of leakage, types of leakage, and descriptions

Source	Type	Description
Human Body	Acoustic	The vibrations generated by a human organ due to the normal functioning of organs
IWMDs	Acoustic	The sound made by electrical components during the normal operation of the device
	EM (unintentional)	The unintentionally-generated EM emanation due to the normal operation of the circuitry inside the device
	EM (wireless)	The EM radiation that is intentionally generated by the device for communication

the medical device and patient’s health condition. In this chapter, we demonstrate how an insulin pump can leak information about its function by emitting unintentional EM radiations. Medical devices may also use EM signals intentionally to wirelessly transmit medical data. Eavesdropping on unencrypted wireless communication has been addressed in several research articles [18, 19]. Moreover, potential information leakage from fully-encrypted data packets has been discussed in computer science literature [408–411]. In this chapter, we focus on the metadata that leaks through wireless communication even when the packets are fully encrypted.

## 5.4 Leaked signals and capture methods

Before discussing various attacks on the privacy of medical data, we need to describe how we capture different types of signals that naturally leak from the human body. Table 5.1 summarizes the sources of physiological information leakage, the types of leakage, and a short description of each form of leakage, which we have used to extract valuable medical information. Then, we briefly describe different capture methods that we have utilized in our experiments.

### 5.4.1 Capturing acoustic signals emanating from body organs

Here, we describe how we can capture the acoustic signals leaked during the normal functioning of lungs and heart. We describe two methods for remotely capturing small vibrations or weak acoustic signals generated by these organs.

#### Displacement-based laser microphone

We have designed and built a displacement-based laser microphone that uses a laser beam to detect sound vibrations from a distance (Fig. 5.2). Laser microphones were invented to eavesdrop on a conversation with a minimal chance of exposure. Although they have been used for surveillance purposes for a long time [412], for the first time, we employ these microphones in the context of a privacy attack on patients' medical data. We have built an inexpensive laser microphone to detect vibrations emanating from the human heart and lungs. This device is based on detecting the varying amounts of reflected laser beam received by a single ambient light sensor. As illustrated in Fig. 5.3, the laser beam forms a small incident angle with the surface. Surface vibration along the normal vector causes displacement of the reflected beam, and as a result, the amount of laser signal reaching the receiver varies for different displacements.

#### Parabolic microphone

The second capture method we propose is based on a parabolic microphone (KJB-Det [413]) to capture weak acoustic signals generated by the lungs. It uses a parabolic reflector to collect and focus sound waves onto a receiver. It amplifies the acoustic signal by concentrating all of the sonic energy at the focal point, thus increasing the signal-to-noise ratio (SNR). KJB-Det comes with parabolic dish that has a diameter



of 50 *cm*. In addition, electronic amplifiers used in KJB-Det can increase the overall level of both the noise and acoustic signal, without degrading the SNR.

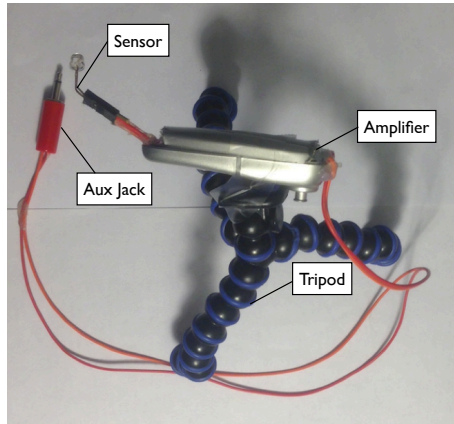


Figure 5.2: The displacement-based laser microphone.

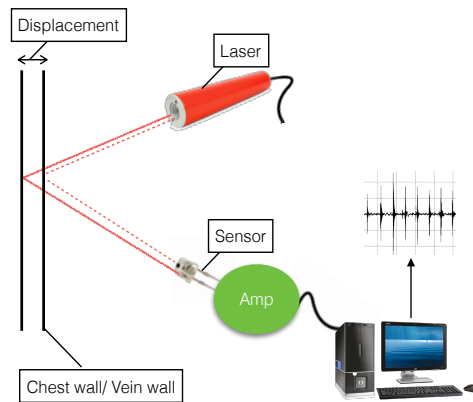


Figure 5.3: Schematic for displacement-based laser microphone: The laser beam forms a small incident angle with the surface. The fraction of light beam received by the light sensor depends on the vibration of the surface.

### 5.4.2 Capturing acoustic signal generated by IWMDs

In order to capture the acoustic signal leaked from IWMDs, several sound-recording equipments can be used, ranging from simple microphones to sophisticated parabolic microphones. In this chapter, we describe two different privacy attacks based on acoustic signals leaked from an insulin pump (electrical motor's sound and acoustic

alarm generated by its safety system) and one privacy attack based on the acoustic leakage from an ambulatory BP monitoring device (acoustic signals generated by the various components of the device when it is measuring BP). In the privacy attack based on the signal generated by insulin pump motor, we capture and amplify the sound of the electrical motor using a parabolic microphone (KJB-Det). In other attacks, we use a simple microphone to record the required acoustic signal.

### 5.4.3 Capturing unintentional EM signals

We use an oscilloscope to detect the unintentionally-generated EM signals. The EM side-channel information that we capture is available during the normal operation of the medical device even when the device is not transmitting any data (e.g., using a USB cable or wireless communication). We capture the raw EM signal directly from the antenna that is connected to the oscilloscope, instead of a filtered and demodulated signal with limited bandwidth. We use an antenna (75 Ohms VHA 9103 Dipol Balun) to improve the SNR for signals in the 25 *MHz* to 500 *MHz* frequency band. Moreover, we check if these EM signals can be captured using a small portable antenna, such as a simple loop of copper wire with 50 *cm* circumference.

EM signals may remain undetected using standard techniques. Spectral analyzers need static carrier signals of significant amplitude. The demodulation process may eliminate the interesting components of unintentionally-emitted EM signals. In addition, the scanning process of wide-band receivers may take a lot of time [414].

### 5.4.4 Capturing the metadata of wireless communication

In order to monitor fully-encrypted wireless communication and extract the metadata from the communication channel, we first need to find the frequency band of the transmission. If the model and type of the device are known, the frequency range can be extracted from manufacturer's documentation.

In general, an IWMD should make its existence and type unknown to unauthorized parties. If a device reveals its existence, its type should still remain hidden to unauthorized persons for many different reasons. For example, the device might be extremely expensive. More importantly, knowing the specific model of a device may provide critical information to potential adversaries. As we elaborate later, if the type, characteristics, and settings of an IWMD are known, designing a tailored attack becomes much easier. A tailored attack is a smart attack based on the specific features and configurations of a known device. Therefore, we assume that the model and type of the IWMD are not known to the attacker.

A fast approach for detecting the frequency band of a wireless transmission is through an oscilloscope that uses a loop of wire as an antenna. The eavesdropper can scan different frequency ranges when the communication channel is active and guess the frequency range. In addition, the frequency band of communication for an unknown IWMD can usually be obtained by scanning some specific bands based on the fact that FDA regulations impose specific limits on the frequency bands of medical devices. The majority of medical devices communicate at 450 *MHz*, 600 *MHz*, 900 *MHz*, 1.4 *GHz*, and 2.4 *GHz*.

After finding the frequency band of transmission, the encrypted packets can be captured using one or multiple universal software radio peripherals (USRPs) [415]. We demonstrate how examining the frequency band of the channel and characteristics of the packets can reveal critical health information.

## 5.5 Proposed privacy attacks

In this section, we propose several privacy attacks to demonstrate how processing physiological leakage from the human body and IWMDs can reveal various medical conditions and provide valuable information about the device (e.g., device type,

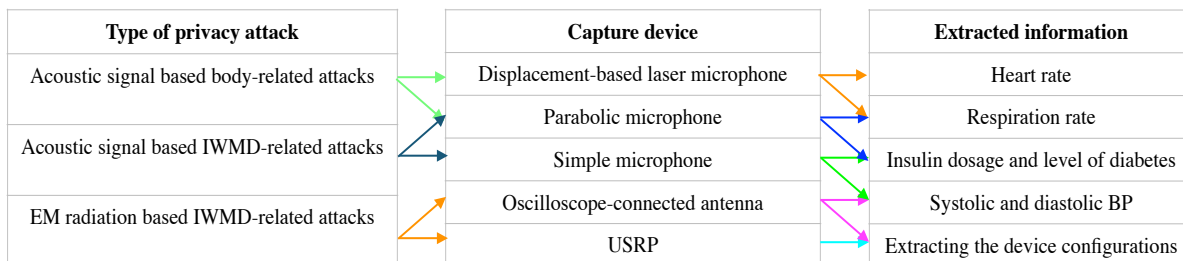


Figure 5.4: Different types of privacy attacks, capture methods, and the private information that each type of attack can extract from different leaked signals

model, and manufacturer). Fig. 5.4 depicts different types of privacy attacks, capture methods that we use to record the leaked signals, and the private information, which each type of attacks can extract from different physiological leaked signals. We demonstrate next several privacy attacks for each type.

### 5.5.1 Acoustic signal based body-related attacks

Here, we first describe a method to estimate the heart and respiration rates from the captured acoustic signal. Then, we discuss the parameters that affect the accuracy and detection range of the attack when each of the two capture methods (parabolic microphone and laser-displacement microphone) is used.

For obtaining the heart and respiration rates, we use a simple algorithm to find the local maxima. In order to reduce the effect of noise, the algorithm ensures that the distance between two consecutive peaks is more than the value of a parameter called *distanceThreshold*. The maximum possible human heart rate (200 pulses per minute) and respiration rate (80 breaths per minute) are used to define *distanceThreshold*. Thus, *distanceThreshold* is set to 300 *ms* and 750 *ms* for the heart and respiration rates, respectively. We perform 20 trials to estimate the heart and respiratory rates based on the leaked acoustic signals. For each trial, we compare our estimates with the actual values. We discuss how accurately our algorithm can estimate the heart

and respiratory rates. We discuss the accuracy of our algorithm for each capture method (parabolic microphone and laser-displacement microphone).

***Laser-displacement microphone:*** we use the laser-displacement microphone for capturing acoustic signals from both the lungs and heart. The sound quality obtained by this microphone depends on two factors: (a) reflection fraction, which is the fraction of the incident beam that is reflected by the surface, and (b) the displacement of the received beam. The first parameter depends on the nature of the surface. For example, the human skin absorbs a large fraction of the incident beam; therefore, the sensor should be placed close to the skin to receive the beam. However, the displacement of the received beam on the sensor decreases as the sensor gets nearer the reflecting surface. We were able to accurately extract the respiration rate from 5 *cm* away. If the person wears a metallic/reflecting necklace, we can point the incident beam towards the necklace instead, which is a better reflector than the human skin. We were able to accurately extract the respiration rate from 6 *m* away when the person wore a flat steel necklace. We also used a displacement-based laser microphone to detect the heart rate. In the absence of an attached reflector surface, the acoustic signal was used by the laser microphone to detect the heart rate with over 95% accuracy at a distance of 5 *cm*. At greater distances, the amount of received beam reduces drastically and the accuracy drops.

***Parabolic microphone:*** The audio gain of a parabolic microphone increases as the frequency increases. The gain of an ideal dish with a diameter of 50 *cm* and a perfect parabolic shape and focus is characterized by a curve starting from 0 *dB* at 200 *Hz*. In order to enhance the amplification of our parabolic microphone, we replaced its dish with a larger dish with a diameter of 1 *m* that provides a 6 *dB* amplification at 200 *Hz*. At lower frequencies, the most important parameters are dish size and the quality of the microphone. The modified parabolic microphone was able to detect the

respiration rate at a distance of 5 *m*. However, the parabolic microphone was unable to detect the heart rate.

### 5.5.2 Acoustic signal based IWMD-related attacks

Here, we describe the privacy attacks that exploit acoustic information leakage from IWMDs. Acoustic signals generated by an IWMD can provide valuable information to an unauthorized party. Each IWMD consists of several components. Some of these components (e.g., electrical motors and relays) can unintentionally produce a capturable sound during normal operation. An unintentionally-generated acoustic signal can be used as a side-channel information to reveal the status of the medical device and the patient's condition. In addition to this class of acoustic signals, some IWMDs intentionally produce acoustic signals to notify the users of conditions that require immediate attention. Many medical devices have alarm systems; among them are insulin pumps, pulse oximetry devices, and BP monitors. These alarms offer necessary warnings to inform patients of changes in their health condition. They usually provide sophisticated mechanisms for safety checks. These alarms make the patient aware of an unusual situation. Generally, the audible frequency range for a human is between 20 *Hz* and 20 *kHz*. Frequency ranges of 2 *kHz* to 4 *kHz* are most easily heard. For this reason, most alarms emit sound in this frequency range. Different acoustic warnings and alarms generated by IWMDs may also provide valuable information to an adversary.

We discuss next different attacks based on unintentionally- and intentionally-generated acoustic signals generated by IWMDs.

#### **Extracting injected dosage and estimating level of diabetes**

Here, we propose privacy attacks based on the acoustic signals leaked from an insulin delivery system (Fig. 5.5). In this medical device, the electrical motor unintentionally

generates acoustic signals and the speaker intentionally produces different alarms as reminders for calibration and high/low glucose, and as predictive high/low glucose alerts. The components marked in red (motor and buzzer) generate the acoustic signals that we can interpret to reveal the medical data.

We present two attacks on an insulin pump using both unintentionally- and intentionally-generated acoustic signals. First, we demonstrate how capturing and interpreting the unintentional acoustic signal generated by its electrical motor can reveal the prescribed dosage, and hence the level of diabetes. Second, we use the acoustic signals generated by its safety system to remotely examine the status of the device and extract the prescribed dosage.

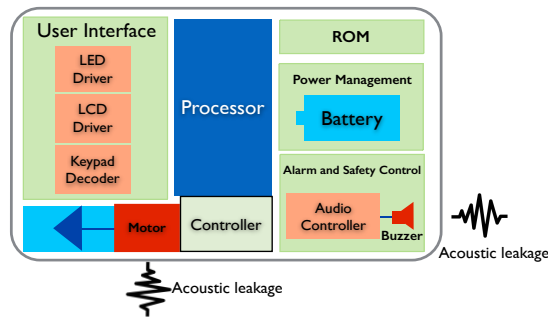


Figure 5.5: A schematic view of an insulin pump. The components marked in red (motor and buzzer) generate the acoustic signals that can be interpreted to reveal the medical data.

***Attack 1: Extracting information from motor sounds of an insulin pump:***

We show below how processing the weak acoustic signal generated by the electrical motor of an insulin pump can reveal the exact amount of injected insulin, and as a result, provide an estimation of initial blood sugar, and level of diabetes. As mentioned earlier, we used a parabolic microphone to capture the acoustic signal in this case. We propose two signal processing algorithms for this attack.

In an insulin pump, a step motor is used in the injection procedure. Our experiments demonstrate that there is a linear relationship between the number of rotation steps of the electrical motor and the amount of injected insulin (Fig. 5.6). Fig. 5.7

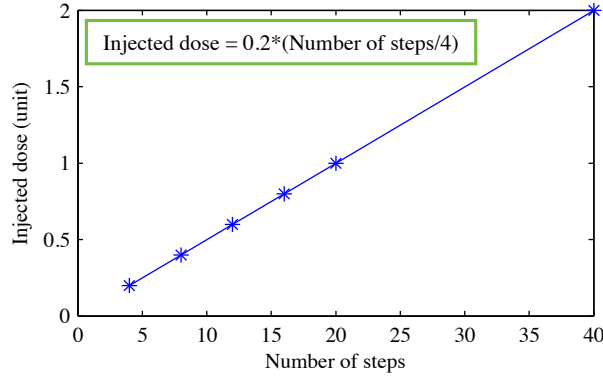


Figure 5.6: Dose of injected insulin vs. the number of rotation steps of the electrical motor.

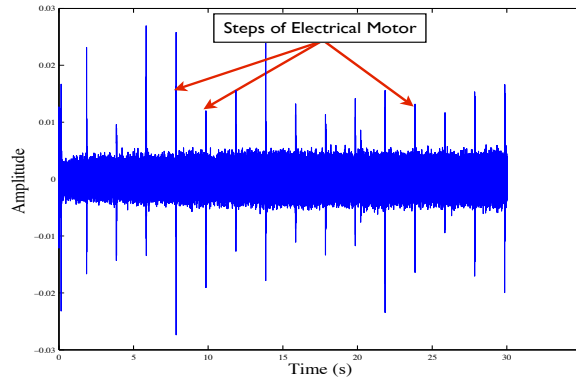


Figure 5.7: Acoustic signal generated by the electrical motor of an insulin pump while injecting 0.8 unit of insulin.

illustrates the acoustic signal generated by the electrical motor while injecting 0.8 unit of insulin. Each peak corresponds to one step of the motor. The first processing algorithm finds the number of peaks. Thus, for this case, the total number of steps is calculated as 16, thereby inferring that 0.8 unit of insulin was injected. *Algorithm 1* shows the pseudo-code of the algorithm. It calculates the exact amount of injected insulin based on the number of motor steps. Its four inputs are: (i) *acousticSignal*, which is the acoustic signal of the electrical motor sampled at 22 kHz, (ii) *distance*, which indicates the minimum acceptable distance between two consecutive peaks (steps), (iii) *threshold*, which is the minimum acceptable amplitude of a peak, and (iv) *widthThreshold*, which is the width of a step in the absence of environmental



noise. We obtain the number of steps from the number of peaks in *acousticSignal* using subroutine *stepCount*. Then, using another subroutine *stepWidth*, we calculate the width of each step that is defined as the time when the peak and its neighboring points are greater than *widthThreshold*. After finding the number of peaks and the width of each peak, we estimate the number of steps that might be corrupted by comparing the width of each peak to *widthThreshold*. If the width is more than *widthThreshold*, it is likely to contain noise in the area around the peak.

*Algorithm 1: Calculating the insulin dosage from the acoustic signal.*

---

Given: *acousticSignal*, *distance*, *threshold*, and *widthThreshold*

---

1.  $steps \leftarrow stepCount(acousticSignal, threshold, distance)$
2.  $widths \leftarrow stepWidth(acousticSignal, threshold, distance)$
3. *for each width in widths*
4.     *if* ( $width > widthThreshold$ )
5.          $noisy \leftarrow noisy + (width/widthThreshold)$
6.     *end*
7. *end*
8. *if* ( $noisy > 3$ )
9.     *Print* “ *Warning: Inaccurate* ”
10.    *return* -1
11. *else*
12.      $dosage \leftarrow \lceil steps/4 \rceil * 0.2$
13.     *Print* *dosage*
14.     *return* 0
15. *end*

---

This algorithm is able to automatically detect the number of peaks in *acousticSignal* that are corrupted. If the number of corrupted locations in *acousticSignal* is more than three, there will not be enough information in *acousticSignal* to reveal the exact insulin dose. Therefore, the attacker should discard that waveform, and try again later when background noise is less powerful.

In order to evaluate and compare our acoustic signal based algorithms, we constructed a test set consisting of 20 acoustic signals generated by the insulin pump when injecting four different doses of 0.2, 0.4, 0.6, and 0.8 unit of insulin (five injections for each dose). We captured the first 10 acoustic signals in a silent office (low-noise environment). We captured the other acoustic signals in the presence of background noise generated by a conversation. The algorithm could extract the injected dose exactly for the first 10 cases. In the presence of the conversation, the algorithm correctly detected the corrupted signal in four cases, and extracted the exact injected dose in the other six cases.

In addition to counting the number of steps, we can calculate the duration of an injection. Calculating the duration is more robust against noise. Using our second algorithm, we show how an adversary can use an estimation of the injection duration to find the exact amount of injected insulin without knowing the exact number of steps.

The amount of injected insulin is quantized to a multiple of 0.2 unit of insulin. As a result, the injection duration is quantized and is a multiple of 7 seconds. For example, the injection of 0.2 and 0.4 unit of insulin takes about 7 and 14 seconds, respectively. Fig. 5.8 shows the amount of injected insulin with respect to injection duration. It shows there is an almost-linear relationship between the amount of injected insulin and injection duration. Therefore, if the attacker can only estimate the injection duration by calculating the time during which the sound of the electrical motor is present, he can find the exact amount of injected insulin even when a large

fraction of the acoustic signal is dominated by background noise and counting the total number of steps is not feasible (Fig. 5.9). Using the test set described earlier, our duration-based algorithm was able to extract the exact amount of insulin in 18 of the 20 cases (10 under low-noise signals and 8 under noisy signals). Similar to the previous method, this algorithm was also able to automatically detect the situations in which the presence of noise affects the computed results.

In summary, capturing and processing the acoustic signal generated by the electrical motor of an insulin pump may reveal the injected dosage, and as a result, reveal the medical condition of the patient. The medical literature suggests that one unit of insulin is required per 50 mg/dl above 120 mg/dl of blood sugar [416]. Therefore, after measuring the insulin dosage, we can also estimate the level of blood sugar before injection.

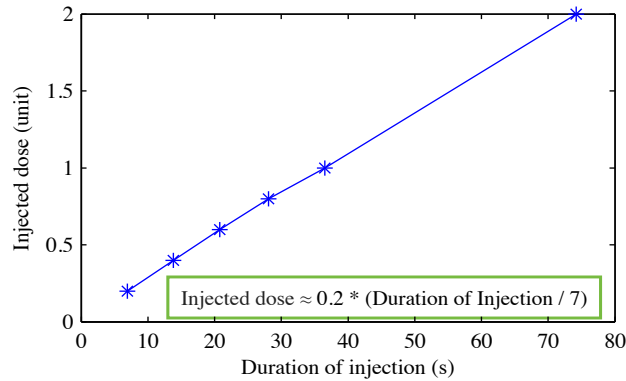


Figure 5.8: Dose of injected insulin vs. injection duration.

**Attack 2: Eavesdropping on alarms of an insulin pump:** We describe below how the safety system of an insulin pump, which intentionally generates acoustic signals to inform patients, can unintentionally leak critical information about the health condition of a patient. As mentioned earlier, alarms are intended to alert patients of special events. The controller unit of the insulin pump (Fig. 5.5) is responsible for handling alerts and alarms, and the speaker generates audible signals in vari-

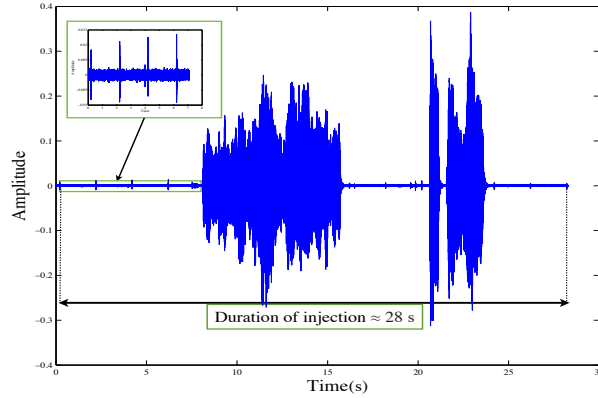


Figure 5.9: Acoustic signal generated by the electrical motor of an insulin pump when 0.8 unit of insulin is injected. For a large fraction of time, the acoustic signal is dominated by background noise, and counting the number of rotation steps is not feasible.

ous situations, including blockage, low/high sugar level, initialization, and end of an injection.

Each injection procedure has four different phases: (i) initialization, (ii) confirmation, (iii) injection, and (iv) end of injection. Fig. 5.10 shows the acoustic signal generated by the alarm system of an insulin pump when a user tries to inject 0.8 unit of insulin. The four phases of the injection procedure are demonstrated in this figure. After the patient sends the injection command, the beginning of the initialization phase is reported by a single beep sound. Then, the user sets the dosage by repeatedly pressing a button. In the confirmation phase, multiple beeps are generated based on the desired dosage. In this phase, one beep is generated by the safety system for every increment of 0.2 unit in insulin dose. However, the frequency of beeps in this phase is  $2\times$  higher than that in the initialization phase. Then, the injection begins and finally the end of injection is reported to the patient by a single beep.

We used three methods to find the exact amount of injected insulin by interpreting the acoustic signal: (i) initialization-based method that counts the number of peaks (beeps) in the initialization phase, (ii) confirmation-based method that counts the number of peaks in the confirmation phase, and (iii) duration-based method that

calculates injection duration. Although the first two methods are straightforward, the third method is more accurate, especially in noisy environments. Similar to *Attack 1*, by extracting the quantized values of injection duration and dose, the exact prescribed dosage can be calculated, even if the attacker cannot count the number of beeps, but only estimate the injection duration. The injected dosage can be directly computed based on the almost-linear relationship between injection duration and injected dosage (Fig. 5.8).

In order to evaluate the accuracy of each algorithm, we constructed a similar test set to the one we used earlier. We captured the acoustic signal from 10 *m* away. The raw signal was amplified using a cheap amplifier before processing. All three methods could accurately extract the injected dose in the low-noise environment. Table 5.2 shows the number of correct and incorrect calculations and accuracy of each method in the noisy environment. The duration-based method showed the best accuracy, where accuracy is defined as the percentage of correctly-calculated doses.

Table 5.2: Accuracy of the three methods for eavesdropping on the alarm system of an insulin pump

Method	Correct	Incorrect	Accuracy (%)
Initialization-based	6	4	60
Confirmation-based	7	3	70
Duration-based	10	0	100

In addition to compromising health-related information of a patient, the status of the medical device, such as blockage and low-battery state, can also be directly extracted by capturing and analyzing the alarms generated by the insulin pump.

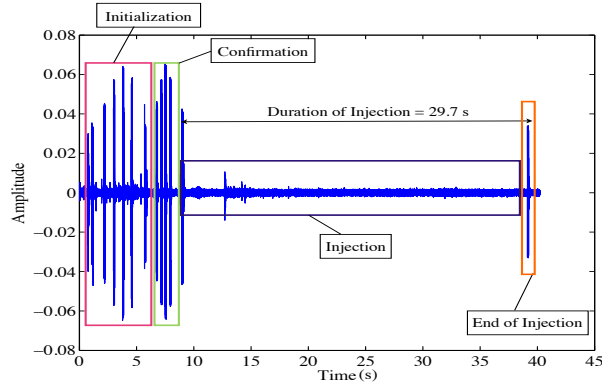


Figure 5.10: Acoustic signal generated by the safety system of an insulin pump when the user tries to inject 0.8 unit of insulin.

### Estimating BP by interpreting leaked acoustic signal of an ambulatory BP monitoring device

In this section, we target an ambulatory BP monitoring device. Fig. 5.11 shows a block diagram of such a device. The components shown in red are the major sources of acoustic leakage. We interpret the sound generated by its electrical pump to estimate the patient's BP, which is the pressure generated by circulating blood upon the walls of blood veins. A simple microphone suffices to capture the acoustic signals from a distance of up to 10 *m* in this case. BP is commonly represented by two numbers (systolic and diastolic), and is measured in millimeters of mercury (*mmHg*). Non-invasive ambulatory BP monitoring is being increasingly used to continuously monitor patients' BP. A digital BP monitor has a cuff and digital pressure sensor. When a user inserts his arm in the cuff, it is automatically inflated by an electric motor. The digital monitor determines the BP and heart rate by measuring the small oscillations when the pressure is slowly released from the cuff. Common BP monitoring devices use a simple algorithm to derive an upper bound on systolic BP. They inflate the cuff to reach the upper bound in every measurement. However, in order to ensure patient's comfort, some new BP devices often use a technology known as fuzzy logic, which anticipates systolic BP to prevent over-inflation. In these devices, the highest pressure

in the cuff is approximately 10 *mmHg* to 15 *mmHg* more than the actual systolic pressure. In this chapter, we have targeted a commercially available BP monitoring system. We choose not to disclose its brand and model number. We discuss how the sound generated by the electrical pump can provide enough information for an eavesdropper to accurately estimate the BP (both systolic and diastolic).

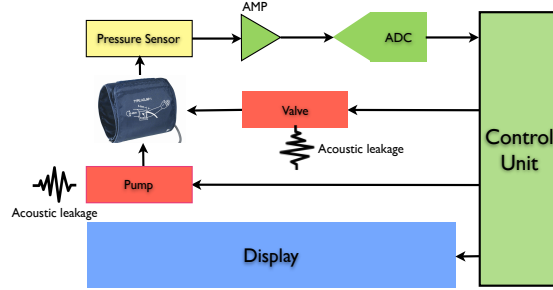


Figure 5.11: Block diagram of an ambulatory BP monitoring device. The components shown in red are the major sources of acoustic leakage.

Our experiments demonstrate that each measurement consists of three consecutive phases: (i) inflation phase in which the cuff pressure increases to reach its upper bound value, (ii) step-wise deflation phase in which the monitoring device opens an air valve to slowly decrease the cuff pressure and measure the BP, and (iii) restart phase. Fig. 5.12 shows the acoustic signal generated during the measurement.

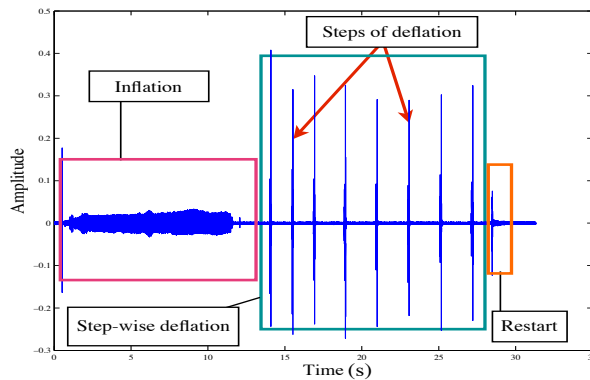


Figure 5.12: Acoustic signal generated by the ambulatory BP monitoring device. Three phases of measurement are shown.

In the BP monitoring device used in our experiments, the cuff pressure decreases about 9 *mmHg* for each step of deflation in the second phase of measurement. In addition, we found that the systolic BP was detected after three or four steps in the step-wise deflation phase, which suggests that the systolic BP should be in the range of  $(P_h - 27)$  *mmHg* to  $(P_h - 36)$  *mmHg*, where  $P_h$  is the maximum cuff pressure in the inflation phase. Moreover, based on our experimental results, the diastolic pressure is usually detected in the range of  $P_l$  *mmHg* to  $(P_l + 9)$  *mmHg*, where  $P_l$  is the minimum cuff pressure during the step-wise deflation phase before the device enters the restart phase. In order to examine the accuracy of the above claim, we used 25 BP measurements. The systolic BP was in the range of  $(P_h - 27)$  *mmHg* to  $(P_h - 36)$  *mmHg* for 21 out of 25 measurements. Moreover, for 23 out of 25 measurements, the diastolic BP was in the range of  $P_l$  *mmHg* to  $(P_l + 9)$  *mmHg*. Therefore, if we can develop a method to detect  $P_h$  and  $P_l$ , the systolic and diastolic pressure can be estimated as  $(P_h - 27 + P_h - 36)/2$  *mmHg* and  $(P_l + P_l + 9)/2$  *mmHg*, respectively.

We describe next how we can use the acoustic signal generated by the electrical pump to extract  $P_h$  and  $P_l$  and thus estimate the BP. The cuff pressure reaches its maximum value at the end of the inflation phase. In order to find the maximum value for an arbitrary measurement, we construct a look-up table that maps the maximum pressure ( $P_h$ ) to the duration of inflation ( $T_h$ ), where  $P_h$  varies from 100 *mmHg* to 180 *mmHg*. For each measurement, we first calculate  $T_h$  by finding the part of the acoustic signal in which the pumping sound is present. Then, we use the look-up table to find  $P_h$ . Thereafter, we count the number of steps before deflation and compute  $P_l = P_h - \text{numberOfSteps} * 9$ . Then, we calculate the range of systolic and diastolic pressures, and report the middle points of these ranges as their estimate. Our experimental results show that for 19 out of 25 arbitrary measurements, this algorithm calculates both systolic and diastolic pressures with maximum absolute error less than 8% (4.5% average absolute error for systolic pressure and 7.0% for



diastolic pressure), where error is defined as the difference between the estimated and actual values divided by the actual value. The main reason for the six failed cases was re-inflation. Re-inflation occurs when the patient suddenly changes his arm position during the step-wise deflation phase. In this case, the monitoring device increases the cuff pressure again. It is easy to modify the method to detect the situation in which re-inflation occurs. *Algorithm 2* gives the pseudo-code for the improved version of our algorithm. We define a function, called *infCount*, which finds the number of inflation phases separated by deflation steps. This improved algorithm automatically detects whether the algorithm is unable to calculate the BP accurately.

### 5.5.3 EM radiation based IWMD-related attacks

We target two classes of EM radiations: (i) unintentional EM radiations that are signals generated by different components of an IWMD (e.g., processor, controller), and (ii) intentional EM radiations that are encrypted wireless communications that transmit medical data. We discuss two EM radiation based attacks using each class of EM radiations, namely from the pump in a BP monitor, and based on the metadata of wireless communications of an insulin pump.

#### Estimating BP from unintentional EM radiations

Here, we discuss an attack based on capturing and analyzing the EM radiation that is unintentionally generated by the BP monitoring device.

Using the EM signals captured from the BP monitoring device, we were able to estimate the patient's BP. EM radiations reveal the activity of the electrical pump in the different phases of a measurement (inflation, step-wise deflation, and restart). The duration of the inflation phase can be revealed by calculating the time when the electrical motor produces the EM radiations, and as a result, the systolic BP can be extracted by using the method discussed earlier. Moreover, by monitoring the activity

of the device in the deflation phase, the number of deflation steps could be detected. Estimating the BP using EM signals was as accurate as when it was estimated from acoustic signals. However, this method can be easily used in a crowded environment, where the acoustic signal may be dominated by background noise.

*Algorithm 2: Estimating systolic and diastolic BP*

---

Given: *acousticSignal*, *table* where *table* :  $T_h \rightarrow P_h$

---

1.  $infNumber \leftarrow infCount(acousticSignal)$
  2.  $if(InfNumber > 1)$
  3.     Print “ Warning: Inaccurate ”
  4.     return - 1
  5. end
  6.  $T_h \leftarrow calculateTimeOfInflation(acousticSignal)$
  7.  $P_h \leftarrow lookUp(T_h, table)$
  8.  $Steps \leftarrow CountPeaks(acousticSignal)$
  9.  $upperSystolic \leftarrow P_h - 27$
  10.  $lowerSystolic \leftarrow P_h - 36$
  11.  $P_l \leftarrow P_h - numberOfSteps * 9$
  12.  $upperDiastolic \leftarrow P_l$
  13.  $lowerDiastolic \leftarrow P_l + 9$
  14.  $systolic \leftarrow \frac{upperSystolic + lowerSystolic}{2}$
  15.  $diastolic \leftarrow \frac{upperDiastolic + lowerDiastolic}{2}$
  16. Print *diastolic*, *systolic*
  17. return 0
-

The activity of the electrical pump in the inflation phase was completely detectable from 15 *cm* away when we used the VHA antenna. Moreover, when we replaced the VHA antenna with a wire of 50 *cm* circumference, we were able to detect the activity from 10 *cm* away. The deflation steps were detectable using the VHA antenna and wire from 10 *cm* and 5 *cm* away, respectively.

### **Extracting insulin dosage regimen from the wireless communication metadata of the insulin pump**

Here, we describe how capturing and processing the metadata leaked from the communication channel of an insulin pump can reveal critical medical information, including the injected dose of insulin, number of injections, and level of diabetes.

Different manufacturers have different priorities and considerations. As a result, the metadata of the communication channel of one device are different from those of others. The metadata-based attack that we discuss next consists of two main steps: (i) the eavesdropper first extracts the metadata from the communication channel to reveal valuable information about the type and model of the IWMD, and (ii) when the device type is known, the attacker designs a tailored attack that specifically targets the known device. We discuss six classes of metadata leaked from the communication channel that can be used to find valuable information about the device: (i) frequency of communication, (ii) time between two consecutive transmissions, (iii) communication protocol, (iv) packet size, (v) detection range, and (vi) modulation protocol. However, in most cases, a subset of these classes can uniquely identify the model and type of the device.

We describe an example of metadata-based privacy attack using the insulin pump delivery system. For the insulin pump we used in this research, the frequency of communication (around 900 *MHz*), time between two packets (5 minutes), and modulation protocol (on-off keying) would be conclusive enough for an adversary to uniquely

identify the insulin pump and its manufacturer. In addition, the detection range (20  $m$ ) and packet size (80  $b$ ) match the information given in the documentation of the device.

We describe a tailored attack against an insulin pump. We assume all communications are fully encrypted. In the first step of the metadata-based attack, we find the model and type of the insulin pump. This specific model comes with a remote control. The remote control is a device that controls and programs the insulin pump and allows the user to deliver a discrete bolus dose or stop/resume insulin delivery. Each button on the remote control sends a specific command to the insulin pump. The size of remote control is usually small to ensure patient's convenience, and as a result, there are only a few buttons on the remote control. Different sequences of buttons on the insulin pump are to be pressed in different situations. For the remote control that we used in our experiment, the patient should use at least three button presses to start the injection: (i) the first button tells the device to initialize the injection, (ii) the second button is used to set the dosage of injection, and (iii) the third button confirms the injection. The patient can press the second button multiple times to increase the dosage. In this scenario, interpreting the number of consecutive packets can uniquely reveal the occurrence of the injection, and the insulin dosage. In order to verify this claim, we designed an experimental setup using the insulin delivery system, its remote control, and a USRP. We performed 10 trials in which the amount of injected insulin varies from 0.2 to 2 units of insulin. All trials confirmed that the amount of injected insulin can be easily computed as:  $dosage = (N - 2) * 0.2$  *unit*, where  $N$  refers to the number of transmitted packets. For example, if seven packets are captured by the USRP in this case, the first and last packets would represent initialization and confirmation. The other five packets can be assumed to be sent to increase the amount of injected insulin. Therefore,  $dosage = (7 - 2) * 0.2 = 1.0$  *unit*.

To sum up, the number of injections can be extracted by counting the number of transmissions that have more than three packets. This approach is completely accurate when the distance between the USRP and the remote control is less than 6  $m$ .

## 5.6 Possible countermeasures

In this section, we briefly discuss some possible countermeasures to protect the patient against the privacy attacks described in this chapter. We hope these initial suggestions would spur further research on countermeasures against such attacks. We discuss different countermeasures for each source of leaked signals (human body and IWMDs). Hiding information that leaks from the body is difficult because there are many local sources of leakage, e.g., lungs, heart, and skin. We can hide some of this information using cloth as a shield. However, since it is typically not possible to cover the whole body, medical information may at least leak from the face. For example, the EM radiation from the face leaks enough information to detect if a person has fever.

As mentioned earlier, many components inside medical devices may generate acoustic or EM signals: the motherboard, communication cables, processor, and actuators. Potential solutions for eliminating the leakage of compromising information from IWMDs can be divided into three main categories: strength reduction, information reduction [417, 418], and noise addition techniques [408, 418, 419]. We describe each category next.

### Signal strength reduction techniques

The main goal of these techniques is to reduce the strength of unintentionally-leaked signals such that their detection range reduces drastically. These methods include circuit redesign, using low-power components, utilizing shielding, and designing iso-

lating containers (i.e., containers that are usually made of a metal mesh and can block acoustic/EM signals of certain frequencies). However, incorporating these techniques will increase IWMD price and thus may not be desirable from a cost perspective.

### **Information reduction techniques**

These techniques focus on minimizing the amount of information leakage. One obvious solution for reducing information leakage from IWMDs is to use standard communication protocols and implementations. If different manufacturers adopt such standards (e.g., they use the same frequency band, modulation protocol, and packet size), unintentionally-leaked signals from various devices would be similar to each other and carry minimum discriminatory information. However, enforcing the use of a single standard communication protocol and a set of design requirements is difficult due to the fact that different medical companies have different priorities. For example, many manufacturers prefer to use standard communication protocols at  $2.4\text{ GHz}$  (e.g., Bluetooth and ZigBee) in their medical devices for connection to smart phones, whereas other manufacturers mainly use a customized communication protocol to minimize energy or increase the communication range.

### **Noise addition techniques**

Such techniques can be implemented in either hardware or software. In software-based defense schemes, IWMDs and their remote controllers can be programmed to produce superfluous packets to significantly degrade the accuracy of attacks based on counting the number of packets or any other statistical analysis. For example, our EM-based attack against the insulin pump can be mitigated as follows. As mentioned earlier, the variation in the number of packets can reveal the exact amount of injected insulin. Our experimental results demonstrate that the total number of packets that might be sent by the remote control to the insulin pump for each injection process is between 3 to 52.

Thus, if the remote control is programmed such that it produces some fake packets for each injection step and always sends 52 packets, then counting the number of packets will not provide any meaningful information. However, for the majority of patients, adding fewer fake packets may be sufficient to drastically reduce the accuracy of the attack. Unfortunately, producing fake packets may drastically increase the energy consumption of the device, and shorten its battery lifetime significantly. Hardware-based countermeasures can also be useful in protecting the user from the privacy attacks based on physiological information leakage. The local sources of leakage (e.g., motherboard, wires, and display board) can be identified during the design or manufacturing process. Afterwards, extra components may be added to generate intended acoustic/EM noise in a specific frequency range to overpower the valuable signal during the normal operation of the device. However, the noise generator should not corrupt intentionally-generated signals (e.g., alarms from the insulin delivery system). Although noise addition techniques can provide promising countermeasures to protect the patient against privacy attacks, they have two main drawbacks. First, they increase the cost of manufacture. Second, adding a noise generator may increase the energy consumption of the device and thus reduce its battery lifetime.

## 5.7 Chapter summary

In this chapter, we discussed two sources, namely the human body and IWMDs, that continuously leak health information under normal operation. We targeted two types of signals for each source: acoustic and EM. We then described a variety of attacks on the privacy of health data by capturing and processing unintentionally-generated leaked signals. Moreover, we discussed the feasibility of using intentionally-generated acoustic signals (as a side-channel information) and EM signals (as a carrier

of metadata) to compromise the patient's health privacy. Finally, we suggested some countermeasures.



## Chapter 6

# DISASTER: Dedicated Intelligent Security Attacks on Sensor-triggered Emergency Responses

In this chapter, we introduce a new class of attacks against cyber-physical systems (CPSs), called *dedicated intelligent security attacks against sensor-triggered emergency responses (DISASTER)*. DISASTER targets safety mechanisms deployed in automation/monitoring CPSs and exploits design flaws and security weaknesses of such mechanisms to trigger emergency responses even in the absence of a real emergency. Launching DISASTER can lead to serious consequences for three main reasons. First, almost all CPSs offer specific emergency responses and, as a result, are potentially susceptible to such attacks. Second, DISASTER can be easily designed to target a large number of CPSs, e.g., the anti-theft systems of all buildings in a residential community. Third, the widespread deployment of insecure sensors in already-in-use

safety mechanisms along with the endless variety of CPS-based applications magnifies the impact of launching DISASTER.

In addition to introducing DISASTER, we describe the serious consequences of such attacks. We demonstrate the feasibility of launching DISASTER against the two most widely-used CPSs: residential and industrial automation/monitoring systems. Moreover, we suggest several countermeasures that can potentially prevent DISASTER and discuss their advantages and drawbacks [420].

## 6.1 Introduction

CPSs offer a transformative approach to automation and monitoring through integration of processing, networking, and control. This combination and active collaboration of computational elements, e.g., powerful base stations, and small embedded devices, e.g., sensors, enable CPSs to reliably and efficiently control physical entities.

Recent and ongoing advances in microelectronics, networking, and computer science have resulted in significant CPS growth. Such systems facilitate automation and monitoring in various application domains, e.g., smart manufacturing lines, smart homes, smart cities, smart grids, and smart vehicles. Moreover, with the emergence of the Internet-of-Things (IoT) paradigm and IoT-enabled CPSs in the last decade, it has become clear that the economic and societal potential of such systems is far beyond what may have been imagined. Thus, major investments have been made worldwide to design and develop CPSs.

As a side effect of the rapid development and pervasive use of CPSs, the number of potential threats and possible attacks against the security of such systems is increasing drastically, while, unfortunately, their security needs are not yet well-recognized [421–423].

An essential component of a majority of CPSs is a safety mechanism, which aims to minimize harm to users' well-being or damage to equipment upon the detection of risks, hazards, or unplanned events. The security of safety mechanisms is an emerging research topic that is attracting increasing attention in academic, industrial as well as governmental research. A few real-world attacks and recent research efforts have demonstrated that generic classes of security attacks, e.g., computer worms, man-in-the-middle attacks, and denial of service (DoS), which have been extensively studied in the network/computer security domains, can be modified to *disable* the safety mechanisms of CPSs. For example, in 2003, the SQL Slammer worm infected the Davis-Besse nuclear power plant in Ohio, USA, and disabled the plant's safety parameter display system and plant process computer for several hours [424]. Stuxnet [121, 122], a real-world high-impact man-in-the-middle attack, was launched against safety mechanisms employed in thousands of industrial CPSs in 2012. Stuxnet faked industrial process control sensor signals so that safety mechanisms of infected systems were disabled, and as a result, their emergency responses were not activated even in the presence of a real emergency. Furthermore, Lamb developed a DoS attack against residential intrusion detection systems in which the attacker continuously jams the communication channel between motion sensors and the base station to suppress the system's alarm that is supposed to be triggered in the presence of an intruder [425].

In this chapter, we present and extensively describe a new class of attacks against CPSs, referred to as *DISASTER*. As opposed to the previously-proposed attacks that mainly aim to **disable** emergency responses of safety mechanisms in the presence of an emergency situation, *DISASTER* attempts to **trigger** the system's emergency responses in the absence of a real emergency.

Our key contributions can be summarized as follows:

1. We introduce *DISASTER* and discuss potential attackers who may be motivated to launch such security attacks.

2. We discuss the impact of DISASTER by describing the consequences of launching such attacks.
3. We examine common design flaws and security weaknesses of safety mechanisms and their components, which may be exploited by an attacker to launch DISASTER.
4. We demonstrate the feasibility of launching DISASTER in realistic scenarios, e.g., residential and industrial automation/monitoring systems.
5. We suggest several countermeasures to proactively address DISASTER, and discuss their advantages and drawbacks.

The remainder of the chapter is organized as follows. Section 6.2 describes the threat model. Section 6.3 describes the typical architecture of CPSs that we consider in this chapter. Then, it discusses different components, design flaws, and security weaknesses of their safety mechanisms. Section 6.4 describes potential consequences of launching DISASTER. Section 6.5 demonstrates how it is feasible to launch the proposed attacks against two real CPSs. Section 6.6 suggests several countermeasures to prevent DISASTER and describes why proactive countermeasures might not always be able to provide sufficient protection against the proposed attacks. Finally, Section 6.7 concludes the chapter.

## **6.2 Threat model**

In this section, we first describe what enables DISASTER and makes CPSs susceptible to such attacks, and discuss why launching DISASTER can be disastrous in real-world scenarios. Second, we discuss who the potential attackers may be who exploit vulnerabilities of CPSs to launch the proposed security attacks, and what their motivations may be.

### 6.2.1 Problem definition

As described later in Section 6.3, in a typical CPS, a centralized processing unit (commonly referred to as base station) obtains a description of the environment based on the data that it collects from different sensors, and it processes the sensory data along with user inputs to control physical objects. Given direct interactions of such a system with both the environment and users, safety and security are two fundamental requirements of CPSs. Safety mechanisms employed in CPSs protect users from undesirable outcomes, risks, hazards, or unplanned events that may result in death, injury, illness, or other harm to individual's well-being, damage to equipment or harm to organizations, while security protocols are focused on protecting the system from intentional attacks [426].

Although safety and security seem to share very similar goals at first glance, a close examination of various safety and security requirements demonstrates that ensuring both safety and security of CPSs is not always possible due to the existence of unavoidable safety-security conflicts [427, 428]. When ensuring both safety and security is not feasible, safety is typically given preference and safety mechanisms willingly sacrifice security of the system to ensure users' safety. For example, modern vehicles commonly support an automatic door unlocking mechanism [429], which opens the vehicle's doors upon the detection of a collision. This safety mechanism ensures passengers' safety by completely disabling the car's security system after detecting an accident.

The unavoidable safety-security conflicts along with different design flaws and security weaknesses of components, e.g., sensors and base stations, used in safety mechanisms facilitate DISASTER. In DISASTER, the attacker exploits such conflicts/weaknesses to *fool the under-attack safety mechanism into falsely labeling a normal situation as an emergency in an attempt to activate emergency responses when they are not needed*. As discussed later in Section 6.4, activating emergency

responses in the absence of an emergency can lead to catastrophic situations, ranging from system shutdown to life-threatening conditions.

Launching DISASTER can have severe negative consequences in real-world scenarios for three reasons. First, since the majority of CPSs offer emergency responses, they are susceptible to such attacks. Second, as demonstrated later in Section 6.5.2, DISASTER can be implemented to simultaneously target a large number of CPSs, e.g., the anti-theft systems of all buildings in a residential community. Third, the widespread use of vulnerable sensors along with the endless variety of CPS-based applications magnifies negative consequences of launching DISASTER.

Despite the fact that safety mechanisms are designed to control hazards and emergency situations and minimize their associated risks, a careless design of a safety mechanism endangers **both** users' safety and the system's security.

## 6.2.2 Potential attackers

Next, we discuss potential attackers who may target CPSs, and what their motivations might be.

As discussed earlier, DISASTER is widely applicable since CPSs used for automation/monitoring are in widespread use in our everyday lives. Such systems may manage a huge amount of information and be used for many services, ranging from industrial management to residential monitoring. This has made such CPSs targets of interest for a multitude of attackers, including, but not limited to, cyberthieves, hackers, occasional hackers, and cyberterrorists. Unfortunately, as described later in Section 6.5.2, an attacker with very limited resources, e.g., a very cheap radio transmitter such as HackRF [430], can easily launch powerful large-scale attacks against CPSs.

As extensively discussed later in Section 6.4, the attackers might launch DISASTER to access restricted areas, cause economic damage to companies or individuals,

trigger life-threatening operations, or halt automation/monitoring processes. Moreover, they might try to make CPS use so inconvenient to the user that he is forced to shut down the whole system.

## **6.3 Typical components and weaknesses of safety mechanisms**

In this section, we first describe the typical architecture of CPSs that we consider in this chapter, and discuss different components of their safety mechanisms, and two main types of emergency responses that they provide. Second, we discuss design flaws and security weaknesses, which are commonly present in widely-used safety mechanisms.

### **6.3.1 Typical CPS architecture**

Fig. 6.1 illustrates a common CPS architecture that includes safety mechanisms. A typical CPS consists of: (i) a base station, which collects and processes environment-related data and controls other components, (ii) wireless sensors that continuously collect data and transmit them to the base station, and (iii) physical objects that are controlled by the base station. State-of-the-art CPSs may also allow the user to remotely control, configure, or access the system over the Internet. The base station gathers data from different sources, e.g., sensors, cloud servers, and user inputs, and processes them to control different physical objects. Furthermore, a majority of modern CPSs have a safety mechanism, which typically needs two extra components: a safety unit and warning devices, e.g., speakers. The safety unit is usually integrated into the base station. When it detects an emergency, e.g., a fire or an accident, it activates warning devices or overrides control signals of physical objects to minimize safety risks associated with the situation. In each application

domain, certain conditions and states are defined as emergency situations in which safety risks are present and should be actively and aggressively addressed.

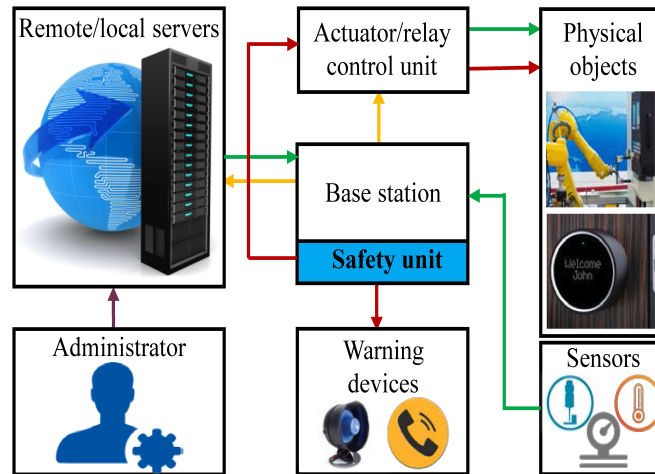


Figure 6.1: Common architecture of CPS. Upon the detection of an emergency, the safety unit directly controls the physical objects or warns the users by activating the passive components.

Although emergency responses vary significantly from one application to another, there are two main types of emergency responses: active and passive. Next, we briefly describe each.

**1. Active response:** Such a response actively attempts to minimize the safety risks by controlling various actuators and components in the system. When the human operator is unable to provide a sufficiently fast response, it is required that the CPS offer an active response to minimize damages associated with the emergency situation. Typically, when a CPS provides an active response, it initiates a specific emergency procedure or halts the system's normal operation. For example, consider an insulin delivery system that continuously monitors blood glucose and injects insulin into the patient's body in order to regulate the blood glucose level. If the system detects a life-threatening low level of blood sugar, it immediately halts the injection procedure to ensure patient safety.

**2. Passive response:** A passive emergency response is provided by the system to warn human operators, proximate people, e.g., residents of a building, or emergency



departments, e.g., fire department, about the need to take immediate action. Unlike an active response, it does not directly control physical entities. For example, consider a simple fire detection system. Upon detecting a fire, the system provides a passive response that activates various notification appliances, e.g., flashing lights and electromechanical horns.

### 6.3.2 Common design flaws and security weaknesses

Due to the inevitable complexities of CPSs, heterogeneity of entities that form them, and limitation of on-sensor resources (e.g., small amount of on-sensor storage), designing completely-secure safety mechanisms and finding perfect safety design strategies are very daunting. As a result, it is easy to find several already-in-market products that are vulnerable to DISASTER. Next, we discuss three design flaws and security weaknesses of safety mechanisms that may enable an attacker to launch such attacks.

#### Using insecure sensors

As mentioned earlier, wireless sensors continuously collect and transmit data that are needed for detecting emergency situations. A fundamental consideration in the design of wireless sensors is choosing the communication protocol. Many manufacturers have decided to design and use customized wireless protocols in an attempt to minimize expenses and maximize battery lifetime. We examined 70 already-in-market sensors from 10 different manufacturers (we reviewed documentations of 62 sensors, and as discussed later in Section 6.5.2, we closely inspected and attacked eight sensors under realistic scenarios) that are widely used in safety mechanisms. We noticed that the communication protocol of each sensor has at least one of the following security weaknesses.

- 1. Lack of data encryption or obfuscation:** Unfortunately, a great number of customized wireless communication protocols used in already-in-market sensors sup-

port neither strong encryption nor obfuscation mechanisms and are, hence, susceptible to various forms of security attacks. In particular, due to the specific requirements of safety systems (e.g., fast response time and monitorability) and common limitations of sensing platforms (e.g., limited on-sensor energy, small amount of available memory, and limited computation power), the majority of sensors utilized in safety mechanisms transmit unencrypted non-obfuscated packets over the communication channel. As a result, an attacker can reverse-engineer the system's communication protocol and generate illegitimate packets (packets not created by legitimate sensors) using his equipment.

**2. *Lack of timestamp:*** A great number of sensors do not include a timestamp (i.e., a sequence of encrypted information identifying when the transmission occurred) in their packets. As a result, the system's base station is unable to distinguish new legitimate packets generated by the sensor from old seemingly legitimate ones, which are recorded and retransmitted by an attacker.

**3. *Using default passwords:*** Setting non-random default passwords at the manufacturing/installation time is a very common mistake that can lead to severe security attacks against the system even when strong encryption mechanisms are utilized to secure the communication channel. It is very common for system administrators or user to forget to change the system's default password at installation time. A recent article provided a list of more than 73,000 cameras in 256 countries that use standard communication protocols and a strong encryption mechanism, yet are not immune to security attacks because they use a default password for encrypting their communications [431].

**4. *Using short sensor identifiers:*** In order to distinguish different sensors from each other and enhance the security of the communication protocol, most sensors include their identifier (also referred to as the pin code or identification number) in all packets they transmit over the communication channel. The base station uses the

sensor's identification code to ensure that the incoming packet comes from one of the already-registered sensors, which are known to the system. However, as demonstrated later in Section 6.5.2, several in-market sensors from well-known manufacturers use very short sensor identifiers (4-8 bits). As a result, they are susceptible to brute-force attacks (i.e., attacks consisting of systematically checking all possible sensor identifiers until the correct one is found).

### **Offering inessential sacrifices**

As mentioned earlier, upon the detection of an emergency situation, automation/monitoring CPSs willingly sacrifice some of their security mechanisms to ensure users' safety. As an example, fire evacuation systems open all doors to enable firefighters to access different rooms and allow the occupants to safely leave the building. Although this evacuation mechanism seems essential to ensuring occupant safety, it might enable an attacker to access restricted areas by triggering an emergency response. This example demonstrates that designers should take both safety and security considerations into account, when designing emergency responses of a CPS.

### **Relying on a single sensor type**

In order to provide a reactive emergency response when required, the automation/monitoring CPS must be able to correctly distinguish abnormal situations from normal ones. In fact, the most important steps in minimizing safety risks is detecting emergency situations. Therefore, before providing any response, the CPS needs to collect sufficient sensory data to obtain a clear description of its environment. If insufficient information is given to the system, it might fail to correctly recognize emergency situations. Unfortunately, in order to minimize costs, the majority of the already-in-use automation/monitoring CPSs only process a single environmental attribute. For example, consider a fire evacuation system that only relies on smoke

detection sensors. Such a system provides an emergency response when at least one of the sensors detects the existence of smoke. Thus, an attacker can easily trigger the emergency response by only targeting a single vulnerable smoke detection sensor.

## **6.4 Potential consequences of launching DISASTER**

As mentioned earlier, CPSs are in widespread use and handle sensitive tasks in various application domains. Hence, launching tailored attacks, like DISASTER, that are applicable to various forms of automation/monitoring CPSs, can lead to serious consequences. Such consequences depend on the type of emergency response activated by the attack. Generally, the negative impact of triggering an active response is more significant than the impact of triggering a passive response due to the fact that the former can actively control various critical operations and even bypass human operators' decisions. Next, we describe possible consequences associated with launching DISASTER.

### **6.4.1 Life-threatening conditions**

Triggering the emergency response of a CPS that handles critical operations, e.g., medical or industrial automation tasks, can lead to serious life-threatening conditions. This can range from conditions affecting an individual to those affecting a large number of people. For example, consider an insulin delivery system that is equipped with a safety mechanism, which monitors the blood glucose and immediately stops the injection procedure when it detects the patient has hypoglycemia, i.e., a life-threatening low level of blood glucose. Triggering the active emergency response of the insulin delivery system immediately shuts down the device. An attacker might be able to trigger such an active response even when the blood glucose level is normal/high

to halt the delivery system and cause hyperglycemia, i.e., a life-threatening high level of blood glucose.

### **6.4.2 Economic collateral damage**

Economic damages refer to monetary losses, including, but not limited to, loss of property, machinery, equipment, and business opportunities, costs of repair or replacement, the economic value of domestic services, and increased medical expenses. Almost all emergency responses have associated costs, even when they are triggered by a real emergency situation. For example, consider a vehicular CPS that is designed to inflate the vehicle's airbags in a collision to provide protection in an accident. In a minor collision that results in the deployment of airbags, the whole dashboard panel, steering wheel, and all airbags have to be replaced. In such cases, the active emergency response provided by the CPS is quite costly. Therefore, if an attacker can activate such an emergency response, he will be able to cause collateral economic damage.

The cost associated with triggering emergency responses varies significantly from one application domain to another. For example, the economic collateral damage that results from triggering an emergency response of a vehicular CPS is much less than that of an industrial CPS that controls a manufacturing line.

### **6.4.3 Overriding access control mechanisms**

In the presence of an emergency situation, a CPS might also be able to command the access control systems that control which users are authorized to access different restricted areas. Such a control is important for two reasons. First, the CPS can facilitate the evacuation procedure in the case of an emergency. Second, the system can lock down particular areas to prevent an intruder from escaping. For example, a residential CPS, which is able to control door locks, may open the main entrance

to ensure that firefighters can easily access restricted areas and residents can safely evacuate the building. However, if an attacker can trigger this safety mechanism in the absence of an emergency situation, he might be able to bypass physical security mechanisms and access restricted areas.

#### **6.4.4 Unintended ignorance**

As mentioned earlier, CPSs provide both passive and active responses to minimize damage associated with an emergency situation. A majority of emergency responses could be extremely annoying to the proximate people if they are activated in the absence of an emergency situation. For example, upon the detection of an emergency situation, a great number of CPSs activate notification appliances, e.g., electromechanical horn and speaker, that generate a high-pitched noise to inform the nearby people about the need to take immediate action. If an attacker launches DISASTER that activates notification appliances several times in a short time frame, the system administrator might be convinced that the system is faulty and turn off the emergency responses. This might lead to serious safety/security risks for the duration the emergency responses remain off.

### **6.5 Launching DISASTER**

In this section, we demonstrate the feasibility of launching DISASTER in realistic scenarios, e.g., residential and industrial automation/monitoring systems. As mentioned in Section 6.3.2, communication protocols utilized in wireless sensors commonly have various security weaknesses. Next, we first briefly describe two well-known types of attacks that exploit security weaknesses of communication protocols to create and transmit illegitimate packets. Second, we demonstrate how an attacker can tailor

these generic forms of attacks to trigger the emergency responses of safety mechanisms and endanger both user safety and system security.

### 6.5.1 Creating and transmitting illegitimate packets

Here, we briefly describe two attacks against sensors that enable the attacker to send illegitimate packets to the base station. In both attacks, we use GNURadio [432], a development toolkit that can be used along with an external radio frequency (RF) hardware, e.g., HackRF [430], to implement various software-defined transmitters/receivers that are implemented as software programs to control external RF devices.

***Attack 1: Retransmitting recorded packets:*** In this approach, an attacker aims to record data packets and retransmit them to the base station without processing or modifying their contents. To do so, the attacker first builds an RF receiver that listens to the communication channel between sensors and the base station and records the transmitted packets. Then, he uses an RF transmitter, which can retransmit previously-recorded packets on the same communication channel. If the frequency of the communication channel is known to the attacker, he can implement the above-mentioned receiver/transmitter using the built-in libraries of GNURadio.

The frequency of the communication channel can be extracted from documents submitted to Federal Communications Commission (FCC). FCC is an independent U.S. government agency that tests all wireless products sold in the U.S. and provides a public database, which includes test reports and documentations of the products [433]. In order to find the frequency of the communication channel used by a sensor, the attacker only needs to find the sensor's documentations by searching its FCC code (i.e., an identification code that specifies the sensor's manufacturer and type) in FCC's public database. FCC codes are commonly written on the sensor's cover.

***Attack 2: Reverse engineering the communication protocol:*** In this approach, the attacker records several data packets and processes them to explore how the communication protocol sends digital data over the communication channel. We describe next how an attacker can reverse-engineer the communication protocol of an arbitrary sensor using HackRF and GNURadio.

1. The attacker first obtains the communication frequency of the sensor and records several packets from the sensor using the method discussed in the previous approach.
2. Then, the attacker finds the modulation type of the communication protocol. The two most commonly-used communication protocols used in wireless sensors are on-off keying (OOK) and binary frequency-shift keying (BFSK). OOK is the simplest form of amplitude-shift keying modulation in which digital data are presented as the presence/absence of a carrier wave, and BFSK is the simplest form of frequency-shift keying (FSK) that uses a pair of discrete frequencies to transmit binary digital data. The modulation type of a communication protocol can be easily detected by examining the Fourier transform of a packet received by HackRF. A single peak (two discrete peaks) in the Fourier transform represents an OOK (BFSK) modulation.
3. After finding the modulation type of a communication protocol, the attacker implements a software-defined demodulator in GNURadio that extracts the transmitted digital data from the recorded analog signal. Fig. 6.2 demonstrates the implementation of an OOK demodulator in GNURadio.
4. If the sensor does not support any encryption mechanism, the attacker can easily examine the digital data to determine what each bit represents, and how he can generate seemingly legitimate packets with arbitrary content.



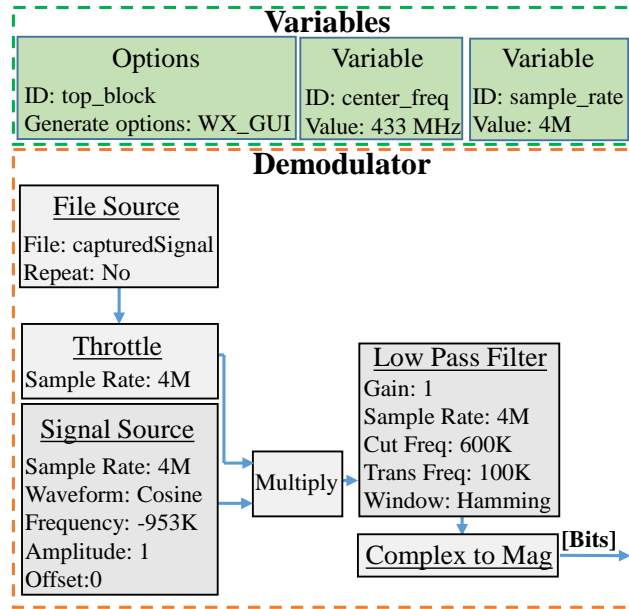


Figure 6.2: The implementation of an OOK demodulator in GNURadio

This approach provides two fundamental advantages over the previous approach. First, the attacker does not need to capture any packets from the actual sensors that he targets. In fact, he can conduct several experiments in a test environment, e.g., a laboratory, to discover potential vulnerabilities in the system. Second, the attacker can improve the quality of the transmitted signal and increase its signal-to-noise ratio in an attempt to launch an attack against the system from a large distance.

### 6.5.2 DISASTER case studies

In this section, we demonstrate the feasibility of launching DISASTER against the two most widely-used automation/monitoring CPSs: residential and industrial.

#### Case I: Residential automation/monitoring CPSs

We first briefly discuss what a typical residential CPS does, what types of sensors are commonly used in such a system, and what emergency responses it offers in the presence of an emergency. Second, we demonstrate how an attacker can use the two

Table 6.1: Different sensors used in a typical residential CPS, their descriptions, and services

Sensor type	Description	Service
Humidity sensor	measures moisture content	Heating/cooling
Temperature sensor	measures the current temperature	Heating/cooling
Light sensor	measures the luminance	Lighting
Motion sensor	detects the presence of a person	Anti-theft mechanism
Door sensor	checks if a door has been opened	Anti-theft mechanism
Smoke detector	detects the presence of smoke/fire	Fire detection

well-known generic types of attacks discussed in Section 6.5.1 to trigger the emergency responses of residential CPSs in real-world scenarios.

***Residential CPSs, their services and emergency responses:*** A residential CPS is mainly designed to offer physical security mechanisms, enhance residents’ convenience, and minimize energy consumption. It can also offer increased quality of life to the residents who need special assistance, e.g., the elderly and disabled people. It processes the data collected by various sensors to control lighting, heating, and cooling, and to monitor/command the security locks of gates and doors. In addition, the base station continuously collects and processes real-time environment-related data gathered by sensors to detect emergency situations. Table 6.1 includes different sensors that are commonly used in residential CPSs, a short description of each sensor, and services that rely on each sensor.

State-of-the-art residential CPSs are able to detect two common emergency situations: fire and ongoing burglary, and provide three typical emergency responses: two passive and one active. Next, we elaborate on these responses and discuss the negative consequences of activating each response.

*Passive response I: Activating warning devices:* In the presence of an emergency situation, notification appliances, e.g., flashing lights, electromechanical horns, or speakers, are activated to warn the proximate people about the need to take immediate action. A majority of notification appliances generate a high-pitched sound to attract the

attention of those nearby. The generated sound could be extremely annoying if it is activated in the absence of an emergency situation. Hence, if a potential attacker can trigger this emergency response several times in the absence of an emergency situation, residents might be convinced that the system is faulty and turn off the emergency response. This might lead to serious safety/security risks and concerns. For example, a burglar might try to trigger the anti-theft alarm several times in a short period of time, e.g., in an hour, in the hope of convincing the user to turn off the monitoring system.

*Passive response II: Informing police/fire department:* Requesting immediate help from the police/fire department, when a real threat is not present, puts firefighters, police officers, as well as the public at risk by needlessly placing heavy, expensive equipment on the streets while wasting fuel and causing traffic jams. Moreover, if an attacker can initiate a help request several times in a short period of time, he might be able to persuade firefighters, police officers, and occupants to believe that when an alarm goes off it is likely a false alarm. As demonstrated later, DISASTER can be launched from a large distance (e.g., over 100 m from the base station). Therefore, an attacker might be able to design a large-scale attack (e.g., he can launch DISASTER using HackRF, while driving in a residential community, to trigger the alarm systems of all houses in the community) to impose significant additional cost on both residents and the responsible governmental department, and convince the residents to turn off their security/safety alarms.

*Active response: Controlling door locks:* As mentioned earlier, a residential automation/monitoring system may be able to automatically control the locks upon the detection of a fire or burglary. In the presence of a fire, it opens the main doors/entrances to ensure that firefighters can enter the affected areas and residents can safely evacuate the building. Moreover, in the presence of an ongoing burglary, it locks the main entrances to ensure that the thief is not able to leave the crime scene until police

officers arrive. Although this emergency response is offered to minimize potential safety risks, triggering this response by an attacker in the absence of an emergency situation could lead to serious security issues. For example, if the attacker triggers the fire evacuation procedure, he will be able to bypass the physical security mechanism of the building by unlocking main entrances. Similarly, the attacker might be able to confine the residents inside the house by initiating the anti-theft lock-down procedure.

***Demonstration of DISASTER against residential CPSs:*** In order to examine the feasibility of launching DISASTER against residential CPSs, we developed two experimental scenarios using the approaches described in Section 6.5. In both scenarios, we targeted three types of sensors (highlighted in red in Table 6.1). The residential CPS processes the data gathered by these sensors to detect emergency situations (fire or burglary). In our experimental setup, we closely inspected six already-in-market sensors (two motion detectors, three smoke detectors, one door sensor) made by well-known manufacturers that cater to the home automation industry. Since these sensors are deployed in numerous already-in-use systems, we choose not to disclose their brand and model number in this chapter.

Next, we describe how the two previously-mentioned generic attacks can be used to launch DISASTER and activate emergency responses of the system.

***Experimental scenario 1: Retransmitting packets:*** In our experimental setup, we captured and retransmitted 20 packets from each sensor (120 packets in all) using the software-defined transmitter/receiver described in Section 6.5.1. Fig. 6.3 demonstrates a packet generated by the door sensor and captured by HackRF. The base station of all the under-experiment sensors accepted previously-recorded packets. This indicates that the packets generated by these sensors include neither a timestamp nor a sequence number. Thus, an attacker can record a packet from each of these sensors

and retransmit it to the base station of the CPS that utilizes the sensor in an attempt to trigger emergency responses.

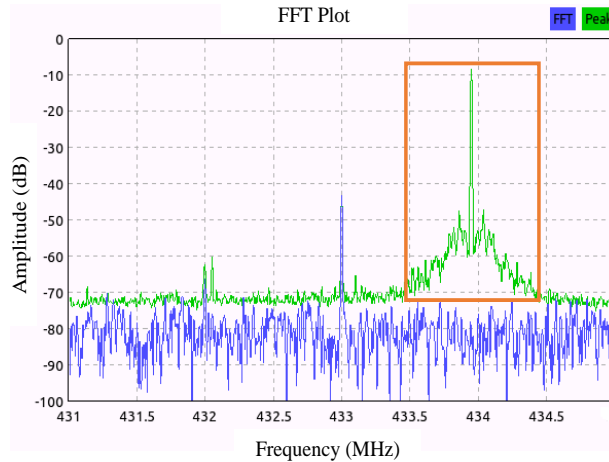


Figure 6.3: The door sensor generates a packet as soon as it detects the door is open. The spike in the fast Fourier transform of the analog signal shows a single transmission using OOK modulation.

In this experimental scenario, we placed HackRF at different distances from each under-experiment sensor to find the maximum recording distance from which the attacker can record a packet using HackRF. Moreover, we increased the distance between HackRF and the base station to find the maximum retransmission distance for each sensor from which a previously-captured packet can be received and accepted by the sensor’s base station. Table 6.2 summarizes results of this experiment for different sensors.

Sensors that enable the anti-theft mechanism (motion and door sensors) transmit data very frequently even when the mechanism is completely disabled. The motion sensor transmits a packet when it detects a moving object, and the door sensor transmits a packet when it detects an open door. For such sensors, an attacker can simply capture a packet when the mechanism is disabled, e.g., when the residents are inside, and retransmit the packet when it is enabled. Unlike motion/door sensors, smoke sensors rarely transmit a packet to the base station since their event-driven transmission protocol only transmits a packet to the base station when an actual threat, e.g.,

Table 6.2: Maximum recording distance and maximum retransmission distance for each sensor in Experimental scenario 1

Sensor	Maximum recording distance (m)	Maximum retransmission distance (m)
Motion sensor I	58	54
Motion sensor II	110	105
Smoke detector I	67	50
Smoke detector II	52	55
Smoke detector III	54	48
Door sensor	56	54

a fire, is present. Thus, capturing and retransmitting a packet that is generated by smoke sensors are difficult and potentially very time-consuming for the attacker. In the second experimental scenario, we discuss how the attacker can reverse-engineer communication protocols deployed in smoke detectors to easily launch DISASTER against the system.

*Experimental scenario 2: Reverse engineering:* As mentioned in Section 6.5, in this approach, the attacker records and demodulates transmitted packets in a test environment, e.g., a laboratory, to examine how a sensor transfers digital data over the communication channel.

We examined the communication protocol used in the six under-experiment sensors. The examination revealed that all sensors share a common security weakness: in order to provide a cost-effective solution, the manufacturers used very simple non-standard transmission protocols that do not provide any cryptographic mechanism. Indeed, the packets transmitted from these sensors to their base stations are neither cryptographically protected nor completely obfuscated. Fig. 6.4 demonstrates the bitstream transmitted by a door sensor to the base station of a residential CPS. The analog signal (Fig. 6.3) captured by HackRF is demodulated using the OOK demodulator (Fig. 6.2). This sensor repeatedly (20 times) transmits a single static packet

(that does not change over time), which includes its 4-bit pin number (a very short sensor identification code), to its base station.

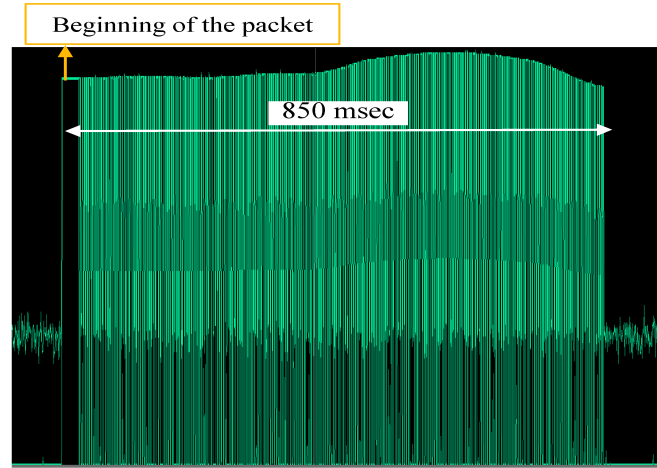


Figure 6.4: The bitstream transmitted by the door sensor to the base station of the residential CPS. The door sensor repeatedly transmits a single static packet, which includes its 4-bit pin number, to its base station.

We were able to completely reverse-engineer the six communication protocols used in these sensors and determine that all of them generate static packets, which include fixed pin numbers. In other words, the only unknown field in the bitstream of an arbitrary packet generated by the sensors was the device’s pin number. Table 6.3 specifies the communication frequency, modulation type, and pin length of each under-experiment sensor.

Table 6.3: Communication frequency, modulation type, and pin length of each residential sensor

Sensor	Communication frequency (MHz)	Modulation	Pin length (bits)
Motion sensor I	433	OOK	4
Motion sensor II	433	OOK	8
Smoke detector I	920	OOK	8
Smoke detector II	920	OOK	8
Smoke detector III	433	OOK	8
Door sensor	433	OOK	4

After completely reverse engineering the protocol, we implemented a brute-force attack using different possible values of the pin numbers of the sensors. We were able to find the actual pin numbers of all sensors in less than five seconds. Then, we placed HackRF at different distances from the base station of the under-experiment sensors and used the maximum transmission power of HackRF to determine the maximum transmission distance from which this attack is possible. Table 6.4 summarizes the results of this experiment for different sensors.

Table 6.4: Maximum transmission distance for each residential sensor in Experimental scenario 2

Sensor	Maximum transmission distance (m)
Motion sensor I	75
Motion sensor II	85
Smoke detector I	75
Smoke detector II	80
Smoke detector III	80
Door sensor	75

## Case II: Industrial automation/monitoring CPS

We first briefly discuss different services and emergency responses offered by a typical industrial CPS. Second, we demonstrate how an attacker can trigger the emergency responses of industrial CPSs.

***Industrial CPSs, their services and emergency responses:*** A typical industrial automation/monitoring CPS offers various automatic mechanisms to operate the equipment, e.g., machinery and boilers, with minimal human intervention, and several approaches that enable remote monitoring of the industrial environment. Generally, industrial automation/monitoring CPSs deal primarily with the automation of manufacturing, quality control, and material-handling processes. In addition, almost all modern industrial automation/monitoring CPSs continuously monitor the



environment to detect emergency situations. These situations need to be aggressively addressed due to the fact they can be catastrophic in a large industrial setting.

State-of-the-art industrial CPSs are able to detect a variety of emergency situations, e.g., a tank overflow, system failure, or a fire. Upon the detection of an emergency situation, they commonly provide four emergency responses, including two passive responses and two active responses. The two passive responses are similar to the ones provided by residential CPSs. Hence, we discuss the two active responses that are commonly offered by industrial CPSs and discuss the negative consequences of activating each response.

*Active response I: Halting normal operation:* A halting procedure is initiated to shut down a part, e.g., a plant or control unit, of the industrial setting or the whole production line when necessary. Upon the detection of an emergency situation, the centralized base station responds by placing the controllable elements, e.g., valves and pumps, into a safe state. For example, a halting procedure controls valves to stop the flow of a hazardous fluid or external gases upon the detection of a dangerous event. This provides protection against possible harm to people, equipment or the environment. Launching DISASTER against an industrial CPS, which activates the halting procedure, may lead to two consequences: production loss and profit penalty. A halting procedure shuts down specific units or the entire facility. This can lead to a significant production loss in chemical industries, e.g., gasoline-centric refinery, where shutting down a unit may stop chemical reactions from completing. Moreover, several time-consuming safety checks need to be done before restarting the normal operation. Thus, the facility might need to be shut down for a substantial amount of time. This could cause a significant impact on profits. For example, an average-sized U.S. Gulf Coast oil refinery loses 68,000 dollars a day for a downed unit [434].

*Active response II: Initiating a damage control mechanism:* Damage control mechanisms include any prudent action aimed at preventing/reducing any expected damage

to the industrial setting, stabilize the situation caused by the damage or alleviate the effects of damage. The main purpose of damage control is to offer a way to return the production line to its normal operation with minimal loss of property or life. A common damage control mechanism in an industrial environment is automatic fire suppression, which employs a combination of dry chemicals and wet agents to extinguish a fire. It applies an extinguishing agent to a three-dimensional enclosed space in order to achieve a concentration of the agent that is sufficient to suppress the fire. A fire suppression system that primarily injects gases into enclosed spaces presents a risk of suffocation. Numerous incidents have been documented where individuals in such spaces have been killed by carbon dioxide agent release [435, 436]. Moreover, the positive pressure caused by these gases may be sufficient to break windows and even walls and destroy the surrounding equipment. Thus, launching DISASTER against an industrial CPS that triggers its fire suppression mechanism may lead to serious consequences, ranging from severe damage to the equipment to life-threatening conditions.

***Demonstration of DISASTER against industrial CPSs:*** In order to investigate the feasibility of launching DISASTER against industrial CPSs, we targeted two industrial systems that use level sensors to monitor liquid level changes in storage tanks (Fig. 6.5). Level monitoring-based safety mechanisms are commonly used in various industrial environments, e.g., the oil industry, to detect an emergency situation that is called tank overflow.

To activate the emergency responses of such a system, the attacker can transmit an illegitimate packet to the base station that indicates that the storage tank is full. Using each of the two approaches described in Section 6.5, an attacker can generate such packets. However, capturing and retransmitting level sensors' regular data packets (i.e., the packets that are periodically transmitted to the base station to report the level of liquid) cannot activate the system's emergency responses. In fact,

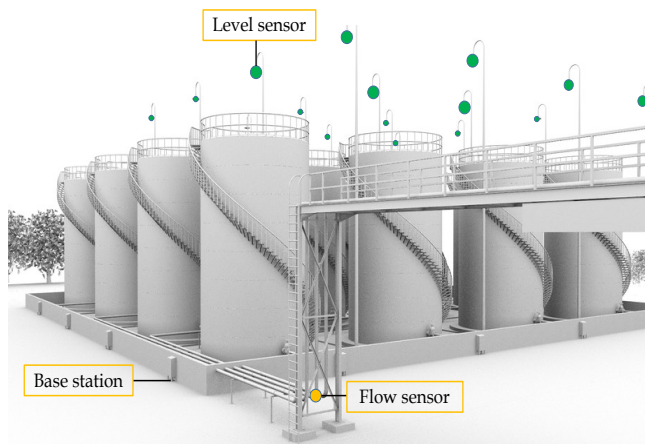


Figure 6.5: A simple industrial automation/monitoring CPS

the attacker needs to record a packet in the presence of a real emergency situation, which is extremely rare in real-world industrial environments, and use it later. Thus, the first approach may not be practical for launching DISASTER against industrial systems described above.

A close examination of two commonly-used industrial level monitoring-based CPSs revealed that none of their sensors uses a secure transmission protocol. Indeed, communications between the sensors and their corresponding base stations are not cryptographically-protected. Therefore, we were able to completely reverse-engineer the communication protocols used in these sensors. To do this, we captured and demodulated 40 data packets (80 packets in all) generated by each sensor. Fig. 6.6 demonstrates the bitstream transmitted by one of the level sensors.

We found that one of the level sensors simply transmits an unencrypted packet that includes a 10-bit pin number and a data field that represents the liquid level in the tank. In order to trigger the emergency response of the CPS that uses this sensor, we transmitted 1024 packets with different pin numbers. We were able to trigger the emergency alarm in less than 10 seconds for this sensor.

We observed that the other sensor transmits unencrypted packets that only contain data and a 1-byte sequence number. Therefore, in order to trigger the emergency

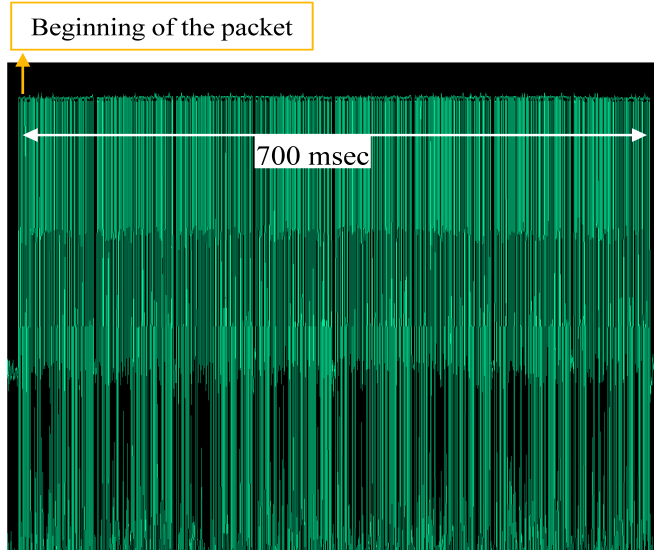


Figure 6.6: The bitstream transmitted by one of the level sensors to the base station of the industrial CPS.

response of the CPS that uses this sensor, an attack can be implemented as follows. The attacker first captures a packet from the sensor and extracts the sequence number. Then he creates and transmits a packet in which the data field is set to its maximum value and the sequence number field is set to the sequence number extracted from the captured packet plus one. We implemented this attack and were able to successfully trigger the emergency responses of the system.

Table 6.5 specifies communication frequency, modulation type, and pin length for each level sensor.

Table 6.5: Communication frequency, modulation type, and pin length for each level sensor

Sensor	Communication frequency (MHz)	Modulation	Pin length (bits)	Sequence number
LS I	433	OOK	10	No
LS II	920	OOK	0 (no pin)	Yes (1 byte)

Moreover, we placed HackRF at different distances from the base stations of the two sensors to find the maximum transmission distance. Table 6.6 summarizes results of this experiment. In real-world industrial CPSs, where signal repeaters (i.e.,

electronic devices that receive signals and retransmit them at a higher power) are in widespread use to support long-range communications, sensors may be located several miles away from the base station. Unfortunately, the attacker can also exploit these repeaters to extend the attack range up to tens of miles, e.g., the attacker can place a HackRF hundred meters away from a repeater that is located several miles away from the under-attack base station of the CPS.

Table 6.6: Maximum transmission distance for each industrial level sensor examined in Experimental scenario 2

Sensor	Maximum transmission distance (m)
LS I	70
LS II	250

## 6.6 Suggested countermeasures

In this section, we first suggest three approaches to mitigate the consequences of launching DISASTER, and for each approach, we briefly describe its limitations and disadvantages. Second, we discuss why preventing DISASTER may not always be feasible due to the existence of unpredictable situations.

### 6.6.1 Proactive countermeasures

Next, we describe three proactive approaches, which can be deployed in the design and verification phases of manufacturing, to prevent DISASTER.

#### Utilizing cryptographic mechanisms

As demonstrated in Section 6.5.2, using simple customized communication protocols to provide short-range communication between sensors and the centralized base station can lead to serious security issues and enable an attacker to reverse-engineer the

protocol. The main weakness of the majority of non-standard communication protocols is that they do not offer any cryptographic mechanisms to ensure confidentiality and integrity of data transmitted by sensors. Utilizing standard communication protocols, which provide strong encryption mechanisms to ensure confidentiality and integrity, or adding encryption mechanisms to customized communication protocols can significantly limit the ability of an attacker to launch a security attack against the system. Bluetooth [245] and ZigBee [247] are instances of standardized communication protocols that offer lightweight encryption mechanisms (e.g., encrypted timestamp and data encryption), yet provide a long battery lifetime. Despite the advantages of encryption mechanisms, utilizing strong encryption in the sensors used in CPS safety mechanisms may not be feasible in the current state of technology due to several domain-specific limitations of CPSs (e.g., lack of enough sources of randomness and limited energy/computation resources) and special requirements of safety mechanisms (e.g., low cost and short response time).

In addition to encryption, obfuscation (i.e., a procedure applied to data to intentionally make them hard to understand without knowing the procedure that was applied) can make reverse engineering of the protocol harder. However, obfuscation cannot truly secure the system since a skilled attacker may eventually be able to reverse-engineer the obfuscation procedure. In fact, obfuscation can only delay (not prevent) reverse engineering of the communication protocol.

### **Security/safety-oriented verification**

As mentioned earlier, common design flaws and security weaknesses of safety mechanisms along with ignorance of common security-safety conflicts/trade-offs can endanger both security and safety of the system. There is a great body of literature on different types of design verification approaches and several commercialized verification approaches that manufacturers can use to detect and address common design

flaws before introducing their product into the market. Such verification approaches have traditionally been used to ensure that a product, service, or system works correctly, meets specific requirements, and fulfills its intended purposes. Unfortunately, traditional verification mechanisms do not typically target a comprehensive set of security and safety requirements. Recently, a few verification approaches [437–440] have begun to take various security and safety considerations into account. Moreover, a few proposals (e.g., [428]) have offered theoretical approaches to detect different safety-security conflicts/trade-offs in CPSs.

Utilizing such newly-proposed approaches can enable designers and manufacturers to predict or detect design flaws, security weaknesses, and safety-security conflicts before releasing a product to the market. However, relying on such methods cannot completely prevent DISASTER due to: (i) the existence of serious disagreements between some security and safety requirements that forces the manufacturer to consider some requirements and ignore others, (ii) inefficiency and imperfections of verification mechanisms, and (iii) unpredictability of threats against CPSs.

### **Designing multimodal systems**

In order to plan and execute an appropriate emergency response, a CPS must reason about its surroundings and obtain a precise description of the environment. Such a system can gather and process data from its surroundings using various types of sensors. Generally, a CPS that uses multiple types of sensors (referred to as a multimodal system) can obtain more information about the environment than a CPS that only relies on one type (referred to as a unimodal system). As a result, multimodal CPSs provide two fundamental advantages over unimodal systems. First, they offer a higher accuracy in detecting emergency situations due to the fact that they can obtain more information about the environment and utilize sensor fusion methods (that combine various sensory data to improve the resolution and accuracy of specific sensor data)

to achieve an accurate description of the environment. Second, multimodal CPSs are typically more difficult to attack since the attacker has to simultaneously target several sensor types to launch DISASTER. For example, a fire detection mechanism that relies on both temperature and smoke detection sensors is clearly more accurate and secure in comparison to a system that only uses smoke detection sensors.

However, multimodal CPSs generally have two disadvantages over unimodal systems: (i) multimodal systems are more complex and expensive, (ii) since the multimodal systems need to process more information, they are slower in detecting emergency situations. Moreover, if all sensors utilized in a multimodal CPS have common design flaws and weaknesses (e.g., all sensors use the same communication protocol that support neither obfuscation nor encryption), launching DISASTER against the multimodal system may not be significantly harder than launching an attack against a unimodal system.

### **6.6.2 Unpredictable situations**

Although the three previously-mentioned approaches can significantly limit the ability of a potential attacker, providing a comprehensive solution for eliminating the security risk associated with DISASTER is hard for two reasons. First, DISASTER might be feasible as a result of the existence of a situation that is not predictable at design time. Second, modeling human errors, e.g., pitfalls in the installation procedure, which might make a system susceptible to the proposed attacks, is very difficult. For instance, suppose a company sends certified installers to install a residential automation system that provides a fire evacuation mechanism, which is able to unlock the doors upon the detection of a fire. A month later, another company installs an air conditioner unit that is accessible from outside the building. In this scenario, an attacker might be able to inject smoke into the residence using the routing paths of the air conditioner and trigger the fire evacuation mechanism even when there is no



fire. In fact, the air conditioner provides the means to a potential attacker to have physical access to the home automation system and trigger its emergency responses.

## 6.7 Chapter summary

In this chapter, we introduced DISASTER, which exploits design flaws and security weaknesses of safety mechanisms deployed in CPSs along with safety-security conflicts to trigger the system's emergency responses even in the absence of a real emergency situation. This can lead to serious consequences, ranging from economic collateral damage to life-threatening conditions.

We examined several already-in-use sensors and listed common design flaws and security weaknesses of safety mechanisms. We discussed the various impacts of DISASTER and described potential consequences of such attacks. We also demonstrated the feasibility of launching DISASTER in realistic scenarios, e.g., residential and industrial automation/monitoring CPSs. Finally, we suggested several countermeasures against the proposed attacks, and discussed how unpredictable situations may give rise to significant security problems in presumably secure CPSs.

# Chapter 7

## CABA: Continuous Authentication Based on BioAura

Most computer systems authenticate users only once at the time of initial login, which can lead to security concerns. Continuous authentication has been explored as an approach for alleviating such concerns. Previous methods for continuous authentication primarily use biometrics, e.g., fingerprint and face recognition, or behaviometrics, e.g., key stroke patterns. We describe CABA, a novel continuous authentication system that is inspired by and leverages the emergence of sensors for pervasive and continuous health monitoring. CABA authenticates users based on their BioAura, an ensemble of biomedical signal streams that can be collected continuously and non-invasively using wearable medical devices. While each such signal may not be highly discriminative by itself, we demonstrate that a collection of such signals, along with robust machine learning, can provide high accuracy levels. We demonstrate the feasibility of CABA through analysis of traces from the MIMIC-II dataset [441]. We propose various applications of CABA, and describe how it can be extended to user identification and adaptive access control authorization. Finally, we discuss possible attacks on the proposed scheme and suggest corresponding countermeasures [37].

## 7.1 Introduction

Authentication refers to the process of verifying a user based on certain credentials, before granting access to a secure system, resource, or area [442]. Traditionally, authentication is only performed when the user initially interacts with the system [443]. In these scenarios, the user faces a knowledge-based authentication challenge, e.g., a password inquiry, and the user is authenticated only if he offers the correct answer, e.g., the password.

Although one-time authentication has been the dominant authentication mechanism for decades [444], several issues spanning user inconvenience to security flaws have been investigated by researchers [445, 446]. For example, the user has to focus on several authentication steps when he tries to unlock a smartphone based on a password/pattern-based authentication method. This may lead to safety risks, e.g., distraction when the user is driving. A serious security flaw of one-time authentication is its inability to detect intruders after initial authentication has been performed. For example, an unauthorized user can access private resources of the authorized user if the latter leaves his authenticated device unattended, or forgets to log out [447].

The above concerns have led to the investigation of continuous authentication mechanisms. Such mechanisms monitor the user's interactions with the device even after initial login to ensure that the initially-authenticated user is still the one using the device. Initial efforts in this direction were based on simple security policies that lock the user's device after a period of inactivity, and ask the user to re-enter the password. However, such schemes may be annoying to users while they still expose a window of vulnerability, leaving much room for improvement [448]. Thus, a rapidly-growing body of literature on the usage of biometrics, i.e., strongly-reliable biological traits such as facial features, and behaviometrics, i.e., measurable behavior such as frequency of keystrokes, for continuous authentication has emerged in the last decade [447, 449].

Recently, wearable medical sensors (WMSs), which measure biomedical signals, e.g., heart rate, blood pressure, and body temperature, have drawn a lot of attention from researchers and begun to be adopted in practice [450, 451]. A recent report by Business Insider [452] claims that 33 million wearable health monitoring devices were sold in 2015. It forecasts that this number will reach 148 million by 2019, and continue to grow rapidly thereafter. We suggest that, since such biomedical signals will be collected anyway for health monitoring purposes, they can also be used to aid authentication. The use of continuously-collected biomedical data for user verification and identification seems promising for three reasons. First, if the biomedical signals are collected by WMSs for medical purposes, using them for authentication does not require any extra device that is not already on the body. Second, this information is collected transparently to the user, i.e., with minimal user involvement. Third, unlike traditional biometrics/behaviometrics, e.g., face features and keystroke patterns, information that may frequently become unavailable, the stream of biomedical signals collected by WMSs is always available when the person is wearing WMSs.

In this chapter, we present CABA, a transparent continuous authentication system based on an ensemble of biomedical signal streams (Biostreams in short) that we call *BioAura*<sup>1</sup>. A Biostream is a sequence of biomedical signal samples that are continuously gathered by a WMS for medical diagnosis and therapeutic purposes. The most important difference between a Biostream and a biometric trait is that a Biostream alone does not have enough discriminatory power to distinguish individuals. Thus, an authentication decision based on a single Biostream, e.g., body temperature or blood pressure, is unlikely to be sufficiently discriminative. However, when multiple Biostreams are combined into a BioAura, it leads to a powerful continuous authentication scheme.

---

<sup>1</sup>Aura is traditionally defined as the energy field around a person. Analogously, we use the term BioAura to define the biological field around a person, manifested as a set of Biostreams.

Our key contributions can be summarized as follows:

1. We suggest a list of design requirements for any continuous authentication system.
2. In order to analyze the discriminatory power of BioAura, we propose a continuous authentication system based on BioAura (called CABA) and investigate it from both accuracy and scalability perspectives.
3. We suggest an adaptive authorization scheme and describe how it can be used to alleviate user inconveniences associated with the use of continuous authentication systems that might falsely reject the user.
4. We describe various possible attacks against the proposed continuous authentication system along with several countermeasures to prevent such attacks.

The rest of the chapter is organized as follows. Section 7.2 describes the requirements that should be targeted in the design of continuous authentication systems and discusses how CABA addresses such requirements. Section 7.3 describes BioAura and the Biostreams that form the proposed BioAura. Section 7.4 discusses the scope of CABA applications. Section 7.5 describes the CABA prototype and our experimental setup. Section 7.6 investigates CABA from both accuracy and scalability perspectives. Section 7.7 describes how CABA can support identification, i.e., the process of recognizing a user without knowing his user ID. Section 7.8 presents an adaptive authorization scheme that can be used along with CABA to enhance user convenience. Section 7.9 discusses possible attacks against the proposed authentication system and describes different countermeasures against each attack. Section 7.10 discusses related work and compares CABA with previously-proposed continuous authentication systems. Section 7.11 briefly describes possible privacy concerns surrounding the use of biomedical signals, how CABA can be used as a stand-alone one-time authentication

system, and the effects of temporal conditions on authentication results. Finally, Section 7.12 concludes the chapter.

## 7.2 Desirable authentication requirements

In this section, we first describe the desirable requirements that every continuous authentication system must satisfy. Then, we discuss how CABA addresses such requirements.

### 7.2.1 Design-octagon

Even though several continuous authentication systems have been proposed in the past, they have not been evaluated against a comprehensive list of design requirements. A few studies, e.g., [453–455], consider a small set of requirements, e.g., cost and accuracy. However, there is no standard list of design requirements that a continuous authentication system must satisfy. We suggest such a list below (that also includes some of the desiderata of typical WMS-based systems, as shown in Fig. 1.5). We call it the *Design-octagon* since it comprises eight design requirements (Fig. 7.1):

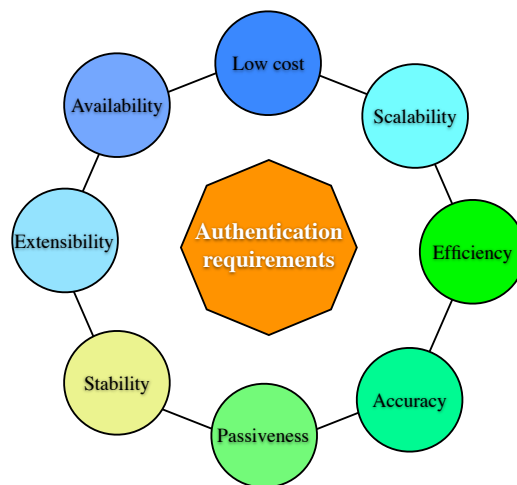


Figure 7.1: Design-octagon: Desiderata for a continuous authentication system.

**1. *Passiveness*:** A user-friendly system must not require frequent user involvement [456]. For example, if the authentication system asks the user to re-enter his credentials often, it may be quite annoying to the user [454].

**2. *Availability*:** The system should provide a reliable authentication system at all time instances [454]. Lack of continuous availability is a significant drawback of several previously-proposed continuous authentication systems – they may often fail due to a lack of sufficient information [457]. For instance, a keyboard-based system may unintentionally reject a legitimate user when he is watching a movie and not using the keyboard.

**3. *High accuracy*:** Undoubtedly, the most important requirement of every authentication system is high accuracy. The system should be able to confidently and accurately distinguish legitimate users from impostors, and reject impostors' requests.

**4. *Scalability*:** The system should be able to handle a growing amount of work when the number of users increases [444]. In particular, its time and space complexity should increase modestly with an increase in the number of users [458].

**5. *Efficiency*:** A short response time, i.e., the time required to capture a test sample, process it, and provide a decision, is very desirable for two reasons. First, it is desirable for the system to quickly authenticate a legitimate user and reject an impostor to ensure user convenience [444]. Second, security may also suffer if there is an appreciable delay. For example, if authorization takes five minutes, an impostor may be able to control the system and access restricted resources in that five-minute timeframe, while the system is still processing.

**6. *Low cost*:** Cost is an important factor in authentication systems used in low-security environments, e.g., in personal computers [454, 459]. In such environments, the cost of adding or modifying the authentication system should ideally be negligible. Thus, systems that do not need extra peripherals, such as retina scanners, would be generally preferred. However, for highly-secure environments, e.g., military bases,

expensive authentication systems could be deployed [455].

**7. Stability:** Any trait that is recorded for processing for authentication purposes must ideally have only slight changes or maintain its pattern over a certain time period [459, 460].

**8. Extensibility:** The authentication system should be able to function on a wide variety of devices regardless of underlying hardware. Ideally, the system should not require dedicated hardware. One of the advantages of password-based authentication is that it can be easily extended to protect a large number of systems, devices, and resources with minimal system modification [444].

### 7.2.2 Addressing desirable requirements

In this subsection, we describe how CABA ensures all of the requirements discussed above.

**1. Passiveness:** In CABA, passiveness is addressed through the use of WMSs. These are small and compact sensors that are specifically designed to take the passiveness requirement into account, since continuous health monitoring needs to minimize user involvement. Thus, passiveness is not only a very desirable requirement for continuous authentication, but also a significant consideration in designing WMSs. Unfortunately, major biometrics-based systems, e.g., fingerprint-based, do not provide a high level of passiveness.

**2. Availability:** The use of WMSs as capture devices also ensures a continuous stream of information since this is also required for continuous health monitoring. However, neither biometrics nor behaviometrics guarantees availability. For example, keyboard/mouse-based continuous authentication systems fail when the user stops using the dedicated peripherals.

**3. Accuracy:** The accuracy of CABA is extensively investigated in Section 7.6 in various experimental scenarios. Section 7.10 demonstrates that the accuracy of



CABA, which is based on an ensemble of weakly discriminative Biostreams, is comparable to previously-proposed systems, which are based on strong biometrics.

**4. Scalability:** The scalability of CABA is investigated in Section 7.6 based on two scalability metrics (time complexity and space complexity). Our analysis shows that an increase in the number of users can be easily handled in this system.

**5. Efficiency:** Authentication can be done in a few milliseconds. For each authentication attempt, the user can immediately provide the required data since the data are already collected using WMSs. The efficiency of the system is described in more detail in Section 7.6.

**6. Low cost:** As discussed later in Section 7.3, the proposed BioAura consists of Biostreams that are collected for continuous health monitoring. If the user is already using a continuous health monitoring system, CABA can offer continuous authentication with minimal cost.

**7. Stability:** Our investigations of different Biostreams and their high authentication accuracy over different timeframes demonstrate that the collected Biostreams maintain their pattern over time. Therefore, they can be used as authentication traits.

**8. Extensibility:** By decoupling the collection of Biostreams from the authenticating device, CABA can be implemented in any general-purpose computing device with sufficient memory capacity and computation power. Unfortunately, neither biometrics- nor behaviometrics-based systems provide significant extensibility. For example, the nature of keyboard/mouse-based authentication schemes inherently limits their applications, i.e., they can only be used for implementing an authentication mechanism in a system that has a keyboard or a mouse.

## 7.3 BioAura

In this section, we first briefly describe how Biostreams can be collected using WMSs. Then, we discuss which Biostreams constitute the BioAura.

As mentioned earlier, BioAura is an ensemble of Biostreams, which are gathered by WMSs for medical diagnosis and continuous health monitoring. The most widely-used scheme for continuous health monitoring consists of two classes of components: (i) WMSs and (ii) a base station [11]. All WMSs transmit their data to the base station either for further processing or long-term storage. In recent years, smartphones have become the dominant base station since they are powerful and ubiquitous, and their energy resources are less limited relative to WMSs [11,461]. Fig. 7.2 illustrates a simple continuous health monitoring system that consists of several small lightweight WMSs, which transmit their biomedical data to the smartphone over a Bluetooth communication link (similar to the left side of the personal health care system illustrated in Fig. 3.1).

Smartphones can perform simple preprocessing to extract values of some important features from the data, and transmit those values. In CABA, the smartphone first executes a very simple feature extraction function that computes the average value of the samples in each Biostream over the last one-minute timeframe of data. Then, it only transmits a feature vector that contains these average values.

As mentioned earlier in Section 7.1, with the expected widespread use of WMSs, CABA can be used to provide a continuous authentication system as a side benefit of continuous health monitoring systems. Our proposed BioAura consists of Biostreams that are essential for routine continuous health monitoring, and their collection needs minimum user involvement. Such Biostreams are expected to be included in long-term continuous health monitoring systems.

Table 7.1 shows the most widely-used Biostreams, their abbreviations/notations used in the medical literature, and their units [11,462]. In this chapter, we exclude

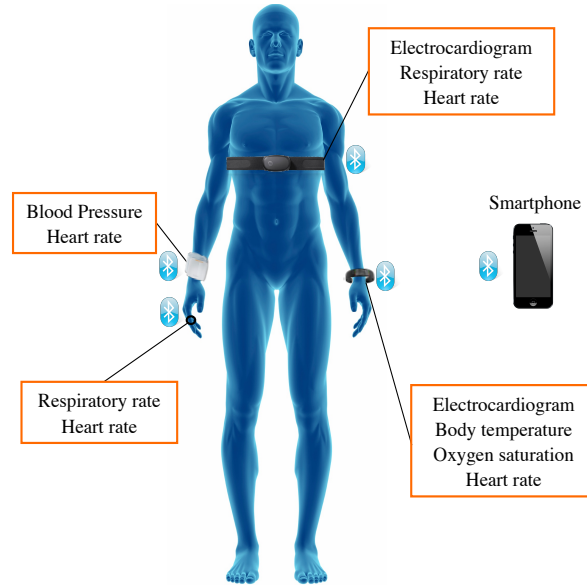


Figure 7.2: A continuous health monitoring system consisting of several small lightweight WMSs that transmit biomedical data to the smartphone.

the first three ones from the proposed BioAura, and include the other nine. Next, we discuss why the three Biostreams are excluded.

**1. *Electroencephalogram (EEG)*:** EEG is excluded from BioAura because it cannot be conveniently captured. The current method for capturing EEG requires the user to wear a cap. Moreover, its capture devices cannot be miniaturized further because electrodes need to form a minimum diameter to be noise-robust [87].

**2. *Electrocardiogram (ECG)*:** Even performing a low-complexity feature extraction on one minute of ECG signals requires at least  $400\times$  more operations than performing a simple statistical feature extraction, e.g., averaging, on the respiratory rate values [463]. This would place a significant computational and energy demand on battery-powered devices such as smartphones and wearables. If we try to avoid the preprocessing, i.e., feature extraction, on the smartphone and just transmit the ECG signals to the authentication system, this would also entail significant energy consumption since ECG waveforms contain at least  $200 \text{ samples/s}$  [11, 464].

**3. *Blood glucose (BG)*:** BG is excluded because currently the devices that mea-

sure BG are invasive, i.e., they require a sample of the user’s blood.

Although we have currently used nine Biostreams to form the BioAura in the prototype implementation, CABA need not necessarily be limited to these nine. As other compact WMSs become available in the future, they could also be made part of the BioAura.

Table 7.1: Biostreams, their abbreviations/notations, and units

Biostream	Abbreviations/Notations	Unit
Electroencephalogram	EEG	$\mu V$
Electrocardiogram	ECG	$\mu V$
Blood glucose	BG	$mg/dL$
Arterial systolic blood pressure	ABPSYS	$mmHg$
Arterial diastolic blood pressure	ABPDIAS	$mmHg$
Arterial average blood pressure	ABPMEAN	$mmHg$
Heart rate	HR	$1/min$
Pulmonary systolic artery pressure	PAPSYS	$mmHg$
Pulmonary diastolic artery pressure	PAPDIAS	$mmHg$
Body temperature	T	<i>Celsius</i>
Oxygen saturation	SPO2	%
Respiratory rate	RESP	$1/min$

## 7.4 Scope of applications

In this section, we describe the possible applications of CABA. The concept of continuous authentication based on BioAura can be used to protect (i) personal computing devices and servers, (ii) software applications, and (iii) restricted physical spaces. Next, we conceptually describe how CABA can be used to protect each domain.

Computing devices, e.g., personal computers, laptops, tablets, and cell phones, or servers can employ two different approaches to utilize CABA: (i) they can use their own computing resources to implement a stand-alone version of CABA, or (ii) they

can simply use decisions made by a version of the scheme implemented on a trusted server. We investigate both approaches.

**Example 1:** Suppose a tablet wants to authenticate its user. The tablet may be unable to dedicate its limited memory/energy resources to support the whole authentication process. In such a scenario, it can use decisions made by a trusted server running CABA. Fig. 7.3 illustrates this scenario. When the user tries to unlock the tablet, it informs the user's smartphone. The smartphone asks the trusted server to open a secure communication channel. The smartphone then sends the information required for specifying the device that needs to be unlocked, e.g., the tablet ID, along with the information that needs to be processed to authenticate the user, e.g., the user ID and a preprocessed frame of data points from his BioAura, to the trusted server. The server then authenticates the user and sends this decision to the tablet. After initial login, the trusted server demands fresh data points at certain intervals.

**Example 2** Suppose the user wants to login to his personal computer. In this case, the computer has enough computational power and energy capacity to implement a stand-alone version of CABA. This case is similar to the one in Example 1, except that there is no need for a trusted server (Fig. 7.4).

Similarly, CABA has the potential to provide continuous authentication for applications that need strong authentication, e.g., e-commerce applications. Its authentication decisions can be made on the same device that runs the application or on a powerful trusted server and then transmitted to the device that runs the application.

**Example 3:** Consider an online banking application that is installed on the user's smartphone. When the user opens the application to access his bank account, the smartphone opens a secure communication channel with the trusted server. Then, the smartphone sends the required information for specifying the application, e.g., the application ID, along with information needed for authenticating the user. The rest of the protocol is the same as before.

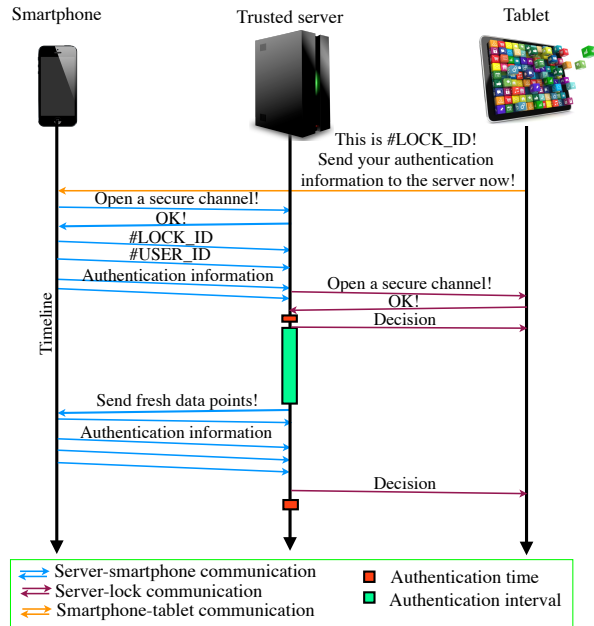


Figure 7.3: The tablet wants to authenticate the user. The vertical arrows depict the timeline.

Finally, CABA can be used to control access to restricted physical spaces, e.g., buildings. Typically, the electronic device that controls the entrance, e.g., a smart lock, would not have enough computation power to use a stand-alone version of CABA. Hence, in such cases, the scheme can be implemented on a trusted server, and decisions then transmitted to the device. This case is similar to the one depicted in Fig. 7.3, with the tablet replaced by the lock.

## 7.5 Implementation and experimental setup

In this section, we first describe our implementation of CABA. We then discuss our experimental setup and different metrics that we used to investigate the proposed system.

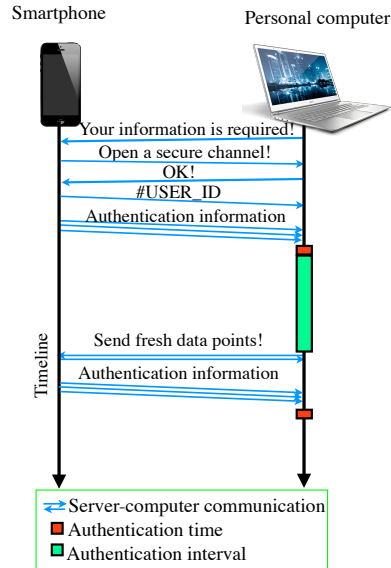


Figure 7.4: The laptop wants to authenticate the user before allowing the user to utilize its resources or software applications.

### 7.5.1 Prototype implementation

Similar to other authentication systems, CABA has two operating phases: (i) enrollment phase in which CABA builds machine learning-based models for each user, given the training data, and (ii) user authentication phase in which the system continuously authenticates the user. The description of the two phases is presented next.

#### Enrollment phase

In the enrollment phase, the authentication system is given a training dataset. The system builds the model using a supervised learning approach, i.e., a machine learning approach in which the model is built based on labeled training data points.

Generally, the amount of information needed to build a model varies from one application to another. As we elaborate later in Section 7.6, we evaluated the number of training data points needed to investigate how much information should be sent to the authentication system to build a reliable and accurate model. Each data point in the training set is nine-dimensional and consists of the average values of

successive measurements of a Biostream over a one-minute timeframe. The value of each dimension is represented using half-precision floating-point format that requires two bytes of storage. Therefore, if the smartphone needs to transmit data points extracted over a one-hour period, it only needs to send 1080 bytes of data to the authentication system over this period.

In order to maintain reliability, CABA should train a new model based on fresh biomedical data obtained at certain intervals. In other words, CABA should update the model regularly to ensure that the model maintains accuracy and can distinguish legitimate users from impostors. The frequency of model update, i.e., how frequently CABA should repeat the enrollment phase, depends on several factors, such as required accuracy and learning time. As we show later in Section 7.6, our experimental results indicate that when CABA re-trains the model every four hours, it achieves the best accuracy and the learning time is only a few minutes. Learning can be done transparently to the user. In other words, CABA can re-train the model while the user continues to be authenticated. For example, suppose the enrollment phase takes five minutes each time and is repeated every four hours, i.e., each model is used for four hours. CABA can start re-training to generate a new model after 3 hours and 55 minutes, and be ready with it after four hours have elapsed.

### **User authentication phase**

In this phase, the system makes decisions using the already-trained model. In a continuous authentication scenario, the system should verify the user's identity at certain intervals. The frequency of authentication depends on several factors, such as the required level of security and the amount of information required for one authentication. In our prototype implementation, CABA re-authenticates the user every minute based on a given nine-dimensional data point  $Y$  that contains the average values of the chosen Biostreams over a specified time interval. When the user approaches the



authentication system and requests authentication, the smartphone performs a simple computation on the already-gathered Biostreams and provides  $Y$ . Therefore, unlike most previously-proposed continuous authentication systems, e.g., keyboard/mouse-based systems, that require the user to wait while they collect authentication information, CABA obtains the required information almost *instantaneously* because the information has already been gathered and stored on the smartphone for the purpose of health monitoring.

Fig. 7.5 illustrates how CABA works when the user requests authentication. In a single verification attempt:

1. The smartphone preprocesses one minute of Biostreams collected from the user’s BioAura. Then, it transmits the preprocessed information ( $Y$ ) along with user ID to the authentication system.
2. The Look-up stage sends  $Y$  to the appropriate classifier in the Jury stage based on the given user ID.
3. The dedicated classifier processes  $Y$  and outputs a binary decision (accept or reject).

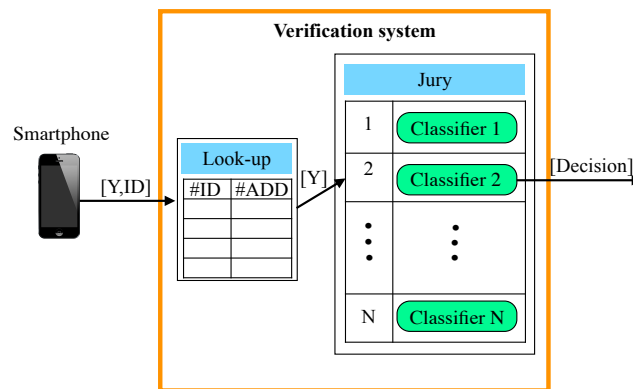


Figure 7.5: User authentication phase: The user’s smartphone provides  $Y$  and the user ID, and CABA outputs the decision.

Next, we provide a detailed description of Look-up and Jury stages.

1. **Look-up stage:** This stage forwards the nine-dimensional vector  $Y$  provided

by the smartphone to the appropriate classifier based on the given user ID. In order to provide a fast search mechanism to find the appropriate classifier, this stage can be implemented using a hash table that associates user IDs with pointers to the classifiers.

**2. Jury stage:** The Jury stage consists of  $N$  binary classifiers, where  $N$  is the number of people who need to be authenticated. The  $i$ -th classifier is trained to only accept the data point  $Y$  that is extracted by the  $i$ -th user's smartphone from his BioAura. The training set of the  $i$ -th classifier consists of the  $i$ -th user's data points labeled as "accept" and others' data points labeled as "reject".

We have used two well-known binary classification methods to build our model: Support Vector Machine (SVM) [258] and Adaptive Boosting (AdaBoost) [465]. Next, we briefly describe each method.

- SVM: The basic concept in an SVM is to find a hyperplane that separates the  $n$ -dimensional data into two classes. However, since the data points in the dataset are not usually linearly separable, SVMs introduce the concept of kernel trick that projects the points into a higher-dimensional space, where they are linearly separable. When no prior knowledge about the dataset is available, SVMs usually demonstrate promising results and generalize well. A great number of previous research studies that perform authentication using machine learning methods only consider SVM with a linear kernel [466] or radial basis function (RBF) kernel [467]. We decided to investigate both.
- AdaBoost: Although SVM has been commonly used in previously-proposed continuous authentication systems in a variety of scenarios, we decided to include AdaBoost as well. The idea behind AdaBoost is to build a highly accurate classifier by combining many weak classifiers that always perform a little bit better than random guessing on every distribution over the training set [465]. Since biomedical signals are individually slightly discriminative, they lead to

weak classifiers, which can be collectively turned into a strong classifier using AdaBoost. Choosing appropriate types of weak classifiers is a significant consideration in AdaBoost. The most commonly used weak learning methods for implementing AdaBoost-based classifiers are decision stumps (also called one-node tree) and decision trees.

### 7.5.2 Experimental setup and metrics

Here, we first describe the parameters and dataset used in our experiments. Then, we discuss the accuracy and scalability metrics used to investigate the proposed authentication system.

#### Experimental parameters and dataset

Next, we discuss the parameters used in our experimental setup and describe the dataset.

**Parameters:** We need the following five parameters in our experiments.

- Dataset length ( $L$ ): This is the duration of Biostreams measurements, i.e., the number of hours of information we have for each person in our data set. In our experiments, we used 14 hours of data for each individual, i.e.,  $L = 14 h$ .
- Dataset dimension ( $n$ ): This is the number of Biostreams that form the BioAura of an individual. In our setup, we have included nine Biostreams for each person, i.e.,  $n = 9$ .
- Dataset size ( $N$ ): This is the number of people in the dataset.
- Training window size ( $TRW$ ): This represents the duration of the signal measurements (expressed in hours) for each individual that we used for training the model in the enrollment phase. For example, if  $TRW$  is 1 hour, it means we

have included 60 data points in our training set, where each point is a nine-dimensional vector consisting of the average values of successive measurements of the nine Biostreams over a one-minute timeframe. We vary TRW in our experiments to study its impact on the model’s accuracy.

- Testing window size ( $TEW$ ): This represents the duration of signal measurements (expressed in hours) for each individual for investigating the accuracy of the trained model in the user authentication phase. We vary the value of TEW in our experiments to investigate its impact on the performance of CABA.

**Dataset:** In order to investigate the accuracy of CABA, we used a freely available multi-parameter dataset, called MIMIC-II [441]. MIMIC-II was gathered in a controlled environment in which each user remains almost stationary during data collection. It has been extensively used in the medical and biomedical fields. It consists of several anonymized high-resolution vital sign trends, waveforms, and sampled biomedical signals for many individuals. For our experiments, we could only find 37 users ( $N = 37$ ) in MIMIC-II for whom the data: (i) include the nine targeted Biostreams, and (ii) are available over several hours (at least 14 hours) with minimal missing values (we excluded a user for whom the data were not available for more than two consecutive hours). Biostreams were sampled using patient monitors (Component Monitoring System Intellivue MP-70 and Philips Healthcare) at the sampling rate of 125 Hz [441].

### **Accuracy metrics**

Next, we describe five metrics that we used for analyzing the accuracy of the proposed authentication system. The first three are traditionally used for examining authentication systems. We define two more to investigate the accuracy in the context of continuous authentication.

- False acceptance rate ( $FAR$ ): This is the ratio of falsely accepted unauthorized users to the total number of invalid requests made by impostors trying to access the system. In the context of continuous authentication, we use the notation  $FAR_{t=TEW}$  to denote FAR under  $TEW$ . A lower FAR is preferred in cases in which security is very important [82].
- False rejection rate ( $FRR$ ): This refers to the ratio of falsely rejected requests to the total number of valid requests made by legitimate users trying to access the system. We use the notation  $FRR_{t=TEW}$  to denote FRR under  $TEW$ . A lower FRR is preferred for user convenience [82].
- Equal error rate ( $EER$ ): This is the point where  $FAR$  equals  $FRR$ . Reporting only  $FRR$  or  $FAR$  does not provide the complete picture because there is a trade-off between the two since we can make one of them low by letting the other one become high. Therefore, we use  $EER$  (instead of  $FRR$  or  $FAR$ ) for reporting CABA's accuracy. As before, we use the notation  $EER_{t=TEW}$  to denote EER under  $TEW$ .
- False acceptance worst-case interval ( $FAW$ ): The output of the authentication system in a time period  $T$  is a sequence of accept/reject decisions. As an example, Fig. 7.6 shows two possible output sequences over a ten-minute authentication timeframe when an impostor is trying to get authenticated. In both sequences, the number of falsely accepted requests is the same. However, in a continuous authentication scenario, the second sequence would be considered worse since the impostor can use the system over a four-minute timeframe without being detected, whereas in the first case the impostor can only use the system over a one-minute timeframe. We define  $FAW$  as the longest time interval (expressed in minutes for CABA) over which an impostor can be falsely

accepted as a legitimate user. In the example of Fig. 7.6,  $FAW$  is one minute and four minutes for the first and second cases, respectively.

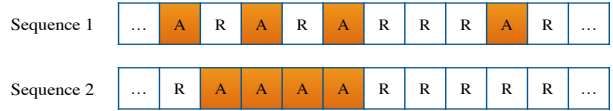


Figure 7.6: Two possible output sequences over a ten-minute authentication time-frame. A (R) refers to an accept (reject) decision.

- False rejection worst-case interval ( $FRW$ ): Analogously to  $FAW$ , we define  $FRW$  as the longest time interval (expressed in minutes) over which a legitimate user might be falsely rejected and marked as an impostor.

### Scalability metrics

As mentioned in Section 7.2, the time and space complexity of the authentication system should increase modestly with an increase in the number of users. In order to investigate the scalability of the proposed method, we express the time and space complexities of CABA using the well-known  $O$  notation, as a function of  $N$  (number of the people in the dataset).

## 7.6 Authentication results

In this section, we investigate CABA from both the accuracy and scalability perspectives.

### 7.6.1 Authentication accuracy

In order to investigate the accuracy of the authentication system, we implemented a prototype of CABA in MATLAB.

The accuracy of a model is generally investigated using a set of data points that is different from the set used in constructing the model. Thus, in order to train and test a

model, the dataset can be divided into two parts: training and test sets. The classical  $K$ -fold cross-validation is not suitable for estimating the performance of a system that processes a time series, i.e., a sequence of data points consisting of successive measurements, because potential local dependencies across observations in a time series define a structure in the data that will be ignored by cross-validation [468]. Thus, in this work, instead of using traditional cross-validation, we designed several experimental scenarios for evaluating the accuracy of the authentication system. We describe these scenarios next.

1. *Baseline*: In the baseline scenario, we break the available dataset into two equal parts, i.e.,  $TEW = TRW = 7 h$ . We use the first half of the dataset (the first seven hours) of each individual to train the model and the second half to test it. We use all the Biostreams, i.e.,  $n = 9$ , to train and test our system. We use two classification methods: SVM and AdaBoost. In the case of SVM, we use two kernels (linear and RBF). In the case of AdaBoost, we consider decision stumps (one-node tree) and decision trees with 5, 10, 15, and 20 nodes as weak classifiers. We run 40 iterations for all Adaboost-based classifiers since we determined experimentally that the training error becomes zero within these many iterations and testing error becomes minimum. The value of  $EER_{t=7h}$  is reported in Table 7.2 for all classifiers. AdaBoost with a tree size of 15, i.e., with 15 nodes in the tree, has the minimum value of  $EER_{t=7h}$ . Increasing tree size usually improves the accuracy of Adaboost-based classifiers. However, using larger trees leads to more complex models, which are more susceptible to overfitting [469]. This can be seen when we move from a tree size of 15 to 20. Table 7.3 summarizes  $FAW$  and  $FRW$  for all classification schemes. Consider RBF SVM as an example. Its  $FAW$  is 4 minutes, which suggests that, in the worst case, an impostor can deceive the authentication system for a 4-minute

Table 7.2: Classifiers and their  $EER_{t=7h}$ 

Type of classifier	Specification	$EER_{t=7h}$ (%)
SVM	Kernel = Linear	3.0
	Kernel = RBF	2.6
AdaBoost	Tree size = 1	3.1
	Tree size = 5	2.9
	Tree size = 10	2.9
	Tree size = 15	2.4
	Tree size = 20	2.5

timeframe. Its  $FRW$  is 3 minutes, which suggests that, in the worst case, a legitimate user is falsely rejected for a stretch of 3 minutes.

Table 7.3: Classifiers and their  $FAW$  and  $FRW$ 

Type of classifier	Specification	$FAW$ (min)	$FRW$ (min)
SVM	Kernel = Linear	4	3
	Kernel = RBF	4	3
AdaBoost	Tree size = 1	5	3
	Tree size = 5	4	3
	Tree size = 10	4	3
	Tree size = 15	4	3
	Tree size = 20	4	4

2. *Biased  $FAR_t/FRR_t$* : Even though it is easier to compare authentication methods based on their  $EER_t$ , we may want to minimize  $FAR_t$  in highly-secure environments in order to ensure that an impostor is not authorized or minimize  $FRR_t$  to enhance user convenience. A low  $FAR_t$  indicates a high security level and a low  $FRR_t$  ensures user convenience. In this experimental scenario, we use the same parameters that are used in the baseline. However, false acceptance and false rejection are penalized differently. We consider two cases: (i) try to make  $FAR_t$  close to zero ( $FAR_{t=7h} < 0.1\%$ ) and measure  $FRR_t$ , and (ii) try to make  $FRR_t$  close to zero ( $FRR_{t=7h} < 0.1\%$ ) and measure  $FAR_t$ . Tables 7.4 and 7.5 summarize the results for these two cases. Based on Table 7.4, CABA can be seen to ensure that impostors are not accepted, but at the cost of an increase



in  $FRR$ . Based on Table 7.5, CABA can be seen to not negatively impact user convenience, i.e., not falsely reject the user, while rejecting impostors in more than 90% of the cases.

Table 7.4: Classifiers and their  $FRR$  ( $FAR \approx 0$ )

Type of classifier	Specification	$FRR(\%)$
SVM	Kernel = Linear	10.2
	Kernel = RBF	9.6
AdaBoost	Tree size = 1	10.0
	Tree size = 5	9.7
	Tree size = 10	8.7
	Tree size = 15	8.4
	Tree size = 20	8.9

Table 7.5: Classifiers and their  $FAR$  ( $FRR \approx 0$ )

Type of classifier	Specification	$FAR(\%)$
SVM	Kernel = Linear	8.9
	Kernel = RBF	7.6
AdaBoost	Tree size = 1	10.7
	Tree size = 5	9.2
	Tree size = 10	7.8
	Tree size = 15	7.6
	Tree size = 20	8.2

3. *Variable window size:* As mentioned earlier, we set the training and testing window sizes to 7 h in the baseline. Here, we change the size of the training and testing windows such that  $TRW = 2, 3, \dots, 12h$  and  $TEW + TRW = 14 h$ . Fig. 7.7 shows the average  $EER_t$  for different classifiers with respect to  $TRW$ . For all classifiers, as we increase  $TRW$  from 2 h to 6 h,  $EER_t$  decreases drastically. Then it remains almost constant until  $TRW$  reaches 11 h. Above this  $TRW$ ,  $EER$  starts increasing for two possible reasons. First, the model may become overfitted. Second, the number of test points may be inadequate.
4. *Moving training window:* In this scenario, the training window moves behind the testing window (Fig. 7.8). We consider  $TEW = TRW = 1, 2, \dots, 7 h$ . Our

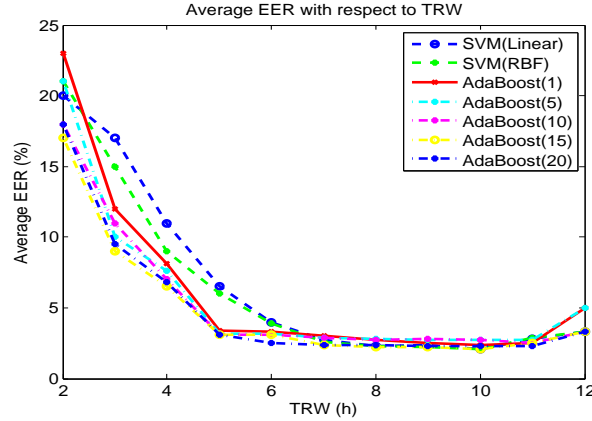


Figure 7.7: Average  $EER_t$  for different classifiers with respect to  $TRW$ .

experimental results demonstrate that this verification scheme provides the best result for  $TEW = TRW = 4 h$ , for which the average  $EER_t$  is 1.9% and the classification method is AdaBoost with a tree size of 15 nodes. This suggests that we can achieve the best accuracy for  $TRW = 4 h$ , under the assumption that the trained model is valid for the next four hours.

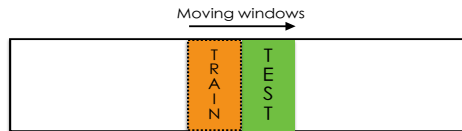


Figure 7.8: Moving training window.

5. *Reducing the number of Biostreams:* We also investigate the impact of dropping a Biostream. Traditionally, feature reduction is used to remove redundant or irrelevant features from the data set before commencing on the training process in order to decrease unnecessary computational cost. However, in our scenario, the main purpose of feature reduction is to investigate how each feature affects accuracy. If CABA can provide an acceptable accuracy with fewer features, fewer WMSs would be required. We dropped one feature at a time and computed  $EER_{t=7h}$  of the system. All other configurations are kept the same as in the baseline. Fig. 7.9 illustrates how  $EER_{t=7h}$  changes for each of the seven clas-

sifiers used in our experiments (two SVM classifiers with different kernel types and five AdaBoost classifiers with different tree sizes) when we drop different Biostreams. The green bar shows the baseline scenario in which no feature is dropped. We can see that dropping the respiratory rate (temperature) has maximum (minimum) negative impact on authentication accuracy. Thus, the most and least important Biostreams are respiratory rate and body temperature, respectively.

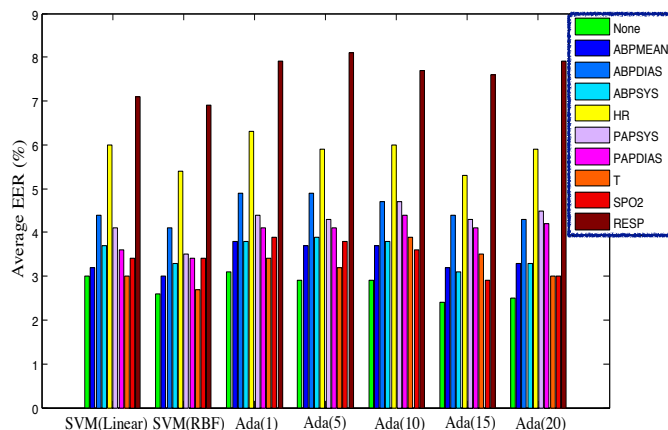


Figure 7.9:  $EER_{t=7h}$  for different classifiers when Biostreams are dropped one at a time. The green bar depicts the baseline scenario in which no feature is dropped. The abbreviations/notations provided in Table 7.1 are used to label other bars.

## 7.6.2 CABA scalability

We discuss below the worst-case time and space complexities of CABA.

### Time complexity

As discussed earlier, CABA can be implemented in such a manner that the time required by the enrollment phase is hidden from the user’s perspective. Hence, we focus on the time complexity of the user authentication process. We found that the required time for processing an authentication request for  $N = 37$  was on the order of a few milliseconds for all classification methods, when CABA was implemented on a

MacBook Pro (2.3 GHz Intel Core i7 processor with 8 GB memory). This suggests that CABA can re-authenticate the user very quickly.

When a person requests authentication by providing his ID and feature vector  $Y$ , the Look-up stage forwards  $Y$  to one and only one classifier in the Jury stage based on the given user ID. Then, the classifier's decision is the final decision of the authentication system. Hence, in order to analyze the time complexity of a single user authentication process, we need to consider the time complexity of the Look-up stage, and one classifier in the Jury stage, as follows:

- Look-up stage: If the Look-up stage is implemented using a hash table that associates user IDs with pointers to classifiers, then its search operation (finding the location of the classifier associated with the user ID) can be performed in  $O(1)$  time.
- One classifier in the Jury stage: The time complexity of the classifier varies from one classification algorithm to another. The time complexities of AdaBoost classifiers and the SVM classifier with a linear kernel do not depend on  $N$ , i.e., they have time complexity of  $O(1)$ . The time complexity of SVM with an RBF kernel is  $O(n_{SV})$ , where  $n_{SV}$  is the number of support vectors. Theoretically,  $n_{SV}$  grows linearly with a linear increase in  $N$ . Thus, the SVM classifier with an RBF kernel has a time complexity of  $O(N)$ .

Hence, the overall time complexity of user authentication is  $O(1)$  for AdaBoost classifiers and the SVM classifier with a linear kernel, and  $O(N)$  for the SVM classifier with an RBF kernel.

## Space complexity

We first investigate how much memory is required for our prototype implementation of CABA. Then, we discuss how the amount of memory required to store the two stages (Look-up and Jury) increases with  $N$ .

The amount of memory required for storing the Look-up stage in our prototype, where  $N = 37$ , was less than 1 *kB*. The amount of memory required for storing a single classifier in the Jury stage varies from tens of bytes (for SVM with a linear kernel) to a few *kB* (for AdaBoost with a tree size of 20). Therefore, the total amount of memory allocated to the authentication system is less than 1 *MB*.

We investigate the space complexity as a function of  $N$ .

- Look-up stage: If the Look-up stage is implemented using a hash table, its space complexity is  $O(N)$ .
- Jury stage: The space complexity of a single classifier in the Jury stage depends on the type of classifier. The space complexities of AdaBoost classifiers and the SVM classifier with a linear kernel do not depend on  $N$ , i.e., they have space complexity of  $O(1)$ . However, the space complexity of the SVM with an RBF kernel is  $O(N)$ . Since the number of classifiers in the Jury stage increases linearly with  $N$ , its space complexity is  $O(N)$  (when an AdaBoost classifier or SVM classifier with a linear kernel is used) or  $O(N^2)$  (when the SVM classifier with the RBF kernel is employed).

## 7.7 Using BioAura for identification

The majority of continuous authentication systems only support continuous verification in which the user provides a user ID and the system checks if the user is the person he purports to be. In this section, we describe how CABA can be slightly

modified to also identify the user from a database of users by processing feature vector  $Y$  provided by the smartphone. An identification scenario consists of four steps. The first three steps are similar to the ones discussed in Section 7.5 for continuous authentication. In the fourth step, CABA processes the decisions of all classifiers in the Jury stage to indicate that the user is not in the database, or conclude that he is, in which case it returns his user ID. This step can be implemented in different ways. In our implementation, CABA processes all outputs of the Jury stage and outputs the user ID if there is only one classifier whose output is an accept decision. Otherwise, it indicates no match. Our experimental results demonstrate that this scheme provides the best result, for which the identification rate is 96.1%, with the AdaBoost classification method with a tree size of 15 nodes. Identification rate is a commonly used metric for this scenario [82]. It is defined as the percentage of attempts correctly identified to the total number of attempts made.

## 7.8 Real-time adaptive authorization

In this section, we first define the concept of authorization. Then, we propose a real-time adaptive authorization (RAA) scheme, which uses the decisions from CABA to provide an extremely flexible access control model. The RAA concept is not limited to CABA. It provides an adjustable access control model for any authorization system that authorizes the user based on decisions of a continuous authentication system.

Authorization is defined as the process of establishing if the user, who has been already authenticated, should be allowed access to a resource, system, or area [470].

Traditional authorization schemes grant a specific access level to the authenticated user based on his user ID. However, the fact that continuous authentication systems have a non-zero  $FRR$  implies that such a simple scheme may unintentionally block a legitimate access when the authentication system fails to recognize a valid user for a

short period of time. Consider a scenario in which a continuous authentication system is used to protect a personal laptop from unauthorized users. The authentication system first authenticates the user. Then, the authorization scheme specifies the user's access level based on the user ID. However, the laptop may log out the user when the authentication scheme falsely rejects him. RAA schemes can be used to alleviate user inconvenience caused by false reject decisions. They continuously adjust the user's access level based on the last decision of the authentication system. Next, we propose an RAA scheme that can be used with a continuous authentication system.

A trust level-based RAA adaptively changes the user's access level based on a parameter called trust level (TRL). TRL is a recently-suggested parameter that represents how much we trust a user based on previous decisions of the continuous authentication system [471]. TRL has a value between 0 and 100, where a higher number indicates a higher level of trust. The initial value of TRL is 100 when the user is authenticated and authorized for the first time. The value of TRL is continuously updated using a trust update procedure after each user authentication. A simple trust update procedure may be to just increase (decrease) the TRL by a constant step after each accept (reject) decision. *Algorithm 1* shows the pseudo-code for such an approach. We need to set two parameters:  $W_{Accept}$  and  $W_{Reject}$ . The values of  $W_{Accept}$  and  $W_{Reject}$  should be chosen such that the TRL value becomes 0 as soon as we detect the presence of an impostor and becomes 100 when we confidently verify that the user is legitimate. Consider AdaBoost classification with a tree size of 15 nodes that yields  $FRW = 3$ . This indicates that the authentication system may falsely reject three consecutive requests of a legitimate user in the worst case. Therefore, if the RAA scheme gets at least four consecutive reject decisions from the authentication system, it becomes confident that the user is an impostor ( $TRL = 0$ ). Hence, we can set  $W_{Reject}$  for this classifier as follows:  $W_{Reject} = \frac{-100}{FRW+1} = \frac{-100}{4} = -25$ .  $FAW = 4$  for the above-mentioned classification method, which indicates that in the worst case, an impostor

may be falsely accepted as a legitimate user in four successive trials. Therefore, if the authentication system outputs five consecutive accept decisions, TRL should become 100. Thus, we can set  $W_{Accept}$  as follows:  $W_{Accept} = \frac{+100}{FAW+1} = \frac{+100}{5} = +20$ .

We can set different threshold values for different applications. We set the threshold value to 100 for accessing email and financial accounts to ensure that the user can access such accounts only when the system is confident that the user is legitimate. However, for less sensitive applications, e.g., simple web surfing, a lower level of trust might be sufficient. Using CABA in conjunction with RAA can enhance user convenience, while ensuring high security for critical applications.

*Algorithm 1: trustUpdate procedure*

---

Given: The latest *decision* of the authentication system and current TRL value

---

1.  $TRL \leftarrow TRL + F_{Update}$ , where

$$F_{Update}(decision) = \begin{cases} W_{Accept}, & \text{if } decision = Accept, \\ W_{Reject}, & \text{otherwise.} \end{cases}$$

2. *If* ( $TRL > 100$ )

3.            $TRL \leftarrow 100$

4. *end*

5. *If* ( $TRL < 0$ )

6.            $TRL \leftarrow 0$

8. *end*

9. *Return*  $TRL$

---



## 7.9 Potential threats and countermeasures

Next, we describe possible attacks/threats against CABA that can be exploited by attackers to bypass CABA. For each attack, we also suggest possible countermeasures.

**1. Eavesdropping:** This is defined as the act of covertly listening to confidential conversations of others [1], which, in our context, can be done by intercepting the communication between two devices using an appropriate equipment, e.g., HackRF [430]. Eavesdropping can occur when unencrypted information is transmitted over an untrusted channel.

**Countermeasures:** The most effective and well-known defense against eavesdropping is encryption. For example, the transmitted message can be encrypted using Advanced Encryption Standard [221]. However, implementing a strong encryption in WMSs may not be possible in the current state of the technology since they have limited energy and memory capacity. Fortunately, eavesdropping does not pose a direct threat to the authentication system. In other words, it is possible to design the authentication system assuming that eavesdropping does occur on the communication between the WMSs and the smartphone. In this case, CABA would require that the data be sent from a smartphone that is previously registered in the system to ensure that the attacker is not able to capture the biomedical information and send the captured information to CABA using another smartphone. The smartphone can send its unique ID over a secure communication link to CABA before transmitting the biomedical information.

**2. Phishing:** This is an attack that attempts to fool the user into submitting his confidential or private information, e.g., username, password, email address, and phone number, to an untrusted server or device [472]. For example, the attacker might attempt to fool the user's smartphone by sending a counterfeit request that asks the smartphone to send its authentication-related information to the attacker's server.

**Countermeasures:** The most effective way to address phishing attacks is to use a

digital certificate, i.e., an electronic document that allows a device to exchange information securely using the public key infrastructure [473]. The certificate carries information about the key and its owner. In CABA, the server’s digital certificate can be examined by the smartphone to ensure that the server is trusted.

**3. Replay attack:** In a replay attack, an attacker records the data, packets, and user’s credentials, which are transmitted between two devices, e.g., a WMS and the smartphone, and exploits them for a malicious purpose. In a replay attack against the authentication system, the attacker attempts to impersonate a legitimate user in order to bypass the authentication procedure and gain full access to the protected device, application, or area. Unlike the attacks based on eavesdropping, in a replay attack, the attacker does not need to interpret the packets. In fact, he can even record encrypted packets and retransmit them in order to bypass the system.

**Countermeasures:** An encrypted timestamp, i.e., a sequence of encrypted information identifying when the transmission occurred, can be utilized to enable the authentication system to check that the packets were not previously recorded. Moreover, the packet should include a field that contains the encrypted information, e.g., a hashed device ID, which can be used in the authentication system to uniquely specify the sender of the packets and check if the sender is known and trusted.

**4. Poisoning attack:** In a poisoning attack, the attacker changes the final learning model by adding precisely-selected invalid data points to the training dataset [161]. In CABA, the attacker might threaten the integrity of the machine learning algorithm by using an untrusted WMS that aims to add malicious data points to the training set.

**Countermeasures:** We describe two types of countermeasures against poisoning attacks.

1. *Outlier detection:* One of the common goals of defenses against poisoning attacks is to reduce the effect of invalid data points on the final result. In a ma-

chine learning method, such invalid data points are considered outliers in the training dataset. Several countermeasures against poisoning attacks have been discussed in [234].

2. *Digitally-signed biomedical information:* A digital signature can be used to check the authenticity of the information. It is a mathematical method for demonstrating the authenticity of a transmitted message. Thus, it provides the means to the recipient to check if the message is created by a legitimate sender. The WMSs and the smartphone can digitally sign the biomedical information before transmitting it.

## 7.10 Comparison between CABA and previously-proposed systems

In this section, we first describe why previously-proposed authentication systems based on biomedical signals (EEG and ECG) may not be well-suited to continuous authentication. Then, we compare CABA to three promising biometrics-/behaviometrics-based continuous authentication systems.

The use of EEG [474] and ECG [86, 475] signals, as biomedical traits with high discriminatory power for user authentication, has received widespread attention in recent years. Although such authentication systems show promising results, they do not provide a convenient method for long-term continuous user authentication for two reasons. First, they commonly need long measurement times and impose a heavy computational load on the system [88]. Second, due to the size/position requirements of the electrodes that enable EEG/ECG acquisition [86, 87], these systems can mainly be used for one-time user authentication (or short-term continuous authentication) systems. For example, the user needs to wear a large cap to collect the data for

EEG-based authentication [474], which is not convenient for long-term continuous authentication.

As mentioned in Section 7.1, several biometrics-/behaviometrics-based continuous authentication systems have been proposed. Among them, facial recognition systems [447, 454, 476, 477], which use facial features (as biometrics), and keyboard-/mouse-based authentication systems [449, 457, 478–481], which rely on keystroke/mouse dynamics (as behaviometrics), are the most promising.

Facial recognition systems make use of low-cost cameras that are commonly built into most laptops. They are accurate when the user looks straight at the webcam. However, their performance is significantly affected by illumination, pose, expression or changes in the image acquisition method [454]. Moreover, the user’s facial images is unavailable when the user turns his head or does not look at the camera. Such systems are also not useful for tablets and smartphones since the user typically does not face a built-in camera in these cases.

Previous keyboard-/mouse-based authentication systems report promising results and provide user authentication in a convenient manner. However, they have four drawbacks that limit their applicability: (i) their performance is easily impacted by environmental variables, such as changes in software environments, input devices, task, or interaction modes [82, 449], (ii) they can only be employed when system has a keyboard/mouse, (iii) the data often become unavailable, e.g., when the user is watching a movie on his computer, and (iv) keyboard-based systems need active involvement of the user for long sessions, e.g., several minutes [457], to guarantee acceptable accuracy, and mouse dynamics based systems have still not reached an acceptable accuracy levels [449].

Unlike most continuous authentication systems that support personal computers and laptops, CABA can be used to protect personal computers, servers, software applications, and restricted physical spaces. Moreover, WMSs ensure a continuous

data stream. This enables the user to freely move and change his posture while being authenticated. In addition, unlike previous systems, CABA can be implemented on any general-purpose computing unit with sufficient memory capacity and computation power.

## **7.11 Discussion**

Here, we address three items not yet explained in detail. First, we discuss an important privacy concern surrounding the use of biomedical signals. Second, we describe how CABA can also be used as a stand-alone one-time authentication system. Third, we discuss the impact of temporal conditions on authentication results.

### **7.11.1 Health information leakage**

An important privacy concern associated with the use of biomedical signals is the possibility of health information leakage. For example, an adversary might extract disease-specific information from such signals, e.g., certain heart rate ranges may be correlated with cardiovascular disease [482]. Exposure of a serious illness or a condition that carries social stigma would naturally raise serious privacy concerns [112]. However, since CABA does not rely on high-precision measurements (it only processes the average values of Biostreams over specific time frames), the amount of health-related information potentially leaked by CABA is less than leaked by EEG/ECG-based approaches that rely on high-quality EEG/ECG signals. Similar concerns have been discussed in previous research efforts for both biometrics and behaviorometrics, and usually addressed by suggesting legislation [483].

### 7.11.2 One-time authentication based on BioAura

CABA can also be used as a stand-alone one-time authentication system. We discuss several such scenarios next.

- **Battery-powered devices:** Incurring overheads of continuous authentication on a battery-powered device may drain its battery quickly, and lead to user inconvenience.
- **Low-security environment:** Continuous authentication may not be required in a low-security environment, e.g., a common room in an apartment.
- **Intentionally-shared resources:** A user might want to intentionally authorize a group of users to access some specific locations or resources. For example, consider a user who uses a smart lock, which grants access to him when he approaches the door of his house. He may want to open the door for his guests and leave the house.

Generally, a continuous authentication system that has high accuracy and a short response time may be able to provide stand-alone one-time authentication or complement a traditional authentication system (whose decision is only considered at the time of initial login). As discussed in Section 7.6, CABA provides an accurate decision within a few milliseconds and, hence, is also useful for one-time authentication.

### 7.11.3 The impact of temporal conditions

The negative impact of temporal conditions, e.g., emotional/physical conditions and changes in posture, gesture or facial expressions, on widely-used biometrics-/behaviometrics-based systems have been discussed earlier [80]. Similarly, some biomedical signals may change significantly due to a change in physical activity. This may negatively impact authentication accuracy. For example, when the user

suddenly starts running, his blood pressure, heart rate, and respiration rate increase. Therefore, if the authentication system has only been trained using data collected when the user was at rest, it might fail to authenticate the user after he finishes running. A solution would be to design a state-aware system that takes different emotional states and physical activities into account. Algorithms exist for recognizing emotional states [484] and the type [485] and intensity [12] of physical activities using WMSs. Such algorithms can be used in conjunction with CABA.

## 7.12 Chapter summary

In this chapter, we proposed CABA, a novel user-transparent system for continuous authentication based on information that is already gathered by WMSs for diagnostic and therapeutic purposes. We described a prototype implementation of CABA and comprehensively investigated its accuracy and scalability. We also described how CABA can be used to support user identification. We then presented an RAA scheme that uses the decisions from CABA to enable flexible access control. We compared CABA to previously-proposed continuous authentication systems (biometrics- and behaviometrics-based), and highlighted its advantages. We discussed several attacks against the proposed authentication system along with their countermeasures. Finally, we briefly described an privacy concerns surrounding the use of biomedical signals, how CABA can also be used for one-time authentication, and impact of temporal conditions on authentication.

# Chapter 8

## Conclusion

The emergence of the Internet of Things (IoT) paradigm provides an opportunity to transform isolated devices into communicating things. As a side effect of rapid advances in the development of IoT-enabled systems, the number of potential security/privacy attacks against such systems, *in particular wearable medical sensor (WMS)-based systems*, has grown exponentially. Therefore, common security threats and privacy concerns need to be studied and addressed in depth. This thesis attempted to explore and address different security/privacy-related issues associated with IoT-enabled systems with a special focus on WMS-based systems.

### 8.1 Thesis summary

In Chapter 1, we discussed different IoT reference models and the scope of IoT applications. We described what security means in the scope of IoT and who the attackers that target the IoT might be, and what motivations they might have. Furthermore, we discussed different WMS-based systems along with their applications, components, and design requirements.

In Chapter 2, we described related work and provided background for several key concepts used in this thesis. We summarized different attacks and threats on the



edge-side layer of IoT and described possible countermeasures against them. We discussed several research directions that are closely related to the domain of WMSs and described how previous research studies have facilitated the design and development of WMS-based systems.

In Chapter 3, we described a secure energy-efficient system for long-term continuous health monitoring. We constructed a wireless body area network (WBAN) using eight biomedical sensors. Furthermore, we presented different processing and transmission schemes and evaluated our schemes using the WBAN. We also examined the storage requirements for long-term analysis and storage. Among the four schemes we evaluated (including the baseline scheme), we showed that the compressive sensing (CS)-based scheme provides the most computational energy savings because it needs to process much fewer signal samples. For low-sample-rate sensors, we can achieve significant energy savings by simply accumulating the raw data before transmitting them to the base station. In addition, the CS-based scheme also allows us to reduce the storage requirements significantly. The results indicate that long-term continuous health monitoring is indeed feasible from both energy and storage points of view.

In Chapter 4, we presented OpSecure, an optical secure communication channel between an implantable medical device (IMD) and an external device, e.g., smartphone, that enables an intrinsically short-range, user-perceptible one-way data transmission (from the external device to the IMD). Based on OpSecure, we proposed a wakeup and a key exchange protocol. In order to evaluate the proposed protocols, we implemented an IMD prototype, that supports both protocols, and developed an Android application, which can be used to wake up the IMD and transmit the shared key from the smartphone to the IMD. We evaluated our prototype implementation using a human body model. Our experimental results indicate that OpSecure can be used to implement both wakeup and key exchange protocols for IMDs with minimal size and energy overheads.

In Chapter 5, we discussed two sources of information leakage, namely the human body and implantable and wearable medical devices (IWMDs), which continuously leak health information. We described two types of signals for each source: acoustic and electromagnetic. We presented a variety of attacks on the privacy of health data by capturing and processing unintentionally-generated leaked signals and also discussed the feasibility of using intentionally-generated acoustic/electromagnetic signals to compromise the patient's health privacy.

In Chapter 6, we discussed Dedicated Intelligent Security Attacks on Sensor-triggered Emergency Responses (DISASTER). It exploits design flaws and security weaknesses of safety mechanisms utilized in cyber-physical systems (CPSs) to trigger the system's emergency responses even when a real emergency situation is not present. We demonstrated that DISASTER can lead to serious consequences, ranging from economic collateral damage to life-threatening conditions. We examined several already-in-use sensors and summarized common design flaws and security weaknesses of safety mechanisms. We demonstrated the possibility of launching DISASTER in realistic scenarios and suggested several countermeasures against the proposed attacks.

In Chapter 7, we proposed a continuous authentication system based on biological aura (CABA). We described a prototype implementation of CABA and examined its accuracy and scalability. We discussed how CABA can be used to support user identification. We presented a real-time adaptive authorization scheme, which uses decisions provided by CABA to enable flexible access control. We compared CABA to previously-proposed continuous authentication systems and highlighted its advantages. We discussed several attacks against the proposed authentication system along with their countermeasures. We also described privacy concerns surrounding the use of biomedical signals, how CABA can also be used for one-time authentication, and impact of temporal conditions on authentication.

## 8.2 Future directions

Next, we describe several avenues along which the proposed schemes and techniques we presented can be further explored.

### Targeting weak links of IoT-enabled systems

The majority of IoT-based services rely on compact battery-powered devices with limited storage and computation resources. Due to the special characteristics of these devices and cost factors considered important by manufacturers, several *already-in-market devices* do not support highly-secure cryptographic protocols. This has led to the emergence of an enormous number of weak links in the network/system that can be exploited by an attacker to target other presumably-secure entities in the network. A few research efforts [486, 487] have recently demonstrated the possibility of targeting weak edge nodes to extract the home user’s WiFi password. Chapman [486] has demonstrated how Internet-connected light bulbs can reveal the user’s WiFi password to the attacker. In [487], a similar attack is discussed, which extracts the WiFi password by targeting the user’s smart lock. The endless variety of IoT applications magnifies the impact of these weak edge nodes. DISASTER, which we described in Chapter 6, also targets insecure sensors in home automation and industrial CPSs. Similar attacks can be proposed and investigated in other application domains.

### Unexpected uses of collected data

The widespread use of ubiquitous computing enabled by IoT technologies has led to the pervasive deployment of Internet-connected sensors in modern day living. In recent years, a few research efforts have attempted to shed light on unexpected uses of different types of environment-/user-related data collected by Internet-connected sensors [488–491]. For example, McKenna et al. have provided a list of privacy-sensitive information, e.g., number of residents, personal habits, and daily routines, that can

be inferred from smart homes' electricity load data collected by smart meters [488]. Despite the existence of previous research efforts, the extent of private information that can be inferred from presumably non-critical data is neither well-known nor well-understood.

### **Promising authentication solutions**

As we described in Chapter 7, password-based authentication has several issues spanning user inconvenience to security flaws. For example, a serious security flaw of one-time password-based authentication is its inability to detect unauthorized users after initial authentication. Such issues have boosted the design and development of continuous authentication mechanisms, e.g., face recognition and keystroke-based authentication systems. In Chapter 7, we presented a novel continuous authentication system based on biomedical signals collected by WMSs and described why the proposed system has an advantage over previously-proposed systems. Similar systems can be designed using another set of biomedical signals, which can potentially address a variety of issues associated with the use of one-time password-based systems. Moreover, researchers may want to investigate the effect of temporal changes in the user's biomedical signals on authentication results.

# Bibliography

- [1] A. Mosenia and N. K. Jha, “A comprehensive study of security of Internet of Things,” *IEEE Trans. Emerging Topics in Computing*, DOI: 10.1109/TETC.2016.2606384, 7 Sept., 2016.
- [2] A. Mosenia, S. Sur-Kolay, A. Raghunathan, and N. K. Jha, “Wearable medical sensor-based system design: A survey,” *under review*.
- [3] D. Singh, G. Tripathi, and A. J. Jara, “A survey of Internet-of-Things: Future vision, architecture, challenges and services,” in *Proc. IEEE World Forum on Internet of Things*, 2014, pp. 287–292.
- [4] L. Atzori, A. Iera, and G. Morabito, “The Internet of Things: A survey,” *Computer Networks*, vol. 54, no. 15, pp. 2787–2805, 2010.
- [5] J. Gubbi, R. Buyya, S. Marusic, and M. Palaniswami, “Internet of Things (IoT): A vision, architectural elements, and future directions,” *Future Generation Computer Systems*, vol. 29, no. 7, pp. 1645–1660, 2013.
- [6] “The Internet of Things reference model,” [http://cdn.iotwf.com/resources/71/IoT\\_Reference\\_Model\\_White\\_Paper\\_June\\_4\\_2014.pdf](http://cdn.iotwf.com/resources/71/IoT_Reference_Model_White_Paper_June_4_2014.pdf), accessed: 10-1-2016.
- [7] C. Sitawarin, A. N. Bhagoji, A. Mosenia, M. Chiang, and P. Mittal, “DARTS: Deceiving autonomous cars with toxic signs,” *arXiv preprint arXiv:1802.06430*, 2018.
- [8] C. Sitawarin, A. N. Bhagoji, A. Mosenia, P. Mittal, and M. Chiang, “Rogue signs: Deceiving traffic sign recognition with malicious ads and logos,” *arXiv preprint arXiv:1801.02780*, 2018.
- [9] A. Mosenia, J. F. Bechara, T. Zhang, P. Mittal, and M. Chiang, “Proc motive: Bringing programmability and connectivity into isolated vehicles,” *Proc. ACM on Interactive, Mobile, Wearable and Ubiquitous Technologies*, vol. 2, no. 1, p. 26, 2018.
- [10] M. Mozaffari-Kermani, M. Zhang, A. Raghunathan, and N. K. Jha, “Emerging frontiers in embedded security,” in *Proc. IEEE Int. Conf. VLSI Design*, 2013, pp. 203–208.

- [11] A. M. Nia, M. Mozaffari-Kermani, S. Sur-Kolay, A. Raghunathan, and N. K. Jha, "Energy-efficient long-term continuous personal health monitoring," *IEEE Trans. Multi-Scale Computing Systems*, vol. 1, no. 2, pp. 85–98, 2015.
- [12] P. Alinia, R. Saeedi, R. Fallahzadeh, A. Rokni, and H. Ghasemzadeh, "A reliable and reconfigurable signal processing framework for estimation of metabolic equivalent of task in wearable sensors," *IEEE J. Selected Topics in Signal Processing*, vol. 10, no. 5, pp. 842–853, 2016.
- [13] C. Anumba, A. Akanmu, and J. Messner, "Towards a cyber-physical systems approach to construction," in *Proc. Construction Research Congress*, 2010, pp. 528–538.
- [14] M. T. Lazarescu, "Design of a WSN platform for long-term environmental monitoring for IoT applications," *IEEE J. Emerging and Selected Topics in Circuits and Systems*, vol. 3, no. 1, pp. 45–54, 2013.
- [15] E. Fleisch, "What is the Internet of Things? An economic perspective," *Economics, Management, and Financial Markets*, vol. 1, no. 2, pp. 125–157, 2010.
- [16] M. Tajima, "Strategic value of RFID in supply chain management," *J. Purchasing and Supply Management*, vol. 13, no. 4, pp. 261–273, 2007.
- [17] M. Zhang, A. Raghunathan, and N. K. Jha, "Trustworthiness of medical devices and body area networks," *Proc. IEEE*, vol. 102, no. 8, pp. 1174–1188, 2014.
- [18] C. Li, A. Raghunathan, and N. K. Jha, "Hijacking an insulin pump: Security attacks and defenses for a diabetes therapy system," in *Proc. IEEE Int. Conf. e-Health Networking Applications and Services*, 2011, pp. 150–156.
- [19] D. Halperin, T. S. Heydt-Benjamin, B. Ransford, S. S. Clark, B. Defend, W. Morgan, K. Fu, T. Kohno, and W. H. Maisel, "Pacemakers and implantable cardiac defibrillators: Software radio attacks and zero-power defenses," in *Proc. IEEE Symp. Security and Privacy*, 2008, pp. 129–142.
- [20] Y. Cherdantseva and J. Hilton, "A reference model of information assurance & security," in *Proc. IEEE Int. Conf. Availability, Reliability and Security*, 2013, pp. 546–555.
- [21] D. B. Parker, *Fighting Computer Crime*. Scribner New York, NY, 1983.
- [22] M. Whitman and H. Mattord, *Principles of Information Security*. Cengage Learning, 2011.
- [23] H. Yin, A. O. Akmandor, A. Mosenia, and N. K. Jha, "Smart healthcare," *Foundations and Trends® in Electronic Design Automation*, vol. 12, no. 4, pp. 401–466, 2018.

- [24] H. Ghayvat, J. Liu, S. C. Mukhopadhyay, and X. Gui, “Wellness sensor networks: A proposal and implementation for smart home for assisted living,” *IEEE Sensors Journal*, vol. 15, no. 12, pp. 7341–7348, 2015.
- [25] S. C. Mukhopadhyay, “Wearable sensors for human activity monitoring: A review,” *IEEE Sensors Journal*, vol. 15, no. 3, pp. 1321–1330, 2015.
- [26] “Olympic medical institute validates Polar RS800 running computer and training system,” [https://www.polar.com/us-en/about\\_polar/news/polar\\_R800](https://www.polar.com/us-en/about_polar/news/polar_R800), accessed: 10-9-2016.
- [27] O. D. Lara and M. A. Labrador, “A survey on human activity recognition using wearable sensors,” *IEEE Communications Surveys & Tutorials*, vol. 15, no. 3, pp. 1192–1209, 2013.
- [28] W. Gao, S. Emaminejad, H. Y. Y. Nyein, S. Challa, K. Chen, A. Peck, H. M. Fahad, H. Ota, H. Shiraki, and D. Kiriya, “Fully integrated wearable sensor arrays for multiplexed in situ perspiration analysis,” *Nature*, vol. 529, no. 7587, pp. 509–514, 2016.
- [29] A. Pantelopoulos and N. G. Bourbakis, “A survey on wearable sensor-based systems for health monitoring and prognosis,” *IEEE Trans. Systems, Man, and Cybernetics*, vol. 40, no. 1, pp. 1–12, 2010.
- [30] S. Park, I. Locher, A. Savvides, M. B. Srivastava, A. Chen, R. Muntz, and S. Yuen, “Design of a wearable sensor badge for smart kindergarten,” in *Proc. IEEE Int. Symp. Wearable Computers*, 2002, pp. 231–238.
- [31] A. B. Barreto, S. D. Scargle, and M. Adjouadi, “A practical EMG-based human-computer interface for users with motor disabilities,” *J. Rehabilitation Research and Development*, vol. 37, no. 1, p. 53, 2000.
- [32] E. O. Thorp, “The invention of the first wearable computer,” in *Proc. IEEE Int. Symp. Wearable Computers*, 1998, pp. 4–8.
- [33] J. Ranck, “The wearable computing market: A global analysis,” *Gigaom Pro*, 2012.
- [34] “Global wearable sensor market to expand at 45.20% CAGR from 2014 to 2020 owing to growing healthcare concerns,” <http://www.transparencymarketresearch.com/pressrelease/wearable-sensor-market.htm>, accessed: 10-9-2016.
- [35] “Sharply falling MEMS prices spur rising demand,” <http://www.semi.org/en/sharply-falling-mems-prices-spur-rising-demand-1>, accessed: 10-9-2016.
- [36] “Global wearable health sensors market,” <http://www.businesswire.com/news/home/20160825005765/en/Global-Wearable-Health-Sensors-Market---Expected>, accessed: 10-9-2016.

- [37] A. Mosenia, S. Sur-Kolay, A. Raghunathan, and N. K. Jha, “CABA: Continuous authentication based on BioAura,” *accepted for publication in IEEE Trans. Computers*, 2016.
- [38] M. Milošević, M. T. Shrove, and E. Jovanov, “Applications of smartphones for ubiquitous health monitoring and wellbeing management,” *J. Information Technology and Applications*, vol. 1, no. 1, pp. 7–14, 2011.
- [39] G. D. Abowd, “What next, UbiComp?: Celebrating an intellectual disappearing act,” in *Proc. ACM Conf. Ubiquitous Computing*, 2012, pp. 31–40.
- [40] “Global wearable sensors market information,” <https://www.marketresearchfuture.com/reports/global-wearable-sensors-market-information-from-2011-to-2021>, accessed: 10-9-2016.
- [41] “Wearable computing devices market,” <http://embedded-computing.com/news/wearable-demand-value-chain-forecast-2020/>, accessed: 10-9-2016.
- [42] “Wearable sensor market to expand sevenfold in five years,” <http://press.ihs.com/press-release/technology/wearable-sensor-market-expand-sevenfold-five-years>, accessed: 10-9-2016.
- [43] “Growth trends, consumer attitudes, and why smart-watches will dominate,” <http://www.businessinsider.com/the-wearable-computing-market-report-2014-10>, accessed: 10-9-2016.
- [44] V. Pejovic, A. Mehrotra, and M. Musolesi, “Anticipatory mobile digital health: Towards personalised proactive therapies and prevention strategies,” *arXiv preprint arXiv:1508.03722*, 2015.
- [45] W. Y. Wong and M. S. Wong, “Smart garment for trunk posture monitoring: A preliminary study,” *Scoliosis and Spinal Disorders*, vol. 3, no. 1, p. 1, 2008.
- [46] A. Crane, S. Doppalapudi, J. O’Leary, P. Ozarek, and C. Wagner, “Wearable posture detection system,” in *Proc. Annual Northeast Bioengineering Conference*, 2014, pp. 1–2.
- [47] E. Sardini, M. Serpelloni, and M. Ometto, “Smart vest for posture monitoring in rehabilitation exercises,” in *Proc. IEEE Sensors Applications Symposium*, 2012, pp. 1–5.
- [48] H. Harms, O. Amft, G. Tröster, M. Appert, R. Müller, and A. Meyer-Heim, “Wearable therapist: Sensing garments for supporting children improve posture,” in *Proc. ACM Int. Conf. Ubiquitous Computing*, 2009, pp. 85–88.
- [49] B. Ainsworth, L. Cahalin, M. Buman, and R. Ross, “The current state of physical activity assessment tools,” *Progress in Cardiovascular Diseases*, vol. 57, no. 4, pp. 387–395, 2015.



- [50] M. de Zambotti, S. Claudatos, S. Inkelis, I. M. Colrain, and F. C. Baker, "Evaluation of a consumer fitness-tracking device to assess sleep in adults," *Chronobiology International*, vol. 32, no. 7, pp. 1024–1028, 2015.
- [51] J. Wei, "How wearables intersect with the Cloud and the Internet of Things: Considerations for the developers of wearables," *IEEE Consumer Electronics Magazine*, vol. 3, no. 3, pp. 53–56, 2014.
- [52] T. L. Koreshoff, T. Robertson, and T. W. Leong, "Internet of Things: A review of literature and products," in *Proc. AMC Australian Computer-Human Interaction Conference: Augmentation, Application, Innovation, Collaboration*, 2013, pp. 335–344.
- [53] D. Malan, T. Fulford-Jones, M. Welsh, and S. Moulton, "CodeBlue: An ad hoc sensor network infrastructure for emergency medical care," in *Proc. Int. Wkshp. Wearable and Implantable Body Sensor Networks*, vol. 5, 2004.
- [54] V. Jones, A. van Halteren, N. Dokovsky, G. Koprnikov, R. Bults, D. Konstantas, and R. Herzog, "Mobile health services based on body area networks," in *Proc. Mobihealth*, 2006, pp. 219–236.
- [55] S. Ozcelik, "Drug infusion systems," *Encyclopedia of Medical Devices and Instrumentation*, pp. 495–508, 2006.
- [56] A. Hadjidj, M. Souil, A. Bouabdallah, Y. Challal, and H. Owen, "Wireless sensor networks for rehabilitation applications: Challenges and opportunities," *J. Network and Computer Applications*, vol. 36, no. 1, pp. 1–15, 2013.
- [57] A. Muro-de-la Herran, B. Garcia-Zapirain, and A. Mendez-Zorrilla, "Gait analysis methods: An overview of wearable and non-wearable systems, highlighting clinical applications," *Sensors*, vol. 14, no. 2, pp. 3362–3394, 2014.
- [58] W. Tao, T. Liu, R. Zheng, and H. Feng, "Gait analysis using wearable sensors," *Sensors*, vol. 12, no. 2, pp. 2255–2283, 2012.
- [59] "Valedo," [https://www.valedotherapy.com/us\\_en/](https://www.valedotherapy.com/us_en/), accessed: 10-9-2016.
- [60] G. Lanfermann, J. Te Vrugt, A. Timmermans, E. Bongers, N. Lambert, and V. Van Acht, "Philips stroke rehabilitation exerciser," *Technical Aids for Rehabilitation*, 2007.
- [61] S. Patel, H. Park, P. Bonato, L. Chan, and M. Rodgers, "A review of wearable sensors and systems with application in rehabilitation," *J. Neuroengineering and Rehabilitation*, vol. 9, no. 1, p. 1, 2012.
- [62] T. Hester, R. Hughes, D. M. Sherrill, B. Knorr, M. Akay, J. Stein, and P. Bonato, "Using wearable sensors to measure motor abilities following stroke," in *Proc. IEEE Int. Wkshp. Wearable and Implantable Body Sensor Networks*, 2006, pp. 4–8.

- [63] A. K. Dey, D. Salber, G. D. Abowd, and M. Futakawa, “The conference assistant: Combining context-awareness with wearable computing,” in *Proc. IEEE Int. Symp. Wearable Computers*, 1999, pp. 21–28.
- [64] E. Keyes, M. P. Johnson, and T. Starner, “Magnetometer-based gesture sensing with a wearable device,” 2015, US Patent 9,141,194.
- [65] D. Kim, O. D. Hilliges, S. Izadi, P. L. Olivier, J. D. J. Shotton, P. Kohli, D. G. Molyneaux, S. E. Hodges, and A. W. Fitzgibbon, “Gesture recognition techniques,” 2014, US Patent 14,280,140.
- [66] M. Roshandel, A. Munjal, P. Moghadam, S. Tajik, and H. Ketabdardar, “Multi-sensor based gestures recognition with a smart finger ring,” in *Proc. Int. Conf. Human-Computer Interaction*. Springer, 2014, pp. 316–324.
- [67] S. K. Card, J. D. Mackinlay, and G. G. Robertson, “A morphological analysis of the design space of input devices,” *ACM Trans. Information Systems*, vol. 9, no. 2, pp. 99–122, 1991.
- [68] A. Ferrone, F. Maita, L. Maiolo, M. Arquilla, A. Castiello, A. Pecora, X. Jiang, C. Menon, and L. Colace, “Wearable band for hand gesture recognition based on strain sensors,” in *Proc. IEEE Int. Conf. Biomedical Robotics and Biomechanics*, 2016, pp. 1319–1322.
- [69] Y. Zhang and C. Harrison, “Tomo: Wearable, low-cost electrical impedance tomography for hand gesture recognition,” in *Proc. ACM Symp. User Interface Software & Technology*, 2015, pp. 167–173.
- [70] Z. Lu, X. Chen, Q. Li, X. Zhang, and P. Zhou, “A hand gesture recognition framework and wearable gesture-based interaction prototype for mobile devices,” *IEEE Trans. Human-Machine Systems*, vol. 44, no. 2, pp. 293–299, 2014.
- [71] R. W. Picard and R. Picard, *Affective Computing*. MIT Press, Cambridge, 1997, vol. 252.
- [72] A. Sano and R. W. Picard, “Stress recognition using wearable sensors and mobile phones,” in *Proc. IEEE Conf. Affective Computing and Intelligent Interaction*, 2013, pp. 671–676.
- [73] J. Wijsman, B. Grundlehner, H. Liu, J. Penders, and H. Hermens, “Wearable physiological sensors reflect mental stress state in office-like situations,” in *Proc. IEEE Conf. Affective Computing and Intelligent Interaction*, 2013, pp. 600–605.
- [74] X. Li, B. Hu, J. Shen, T. Xu, and M. Retcliffe, “Mild depression detection of college students: An EEG-based solution with free viewing tasks,” *J. Medical Systems*, vol. 39, no. 12, pp. 1–6, 2015.

- [75] H. W. Guo, Y. S. Huang, J. C. Chien, and J. S. Shieh, "Short-term analysis of heart rate variability for emotion recognition via a wearable ECG device," in *Proc. IEEE Int. Conf. Intelligent Informatics and Biomedical Sciences*, 2015, pp. 262–265.
- [76] T. O. Meservy, M. L. Jensen, J. Kruse, J. K. Burgoon, J. F. Nunamaker, D. P. Twitchell, G. Tsechpenakis, and D. N. Metaxas, "Deception detection through automatic, unobtrusive analysis of nonverbal behavior," *IEEE Intelligent Systems*, vol. 20, no. 5, pp. 36–43, 2005.
- [77] M. Sung and A. Pentland, "PokerMetrics: Stress and lie detection through non-invasive physiological sensing," *Ph.D. thesis, MIT Media Laboratory*, 2005.
- [78] M. R. Bhutta, M. J. Hong, Y.-H. Kim, and K.-S. Hong, "Single-trial lie detection using a combined fNIRS-polygraph system," *Frontiers in Psychology*, vol. 6, p. 709, 2015.
- [79] P. S. Teh, A. B. J. Teoh, and S. Yue, "A survey of keystroke dynamics biometrics," *The Scientific World Journal*, vol. 2013, 2013.
- [80] K. Delac and M. Grgic, "A survey of biometric recognition methods," in *Proc. IEEE Int. Symp. Electronics in Marine*, 2004, pp. 184–193.
- [81] W. Khalifa, A. Salem, M. Roushdy, and K. Revett, "A survey of EEG based user authentication schemes," in *Proc. IEEE Int. Conf. Informatics and Systems*, 2012, pp. 55–60.
- [82] S. P. Banerjee and D. L. Woodard, "Biometric authentication and identification using keystroke dynamics: A survey," *J. Pattern Recognition Research*, vol. 7, no. 1, pp. 116–139, 2012.
- [83] D. Gafurov, E. Snekenes, and P. Bours, "Gait authentication and identification using wearable accelerometer sensor," in *Proc. IEEE Wkshp. Automatic Identification Advanced Technologies*, 2007, pp. 220–225.
- [84] A. Ferrari, D. Puccinelli, and S. Giordano, "Gesture-based soft authentication," in *Proc. IEEE Int. Conf. Wireless and Mobile Computing, Networking and Communications*, 2015, pp. 771–777.
- [85] M. Phothisonothai, "An investigation of using SSVEP for EEG-based user authentication system," in *Proc. IEEE Asia-Pacific Signal and Information Processing Association Annual Summit and Conference*, 2015, pp. 923–926.
- [86] Z. Zhao, L. Yang, D. Chen, and Y. Luo, "A human ECG identification system based on ensemble empirical mode decomposition," *Sensors*, vol. 13, no. 5, pp. 6832–6864, 2013.
- [87] M. Teplan, "Fundamentals of EEG measurement," *Measurement Science Review*, vol. 2, no. 2, pp. 1–11, 2002.

- [88] I. Nakanishi, S. Baba, and C. Miyamoto, “EEG based biometric authentication using new spectral features,” in *Proc. IEEE Int. Symp. Intelligent Signal Processing and Communication Systems*, 2009, pp. 651–654.
- [89] J. Schneider, D. Börner, P. Van Rosmalen, and M. Specht, “Augmenting the senses: A review on sensor-based learning support,” *Sensors*, vol. 15, no. 2, pp. 4097–4133, 2015.
- [90] J. A. Kulik and J. Fletcher, “Effectiveness of intelligent tutoring systems: A meta-analytic review.” *Review of Educational Research*, vol. 86, no. 1, pp. 42–78, 2016.
- [91] B. Goldberg, “Intelligent tutoring gets physical: Coaching the physical learner by modeling the physical world,” in *Proc. Int. Conf. Augmented Cognition*. Springer, 2016, pp. 13–22.
- [92] T. Großhauser, B. Bläsing, C. Spieth, and T. Hermann, “Wearable sensor-based real-time sonification of motion and foot pressure in dance teaching and training,” *J. Audio Engineering Society*, vol. 60, no. 7/8, pp. 580–589, 2012.
- [93] H. Alemdar and C. Ersoy, “Wireless sensor networks for healthcare: A survey,” *Computer Networks*, vol. 54, no. 15, pp. 2688–2710, 2010.
- [94] K. Patrick, W. G. Griswold, F. Raab, and S. S. Intille, “Health and the mobile phone,” *American J. Preventive Medicine*, vol. 35, no. 2, p. 177, 2008.
- [95] R. P. Padhy, M. R. Patra, and S. C. Satapathy, “Design and implementation of a Cloud based rural healthcare information system model,” *Universal J. Applied Computer Science and Information Technology*, vol. 2, no. 1, pp. 149–157, 2012.
- [96] H. Thabit and R. Hovorka, “Closed-loop insulin delivery in Type-1 diabetes,” *Endocrinology and Metabolism Clinics of North America*, vol. 41, no. 1, pp. 105–117, 2012.
- [97] D. Culler, J. Hill, M. Horton, K. Pister, R. Szewczyk, and A. Wood, “Mica: The commercialization of microsensor motes,” *Sensor Technology and Design*, vol. 19, pp. 40–48, 2002.
- [98] T. Rault, A. Bouabdallah, and Y. Challal, “Energy efficiency in wireless sensor networks: A top-down survey,” *Computer Networks*, vol. 67, pp. 104–122, 2014.
- [99] S. E. Kerick, K. S. Oie, and K. McDowell, “Assessment of EEG signal quality in motion environments,” Defense Technical Information Center Document, Tech. Rep., 2009.
- [100] D. Halperin, T. S. Heydt-Benjamin, K. Fu, T. Kohno, and W. H. Maisel, “Security and privacy for implantable medical devices,” *IEEE Pervasive Computing*, vol. 7, no. 1, pp. 30–39, 2008.

- [101] T. Pylvänäinen, “Automatic and adaptive calibration of 3D field sensors,” *Applied Mathematical Modelling*, vol. 32, no. 4, pp. 575–587, 2008.
- [102] A. Krohn, M. Beigl, C. Decker, U. Kochendörfer, P. Robinson, and T. Zimmer, “Inexpensive and automatic calibration for acceleration sensors,” in *Proc. Int. Symp. Ubiquitous Computing Systems*, 2004, pp. 245–258.
- [103] S. Bhunia, M. S. Hsiao, M. Banga, and S. Narasimhan, “Hardware Trojan attacks: Threat analysis and countermeasures,” *Proc. IEEE*, vol. 102, no. 8, pp. 1229–1247, 2014.
- [104] H. Salmani and M. M. Tehranipoor, “Vulnerability analysis of a circuit layout to hardware Trojan insertion,” *IEEE Trans. Information Forensics and Security*, vol. 11, no. 6, pp. 1214–1225, 2016.
- [105] T. Wehbe, V. J. Mooney, D. C. Keezer, and N. B. Parham, “A novel approach to detect hardware Trojan attacks on primary data inputs,” in *Proc. ACM Wkshp. Embedded Systems Security*, 2015, p. 2.
- [106] S. Bhasin and F. Regazzoni, “A survey on hardware Trojan detection techniques,” in *Proc. IEEE Int. Symp. Circuits and Systems*, 2015, pp. 2021–2024.
- [107] D. M. Shila and V. Venugopal, “Design, implementation and security analysis of hardware Trojan threats in FPGA,” in *Proc. IEEE Int. Conf. Communications*, 2014, pp. 719–724.
- [108] M. Tehranipoor and F. Koushanfar, “A survey of hardware Trojan taxonomy and detection,” *IEEE Design and Test of Computers*, vol. 27, no. 1, pp. 10–25, 2010.
- [109] “NSA TEMPEST Series,” <http://cryptome.org/#NSA--TS>, accessed: 10-1-2016.
- [110] H. Tanaka, “Information leakage via electromagnetic emanations and evaluation of TEMPEST countermeasures,” in *Information Systems Security*. Springer, 2007, pp. 167–179.
- [111] M. Vuagnoux and S. Pasini, “Compromising electromagnetic emanations of wired and wireless keyboards,” in *Proc. USENIX Security Symposium*, 2009, pp. 1–16.
- [112] A. M. Nia, S. Sur-Kolay, A. Raghunathan, and N. K. Jha, “Physiological information leakage: A new frontier in health information security,” *IEEE Trans. Emerging Topics in Computing*, vol. 4, no. 3, pp. 321–334, 2016.
- [113] A. Brandt and J. Buron, “Home automation routing requirements in low-power and lossy networks,” <https://tools.ietf.org/html/rfc5826>, accessed: 10-1-2016.

- [114] S. Seys and B. Preneel, “Authenticated and efficient key management for wireless ad-hoc networks,” in *Proc. 24th Symp. Information Theory in the Benelux*, 2003, pp. 195–202.
- [115] T. Martin, M. Hsiao, D. Ha, and J. Krishnaswami, “Denial-of-service attacks on battery-powered mobile computers,” in *Proc. IEEE 2nd Conf. Pervasive Computing and Communications*, 2004, pp. 309–318.
- [116] M. Khouzani and S. Sarkar, “Maximum damage battery depletion attack in mobile sensor networks,” *IEEE Trans. Automatic Control*, vol. 56, no. 10, pp. 2358–2368, 2011.
- [117] A. Agah and S. K. Das, “Preventing DoS attacks in wireless sensor networks: A repeated game theory approach,” *Int. J. Network Security*, vol. 5, no. 2, pp. 145–153, 2007.
- [118] E. Y. Vasserman and N. Hopper, “Vampire attacks: Draining life from wireless ad-hoc sensor networks,” *IEEE Trans. Mobile Computing*, vol. 12, no. 2, pp. 318–332, 2013.
- [119] F. Stajano, “The resurrecting duckling,” in *Proc. Security Protocols*. Springer, 2000, pp. 183–194.
- [120] M. Shahrada, A. Mosenia, L. Song, M. Chiang, D. Wentzlaff, and P. Mittal, “Acoustic denial of service attacks on HDDs,” *arXiv preprint arXiv:1712.07816*, 2017.
- [121] A. Matrosov, E. Rodionov, D. Harley, and J. Malcho, “Stuxnet under the microscope,” ESET LLC, Tech. Rep., 2011.
- [122] A. A. Cárdenas, S. Amin, Z.-S. Lin, Y.-L. Huang, C.-Y. Huang, and S. Sastry, “Attacks against process control systems: Risk assessment, detection, and response,” in *Proc. ACM 6th Symp. Information, Computer and Communications Security*, 2011, pp. 355–366.
- [123] X. Wang, S. Chellappan, W. Gu, W. Yu, and D. Xuan, “Search-based physical attacks in sensor networks,” in *Proc. IEEE 14th Int. Conf. Computer Communications and Networks*, 2005, pp. 489–496.
- [124] A. Becher, Z. Benenson, and M. Dornseif, *Tampering with Notes: Real-world Physical Attacks on Wireless Sensor Networks*. Springer, 2006.
- [125] R. Anderson and M. Kuhn, “Tamper resistance—a cautionary note,” in *Proc. 2nd USENIX Wkshp. Electronic Commerce*, vol. 2, 1996, pp. 1–11.
- [126] M. Zorzi, A. Gluhak, S. Lange, and A. Bassi, “From today’s Intranet of Things to a future Internet of Things: A wireless-and mobility-related view,” *IEEE Wireless Communications*, vol. 17, no. 6, pp. 44–51, 2010.

- [127] G. Hernandez, O. Arias, D. Buentello, and Y. Jin, “Smart Nest thermostat: A smart spy in your home,” in *Proc. Black Hat USA*, 2014.
- [128] B. Parno, A. Perrig, and V. Gligor, “Distributed detection of node replication attacks in sensor networks,” in *Proc. IEEE Symp. Security and Privacy*, 2005, pp. 49–63.
- [129] J. P. Walters, Z. Liang, W. Shi, and V. Chaudhary, “Wireless sensor network security: A survey,” *Security in Distributed, Grid, Mobile, and Pervasive Computing*, vol. 1, p. 367, 2007.
- [130] H. Chan, A. Perrig, and D. Song, “Random key predistribution schemes for sensor networks,” in *Proc. IEEE Symp. Security and Privacy*, 2003, pp. 197–213.
- [131] G. Padmavathi and D. Shanmugapriya, “A survey of attacks, security mechanisms and challenges in wireless sensor networks,” *arXiv preprint arXiv:0909.0576*, 2009.
- [132] A. Juels, R. L. Rivest, and M. Szydlo, “The blocker tag: Selective blocking of RFID tags for consumer privacy,” in *Proc. ACM 10th Conf. Computer and Communications Security*, 2003, pp. 103–111.
- [133] S. A. Weis, S. E. Sarma, R. L. Rivest, and D. W. Engels, “Security and privacy aspects of low-cost radio frequency identification systems,” in *Security in Pervasive Computing*. Springer, 2004, pp. 201–212.
- [134] A. Juels, “RFID security and privacy: A research survey,” *IEEE J. Selected Areas in Communications*, vol. 24, no. 2, pp. 381–394, 2006.
- [135] P. Peris-Lopez, J. C. Hernandez-Castro, J. M. Estevez-Tapiador, and A. Ribagorda, “RFID systems: A survey on security threats and proposed solutions,” in *Proc. Personal Wireless Communications*. Springer, 2006, pp. 159–170.
- [136] S. H. Weingart, “Physical security devices for computer subsystems: A survey of attacks and defenses,” in *Proc. Cryptographic Hardware and Embedded Systems*. Springer, 2000, pp. 302–317.
- [137] M. Lehtonen, D. Ostojic, A. Ilic, and F. Michahelles, “Securing RFID systems by detecting tag cloning,” in *Pervasive Computing*. Springer, 2009, pp. 291–308.
- [138] J. Westhues, “Hacking the prox card,” *RFID: Applications, Security, and Privacy*, pp. 291–300, 2005.
- [139] D. N. Duc and K. Kim, “Defending RFID authentication protocols against DoS attacks,” *Computer Communications*, vol. 34, no. 3, pp. 384–390, 2011.

- [140] T. Karygiannis, B. Eydt, G. Barber, L. Bunn, and T. Phillips, “Guidelines for securing radio frequency identification (RFID) systems,” *NIST Special Publication*, vol. 80, pp. 1–154, 2007.
- [141] T. Karygiannis, B. Eydt, G. Barber, and L. Bunn, “DHS emerging applications and technology subcommittee,” [http://www.dhs.gov/xlibrary/assets/privacy/privacy\\_advcom\\_rpt\\_rfid\\_draft.pdf](http://www.dhs.gov/xlibrary/assets/privacy/privacy_advcom_rpt_rfid_draft.pdf), accessed: 10-1-2016.
- [142] G. Hancke, “Eavesdropping attacks on high-frequency RFID tokens,” in *Proc. 4th Wkshp. RFID Security*, 2008, pp. 100–113.
- [143] Y. Zhou and D. Feng, “Side-channel attacks: Ten years after its publication and the impacts on cryptographic module security testing.” *IACR Cryptology ePrint Archive*, vol. 2005, p. 388, 2005.
- [144] A. Mukherjee, “Physical-layer security in the Internet of Things: Sensing and communication confidentiality under resource constraints,” *Proc. IEEE*, vol. 103, no. 10, pp. 1747–1761, 2015.
- [145] G. Noubir and G. Lin, “Low-power DoS attacks in data wireless LANs and countermeasures,” *ACM SIGMOBILE Mobile Computing and Communications Review*, vol. 7, no. 3, pp. 29–30, 2003.
- [146] Q. I. Sarhana, “Security attacks and countermeasures for wireless sensor networks: Survey,” *Int. J. Current Engineering and Technology*, pp. 628–635, 2013.
- [147] A. D. Wood, J. Stankovic, and G. Zhou, “DEEJAM: Defeating energy-efficient jamming in IEEE 802.15. 4-based wireless networks,” in *Proc. IEEE 4th Communications Society Conf. Sensor, Mesh and Ad-Hoc Communications and Networks*, 2007, pp. 60–69.
- [148] M. Wilhelm, I. Martinovic, J. B. Schmitt, and V. Lenders, “Short paper: Reactive jamming in wireless networks: How realistic is the threat?” in *Proc. ACM 4th Conf. Wireless Network Security*, 2011.
- [149] A. Mpitzopoulos, D. Gavalas, C. Konstantopoulos, and G. Pantziou, “A survey on jamming attacks and countermeasures in WSNs,” *IEEE Communications Surveys & Tutorials*, vol. 11, no. 4, pp. 42–56, 2009.
- [150] Z. Karakehayov, “Using REWARD to detect team black-hole attacks in wireless sensor networks,” in *Proc. Wkshp. Real-World Wireless Sensor Networks*, 2005, pp. 20–21.
- [151] B. Revathi and D. Geetha, “A survey of cooperative black and gray hole attack in MANET,” *Int. J. Computer Science and Management Research*, vol. 1, no. 2, pp. 205–208, 2012.



- [152] O. Garcia-Morchon, S. Kumar, R. Struik, S. Keoh, and R. Hummen, “Security considerations in the IP-based Internet of Things,” <https://tools.ietf.org/html/draft-garcia-core-security-04>, accessed: 10-1-2016.
- [153] L. Wallgren, S. Raza, and T. Voigt, “Routing attacks and countermeasures in the RPL-based Internet of Things,” *Int. J. Distributed Sensor Networks*, vol. 2013, 2013.
- [154] V. P. Singh, S. Jain, and J. Singhai, “Hello flood attack and its countermeasures in wireless sensor networks,” *Int. J. Computer Science*, vol. 7, no. 3, p. 23, 2010.
- [155] J. R. Douceur, “The Sybil attack,” in *Peer-to-peer Systems*. Springer, 2002, pp. 251–260.
- [156] I. Stojmenovic and S. Wen, “The fog computing paradigm: Scenarios and security issues,” in *Proc. IEEE Federated Conf. Computer Science and Information Systems*, 2014, pp. 1–8.
- [157] I. Stojmenovic, S. Wen, X. Huang, and H. Luan, “An overview of fog computing and its security issues,” *J. Concurrency and Computation: Practice and Experience*, 2015. [Online]. Available: <http://dx.doi.org/10.1002/cpe.3485>
- [158] B. A. Martin, F. Michaud, D. Banks, A. Mosenia, R. Zolfonoon, S. Irwan, S. Schrecker, and J. K. Zao, “OpenFog security requirements and approaches,” in *Proc. IEEE Fog World Congress*, 2017, pp. 1–6.
- [159] S. W. Boyd and A. D. Keromytis, “SQLrand: Preventing SQL injection attacks,” in *Applied Cryptography and Network Security*. Springer, 2004, pp. 292–302.
- [160] M. Barreno, B. Nelson, R. Sears, A. D. Joseph, and J. D. Tygar, “Can machine learning be secure?” in *Proc. ACM Symp. Information, Computer and Communications Security*, 2006, pp. 16–25.
- [161] B. Biggio, B. Nelson, and P. Laskov, “Poisoning attacks against support vector machines,” *arXiv preprint arXiv:1206.6389*, 2012.
- [162] L. Huang, A. D. Joseph, B. Nelson, B. I. Rubinstein, and J. Tygar, “Adversarial machine learning,” in *Proc. ACM 4th Wkshp. Security and Artificial Intelligence*, 2011, pp. 43–58.
- [163] B. I. Rubinstein, B. Nelson, L. Huang, A. D. Joseph, S.-H. Lau, S. Rao, N. Taft, and J. Tygar, “Stealthy poisoning attacks on PCA-based anomaly detectors,” *ACM SIGMETRICS Performance Evaluation Review*, vol. 37, no. 2, pp. 73–74, 2009.
- [164] K. Hong, D. Lillethun, U. Ramachandran, B. Ottenwalder, and B. Koldehofe, “Mobile fog: A programming model for large-scale applications on the Internet of Things,” in *Proc. ACM 2nd SIGCOMM Wkshp. Mobile Cloud Computing*, 2013, pp. 15–20.

- [165] B. Grobauer, T. Walloschek, and E. Stocker, “Understanding cloud computing vulnerabilities,” *IEEE Security Privacy*, vol. 9, no. 2, pp. 50–57, Mar. 2011.
- [166] A. Nejat, S. M. H. Shekarian, and M. S. Zamani, “A study on the efficiency of hardware Trojan detection based on path-delay fingerprinting,” *Microprocessors and Microsystems*, vol. 38, no. 3, pp. 246–252, 2014.
- [167] N. Yoshimizu, “Hardware Trojan detection by symmetry breaking in path delays,” in *Proc. IEEE Int. Symp. Hardware-Oriented Security and Trust*, 2014, pp. 107–111.
- [168] A. N. Nowroz, K. Hu, F. Koushanfar, and S. Reda, “Novel techniques for high-sensitivity hardware Trojan detection using thermal and power maps,” *IEEE Trans. Computer-Aided Design of Integrated Circuits and Systems*, vol. 33, no. 12, pp. 1792–1805, 2014.
- [169] T. Iwase, Y. Nozaki, M. Yoshikawa, and T. Kumaki, “Detection technique for hardware Trojans using machine learning in frequency domain,” in *Proc. IEEE 4th Global Conf. Consumer Electronics*. IEEE, 2015, pp. 185–186.
- [170] M. Tehranipoor, H. Salmani, and X. Zhang, “Hardware Trojan detection: Untrusted manufactured integrated circuits,” in *Integrated Circuit Authentication*. Springer, 2014, pp. 31–38.
- [171] K. Hu, A. N. Nowroz, S. Reda, and F. Koushanfar, “High-sensitivity hardware Trojan detection using multimodal characterization,” in *Proc. IEEE Design, Automation & Test in Europe Conference & Exhibition*, 2013, pp. 1271–1276.
- [172] S. S. Clark, B. Ransford, A. Rahmati, S. Guineau, J. Sorber, W. Xu, and K. Fu, “WattsUpDoc: Power side channels to nonintrusively discover untargeted malware on embedded medical devices,” in *Proc. USENIX Wkshp. Health Information Technologies*, 2013.
- [173] M. Mognna, K. Markantonakis, D. Naccache, and K. Mayes, “Verifying software integrity in embedded systems: A side channel approach,” in *Proc. Int. Wkshp. Constructive Side-Channel Analysis and Secure Design*, 2014, pp. 261–280.
- [174] M. Mognna, K. Markantonakis, and K. Mayes, “The B-side of side channel leakage: Control flow security in embedded systems,” in *Proc. Int. Conf. Security and Privacy in Communication Systems*, 2013, pp. 288–304.
- [175] H. Sayadi, A. SM PD, S. R. Houmansadr, and H. Homayoun, “Comprehensive assessment of run-time hardware-supported malware detection using general and ensemble learning,” in *Proc. ACM Int. Conf. Computing Frontiers*, 2018.
- [176] H. Sayadi, N. Patel, A. Sasan, S. Rafatirad, H. Homayoun *et al.*, “Ensemble learning for effective run-time hardware-based malware detection: A comprehensive analysis and classification,” in *Proc. 55th Annual Design Automation Conference*. ACM, 2018, p. 1.

- [177] N. Lesperance, S. Kulkarni, and K.-T. Cheng, “Hardware Trojan detection using exhaustive testing of K-bit subspaces,” in *Proc. IEEE Asia and South Pacific Design Automation Conference*, 2015, pp. 755–760.
- [178] X. Ye, J. Feng, H. Gong, C. He, and W. Feng, “An anti-Trojans design approach based on activation probability analysis,” in *Proc. IEEE Int. Conf. Electron Devices and Solid-State Circuits*, 2015, pp. 443–446.
- [179] R. S. Chakraborty, F. Wolff, S. Paul, C. Papachristou, and S. Bhunia, “MERO: A statistical approach for hardware Trojan detection,” in *Proc. Cryptographic Hardware and Embedded Systems*. Springer, 2009, pp. 396–410.
- [180] S. S. Doumit and D. P. Agrawal, “Self-organized criticality and stochastic learning based intrusion detection system for wireless sensor networks,” in *Proc. IEEE Conf. Military Communications*, vol. 1, 2003, pp. 609–614.
- [181] C.-C. Su, K.-M. Chang, Y.-H. Kuo, and M.-F. Horng, “The new intrusion prevention and detection approaches for clustering-based sensor networks [wireless sensor networks],” in *Proc. IEEE Conf. Wireless Communications and Networking*, vol. 4, 2005, pp. 1927–1932.
- [182] A. Agah, S. K. Das, K. Basu, and M. Asadi, “Intrusion detection in sensor networks: A non-cooperative game approach,” in *Proc. IEEE 3rd Int. Symp. Network Computing and Applications*, 2004, pp. 343–346.
- [183] A. P. R. da Silva, M. H. Martins, B. P. Rocha, A. A. Loureiro, L. B. Ruiz, and H. C. Wong, “Decentralized intrusion detection in wireless sensor networks,” in *Proc. ACM 1st Int. Wkshp. Quality of Service & Security in Wireless and Mobile Networks*, 2005, pp. 16–23.
- [184] M. S. I. Mamun, A. Kabir, M. Hossen, M. Khan, and R. Hayat, “Policy based intrusion detection and response system in hierarchical WSN architecture,” *arXiv preprint arXiv:1209.1678*, 2012.
- [185] A. D. Wood and J. Stankovic, “Denial of service in sensor networks,” *IEEE Computer*, vol. 35, no. 10, pp. 54–62, 2002.
- [186] M. Zhang and N. K. Jha, “FinFET-based power management for improved DPA resistance with low overhead,” *ACM J. Emerging Technologies in Computing Systems*, vol. 7, no. 3, p. 10, 2011.
- [187] V. Sundaresan, S. Rammohan, and R. Vemuri, “Defense against side-channel power analysis attacks on microelectronic systems,” in *Proc. IEEE National Conf. Aerospace and Electronics*, 2008, pp. 144–150.
- [188] D. A. Osvik, A. Shamir, and E. Tromer, “Cache attacks and countermeasures: The case of AES,” in *Topics in Cryptology*. Springer, 2006, pp. 1–20.

- [189] C. Wachsmann and A.-R. Sadeghi, “Physically Unclonable Functions (PUFs): Applications, models, and future directions,” *Synthesis Lectures on Information Security, Privacy, and Trust*, vol. 5, no. 3, pp. 1–91, 2014.
- [190] K. Rosenfeld, E. Gavas, and R. Karri, “Sensor physical unclonable functions,” in *Proc. IEEE Int. Symp. Hardware-Oriented Security and Trust*, 2010, pp. 112–117.
- [191] A. Kanuparthi, R. Karri, and S. Addepalli, “Hardware and embedded security in the context of Internet of Things,” in *Proc. Wkshp. Security, Privacy and Dependability for Cyber Vehicles*, 2013, pp. 61–64.
- [192] U. Guin, D. DiMase, and M. Tehranipoor, “Counterfeit integrated circuits: Detection, avoidance, and the challenges ahead,” *J. Electronic Testing*, vol. 30, no. 1, pp. 9–23, 2014.
- [193] Y. W. Law, Y. Zhang, J. Jin, M. Palaniswami, and P. Havinga, “Secure rateless deluge: Pollution-resistant reprogramming and data dissemination for wireless sensor networks,” *EURASIP J. Wireless Communications and Networking*, vol. 2011, p. 5, 2011.
- [194] J.-J. Quisquater and D. Samyde, “Electromagnetic analysis (EMA): Measures and counter-measures for smart cards,” in *Smart Card Programming and Security*. Springer, 2001, pp. 200–210.
- [195] A. Juels and J. Brainard, “Soft blocking: Flexible blocker tags on the cheap,” in *Proc. ACM Wkshp. Privacy in the Electronic Society*, 2004, pp. 1–7.
- [196] S. Kinoshita, F. Hoshino, T. Komuro, A. Fujimura, and M. Ohkubo, “Low-cost RFID privacy protection scheme,” *IPS Journal*, vol. 45, no. 8, pp. 2007–2021, 2004.
- [197] M. R. Rieback, B. Crispo, and A. S. Tanenbaum, “RFID guardian: A battery-powered mobile device for RFID privacy management,” in *Proc. Information Security and Privacy*. Springer, 2005, pp. 184–194.
- [198] M. Feldhofer, S. Dominikus, and J. Wolkerstorfer, “Strong authentication for RFID systems using the AES algorithm,” in *Cryptographic Hardware and Embedded Systems*. Springer, 2004, pp. 357–370.
- [199] P. Peris-Lopez, J. C. Hernandez-Castro, J. M. Estevez-Tapiador, and A. Ribagorda, “ $M^2AP$ : A minimalist mutual-authentication protocol for low-cost RFID tags,” in *Ubiquitous Intelligence and Computing*. Springer, 2006, pp. 912–923.
- [200] M. Jung, H. Fiedler, and R. Lerch, “8-bit microcontroller system with area efficient AES coprocessor for transponder applications,” in *Proc. Ecrypt Wkshp. RFID and Lightweight Crypto*, 2005, pp. 32–43.

- [201] E. Y. Choi, S. M. Lee, and D. H. Lee, “Efficient RFID authentication protocol for ubiquitous computing environment,” in *Proc. Embedded and Ubiquitous Computing*. Springer, 2005, pp. 945–954.
- [202] T. Dimitriou, “A lightweight RFID protocol to protect against traceability and cloning attacks,” in *Proc. IEEE 1st Int. Conf. Security and Privacy for Emerging Areas in Communications Networks*, 2005, pp. 59–66.
- [203] S. M. Lee, Y. J. Hwang, D. H. Lee, and J. I. Lim, “Efficient authentication for low-cost RFID systems,” in *Computational Science and Its Applications*. Springer, 2005, pp. 619–627.
- [204] G. Avoine and P. Oechslin, “A scalable and provably secure hash-based RFID protocol,” in *Proc. IEEE 3rd Int. Conf. Pervasive Computing and Communications*, 2005, pp. 110–114.
- [205] M. Ohkubo, K. Suzuki, and S. Kinoshita, “Hash-chain based forward-secure privacy protection scheme for low-cost RFID,” in *Proc. Scandinavian Conference on Information Systems*, vol. 2004, 2004, pp. 719–724.
- [206] D. Molnar and D. Wagner, “Privacy and security in library RFID: Issues, practices, and architectures,” in *Proc. ACM 11th Conf. Computer and Communications Security*, 2004, pp. 210–219.
- [207] I. Vajda and L. Buttyán, “Lightweight authentication protocols for low-cost RFID tags,” in *Proc. 2nd Wkshp. Security in Ubiquitous Computing*, 2003.
- [208] P. F. Cortese, F. Gemmiti, B. Palazzi, M. Pizzonia, and M. Rimondini, “Efficient and practical authentication of PUF-based RFID tags in supply chains,” in *Proc. IEEE Int. Conf. RFID-Technology and Applications*, 2010, pp. 182–188.
- [209] D. Moriyama, S. Matsuo, and M. Yung, “PUF-based RFID authentication secure and private under complete memory leakage,” *Int. Assoc. Cryptologic Research Cryptology ePrint Archive*, p. 712, 2013.
- [210] H.-H. Huang, L.-Y. Yeh, W.-J. Tsaur *et al.*, “Ultra-lightweight mutual authentication and ownership transfer protocol with PUF for Gen2 V2 RFID systems,” in *Proc. Int. Conf. Engineers and Computer Scientists*, vol. 2, 2016.
- [211] S. Mauw and S. Piramuthu, “A PUF-based authentication protocol to address ticket-switching of RFID-tagged items,” in *Proc. Int. Wkshp. Security and Trust Management*, 2012, pp. 209–224.
- [212] C. Karlof and D. Wagner, “Secure routing in wireless sensor networks: Attacks and countermeasures,” *Ad-hoc Networks*, vol. 1, no. 2, pp. 293–315, 2003.
- [213] K. Sanzgiri, B. Dahill, B. N. Levine, C. Shields, and E. M. B. Royer, “A secure routing protocol for ad-hoc networks,” in *Proc. IEEE 10th Int. Conf. Network Protocols*, 2002, pp. 78–87.

- [214] P. Papadimitratos and Z. J. Haas, “Secure routing for mobile ad hoc networks,” in *Proc. SCS Communication Networks and Distributed Systems Modeling and Simulation Conference*, 2002, pp. 193–204.
- [215] R. Bonetto, N. Bui, V. Lakkundi, A. Olivereau, A. Serbanati, and M. Rossi, “Secure communication for smart IoT objects: Protocol stacks, use cases and practical examples,” in *Proc. IEEE Int. Symp. World of Wireless, Mobile and Multimedia Networks*, 2012, pp. 1–7.
- [216] M. Čagalj, S. Čapkun, and J.-P. Hubaux, “Wormhole-based antijamming techniques in sensor networks,” *IEEE Trans. Mobile Computing*, vol. 6, no. 1, pp. 100–114, 2007.
- [217] A. Abduvaliyev, A.-S. Pathan, J. Zhou, R. Roman, and W.-C. Wong, “On the vital areas of intrusion detection systems in wireless sensor networks,” *IEEE Communications Surveys & Tutorials*, vol. 15, no. 3, pp. 1223–1237, 2013.
- [218] Y. Wang, H. Yang, X. Wang, and R. Zhang, “Distributed intrusion detection system based on data fusion method,” in *Proc. 5th World Congress on Intelligent Control and Automation*, June 2004, pp. 4331–4334.
- [219] S. Raza, L. Wallgren, and T. Voigt, “SVELTE: Real-time intrusion detection in the Internet of Things,” *Ad-hoc Networks*, vol. 11, no. 8, pp. 2661–2674, 2013.
- [220] C. Liu, J. Yang, Y. Zhang, R. Chen, and J. Zeng, “Research on immunity-based intrusion detection technology for the Internet of Things,” in *Proc. IEEE 7th Int. Conf. Natural Computation*, vol. 1, 2011, pp. 212–216.
- [221] J. Daemen and V. Rijmen, *The Design of Rijndael: AES-The Advanced Encryption Standard*. Springer Science and Business Media, 2013.
- [222] M. Bellare, A. Desai, E. Jorjani, and P. Rogaway, “A concrete security treatment of symmetric encryption,” in *Proc. IEEE 38th Symp. Foundations of Computer Science*, 1997, pp. 394–403.
- [223] M. Katagi and S. Moriai, “Lightweight cryptography for the Internet of Things,” *Sony Corporation*, pp. 7–10, 2008.
- [224] T. Shirai, K. Shibutani, T. Akishita, S. Moriai, and T. Iwata, “The 128-bit blockcipher CLEFIA,” in *Proc. Fast Software Encryption*. Springer, 2007, pp. 181–195.
- [225] A. Bogdanov, L. R. Knudsen, G. Leander, C. Paar, A. Poschmann, M. J. Robshaw, Y. Seurin, and C. Vikkelsoe, *PRESENT: An Ultra-lightweight Block Cipher*. Springer, 2007.
- [226] R. Kumar and S. Rajalakshmi, “Mobile sensor cloud computing: Controlling and securing data processing over smart environment through mobile sensor cloud computing,” in *Proc. IEEE Int. Conf. Computer Sciences and Applications*, 2013, pp. 687–694.

- [227] S. Misra and A. Vaish, “Reputation-based role assignment for role-based access control in wireless sensor networks,” *Computer Communications*, vol. 34, no. 3, pp. 281–294, 2011.
- [228] C. Ozturk, Y. Zhang, and W. Trappe, “Source-location privacy in energy-constrained sensor network routing,” in *Proc. ACM 2nd Wkshp. Security of Ad-hoc and Sensor Networks*, 2004, pp. 88–93.
- [229] M. Howard and S. Lipner, *The Security Development Lifecycle*. O’Reilly Media, Incorporated, 2009.
- [230] H. Mouratidis and P. Giorgini, “Security attack testing (SAT): Testing the security of information systems at design time,” *Information Systems*, vol. 32, no. 8, pp. 1166–1183, 2007.
- [231] B. I. Rubinstein, B. Nelson, L. Huang, A. D. Joseph, S.-H. Lau, S. Rao, N. Taft, and J. Tygar, “ANTIDOTE: Understanding and defending against poisoning of anomaly detectors,” in *Proc. ACM 9th SIGCOMM Conf. Internet Measurement*, 2009, pp. 1–14.
- [232] B. Biggio, I. Corona, G. Fumera, G. Giacinto, and F. Roli, “Bagging classifiers for fighting poisoning attacks in adversarial classification tasks,” in *Multiple Classifier Systems*. Springer, 2011, pp. 350–359.
- [233] L. Breiman, “Bagging predictors,” *Machine Learning*, vol. 24, no. 2, pp. 123–140, 1996.
- [234] M. Mozaffari-Kermani, S. Sur-Kolay, A. Raghunathan, and N. K. Jha, “Systematic poisoning attacks on and defenses for machine learning in healthcare,” *IEEE J. Biomedical and Health Informatics*, vol. 19, no. 6, pp. 1893–1905, Nov. 2015.
- [235] S. Son, K. S. McKinley, and V. Shmatikov, “Diglossia: Detecting code injection attacks with precision and efficiency,” in *Proc. ACM SIGSAC Conf. Computer & Communications Security*, 2013, pp. 1181–1192.
- [236] V. Luong, “Intrusion detection and prevention system: SQL-injection attacks,” Master’s thesis, San Jose State University, 2010.
- [237] F. S. Rietta, “Application layer intrusion detection for SQL injection,” in *Proc. ACM 44th Southeast Regional Conference*, 2006, pp. 531–536.
- [238] W. G. Halfond and A. Orso, “AMNESIA: Analysis and monitoring for NEutralizing SQL-injection attacks,” in *Proc. 20th IEEE/ACM Int. Conf. Automated Software Engineering*, 2005, pp. 174–183.
- [239] B. E. Jonsson, “An empirical approach to finding energy efficient ADC architectures,” in *Proc. IEEE Analog-to-Digital Forum*, 2011, pp. 1–6.

- [240] S.-W. M. Chen and R. W. Brodersen, “A 6-bit 600-ms/s 5.3-mW asynchronous ADC in 0.13 $\mu$ m-CMOS,” *IEEE J. Solid-State Circuits*, vol. 41, no. 12, pp. 2669–2680, 2006.
- [241] C.-C. Lu, “A 1.2 V 10-bit 5 MS/s CMOS cyclic ADC,” in *Proc. IEEE Int. Symp. Circuits and Systems*, 2013, pp. 1986–1989.
- [242] T. Morita, “Delta-sigma ADC,” 2013, US Patent 8,466,821.
- [243] “ANT basics,” <https://www.thisisant.com/developer/ant/ant-basics>, accessed: 10-9-2016.
- [244] P. Baronti, P. Pillai, V. W. Chook, S. Chessa, A. Gotta, and Y. F. Hu, “Wireless sensor networks: A survey on the state of the art and the 802.15.4 and ZigBee standards,” *Computer Communications*, vol. 30, no. 7, pp. 1655–1695, 2007.
- [245] C. Gomez, J. Oller, and J. Paradells, “Overview and evaluation of Bluetooth Low Energy: An emerging low-power wireless technology,” *Sensors*, vol. 12, no. 9, pp. 11 734–11 753, 2012.
- [246] N. Kane, M. Simmons, D. John, D. Thompson, and D. Basset, “Validity of the Nike+ device during walking and running,” *Int. J. Sports Medicine*, vol. 31, no. 02, pp. 101–105, 2010.
- [247] A. Dementyev, S. Hodges, S. Taylor, and J. Smith, “Power consumption analysis of Bluetooth Low Energy, ZigBee and ANT sensor nodes in a cyclic sleep scenario,” in *Proc. IEEE Wireless Symposium*, 2013, pp. 1–4.
- [248] B. Gholami, S. Yoon, and V. Pavlovic, “Decentralized approximate bayesian inference for distributed sensor network,” in *Proc. Thirtieth AAAI Conf. Artificial Intelligence*, 2016, pp. 1582–1588.
- [249] B. Babagholami-Mohamadabadi, S. Yoon, and V. Pavlovic, “Mean field variational inference using bregman ADMM for distributed camera network,” in *Proc. ACM Int. Conf. Distributed Smart Cameras*, 2015, pp. 209–210.
- [250] H. Ghasemzadeh and R. Jafari, “Data aggregation in body sensor networks: A power optimization technique for collaborative signal processing,” in *Proc. IEEE Communications Society Conf. Sensor, Mesh and Ad Hoc Communications and Networks*, 2010, pp. 1–9.
- [251] N. Kimura and S. Latifi, “A survey on data compression in wireless sensor networks,” in *Proc. IEEE Int. Conf. Information Technology: Coding and Computing*, vol. 2, 2005, pp. 8–13.
- [252] M. A. Razzaque, C. Bleakley, and S. Dobson, “Compression in wireless sensor networks: A survey and comparative evaluation,” *ACM Trans. Sensor Networks*, vol. 10, no. 1, p. 5, 2013.



- [253] R. G. Baraniuk, “Compressive sensing,” *IEEE Signal Processing Magazine*, vol. 24, no. 4, pp. 118–120, 2007.
- [254] M. Shoaib, K. H. Lee, N. K. Jha, and N. Verma, “A 0.6-107 $\mu$ W energy-scalable processor for seizure detection with compressively-sensed EEG,” *IEEE Trans. Circuits and Systems I*, vol. 61-I, no. 4, pp. 1105–1118, Apr. 2014.
- [255] M. Zhang, M. M. Kermani, A. Raghunathan, and N. K. Jha, “Energy-efficient and secure sensor data transmission using encompression,” in *Proc. IEEE Int. Conf. VLSI Design*, 2013, pp. 31–36.
- [256] S. R. Safavian and D. Landgrebe, “A survey of decision tree classifier methodology,” *IEEE Trans. Systems, Man, and Cybernetics*, vol. 21, no. 3, pp. 660–674, 1991.
- [257] Y. Freund and R. E. Schapire, “Large margin classification using the perceptron algorithm,” *Machine Learning*, vol. 37, no. 3, pp. 277–296, 1999.
- [258] J. A. Suykens and J. Vandewalle, “Least squares support vector machine classifiers,” *Neural Processing Letters*, vol. 9, no. 3, pp. 293–300, 1999.
- [259] B. Liu, Z. Zhang, G. Xu, H. Fan, and Q. Fu, “Energy efficient telemonitoring of physiological signals via compressed sensing: A fast algorithm and power consumption evaluation,” *Biomedical Signal Processing and Control*, vol. 11, pp. 80–88, 2014.
- [260] M. Shoaib, N. K. Jha, and N. Verma, “Algorithm-driven architectural design space exploration of domain-specific medical-sensor processors,” *IEEE Trans. Very Large Scale Integration Systems*, vol. 21, no. 10, pp. 1849–1862, Oct. 2013.
- [261] Y. Liang, X. Zhou, Z. Yu, and B. Guo, “Energy-efficient motion related activity recognition on mobile devices for pervasive healthcare,” *Mobile Networks and Applications*, vol. 19, no. 3, pp. 303–317, 2014.
- [262] D. Millett, “Hans Berger: From psychic energy to the EEG,” *Perspectives in Biology and Medicine*, vol. 44, no. 4, pp. 522–542, 2001.
- [263] S. K. Vashist, “Non-invasive glucose monitoring technology in diabetes management: A review,” *Analytica Chimica Acta*, vol. 750, pp. 16–27, 2012.
- [264] A. J. Bandodkar, W. Jia, C. Yardımcı, X. Wang, J. Ramirez, and J. Wang, “Tattoo-based noninvasive glucose monitoring: A proof-of-concept study,” *Analytical Chemistry*, vol. 87, no. 1, pp. 394–398, 2014.
- [265] V. F. Curto, S. Coyle, R. Byrne, N. Angelov, D. Diamond, and F. Benito-Lopez, “Concept and development of an autonomous wearable micro-fluidic platform for real time pH sweat analysis,” *Sensors and Actuators B: Chemical*, vol. 175, no. 4, pp. 263–270, 2012.

- [266] S. Subashini and V. Kavitha, “A survey on security issues in service delivery models of Cloud computing,” *J. Network and Computer Applications*, vol. 34, no. 1, pp. 1–11, 2011.
- [267] A.-S. K. Pathan, H.-W. Lee, and C. S. Hong, “Security in wireless sensor networks: Issues and challenges,” in *Proc. IEEE Int. Conf. Advanced Communication Technology*, vol. 2, 2006, p. 6.
- [268] M. Al Ameen, J. Liu, and K. Kwak, “Security and privacy issues in wireless sensor networks for healthcare applications,” *J. Medical Systems*, vol. 36, no. 1, pp. 93–101, 2012.
- [269] M. M. Patel and A. Aggarwal, “Security attacks in wireless sensor networks: A survey,” in *Proc. IEEE Int. Conf. Intelligent Systems and Signal Processing*, 2013, pp. 329–333.
- [270] J. Zhen, J. Li, M. J. Lee, and M. Anshel, “A lightweight encryption and authentication scheme for wireless sensor networks,” *Int. J. Security and Networks*, vol. 1, no. 3-4, pp. 138–146, 2006.
- [271] C. H. Lim and T. Korkishko, “mCrypton—a lightweight block cipher for security of low-cost RFID tags and sensors,” in *Proc. Int. Wkshp. Information Security Applications*, 2005, pp. 243–258.
- [272] Y. Kim, W. S. Lee, V. Raghunathan, N. K. Jha, and A. Raghunathan, “Vibration-based secure side channel for medical devices,” in *Proc. IEEE Design Automation Conference*, 2015, pp. 1–6.
- [273] C. Wang, X. Guo, Y. Wang, Y. Chen, and B. Liu, “Friend or foe?: Your wearable devices reveal your personal PIN,” in *Proc. ACM Asia Conf. Computer and Communications Security*, 2016, pp. 189–200.
- [274] H. Wang, T. T.-T. Lai, and R. Roy Choudhury, “Mole: Motion leaks through smartwatch sensors,” in *Proc. ACM Annual Int. Conf. Mobile Computing and Networking*, 2015, pp. 155–166.
- [275] X. Liu, Z. Zhou, W. Diao, Z. Li, and K. Zhang, “When good becomes evil: Keystroke inference with smartwatch,” in *Proc. ACM SIGSAC Conf. Computer and Communications Security*, 2015, pp. 1273–1285.
- [276] J. Kim, T. Lee, J. Kim, and H. Ko, “Ambient light cancellation in photoplethysmogram application using alternating sampling and charge redistribution technique,” in *Proc. Annual Int. Conf. IEEE Engineering in Medicine and Biology Society*, 2015, pp. 6441–6444.
- [277] P. E. Clayson, S. A. Baldwin, and M. J. Larson, “How does noise affect amplitude and latency measurement of event-related potentials (ERPs)? a methodological critique and simulation study,” *Psychophysiology*, vol. 50, no. 2, pp. 174–186, 2013.

- [278] S. Salehizadeh, D. K. Dao, J. W. Chong, D. McManus, C. Darling, Y. Mendelson, and K. H. Chon, “Photoplethysmograph signal reconstruction based on a novel motion artifact detection-reduction approach,” *Annals of Biomedical Engineering*, vol. 42, no. 11, pp. 2251–2263, 2014.
- [279] H. Han and J. Kim, “Artifacts in wearable photoplethysmographs during daily life motions and their reduction with least mean square based active noise cancellation method,” *Computers in Biology and Medicine*, vol. 42, no. 4, pp. 387–393, 2012.
- [280] O. Banos, M. A. Toth, M. Damas, H. Pomares, and I. Rojas, “Dealing with the effects of sensor displacement in wearable activity recognition,” *Sensors*, vol. 14, no. 6, pp. 9995–10 023, 2014.
- [281] P. Alinia, R. Saeedi, B. Mortazavi, A. Rokni, and H. Ghasemzadeh, “Impact of sensor misplacement on estimating metabolic equivalent of task with wearables,” in *Proc. Int. Conf. Wearable and Implantable Body Sensor Networks*, 2015, pp. 1–6.
- [282] B. Chandrakar, O. Yadav, and V. Chandra, “A survey of noise removal techniques for ECG signals,” *Int. J. Advanced Research in Computer and Communication Engineering*, vol. 2, no. 3, pp. 1354–1357, 2013.
- [283] J. A. Urigüen and B. Garcia-Zapirain, “EEG artifact removal—state-of-the-art and guidelines,” *J. Neural Engineering*, vol. 12, no. 3, p. 31001, 2015.
- [284] J. Almazán, L. M. Bergasa, J. J. Yebes, R. Barea, and R. Arroyo, “Full auto-calibration of a smartphone on board a vehicle using IMU and GPS embedded sensors,” in *Proc. IEEE Intelligent Vehicles Symposium*, 2013, pp. 1374–1380.
- [285] M. Kok, J. D. Hol, T. B. Schön, F. Gustafsson, and H. Luinge, “Calibration of a magnetometer in combination with inertial sensors,” in *Proc. IEEE Int. Conf. Information Fusion*, 2012, pp. 787–793.
- [286] Y. Li, J. Georgy, X. Niu, Q. Li, and N. El-Sheimy, “Autonomous calibration of MEMS gyros in consumer portable devices,” *IEEE Sensors Journal*, vol. 15, no. 7, pp. 4062–4072, 2015.
- [287] J. Andreu-Perez, C. C. Poon, R. D. Merrifield, S. T. Wong, and G.-Z. Yang, “Big data for health,” *IEEE J. Biomedical and Health Informatics*, vol. 19, no. 4, pp. 1193–1208, 2015.
- [288] S. Redmond, N. Lovell, G. Yang, A. Horsch, P. Lukowicz, L. Murrugarra, and M. Marschollek, “What does big data mean for wearable sensor systems?” *Yearbook of Medical Informatics*, vol. 9, no. 1, pp. 135–142, 2014.
- [289] N. Eagle and A. S. Pentland, “Reality mining: Sensing complex social systems,” *Personal and Ubiquitous Computing*, vol. 10, no. 4, pp. 255–268, 2006.

- [290] C. Gurrin, A. F. Smeaton, and A. R. Doherty, “Lifelogging: Personal big data,” *Foundations and Trends in Information Retrieval*, vol. 8, no. 1, pp. 1–125, 2014.
- [291] D.-S. Lee, S. Bhardwaj, E. Alasaarela, and W.-Y. Chung, “An ECG analysis on sensor node for reducing traffic overload in u-healthcare with wireless sensor network,” in *Proc. IEEE Sensors*, 2007, pp. 256–259.
- [292] N. Tang, “Big data cleaning,” in *Proc. Asia-Pacific Web Conference*, 2014, pp. 13–24.
- [293] E. Rahm and H. H. Do, “Data cleaning: Problems and current approaches,” *IEEE Data Eng. Bull.*, vol. 23, no. 4, pp. 3–13, 2000.
- [294] M. Dallachiesa, A. Ebaid, A. Eldawy, A. Elmagarmid, I. F. Ilyas, M. Ouzzani, and N. Tang, “NADEEF: A commodity data cleaning system,” in *Proc. ACM SIGMOD Int. Conf. Management of Data*, 2013, pp. 541–552.
- [295] Z. Khayyat, I. F. Ilyas, A. Jindal, S. Madden, M. Ouzzani, P. Papotti, J.-A. Quiané-Ruiz, N. Tang, and S. Yin, “Bigdancing: A system for big data cleansing,” in *Proc. ACM SIGMOD Int. Conf. Management of Data*, 2015, pp. 1215–1230.
- [296] Q. Zhang, L. Cheng, and R. Boutaba, “Cloud computing: State-of-the-art and research challenges,” *J. Internet Services and Applications*, vol. 1, no. 1, pp. 7–18, 2010.
- [297] R. Moreno-Vozmediano, R. S. Montero, and I. M. Llorente, “Key challenges in Cloud computing: Enabling the future Internet of services,” *IEEE Internet Computing*, vol. 17, no. 4, pp. 18–25, 2013.
- [298] A. N. Toosi, R. N. Calheiros, and R. Buyya, “Interconnected Cloud computing environments: Challenges, taxonomy, and survey,” *ACM Computing Surveys*, vol. 47, no. 1, pp. 7–47, 2014.
- [299] C. Rong, S. T. Nguyen, and M. G. Jaatun, “Beyond lightning: A survey on security challenges in Cloud computing,” *Computers & Electrical Engineering*, vol. 39, no. 1, pp. 47–54, 2013.
- [300] C. Cérin, C. Coti, P. Delort, F. Diaz, and M. Gagnaire, “Downtime statistics of current Cloud solutions,” International Working Group on Cloud Computing Resiliency, Tech. Rep., 2013.
- [301] K. V. Vishwanath and N. Nagappan, “Characterizing Cloud computing hardware reliability,” in *Proc. ACM Symp. Cloud Computing*, 2010, pp. 193–204.
- [302] P. Garraghan, I. S. Moreno, P. Townend, and J. Xu, “An analysis of failure-related energy waste in a large-scale Cloud environment,” *IEEE Trans. Emerging Topics in Computing*, vol. 2, no. 2, pp. 166–180, 2014.

- [303] Y. Wei and M. B. Blake, “Service-oriented computing and Cloud computing: Challenges and opportunities,” *IEEE Internet Computing*, vol. 14, no. 6, p. 72, 2010.
- [304] S. M. Habib, S. Ries, and M. Muhlhauser, “Cloud computing landscape and research challenges regarding trust and reputation,” in *Proc. Int. Conf. Ubiquitous Intelligence & Computing*, 2010, pp. 410–415.
- [305] H. Abu-Libdeh, L. Princehouse, and H. Weatherspoon, “RACS: A case for Cloud storage diversity,” in *Proc. ACM Symp. Cloud Computing*, 2010, pp. 229–240.
- [306] M. Shahrad and D. Wentzlaff, “Availability knob: Flexible user-defined availability in the Cloud,” in *Proc. ACM Symp. Cloud Computing*, 2016, pp. 410–415.
- [307] K. Ren, C. Wang, and Q. Wang, “Security challenges for the public Cloud,” *IEEE Internet Computing*, vol. 16, no. 1, pp. 69–73, 2012.
- [308] L. Popa, M. Yu, S. Y. Ko, S. Ratnasamy, and I. Stoica, “Cloudpolice: Taking access control out of the network,” in *Proc. 9th ACM SIGCOMM Wkshp. Hot Topics in Networks*, 2010, p. 7.
- [309] X.-Y. Li, Y. Shi, Y. Guo, and W. Ma, “Multi-tenancy based access control in Cloud,” in *Proc. IEEE Int. Conf. Computational Intelligence and Software Engineering*, 2010, pp. 1–4.
- [310] J. M. A. Calero, N. Edwards, J. Kirschnick, L. Wilcock, and M. Wray, “Toward a multi-tenancy authorization system for Cloud services,” *IEEE Security & Privacy*, vol. 8, no. 6, pp. 48–55, 2010.
- [311] R. Masood, M. A. Shibli, Y. Ghazi, A. Kanwal, and A. Ali, “Cloud authorization: Exploring techniques and approach towards effective access control framework,” *Frontiers of Computer Science*, vol. 9, no. 2, pp. 297–321, 2015.
- [312] A. Alamri, W. S. Ansari, M. M. Hassan, M. S. Hossain, A. Alelaiwi, and M. A. Hossain, “A survey on sensor-Cloud: Architecture, applications, and approaches,” *Int. J. Distributed Sensor Networks*, vol. 2013, 2013.
- [313] D. Petcu, G. Macariu, S. Panica, and C. Crăciun, “Portable Cloud applications—from theory to practice,” *Future Generation Computer Systems*, vol. 29, no. 6, pp. 1417–1430, 2013.
- [314] G. Nan, Z. Mao, M. Yu, M. Li, H. Wang, and Y. Zhang, “Stackelberg game for bandwidth allocation in Cloud-based wireless live-streaming social networks,” *IEEE Systems Journal*, vol. 8, no. 1, pp. 256–267, 2014.

- [315] G. Wei, A. V. Vasilakos, Y. Zheng, and N. Xiong, “A game-theoretic method of fair resource allocation for Cloud computing services,” *J. Supercomputing*, vol. 54, no. 2, pp. 252–269, 2010.
- [316] S. Ullah, H. Higgins, B. Braem, B. Latre, C. Blondia, I. Moerman, S. Saleem, Z. Rahman, and K. S. Kwak, “A comprehensive survey of wireless body area networks,” *J. Medical Systems*, vol. 36, no. 3, pp. 1065–1094, 2012.
- [317] J. Ko, C. Lu, M. B. Srivastava, J. A. Stankovic, A. Terzis, and M. Welsh, “Wireless sensor networks for healthcare,” *Proc. IEEE*, vol. 98, no. 11, pp. 1947–1960, 2010.
- [318] B. Latré, B. Braem, I. Moerman, C. Blondia, and P. Demeester, “A survey on wireless body area networks,” *Wireless Networks*, vol. 17, no. 1, pp. 1–18, 2011.
- [319] C. Otto, A. Milenkovic, C. Sanders, and E. Jovanov, “System architecture of a wireless body area sensor network for ubiquitous health monitoring,” *J. Mobile Multimedia*, vol. 1, no. 4, pp. 307–326, 2006.
- [320] K. Wac, A. Van Halteren, and D. Konstantas, “QoS-predictions service: Infrastructural support for proactive QoS-and context-aware mobile services (position paper),” in *On the Move to Meaningful Internet Systems*. Springer, 2006, pp. 1924–1933.
- [321] E. J. Candes and M. B. Wakin, “An introduction to compressive sampling,” *IEEE Signal Processing Magazine*, vol. 25, no. 2, pp. 21–30, 2008.
- [322] M. Shoaib, N. K. Jha, and N. Verma, “Signal processing with direct computations on compressively-sensed data,” *IEEE Trans. VLSI Systems*, vol. 23, no. 1, pp. 30–43, Jan. 2015.
- [323] C. B. Wilson, “Sensors in medicine,” *Western J. Medicine*, vol. 171, no. 5-6, p. 322, 1999.
- [324] J. Yick, B. Mukherjee, and D. Ghosal, “Wireless sensor network survey,” *Computer Networks*, vol. 52, no. 12, pp. 2292–2330, 2008.
- [325] L. D. Durosier, G. Green, I. Batkin, A. J. Seely, M. G. Ross, B. S. Richardson, and M. G. Frasc, “Sampling rate of heart rate variability impacts the ability to detect acidemia in ovine fetuses near-term,” *Frontiers in Pediatrics*, vol. 2, p. 38, 2014.
- [326] V. N. Hegde, R. Deekshit, and P. S. Satyanarayana, “Heart rate variability analysis for abnormality detection using time frequency distribution – smoothed pseudo Winger Ville method,” *Power (dB)*, vol. 30, no. 20, p. 10, 2013.
- [327] G. Mancia, A. Zanchetti, E. Agebiti-Rosei, G. Benemio, R. De Cesaris, R. Fogari, A. Pessino, C. Porcellati, A. Salvetti, B. Trimarco *et al.*, “Ambulatory blood

- pressure is superior to clinic blood pressure in predicting treatment-induced regression of left ventricular hypertrophy,” *Circulation*, vol. 95, no. 6, pp. 1464–1470, 1997.
- [328] M. Adibuzzaman, G. C. Kramer, L. Galeotti, S. J. Merrill, D. G. Strauss, and C. G. Scully, “The mixing rate of the arterial blood pressure waveform Markov chain is correlated with shock index during hemorrhage in anesthetized swine,” in *Proc. IEEE 36th Annual Int. Conf. Engineering in Medicine and Biology Society*, 2014, pp. 3268–3271.
- [329] A. Evans and E. H. Winslow, “Oxygen saturation and hemodynamic response in critically ill, mechanically ventilated adults during intrahospital transport,” *American J. Critical Care*, vol. 4, no. 2, pp. 106–111, 1995.
- [330] C. O. F. Kamlin, C. P. F. O’Donnell, P. G. Davis, and C. J. Morley, “Oxygen saturation in healthy infants immediately after birth,” *J. Pediatrics*, vol. 148, no. 5, pp. 585–589, 2006.
- [331] C. Simon, C. Gronfier, J. Schlienger, and G. Brandenberger, “Circadian and ultradian variations of leptin in normal man under continuous enteral nutrition: Relationship to sleep and body temperature,” *J. Clinical Endocrinology and Metabolism*, vol. 83, no. 6, pp. 1893–1899, 1998.
- [332] H. G. Piper, J. L. Alexander, A. Shukla, F. Pigula, J. M. Costello, P. C. Laussen, T. Jaksic, and M. S. Agus, “Real-time continuous glucose monitoring in pediatric patients during and after cardiac surgery,” *J. Pediatrics*, vol. 118, no. 3, pp. 1176–1184, 2006.
- [333] C. Wan-Young, L. Young-Dong, and J. Sang-Joong, “A wireless sensor network compatible wearable u-healthcare monitoring system using integrated ECG, accelerometer and SpO<sub>2</sub>,” in *Proc. IEEE 30th Annual Int. Conf. Engineering in Medicine and Biology Society*, 2008, pp. 1529–1532.
- [334] Y. Cho, Y. Nam, Y. Choi, and W. Cho, “SmartBuckle: Human activity recognition using a 3-axis accelerometer and a wearable camera,” in *Proc. 2nd Int. Wkshp. Systems and Networking Support for Health Care and Assisted Living Environments*, 2008, p. 7.
- [335] K. Sankaran, M. Zhu, X. F. Guo, A. L. Ananda, M. C. Chan, and L. Peh, “Using mobile phone barometer for low-power transportation context detection,” in *Proc. ACM Conf. Embedded Network Sensor Systems*, 2014, pp. 191–205.
- [336] A. S. Berson, F. Y. Lau, J. M. Wojick, and H. V. Pipberger, “Distortions in infant electrocardiograms caused by inadequate high-frequency response,” *American Heart Journal*, vol. 93, no. 6, pp. 730–734, 1977.

- [337] F. Simon, J. P. Martinez, P. Laguna, B. Van Grinsven, C. Rutten, and R. Houben, "Impact of sampling rate reduction on automatic ECG delimitation," in *Proc. IEEE 29th Annual Int. Conf. Engineering in Medicine and Biology Society*, 2007, pp. 2587–2590.
- [338] J. D. Jirsch, E. Urrestarazu, P. LeVan, A. Olivier, F. Dubeau, and J. Gotman, "High-frequency oscillations during human focal seizures," *Brain*, vol. 129, no. 6, pp. 1593–1608, 2006.
- [339] J. Engel Jr., A. Bragin, R. Staba, and I. Mody, "High-frequency oscillations: What is normal and what is not?" *Epilepsia*, vol. 50, no. 4, pp. 598–604, 2009.
- [340] M. Chen, O. Boric-Lubecke, V. Lubecke, and X. Wang, "Analog signal processing for heart rate extraction," in *Proc. IEEE 27th Annual Int. Conf. Engineering in Medicine and Biology Society*, 2005, pp. 6671–6674.
- [341] M. T. Dastjerdi, "An analog VLSI front end for pulse oximetry," Ph.D. dissertation, Dept. of Electrical Engineering and Computer Science, Massachusetts Institute of Technology, 2006.
- [342] H. Y. Yang and R. Sarpeshkar, "A bio-inspired ultra-energy-efficient analog-to-digital converter for biomedical applications," *IEEE Trans. Circuits and Systems I*, vol. 53, no. 11, pp. 2349–2356, 2006.
- [343] "Glucose meter fundamentals and design," [http://freescale.com/files/microcontrollers/doc/app\\_note/AN4364.pdf](http://freescale.com/files/microcontrollers/doc/app_note/AN4364.pdf), accessed: 10-1-2016.
- [344] "Low-power 12-bit, 3-axis accelerometer," [http://cache.freescale.com/files/sensors/doc/fact\\_sheet/MMA8450QFS.pdf](http://cache.freescale.com/files/sensors/doc/fact_sheet/MMA8450QFS.pdf), accessed: 10-1-2016.
- [345] C. Park, P. H. Chou, Y. Bai, R. Matthews, and A. Hibbs, "An ultra-wearable, wireless, low power ECG monitoring system," in *Proc. IEEE Conf. Biomedical Circuits and Systems*, 2006, pp. 241–244.
- [346] C. J. Deepu, X. Zhang, W. Liew, D. Wong, and Y. Lian, "An ECG-SoC with 535 nW/channel lossless data compression for wearable sensors," in *Proc. IEEE Asian Conf. Solid-State Circuits*, 2013, pp. 145–148.
- [347] L. Yan and H. Yoo, "A low-power portable ECG touch sensor with two dry metal contact electrodes," *J. Semiconductor Technology and Science*, vol. 10, no. 4, pp. 300–308, 2010.
- [348] M. K. Delano, "A long term wearable electrocardiogram (ECG) measurement system," Ph.D. dissertation, Massachusetts Institute of Technology, 2012.
- [349] D. Yates, E. Lopez-Morillo, R. G. Carvajal, J. Ramirez-Angulo, and E. Rodriguez-Villegas, "A low-voltage low-power front-end for wearable EEG systems," in *Proc. IEEE 29th Annual Int. Conf. Engineering in Medicine and Biology Society*, 2007, pp. 5282–5285.



- [350] M. Mollazadeh, K. Murari, H. Schwerdt, X. Wang, N. Thakor, and G. Cauwenberghs, “Wireless multichannel acquisition of neuropotentials,” in *Proc. IEEE Conf. Biomedical Circuits and Systems*, 2008, pp. 49–52.
- [351] I. F. Akyildiz, W. Su, Y. Sankarasubramaniam, and E. Cayirci, “A survey on sensor networks,” *IEEE Communications Magazine*, vol. 40, no. 8, pp. 102–114, 2002.
- [352] C. Doukas, T. Pliakas, and I. Maglogiannis, “Mobile healthcare information management utilizing cloud computing and Android OS,” in *Proc. IEEE Int. Conf. Engineering in Medicine and Biology Society*, 2010, pp. 1037–1040.
- [353] N. Verma and A. P. Chandrakasan, “An ultra low energy 12-bit rate-resolution scalable SAR ADC for wireless sensor nodes,” *IEEE J. Solid-State Circuits*, vol. 42, no. 6, pp. 1196–1205, 2007.
- [354] D. Ho, K. Iniewski, S. Kasnavi, A. Ivanov, and S. Natarajan, “Ultra-low power 90nm 6T SRAM cell for wireless sensor network applications,” *Networks*, vol. 1, p. 3, 2006.
- [355] Q. Zhao and L. Zhang, “ECG feature extraction and classification using Wavelet transform and support vector machines,” in *Proc. IEEE Int. Conf. Neural Networks and Brain*, vol. 2, 2005, pp. 1089–1092.
- [356] K. H. Lee, S.-Y. Kung, and N. Verma, “Low-energy formulations of support vector machine kernel functions for biomedical sensor applications,” *J. Signal Processing Systems*, vol. 69, no. 3, pp. 339–349, 2012.
- [357] A. H. Shoeb, “Application of machine learning to epileptic seizure onset detection and treatment,” Ph.D. dissertation, Division of Health Sciences and Technology, Massachusetts Institute of Technology, 2009.
- [358] P. D. Williamson, D. D. Spencer, S. S. Spencer, R. A. Novelly, and R. H. Mattson, “Complex partial seizures of frontal lobe origin,” *Annals of Neurology*, vol. 18, no. 4, pp. 497–504, 1985.
- [359] B. Babagholami-Mohamadabadi, A. Jourabloo, A. Zarghami, and S. Kasaei, “A bayesian framework for sparse representation-based 3-d human pose estimation,” *IEEE Signal Processing Letters*, vol. 21, no. 3, pp. 297–300, 2014.
- [360] B. Babagholami-Mohamadabadi, A. Zarghami, M. Zolfaghari, and M. S. Baghshah, “PSSDL: Probabilistic semi-supervised dictionary learning,” in *Joint European Conf. Machine Learning and Knowledge Discovery in Databases*, 2013, pp. 192–207.
- [361] L. F. Polania, R. E. Carrillo, M. Blanco-Velasco, and K. E. Barner, “Compressed sensing based method for ECG compression,” in *Proc. IEEE Int. Conf. Acoustics, Speech and Signal Processing*, 2011, pp. 761–764.

- [362] M. L. Brown, W. J. Williams, and A. O. Hero, “Non-orthogonal Gabor representation of event-related potentials,” in *Proc. IEEE Int. Conf. Engineering in Medicine and Biology Society*, 1993, pp. 314–315.
- [363] P. J. Durka and K. J. Blinowska, “A unified time-frequency parametrization of EEGs,” *IEEE Engineering in Medicine and Biology Magazine*, vol. 20, no. 5, pp. 47–53, 2001.
- [364] S. Aviyente, E. M. Bernat, S. M. Malone, and W. G. Iacono, “Analysis of event related potentials using PCA and matching pursuit on the time-frequency plane,” in *Proc. IEEE Int. Conf. Engineering in Medicine and Biology Society*, 2006, pp. 2454–2457.
- [365] A. Boroumand, S. Ghose, Y. Kim, R. Ausavarungnirun, E. Shiu, R. Thakur, D. Kim, A. Kuusela, A. Knies, P. Ranganathan *et al.*, “Google workloads for consumer devices: Mitigating data movement bottlenecks,” in *Proc. ACM Twenty-Third Int. Conf. Architectural Support for Programming Languages and Operating Systems*, 2018, pp. 316–331.
- [366] A. Boroumand, S. Ghose, M. Patel, H. Hassan, B. Lucia, K. Hsieh, K. T. Malladi, H. Zheng, and O. Mutlu, “LazyPIM: An efficient cache coherence mechanism for processing-in-memory,” *IEEE Computer Architecture Letters*, vol. 16, no. 1, pp. 46–50, 2017.
- [367] K. Hsieh, S. Khan, N. Vijaykumar, K. K. Chang, A. Boroumand, S. Ghose, and O. Mutlu, “Accelerating pointer chasing in 3D-stacked memory: Challenges, mechanisms, evaluation,” in *Proc. IEEE Int. Conf. Computer Design*, 2016, pp. 25–32.
- [368] V. Seshadri, K. Hsieh, A. Boroumand, D. Lee, M. A. Kozuch, O. Mutlu, P. B. Gibbons, and T. C. Mowry, “Fast bulk bitwise AND and OR in DRAM,” *IEEE Computer Architecture Letters*, vol. 14, no. 2, pp. 127–131, 2015.
- [369] H. Sayadi, N. Patel, A. Sasan, and H. Homayoun, “Machine learning-based approaches for energy-efficiency prediction and scheduling in composite cores architectures,” in *Proc. Int. Conf. Computer Design*, 2017, pp. 129–136.
- [370] H. Sayadi, D. Pathak, I. Savidis, and H. Homayoun, “Power conversion efficiency-aware mapping of multithreaded applications on heterogeneous architectures: A comprehensive parameter tuning,” in *Proc. IEEE Asia Design Automation Conference*, 2018, pp. 70–75.
- [371] H. Sayadi and H. Homayoun, “Scheduling multithreaded applications onto heterogeneous composite cores architecture,” in *Proc. Int. Conf. Green and Sustainable Computing*, 2017, pp. 1–8.
- [372] A. Mosenia and N. K. Jha, “OpSecure: A secure optical communication channel for implantable medical devices,” *under review*.

- [373] S. Gollakota, H. Hassanieh, B. Ransford, D. Katabi, and K. Fu, “They can hear your heartbeats: Non-invasive security for implantable medical devices,” *ACM SIGCOMM Computer Communication Review*, vol. 41, no. 4, pp. 2–13, 2011.
- [374] M. Zhang, A. Raghunathan, and N. K. Jha, “MedMon: Securing medical devices through wireless monitoring and anomaly detection,” *IEEE Trans. Biomedical Circuits and Systems*, vol. 7, no. 6, pp. 871–881, 2013.
- [375] S. Lee, K. Fu, T. Kohno, B. Ransford, and W. H. Maisel, “Clinically significant magnetic interference of implanted cardiac devices by portable headphones,” *Heart Rhythm*, vol. 6, no. 10, pp. 1432–1436, 2009.
- [376] C. Hu, F. Zhang, X. Cheng, X. Liao, and D. Chen, “Securing communications between external users and wireless body area networks,” in *Proc. ACM Wkshp. Hot Topics on Wireless Network Security and Privacy*, 2013, pp. 31–36.
- [377] N. R. Potlapally, S. Ravi, A. Raghunathan, and N. K. Jha, “A study of the energy consumption characteristics of cryptographic algorithms and security protocols,” *IEEE Trans. Mobile Computing*, vol. 5, no. 2, pp. 128–143, Feb. 2006.
- [378] C. Strydis, D. Zhu, and G. N. Gaydadjiev, “Profiling of symmetric-encryption algorithms for a novel biomedical-implant architecture,” in *Proc. ACM Conf. Computing Frontiers*, 2008, pp. 231–240.
- [379] S. Schechter, “Security that is meant to be skin deep,” Microsoft Research, Tech. Rep., Apr. 2010.
- [380] T. Denning, A. Borning, B. Friedman, B. T. Gill, T. Kohno, and W. H. Maisel, “Patients, pacemakers, and implantable defibrillators: Human values and security for wireless implantable medical devices,” in *Proc. ACM SIGCHI Conf. Human Factors in Computing Systems*, 2010, pp. 917–926.
- [381] K. K. Venkatasubramanian, A. Banerjee, and S. K. Gupta, “EKG-based key agreement in body sensor networks,” in *Proc. IEEE Int. Conf. Computer Communications*, 2008, pp. 1–6.
- [382] F. Xu, Z. Qin, C. C. Tan, B. Wang, and Q. Li, “IMDGuard: Securing implantable medical devices with the external wearable guardian,” in *Proc. IEEE Int. Conf. Computer Communications*, 2011, pp. 1862–1870.
- [383] M. Rostami, A. Juels, and F. Koushanfar, “Heart-to-heart (H2H): Authentication for implanted medical devices,” in *Proc. ACM SIGSAC Conf. Computer & Communications Security*, 2013, pp. 1099–1112.
- [384] T. Halevi and N. Saxena, “Acoustic eavesdropping attacks on constrained wireless device pairing,” *IEEE Trans. Information Forensics and Security*, vol. 8, no. 3, pp. 563–577, 2013.

- [385] J. Vučić, C. Kottke, S. Nerreter, K.-D. Langer, and J. W. Walewski, “513 Mbit/s visible light communications link based on DMT-modulation of a white LED,” *J. Lightwave Technology*, vol. 28, no. 24, pp. 3512–3518, 2010.
- [386] F.-M. Wu, C.-T. Lin, C.-C. Wei, C.-W. Chen, H.-T. Huang, and C.-H. Ho, “1.1-Gb/s white-LED-based visible light communication employing carrier-less amplitude and phase modulation,” *IEEE Photonics Technology Letters*, vol. 24, no. 19, pp. 1730–1732, 2012.
- [387] “Is your defibrillator beeping?” <https://keepyourhearthealthy.wordpress.com/2011/01/02/is-your-defibrillator-beeping/>, accessed: 10-9-2016.
- [388] “ATmega168,” <http://www.atmel.com/devices/atmega168.aspx>, accessed: 10-9-2016.
- [389] “Ambient light sensor,” <https://www.sparkfun.com/datasheets/Sensors/>, accessed: 10-9-2016.
- [390] “Simblee,” <https://www.simblee.com/index.html>, accessed: 10-9-2016.
- [391] S. S. Clark and K. Fu, “Recent results in computer security for medical devices,” in *Proc. Int. Conf. Wireless Mobile Communication and Healthcare*, 2011, pp. 111–118.
- [392] “RGB image classification using Euclidean distance,” <http://www.math.ttu.edu/outreach/sumac/pics/lhs.pdf>, accessed: 10-9-2016.
- [393] J. C. Haartsen, “The bluetooth radio system,” *IEEE Personal Communications*, vol. 7, no. 1, pp. 28–36, 2000.
- [394] F. Mokhayeri, M. R. Akbarzadeh-T, and S. Toosizadeh, “Mental stress detection using physiological signals based on soft computing techniques,” in *Proc. 18th Iranian Conf. Biomedical Engineering*, Dec. 2011, pp. 232–237.
- [395] B. Kaur, J. J. Durek, B. L. O’Kane, N. Tran, S. Moses, M. Luthra, and V. N. Ikonomidou, “Heart rate variability (HRV): An indicator of stress,” in *Proc. SPIE Sensing Technology + Applications*, 2014, pp. 91 180V–91 180V8.
- [396] G. N. Dikecligil and L. R. Mujica-Parodi, “Ambulatory and challenge-associated heart rate variability measures predict cardiac responses to real-world acute emotional stress,” *Biological Psychiatry*, vol. 67, no. 12, pp. 1185–1190, 2010.
- [397] D. Svard, A. Cichocki, and A. Alvandpour, “Design and evaluation of a capacitively-coupled sensor readout circuit toward contact-less ECG and EEG,” in *Proc. IEEE Biomedical Circuits and Systems Conference*, 2010, pp. 302–305.
- [398] T. G. Buchman, P. K. Stein, and B. Goldstein, “Heart rate variability in critical illness and critical care,” *Current Opinion in Critical Care*, vol. 8, no. 4, pp. 311–315, 2002.

- [399] M. T. Bradley and M. P. Janisse, “Accuracy demonstrations, threat, and the detection of deception: Cardiovascular, electrodermal, and pupillary measures,” *Psychophysiology*, vol. 18, no. 3, pp. 307–315, 1981.
- [400] H. Pasterkamp, S. S. Kraman, and G. R. Wodicka, “Respiratory sounds: Advances beyond the stethoscope,” *American J. Respiratory and Critical Care Medicine*, vol. 156, no. 3, pp. 974–987, 1997.
- [401] N. Arora, D. Martins, D. Ruggerio, E. Tousimis, A. J. Swistel, M. P. Osborne, and R. M. Simmons, “Effectiveness of a noninvasive digital infrared thermal imaging system in the detection of breast cancer,” *The American J. Surgery*, vol. 196, no. 4, pp. 523–526, 2008.
- [402] J. B. Mercer and E. F. J. Ring, “Fever screening and infrared thermal imaging: Concerns and guidelines,” *Thermology International*, vol. 19, no. 3, pp. 67–69, 2009.
- [403] L. J. Jiang, E. Y. K. Ng, A. C. B. Yeo, S. Wu, F. Pan, W. Y. Yau, J. H. Chen, and Y. Yang, “A perspective on medical infrared imaging,” *J. Medical Engineering and Technology*, vol. 29, no. 6, pp. 257–267, 2005.
- [404] M. Backes, M. Dürmuth, S. Gerling, M. Pinkal, and C. Sporleder, “Acoustic side-channel attacks on printers,” in *Proc. USENIX Security Symposium*, 2010, pp. 307–322.
- [405] L. Zhuang, F. Zhou, and J. D. Tygar, “Keyboard acoustic emanations revisited,” in *Proc. ACM Conf. Computer and Communications Security*, 2005, pp. 373–382.
- [406] H. Tanaka, “Evaluation of information leakage via electromagnetic emanation and effectiveness of Tempest,” *IEICE Trans. Information and Systems*, vol. 91, no. 5, pp. 1439–1446, 2008.
- [407] ———, “Information leakage via electromagnetic emanations and evaluation of Tempest countermeasures,” *Information Systems Security*, pp. 167–179, 2007.
- [408] S. Chen, R. Wang, X. Wang, and K. Zhang, “Side-channel leaks in web applications: A reality today, a challenge tomorrow,” in *Proc. IEEE Symp. Security and Privacy*, 2010, pp. 191–206.
- [409] X. Luo, P. Zhou, E. W. Chan, W. Lee, R. K. Chang, and R. Perdisci, “HTTPOS: Sealing information leaks with browser-side obfuscation of encrypted flows,” in *Proc. Network and Distributed System Security Symposium*, 2011.
- [410] H. Shulman, “Pretty bad privacy: Pitfalls of DNS encryption,” in *Proc. ACM 13th Wkshp. Privacy in the Electronic Society*, 2014, pp. 191–200.

- [411] S. Kadloor, X. Gong, N. Kiyavash, T. Tezcan, and N. Borisov, “Low-cost side channel remote traffic analysis attack in packet networks,” in *Proc. IEEE Int. Conf. Communications*, 2010, pp. 1–5.
- [412] T. Wang, Z. Zhu, and A. Divakaran, “Long range audio and audio-visual event detection using a laser Doppler vibrometer,” in *Proc. SPIE Defense, Security, and Sensing*, 2010, p. 77040J.
- [413] “Detect ear - DET EAR,” <http://www.kjbsecurity.com/products/detail/detect-ear/117/>, accessed: 02-1-2015.
- [414] M. Vuagnoux and P. Sylvain, “Compromising electromagnetic emanations of wired and wireless keyboards,” in *Proc. USENIX Security Symposium*, 2009, pp. 1–16.
- [415] M. Ettus, “USRP user’s and developer’s guide,” *Ettus Research LLC*, 2005.
- [416] K. L. Herbst and I. B. Hirsch, “Insulin strategies for primary care providers,” *Clinical Diabetes*, vol. 20, no. 1, pp. 11–17, 2002.
- [417] D. Agrawal, B. Archambeault, J. R. Rao, and P. Rohatgi, “The EM side channel(s),” in *Cryptographic Hardware and Embedded Systems*. Springer, 2003, pp. 29–45.
- [418] K. Pongaliur, Z. Abraham, A. X. Liu, L. Xiao, and L. Kempel, “Securing sensor nodes against side channel attacks,” in *Proc. IEEE 11th Symp. High Assurance Systems Engineering*, 2008, pp. 353–361.
- [419] J. Deng, R. Han, and S. Mishra, “Countermeasures against traffic analysis attacks in wireless sensor networks,” in *Proc. IEEE First Int. Conf. Security and Privacy for Emerging Areas in Communications Networks*, 2005, pp. 113–126.
- [420] A. Mosenia, S. Sur-Kolay, A. Raghunathan, and N. K. Jha, “Disaster: Dedicated intelligent security attacks on sensor-triggered emergency responses,” *under review*.
- [421] A. A. Cárdenas, S. Amin, B. Sinopoli, A. Giani, A. Perrig, and S. Sastry, “Challenges for securing cyber physical systems,” in *Proc. Wkshp. Future Directions in Cyber Physical Systems Security*, 2009.
- [422] R. R. Rajkumar, I. Lee, L. Sha, and J. Stankovic, “Cyber physical systems: The next computing revolution,” in *Proc. ACM Design Automation Conference*, 2010, pp. 731–736.
- [423] C. Neuman, “Challenges in security for cyber physical systems,” in *Proc. Wkshp. Future Directions in Cyber Physical Systems Security*, vol. 7, 2009.

- [424] N. Veerasamy, M. Grobler, and B. Von Solms, “Building an ontology for cyberterrorism,” in *Proc. European Conf. Information Warfare and Security*, 2012, p. 286.
- [425] L. Lamb, “Home insecurity: No alarms, false alarms, and SIGINT,” Oak Ridge National Laboratory, Tech. Rep., 2014.
- [426] G. Sabaliauskaite and A. P. Mathur, “Aligning cyber-physical system safety and security,” in *Proc. Complex Systems Design & Management Asia*. Springer, 2015, pp. 41–53.
- [427] M. Li, W. Lou, and K. Ren, “Data security and privacy in wireless body area networks,” *IEEE Wireless Communications*, vol. 17, no. 1, pp. 51–58, 2010.
- [428] M. Sun, S. Mohan, L. Sha, and C. Gunter, “Addressing safety and security contradictions in cyber-physical systems,” in *Proc. Wkshp Future Directions in Cyber-Physical Systems Security*, 2009.
- [429] A. Parvulescu, “System for automatically unlocking an automotive child safety door lock,” June 2000, US Patent 6,081,758.
- [430] “HackRF One,” <https://greatscottgadgets.com/hackrf/>, accessed: 10-1-2016.
- [431] “Peeping into 73,000 unsecured security cameras,” <http://www.networkworld.com/article/2844283/microsoft-subnet/peeping-into-73-000-unsecured-security-cameras-thanks-to-default-passwords.html>, accessed: 10-1-2016.
- [432] “GNURadio,” <http://gnuradio.org/redmine/projects/gnuradio/wiki>, accessed: 10-1-2016.
- [433] “Federal Communication Commission,” <https://www.fcc.gov>, accessed: 10-1-2016.
- [434] P. J. Christensen, W. H. Graf, and T. W. Yeung, “Refinery power failures: Causes, costs and solutions,” *Petroleum Technology Quarterly*, vol. 18, no. 4, 2013.
- [435] “Sheffield forgemasters fined after worker’s death,” <http://www.thestar.co.uk/news/local/breaking-sheffield-forgemasters-fined-after-worker-s-death-1-6326832>, accessed: 10-1-2016.
- [436] “If the fire doesn’t kill you, the  $CO_2$  might,” <http://www.analoxsensortechnology.com/blog/2015/08/>, accessed: 10-1-2016.
- [437] R. Akella and B. M. McMillin, “Model-checking BNDC properties in cyber-physical systems,” in *Proc. 33rd IEEE Int. Computer Software and Applications Conference*, vol. 1, 2009, pp. 660–663.

- [438] R. Akella, H. Tang, and B. M. McMillin, “Analysis of information flow security in cyber-physical systems,” *Int. J. Critical Infrastructure Protection*, vol. 3, no. 3, pp. 157–173, 2010.
- [439] C. Li, A. Raghunathan, and N. K. Jha, “Improving the trustworthiness of medical device software with formal verification methods,” *IEEE Embedded Systems Letters*, vol. 5, no. 3, pp. 50–53, 2013.
- [440] Z. Jiang, M. Pajic, R. Alur, and R. Mangharam, “Closed-loop verification of medical devices with model abstraction and refinement,” *Int. J. Software Tools for Technology Transfer*, vol. 16, no. 2, pp. 191–213, 2014.
- [441] M. Saeed, M. Villarroel, A. T. Reisner, G. Clifford, L.-W. Lehman, G. Moody, T. Heldt, T. H. Kyaw, B. Moody, and R. G. Mark, “Multiparameter intelligent monitoring in intensive care II (MIMIC-II): A public-access intensive care unit database,” *Critical Care Medicine*, vol. 39, no. 5, p. 952, 2011.
- [442] P. S. Teh, A. B. J. Teoh, and S. Yue, “A survey of keystroke dynamics biometrics,” *The Scientific World Journal*, vol. 2013, 2013.
- [443] T. Sim, S. Zhang, R. Janakiraman, and S. Kumar, “Continuous verification using multimodal biometrics,” *IEEE Trans. Pattern Analysis and Machine Intelligence*, vol. 29, no. 4, pp. 687–700, 2007.
- [444] J. Bonneau, C. Herley, P. C. Van Oorschot, and F. Stajano, “The quest to replace passwords: A framework for comparative evaluation of web authentication schemes,” in *Proc. IEEE Symp. Security and Privacy*, 2012, pp. 553–567.
- [445] A. J. Aviv, K. Gibson, E. Mossop, M. Blaze, and J. M. Smith, “Smudge attacks on smartphone touch screens,” in *Proc. USENIX Wkshp. Offensive Technologies*, vol. 10, 2010, pp. 1–7.
- [446] C. Ma, D. Wang, and S. Zhao, “Security flaws in two improved remote user authentication schemes using smart cards,” *Int. J. Communication Systems*, vol. 27, no. 10, pp. 2215–2227, 2014.
- [447] K. Niinuma, U. Park, and A. K. Jain, “Soft biometric traits for continuous user authentication,” *IEEE Trans. Information Forensics and Security*, vol. 5, no. 4, pp. 771–780, 2010.
- [448] S. Egelman, S. Jain, R. S. Portnoff, K. Liao, S. Consolvo, and D. Wagner, “Are you ready to lock?” in *Proc. ACM Conf. Computer and Communications Security*, 2014, pp. 750–761.
- [449] C. Shen, Z. Cai, and X. Guan, “Continuous authentication for mouse dynamics: A pattern-growth approach,” in *Proc. IEEE Int. Conf. Dependable Systems and Networks*, 2012, pp. 1–12.



- [450] A. Pantelopoulos and N. G. Bourbakis, “A survey on wearable sensor-based systems for health monitoring and prognosis,” *IEEE Trans. Systems, Man, and Cybernetics*, vol. 40, no. 1, pp. 1–12, 2010.
- [451] R. Gravina, P. Alinia, H. Ghasemzadeh, and G. Fortino, “Multi-sensor fusion in body sensor networks: State-of-the-art and research challenges,” *Information Fusion*, vol. 35, pp. 68–80, 2017.
- [452] “Growth trends, consumer attitudes, and why smart-watches will dominate,” <http://www.businessinsider.com/the-wearable-computing-market-report-2014-10>, accessed: 08-1-2015.
- [453] M. Mihajlov and B. Jerman-Blažič, “On designing usable and secure recognition-based graphical authentication mechanisms,” *Interacting with Computers*, vol. 23, no. 6, pp. 582–593, 2011.
- [454] K. Niinuma and A. K. Jain, “Continuous user authentication using temporal information,” in *Proc. SPIE Defense, Security, and Sensing*, 2010, p. 76670L.
- [455] S. Liu and M. Silverman, “A practical guide to biometric security technology,” *IEEE IT Professional*, vol. 3, no. 1, pp. 27–32, 2001.
- [456] W. Shi, J. Yang, Y. Jiang, F. Yang, and Y. Xiong, “Senguard: Passive user identification on smartphones using multiple sensors,” in *Proc. IEEE Int. Conf. Wireless and Mobile Computing, Networking and Communications*, 2011, pp. 141–148.
- [457] J. Roth, X. Liu, and D. Metaxas, “On continuous user authentication via typing behavior,” *IEEE Trans. Image Processing*, vol. 23, no. 10, pp. 4611–4624, 2014.
- [458] N. Bartlow and B. Cukic, “Evaluating the reliability of credential hardening through keystroke dynamics,” in *Proc. Int. Symp. Software Reliability Engineering*, vol. 6, 2006, pp. 117–126.
- [459] E. Alsolami, “An examination of keystroke dynamics for continuous user authentication,” Ph.D. dissertation, Dept. of Computer Science and Software Engineering, Queensland University of Technology, 2012.
- [460] M. Schuckers, “Some statistical aspects of biometric identification device performance,” *Stats Magazine*, vol. 3, 2001.
- [461] A. Bourouis, M. Feham, and A. Bouchachia, “Ubiquitous mobile health monitoring system for elderly (UMHMSE),” *arXiv preprint arXiv:1107.3695*, 2011.
- [462] U. Varshney, “Pervasive healthcare and wireless health monitoring,” *Mobile Networks and Applications*, vol. 12, no. 2-3, pp. 113–127, 2007.

- [463] E. B. Mazomenos, D. Biswas, A. Acharyya, T. Chen, K. Maharatna, J. Rosen-  
garten, J. Morgan, and N. Curzen, “A low-complexity ECG feature extraction  
algorithm for mobile healthcare applications,” *IEEE J. Biomedical and Health  
Informatics*, vol. 17, no. 2, pp. 459–469, 2013.
- [464] P. R. Rijnbeek, J. A. Kors, and M. Witsenburg, “Minimum bandwidth re-  
quirements for recording of pediatric electrocardiograms,” *Circulation*, vol. 104,  
no. 25, pp. 3087–3090, 2001.
- [465] Y. Freund, R. Schapire, and N. Abe, “A short introduction to boosting,” *J.  
Japanese Society For Artificial Intelligence*, vol. 14, pp. 771–780, 1999.
- [466] H. Gascon, S. Uellenbeck, C. Wolf, and K. Rieck, “Continuous authentication  
on mobile devices by analysis of typing motion behavior,” in *Proc. Sicherheit*,  
2014, pp. 1–12.
- [467] Z. Sitová, J. Šeděnka, Q. Yang, G. Peng, G. Zhou, P. Gasti, and K. S. Balagani,  
“HMOG: New behavioral biometric features for continuous authentication of  
smartphone users,” *IEEE Trans. Information Forensics and Security*, vol. 11,  
no. 5, pp. 877–892, 2016.
- [468] S. Arlot and A. Celisse, “A survey of cross-validation procedures for model  
selection,” *Statistics Surveys*, vol. 4, pp. 40–79, 2010.
- [469] D. Mease and A. Wyner, “Evidence contrary to the statistical view of boosting,”  
*J. Machine Learning Research*, vol. 9, pp. 131–156, 2008.
- [470] S. P. Miller, B. C. Neuman, J. I. Schiller, and J. H. Saltzer, “Kerberos authen-  
tication and authorization system,” in *Proc. Project Athena Technical Plan*,  
1987.
- [471] I. Deutschmann, P. Nordstrom, and L. Nilsson, “Continuous authentication  
using behavioral biometrics,” *IEEE IT Professional*, vol. 15, no. 4, pp. 12–15,  
2013.
- [472] C. Abad, “The economy of phishing: A survey of the operations of the phishing  
market,” *First Monday*, vol. 10, no. 9, 2005.
- [473] R. Dhamija, J. D. Tygar, and M. Hearst, “Why phishing works,” in *Proc. ACM  
Conf. Human Factors In Computing Systems*, 2006, pp. 581–590.
- [474] J. Sohankar, K. Sadeghi, A. Banerjee, and S. K. Gupta, “E-bias: A perva-  
sive EEG-based identification and authentication system,” in *Proc. 11th ACM  
Symp. QoS and Security for Wireless and Mobile Networks*, 2015, pp. 165–172.
- [475] R. D. Labati, R. Sassi, and F. Scotti, “ECG biometric recognition: Permanence  
analysis of QRS signals for 24 hours continuous authentication,” in *Proc. IEEE  
Int. Wkshp. Information Forensics and Security*, 2013, pp. 31–36.

- [476] D. Crouse, H. Han, D. Chandra, B. Barbelo, and A. K. Jain, “Continuous authentication of mobile user: Fusion of face image and inertial measurement unit data,” in *Proc. IEEE Int. Conf. Biometrics*, 2015, pp. 135–142.
- [477] P.-W. Tsai, M. K. Khan, J.-S. Pan, and B.-Y. Liao, “Interactive artificial bee colony supported passive continuous authentication system,” *IEEE Systems Journal*, vol. 8, no. 2, pp. 395–405, 2014.
- [478] S. Mondal and P. Bours, “Context independent continuous authentication using behavioural biometrics,” in *Proc. IEEE Int. Conf. Identity, Security and Behavior Analysis*, 2015, pp. 1–8.
- [479] I. Traore, I. Woungang, Y. Nakkabi, M. S. Obaidat, A. A. E. Ahmed, and B. Khalilian, “Dynamic sample size detection in learning command line sequence for continuous authentication,” *IEEE Trans. Systems, Man, and Cybernetics*, vol. 42, no. 5, pp. 1343–1356, 2012.
- [480] P. Bours and S. Mondal, “Performance evaluation of continuous authentication systems,” *IET Biometrics*, vol. 4, no. 4, pp. 220–226, 2015.
- [481] R. E. Smith, *Authentication: From Passwords to Public Keys*. Addison-Wesley Longman Publishing Co., 2001.
- [482] K. Fox, J. S. Borer, A. J. Camm, N. Danchin, R. Ferrari, J. L. L. Sendon, P. G. Steg, J.-C. Tardif, L. Tavazzi, and M. Tendera, “Resting heart rate in cardiovascular disease,” *J. American College of Cardiology*, vol. 50, no. 9, pp. 823–830, 2007.
- [483] D. R. Carpenter, A. J. McLeod Jr., and J. G. Clark, “Using biometric authentication to improve fire ground accountability: An assessment of firefighter privacy concerns,” in *Proc. Americas Conference on Information Systems*, p. 11, 2008.
- [484] C. Peter, E. Ebert, and H. Beikirch, “A wearable multi-sensor system for mobile acquisition of emotion-related physiological data,” in *Proc. Int. Conf. Affective Computing and Intelligent Interaction*, 2005, pp. 691–698.
- [485] T. Denning, A. Andrew, R. Chaudhri, C. Hartung, J. Lester, G. Borriello, and G. Duncan, “BALANCE: Towards a usable pervasive wellness application with accurate activity inference,” in *Proc. Wkshp. ACM Mobile Computing Systems and Applications*, 2009, p. 5.
- [486] “Use Smart Doorbell to Hack WiFi Password,” <http://thehackernews.com/2016/01/doorbell-hacking-wifi-pasword.html/>, accessed: 2-1-2016.
- [487] “Hacking into Internet Connected Light Bulbs,” <http://www.contextis.com/resources/blog/hacking-internet-connected-light-bulbs/>, accessed: 2-1-2016.

- [488] E. McKenna, I. Richardson, and M. Thomson, “Smart meter data: Balancing consumer privacy concerns with legitimate applications,” *Energy Policy*, vol. 41, pp. 807–814, 2012.
- [489] Y. Michalevsky, A. Schulman, G. A. Veerapandian, D. Boneh, and G. Nakibly, “Powerspy: Location tracking using mobile device power analysis,” in *Proc. USENIX Security Symposium*, 2015, pp. 785–800.
- [490] J. Han, E. Owusu, L. T. Nguyen, A. Perrig, and J. Zhang, “Accomplice: Location inference using accelerometers on smartphones,” in *Proc. IEEE Int. Conf. Communication Systems and Networks*, 2012, pp. 1–9.
- [491] L. Cai and H. Chen, “TouchLogger: Inferring keystrokes on touch screen from smartphone motion,” in *Proc. USENIX Wkshp. Hot Topics in Security*, 2011, pp. 9–9.